ADAPTIVE ITERATIVE RECEIVERS FOR LAYERED SPACE TIME CODED CDMA SYSTEMS

TEAV KEOV KOLYAN

A THESIS SUBMITTED IN PARTIAL FULFILLMENT

OF THE REQUIREMENT FOR THE DEGREE OF

MASTER OF ENGINEERING IN INFORMATION ENGINEERING

FACULTY OF ENGINEERING

KING MONGKUT'S INSTITUTE OF TECHNOLOGY LADKRABANG

2010

KMITL-2010-EN-M-230-128

หัวข้อวิทยานิพนธ์	**เครื่องรับแบบปรับค่าวนรอบสำหรับระบบ CDMA ที่มีการเข้ารหัสเลเยอร์สเปซไทม์**
นักศึกษา	Miss. Teav Keov Kolyan
รหัสประจำตัว	51601251
ปริญญา	วิศวกรรมศาสตรมหาบัณฑิต
สาขาวิชา	วิศวกรรมสารสนเทศ
พ.ศ.	2553
อาจารย์ที่ปรึกษาวิทยานิพนธ์	ผศ.ดร. พิทักษ์ ธรรมวาริน

บทคัดย่อ

ระบบการสื่อสารไร้สายเป็นหนึ่งในสาขาที่มีความเปลี่ยนแปลงอย่างรวดเร็วในระบบการสื่อสารในปัจจุบัน อย่างไรก็ตามเนื่องจากการเชื่อมต่อของระบบการสื่อสารไร้สายยังไม่มีเสถียรภาพที่เพียงพอและมีความจุของระบบน้อย อันเนื่องมาจาก ช่องสัญญาณการจางหายหลายทิศทาง และสัญญาณรบกวนที่เกิดขึ้นในระบบ เช่นสัญญาณแทรกสอดของช่องสัญญาณร่วม (Co-channel Interference CCI) และสัญญาณแทรกสอดเนื่องจากการเข้าถึงของผู้ใช่หลายคน (Multiple Access Interference MAI) ดังนั้นในวิทยานิพนธ์นี้จึงนำเสนอ เครื่องรับสัญญาณที่มีโครงสร้างใหม่ 2 โครงสร้าง ที่มีระบบการเข้ารหัสแบบเลเยอร์สเปสไทม์ (Layered Space-time Coding (LSTC)) และ Multiple Input Multiple Output (MIMO) สำหรับการประยุกต์ใช้งานในระบบการสื่อสารไร้สายแบบ LSTC-CDMA

เครื่องรับสัญญาณที่ถูกออกแบบเรียกว่า เครื่องรับสัญญาณ LSTC-CDMA แบบปรับค่าได้วนซ้ำ และเครื่องรับสัญญาณแบบ G-RAKE LSTC-CDMA แบบปรับค่าได้วนซ้ำ เครื่องรับสัญญาณที่นำเสนอ ถูกศึกษาในปริภูมิเวลาและความถี่ โดยประกอบด้วยการตรวจจับสัญญาณแบบปรับค่าได้วนซ้ำและการเข้ารหัสสัญญาณ เทคนิคการปรับค่าแบบ Least Mean Square (LMS), Partial Filtered Gradient LMS (PFGLMS) และ Recursive Least Square (RLS) ได้ถูกนำมาใช้ในกระบวนการการปรับค่าเพื่อขจัดสัญญาณรบกวนออกจากระบบ นอกจากนี้ความซับซ้อนในการคำนวณของระบบการตรวจจับสัญญาณแบบปรับค่าได้ในปริภูมิเวลาและความถี่ถูกพิจารณา และพบว่าความซับซ้อนในการคำนวณของเครื่องรับสัญญาณแบบปรับค่าได้วนซ้ำในปริภูมิความถี่ที่นำเสนอลดลงอย่างมากเมื่อเปรียบเทียบกับเครื่องรับสัญญาณแบบปรับค่าได้วนซ้ำในปริภูมิเวลา

เครื่องรับสัญญาณ LSTC-CDMA แบบปรับค่าวนซ้ำถูกตรวจสอบภายในช่องสัญญาณของการจางหายอย่างรวดเร็วและอย่างช้า (Fast and Slow fading Channel) ด้วยจำนวนของสายอากาศส่งและรับที่ต่างๆกัน จากผลการทดลองพบว่าอัตราการผิดพลาดของบิต (BER) จะเพิ่มขึ้นเมื่ออัตราการจางหายในช่องสัญญาณเพิ่มขึ้น จำนวนของสายอากาศส่งและรับที่ใช้ในการทดลอง 2x4 จะให้ประสิทธิภาพของระบบดีที่สุดระหว่างจำนวนของสายอากาศส่งและรับ 2x2 4x4 และ 4x2 นอกจากนี้ จำนวนของ Finger ในโครงสร้างของเครื่องรับสัญญาณแบบ G-RAKE LSTC-CDMA แบบปรับค่าได้วนซ้ำ ที่มีจำนวน 3 Fingers และ 6 Fingers ได้ถูกนำมาใช้ ประสิทธิภาพของเครื่องรับที่นำเสนอเมื่อเพิ่มจำนวนของ Finger ให้มากกว่าจำนวนของทิศทางของช่องสัญญาณจางหาย พบว่าประสิทธิภาพของเครื่องรับสัญญาณในปริภูมิเวลาและความถี่ให้ผลลัพท์ที่เหมือนกัน นอกจากนี้เครื่องรับสัญญาณที่ใช้เทคนิคการปรับค่าแบบ RLS จะให้ประสิทธิภาพดีกว่าเครื่องรับที่ใช้เทคนิคการปรับค่าแบบ LMS และ PFGLMS เครื่องรับสัญญาณแบบ G-RAKE LSTC-CDMA แบบปรับค่าวนซ้ำ มีประสิทธิภาพที่ดีกว่า เครื่องรับสัญญาณแบบ LSTC-CDMA แบบปรับค่าวนซ้ำ

สุดท้ายผลการทดลองได้แสดงให้เห็นว่าเครื่องรับสัญญาณที่ได้ออกแบบมีความสามารถในการเอาชนะผลของการจางหายของช่องสัญญาณแบบหลายทิศทาง และขจัดสัญญาณแทรกสอดที่ไม่ต้องการออกจากระบบได้ โดยความซับซ้อนในการคำนวณที่ต่ำ และมีความเร็วในการปรับค่าของระบบที่เหมาะสม

Thesis Title	Adaptive Iterative Receivers for Layered Space Time Coded CDMA Systems
Student	Miss. Teav Keov Kolyan
Student ID.	51601251
Degree	Master of Engineering
Program	Information Engineering
Year	2010
Thesis Advisor	Asst. Prof. Dr. Pitak Thumwarin

ABSTRACT

Wireless communication system is one of the most vibrant areas in the communication field today. However, wireless communication links become unreliable and have fundamentally low capacity due to the effect of multipath fading channels and the systems interferences such as Co-Channel Interference (CCI) and Multiple Access Interference (MAI). Therefore, two new structure receivers in Layered Space-Time Coding (LSTC) and Multiple Input Multiple Output (MIMO) with Direct Sequence Code Division Multiple Access (DS-CDMA) systems for applications in downlink wireless communications have been proposed in this thesis.

The designed receivers are called adaptive iterative LSTC-CDMA receiver and adaptive iterative Generalized RAKE (G-RAKE) LSTC-CDMA receiver. The proposed receivers, based on a joint adaptive iterative detection and decoding algorithm, are investigated in both time and frequency domains. Specifically, Least Means Square (LMS), Partially Filtered Gradient LMS (PFGLMS) and Recursive Least Squares (RLS) algorithms are used in the adaptation process under the interference suppression and cancelation techniques. Moreover, the computational complexities of these adaptive detection algorithms in time and frequency domain are investigated. It is shown that the numbers of complexity of the proposed adaptive iterative receivers in frequency domain are significantly reduced in comparison with those in time domain.

The adaptive iterative LSTC-CDMA receiver is investigated in both fast and slow fading channels with a various number of antennas. The performance results show that the average Bit-Error Rate (BER) of the proposed adaptive receiver increases when the fading rate is increased and the 2x4 antennas system achieves the best performances among 2x2, 4x4 and 4x2 antennas systems. 3 fingers

and 6 fingers G-RAKE structures are utilized in the adaptive G-RAKE LSTC-CDMA receiver. The performance of the proposed receiver improves when the number of fingers is increased beyond the number of resolvable multipath. Furthermore, the results show that the performances of both proposed receivers in frequency domain have the same performances as those in time domain. However, the RLS based receivers have better performances than PFGLMS and LMS based receivers; and the adaptive iterative G-RAKE LSTC-CDMA receiver outperforms the adaptive iterative LSTC-CDMA receiver.

Finally, the simulation results prove that the designed receivers successfully have the ability to combat the effect of multipath fading channels and also to cancel the system interferences with low computational complexities and fast convergence speeds.

ACKNOWLEDGEMENTS

This thesis concludes two years' study at King Mongkut's Institute of Technology Ladkrabang (KMITL). Without the generous contributions from many individuals, it would never have been accomplished.

First, I would like to sincerely appreciate to my advisor, Asst. Prof. Dr. Pitak Thumwarin, for his limitless supports and valuable supervision. I would also like to thank him for being approachable, friendly and encouraging.

I would like to express my gratitude to my co-advisor, Dr. Chakree Teekapakvisit, for his valuable recommendations, helpful guidance and kindly advises. With great perception, he defined the early directions of my research and has continuously provided generous support along the way of my graduate study. I am perpetually proud to have been his student.

In particular, I am grateful for the financial support from ASEAN University Network/Southeast Asia Engineering Education Development Network (AUN/SEED-Net). Without their scholarship, I would not have been able to reach this point in my research. Moreover, I also extend my sincere appreciation to KMITL for giving me the admission to conduct my master research during two years in the school of computer engineering.

Throughout my overseas studies, I could not forget the grateful helps from Assoc. Prof. Dr. Pitikhate Sooraksa and Asst. Prof. Kitdakorn Klomkarn who have given me countless advices regarding to academic and personal problems. My sincere gratitude also goes to all professors, lecturers and supporting staffs in faculty engineering, who always continuously encouraged, helped and gave me a guideline during the whole period of my study. To all my friends and colleagues both in Cambodia and Thailand, I wish to express many thanks for the enjoyable and stimulating atmosphere that they helped to provide with their companion and friendship.

Last but not least, I am substantially indebted to my parents and my sister. Their encouragement, inspiration, dedication and persistent supports are enormous sources of energy for me. It is their tolerance and love that carry me through the peaks and troughs of my entire life.

Bangkok, Thailand — Teav Keov Kolyan

August, 2010

Table of Contents

List of Tables

Table Page

List of Figures

Figure Page

List of Abbreviations

APP	A Posteriori Probabilities
AWGN	Additive White Gaussian Noise
BPSK	Binary Phase Shift Keying
BER	Bit-Error Rate
BC	Broadcast Channel
CSI	Channel State Information
CCI	Co-Channel Interference
CDMA	Code Division Multiple Access
DLST	Diagonal Layered Space-Time
DS-CDMA	Direct Sequence CDMA
FFT	Fast Fourier Transform
FDMA	Frequency Division Multiple Access
FDE	Frequency Domain Equalizer
FH-CDMA	Frequency Hopping CDMA
G-RAKE	Generalized RAKE
HLST	Horizontal Layered Space-Time
i.i.d	independent identically distributed
ISI	Inter-Symbol Interference
IFFT	Inverse Fast Fourier Transform
LST	Layered Space-Time
LSTC	Layered Space-Time Coding
LMS	Least Means Square
LOS	Line Of Sight
MF	Matched Filter
MAP	Maximum A Posteriori Probability
ML	Maximum Likelihood
MSE	Mean Square Error
MMSE	Minimum Mean Square Error
MAC	Multiple Access Channel
MAI	Multiple Access Interference

MIMO	Multiple Input Multiple Output
PIC	Parallel Interference Cancellers
PFGLMS	Partially Filtered Gradient LMS
pdf	probability density function
PG	Processing Gain
PN	Pseudo Noise
RLS	Recursive Least Squares
S/P	Serial-to-Parallel
SNR	Signal to Noise Ratio
STBC	Space-Time Block Codes
STC	Space-Time Coding
STTC	Space-Time Trellis Codes
SM	Spatial Multiplexing
SIC	Successive Interference Cancellers
TLST	Threaded Layered Space-Time
TDMA	Time Division Multiple Access
TDE	Time-Domain Equalizer
TH-CDMA	Time Hopping CDMA
VBLAST	Vertical Bell Laboratories Layered Space-Time
VLST	Vertical Layered Space-Time
ZF	Zero-Forcing

Chapter 1

Introduction

This chapter describes the background and motivation of this work by introducing the research field, presenting the principal research problems and explaining the main research objectives. A concise outline for the remainders of the thesis is provided at the end of this chapter.

1.1 Background

Wireless communication systems have become increasingly important not only for professional applications but also for many fields in people's daily routine and in consumer electronics. Moreover, the demand for faster and easier ways to communicate and transfer information worldwide with real time processing is increasing. Therefore, the demands for capacity in wireless communications have been rapidly increasing worldwide. However, the signal transmission quality in wireless communication has deteriorated due to the modernization of the urban cities with skyscrapers and other manmade obstacles. These obstacles and demands are driving communication technology towards a higher data rate, higher mobility, and higher carrier frequencies in order to enable reliable transmission over wireless communication systems.

Recent research in information theory has shown that large gains in capacity of communication over wireless channels are feasible in multiple-input multiple-output (MIMO) systems [1, 2]. An effective and practical way to approach the optimal capacity of MIMO wireless channels is to employ space-time coding (STC) [3]. Through this approach, simultaneous diversity and coding gains can be obtained, as well as high spectral efficiency. STC and related MIMO signal processing soon evolved into a most vibrant research area in wireless communications.

A popular technique to efficiently utilize the available wireless MIMO communication resources is multiple access technique. It has been successfully demonstrated in theory as well as in practice that a code division multiple access (CDMA) system can offer higher bandwidth efficiency than its predecessors, such as the frequency division multiple access (FDMA) and time division multiple access (TDMA) techniques [4]. In order to improve the throughput of the wireless system, the combination of layered space-time coding (LSTC) and CDMA technique, named as LSTC-CDMA, has been intensively studied. However, this implementation generates co-channel interference (CCI) from the adjacent layers and multiple access interference (MAI) from other users. Both interferences will degrade the system performance seriously. Hence, the recent research challenge is shifted towards the interference suppression and cancellation at the receiver end of wireless communication systems.

1.2 Research Motivations

Generally, MIMO channels are only associated with multiple antenna systems [5]. However, the use of multiple antennas, along with multipath and multiple users, to transmit information data simultaneously in the same channel introduces not only inter-symbol interference (ISI), but also CCI and MAI, which limit the performance of the whole system. Therefore, one of the key challenges in designing multiuser communications systems is to mitigate the interferences. Many advanced signal processing techniques proposed to mitigate interference fall largely into multiuser detections.

The simplest detection technique of CDMA systems is a single user matched filter (MF) [6] or the conventional MF detector. In the multiuser systems, the conventional MF of a desired user will suffer from the MAI. The motivated studies of multiuser detection techniques for CDMA systems were started with the work of Verdu [7, 8]. He introduced an optimal approach based on maximum likelihood (ML) algorithm. Although the ML detector can nearly eliminate the degradation in performance due to multiuser interference, it had two main drawbacks: complexity and required side information. Later on, another optimal approach based on maximum a posteriori probability (MAP) algorithm [9] was introduced with similar structure and drawbacks. Due to the high complexity of the optimal detectors, the linear and decision feedback detectors have been discussed. Linear detectors, such as zero-forcing (ZF) detection and minimum mean squared error (MMSE) detection [10], are generally much less complex than the optimal detector, making them practical for most applications. They can suppress the interference by means of linear processing. However, the computational complexity of the system is still increased [11] by using the iterative technique. Hence, some of decision feedback detectors, such as successive interference cancellers (SIC) and parallel interference cancellers (PIC) [11-15], have been developed. The ability of both detectors is to remove the MAI from the received signal with relatively low computational complexity [12]. However, the decision feedback detectors have difficulty when MIMO CDMA system is presented because it fails with the present of CCI.

Therefore, the adaptive detection technique in STC communications systems was proposed in [16]. It was shown that the proposed method can effectively suppress CCI while preserving the space-time structure. As the result, CCI can be reduced but MAI is still a huge problem, degrading the performance and yielding channel estimation inaccurate in a high interference environment. A non-linear adaptive iterative receiver has been studied in [17,18]. It contains a feed-forward filter to detect the desired signals and a feedback filter to cancel the interferences under an iterative format. The system performance can be improved significantly. However, the complexity is increased because of the feedback filter, compared to the linear system which has only the feed forward filter.

Thus, the computational complexity is an important issue that impacts on receiver design. Therefore, such a high computational complexity receivers make its detectors become impractical in a real system. This motivates the author to focus on investigating adaptive multiuser detection algorithms with a good performance and a complexity trade-offs.

1.3 Research Objectives and Contributions

In this study, two new receivers' structures in space-time coding and MIMO direct sequence (DS)-CDMA systems for application in downlink wireless communication are presented. The objective of the proposed receivers is to improve the system performances which include the abilities to mitigate the problems of interferences and multipath fading by improving the system convergence speed and reducing the complexity. Specifically, adaptive detection algorithms play an important role in designing these downlink LSTC-CDMA receivers. Two main contributions of this research work are presented.

Due to the high computational complexity in the non-adaptive MMSE receivers, an adaptive iterative receiver for LSTC-CDMA systems has been presented in this thesis. The proposed receivers are firstly investigated in time domain system. Then, they are also designed in frequency domain based on the frequency domain equalizer (FDE) [9]. This results in a significant reduction in the computational complexity with performance comparable to time-domain equalizer (TDE) [9]. The receiver is based on a joint adaptive iterative detection and decoding algorithm. Least means square (LMS) [19] detection algorithm and MAP decoding algorithm are utilized in the receiver structure in order to reduce the computational complexity and improve the system performance. A partially filtered gradient LMS (PFGLMS) algorithm [20] is also proposed to improve the convergence speed of the LMS based receiver with a slight increase in complexity. In reality, recursive least squares (RLS) algorithm has higher computational requirement than LMS and PFGLMS but has a faster convergence speed [21]. So, the RLS algorithm is also studied based on this trade-offs. The system performances are evaluated by using the results from computer simulation in trading with the complexity computation in both time and frequency domain for various number of antennas. Successfully, the performance results prove that the proposed receiver can effectively mitigate the CCI and MAI by using the interference suppression and cancellation techniques. Moreover, the simulation results show that the proposed receiver based on RLS algorithm yields a faster convergence speed and better tracking ability with a slightly increase in the complexity than that of LMS and PFGLMS algorithm. Finally, it is proved that the system performances of the time and frequency domain approaches are identical.

Generally, it is a difficult task to enlarge the network capacity and improve the quality of service due to the multipath fading of wireless channel. The number of multipath signals is unknown and difficult to predict. However, a RAKE receiver allows each arriving multipath signal to be individually demodulated and then combined to produce a stronger and more accurate signal [22]. The simple RAKE receiver structure is proposed, in which the values produced by RAKE fingers are combined to generate a decision statistics [23]. Optimizing the RAKE receiver for the CDMA downlink was presented in [24]. Furthermore, the generalized RAKE (G-RAKE) receivers for interference suppression and multipath mitigation have been developed in [23-25]. Compared to the conventional RAKE receiver, this generalized RAKE receiver has more fingers and has different combining weights. G-RAKE reception in DS-CDMA systems has been described in detail in [26]. They proved that G-RAKE receiver can theoretically provide significant gains in performance by suppressing interference and combat the effect of multipath channels compared to adaptive CDMA receiver.

As a result, the G-RAKE reception is applied in the LSTC-CDMA receiver structure to improve the system performance in multipath fading channels. Therefore, a Generalized RAKE LSTC-CDMA receiver for interference suppression and multipath mitigation has also been proposed in this thesis. The adaptive detection algorithms are used for both feed-forward filter and feedback filter in the adaptive detection in order to determine the weight coefficient of each finger element. Consequently, the proposed adaptive detector, based on LMS, PFGLMS, and RLS algorithm, are investigated whereby the systems performances are compared to each other in both time and frequency domain system. The performance of the system is evaluated by using the simulation results for various numbers of RAKE fingers. The simulation results show that the system performance improves when the number of fingers is increased beyond the number of resolvable multipath. Furthermore, RLS based receiver achieves the best performance among that of LMS and PFGLMS. Finally, the simulation results also show that the G-RAKE LSTC-CDMA receiver yields a faster convergence speed and have a better tracking ability than that of adaptive iterative LSTC-CDMA receiver.

1.4 Thesis Outline

The thesis has six chapters. Chapter 3, 4, and 5 contain the main contributions. As a guide to read this thesis, its structures are organized and briefly summarized as follows.

Chapter 1 introduces a short review of the wireless communications revolutions and the existing problems in this rapidly-evolving field, as well as the motivation and contributions of this research work.

Chapter 2 describes some fundamentals of wireless MIMO systems that related to this thesis. It focus mainly on MIMO system model, multiple access techniques, fading channels, architectures of space-time coding and more importantly some useful multiuser detection techniques.

Chapter 3 presents the adaptive iterative LSTC-CDMA receiver in both time domain and frequency domain in MIMO Rayleigh fading channels. The LMS, PFGLMS and RLS algorithms are used in the feed forward and feedback filter of the adaptive detector in order to cancels CCI and mitigates MAI. The computational complexity of each adaptive algorithm is calculated in both time and frequency domain.

Chapter 4 provides the proposed Generalized RAKE LSTC-CDMA receiver based on LMS, RLS, and PFGLMS detection algorithms in time and frequency domain system. The system models of the proposed transmitter and receiver are presented based on a joint structure between the G-RAKE receiver and LSTC-CDMA receiver.

Chapter 5 gives the performances results of the adaptive iterative LSTC-CDMA receiver and G-RAKE LSTC-CDMA receiver. Both proposed receivers are investigated based on adaptive detection algorithms such as LMS, PFGLMS and RLS in time and frequency domain system. In addition, the performances of the proposed schemes are also compared with each other through simulation results.

Chapter 6 concludes the thesis by summarizing main results and discussing potential future research works.

Chapter 2

Wireless MIMO Systems

A brief introduction to wireless multiple input multiple output (MIMO) channel characteristics is presented in this chapter. Two main techniques for realizing a MIMO system, namely space-time coding and spatial multiplexing, are explained. Then, the detail description of fading channels model, multiuser interferences, and multiple access techniques are presented. Finally, the literature reviews of various multiuser detection techniques are briefly described at the end of this chapter.

2.1 Introduction

For several last decades, wireless system designers are facing a number of challenges. Novel communication and information services are being introduced almost daily. These include the increasing demand for higher data rates, better quality of service and higher network capacity. In recent years, MIMO systems have emerged as a most promising technology in these measures. MIMO communication systems can be defined intuitively [27, 28] by considering that multiple antennas are used at the transmitting end as well as at the receiving end. In principle, using multi-element antenna arrays at both ends of the link can dramatically enhance the system capacity [29] by increasing the data rate and add diversity to improve the quality of the communication. The key principle that will enable ultimate capacity utilization in wireless MIMO system is the use of space-time coding and spatial multiplexing. However, the implementation of these two techniques yields various forms of interferences at the receiver end of a wireless system. Hence, various designs of transceivers with the combination of MIMO systems, various multiple access techniques, and appropriate types of multiuser detection algorithms have been developed in order to overcome the effects of these interfering scenarios and to improve the system capacity.

2.2 MIMO Multiuser Systems

2.2.1 MIMO System Model

Multiple-input multiple-output communication techniques have been an important area for the next-generation wireless systems because of their potential for high capacity, increased diversity and interference suppression [30]. A MIMO channel with N transmit antennas and M receive antennas is depicted in Figure 2.1. The information bits are first sent into the system by the source. Then, it is transformed into the transmitted signal by a transmitter. Next, the signal passes through the wireless channel. Finally, the desired signals are detected by multiple receive antennas.

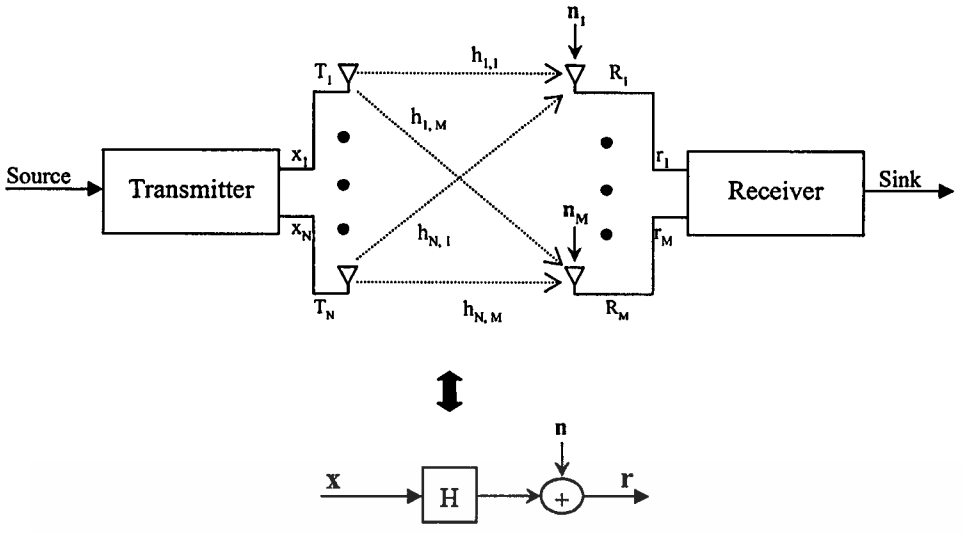

Figure 2.1 MIMO wireless link.

The transmitted signals in each symbol period are represented by an $(N \times 1)$ column matrix $\mathbf{X}$ which is denoted as:

$$\mathbf{X} = [\mathbf{X}_1, \ldots, \mathbf{X}_N]^T \tag{2.1}$$

where $\mathbf{X}_i$ refers to the transmitted signal from antenna i-th and $i = [1,..,N]$.

A wireless channel is typically represented as a matrix $\mathbf{H}$ of dimension $(N \times M)$, where each of the coefficients $h_{j,i}$ represents a sample of complex random variable that describes the channel between the j-th receive antenna and the i-th transmit antenna, as shown below:

$$\mathbf{H} = \begin{bmatrix} h_{1,1} & h_{1,2} & \cdots & h_{1,N} \\ h_{2,1} & h_{2,2} & \cdots & h_{2,N} \\ \cdots & \cdots & \cdots & \cdots \\ h_{M,1} & h_{M,2} & \cdots & h_{M,N} \end{bmatrix} \tag{2.2}$$

The total received signal at the receive antennas j-th is expressed as:

$$r_j = \sum_{i=1}^{N} h_{ji} x_i + n_j \tag{2.3}$$

where n_j is a zero mean independent identically distributed (i.i.d) additive white Gaussian noise (AWGN) complex sample at the receive antenna j-th. So, the total received signal vector, denoted by an $(M \times 1)$ column matrix $\mathbf{r}$, can be represented as:

$$\mathbf{r} = \mathbf{H}\mathbf{x} + \mathbf{n} \tag{2.4}$$

where $\mathbf{r} = [r_1, \ldots, r_M]^T$ and $\mathbf{n} = [n_1, \ldots, n_M]^T$.

2.2.2 Spatial Multiplexing

The basic principle of spatial multiplexing (SM) is to transmit essentially independent data from each antenna. Then at the receiver, the multi-antenna signal is separated with appropriate detection techniques. In SM systems which is shown in Figure 2.2, the input data stream is de-multiplexed into N separate streams, using a serial-to-parallel (S/P) converter, and each stream is transmitted from an independent antenna. The received signal is then passed through the detector, which is similar to a multiuser detector and treats separate streams as separate users of a multiuser channel.

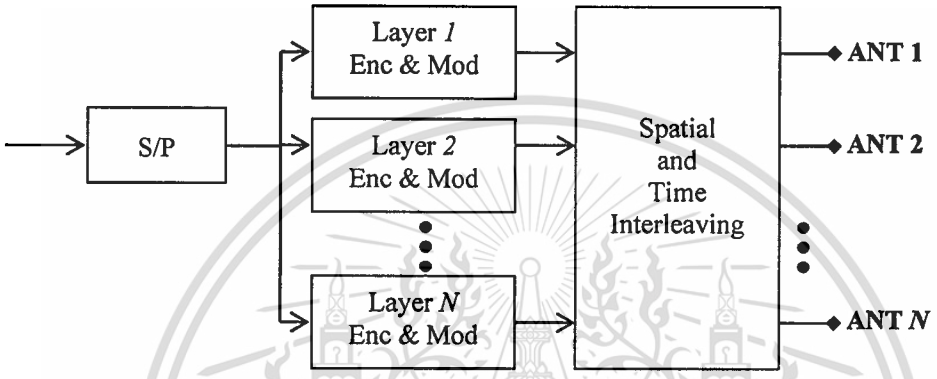

Figure 2.2 Spatial Multiplexing system model.

The SM technique is utilized when that the channels between any transmit and any receive antennas are uncorrelated from one another. Then, different information data can be allocated to different transmit antennas and transmitted simultaneously through the MIMO channel to the receive antennas. The received signal at the receive antenna is the superposition of the signals coming from all the transmit antennas and additive noise. Because the signal corresponding to every transmit antenna has a particular spatial signature at a receive antenna, it will be able to detect the individual signals transmitted by each of antennas and separate them at the receiver. This operation obviously increases the spectral efficiency of the system by a factor equal to the number of transmit antennas. Thus, the throughput of an SM scheme is N symbols per channel for a MIMO channel with N transmit antennas. However, the N-fold increase in throughput will generally come at the cost of a low diversity gain compared to space-time coding. On the other hand, as shown by B. Vucetic and J. Yuan [31] and H. Jafarhani [32], space-time codes provide a diversity gain equal to the product of the number of transmit and receive antennas NM.

2.2.3 Space-Time Coding

An effective and practical way to approaching the capacity of MIMO wireless channels is to employ space-time (ST) coding [33]. Space-time codes (STC) were first introduced by Tarokh et al. [33, 34] in 1998 as a novel means of providing transmit diversity for multiple antennas in fading channels. The space-time coding scheme is essentially defined as a joint design of coding, modulation, transmit and receive diversity, which is designed for use with multiple transmits antennas. Moreover, space-time coding can achieve transmit diversity and power gain over spatially uncoded systems without sacrificing the bandwidth.

Two main approaches in STC structures, namely space-time block codes (STBC) [35] and space-time trellis codes (STTC) [33] were firstly studied. The space-time block codes can achieve the full transmit diversity specified by the number of the transmit antennas. However, no coding gain can be provided by space-time block codes, while non-full rate space-time block codes can introduce bandwidth expansion. On the other hand, space-time trellis codes provide both diversity and coding gain. In principle, space-time trellis codes have a major drawback. The maximum likelihood decoder complexity grows exponentially with the number of bits per symbol, thus limiting achievable data rates. Later, Foschini [36] proposed other STC approaches, namely layered space-time (LST) architecture. It can attain a tight lower bound on the MIMO channel capacity and overcome the weakness of STTC scheme. Therefore, LST architecture is utilized in this thesis and its main features will be presented briefly in section 2.6.

However, a central issue in these coding schemes is the exploitation of multipath effects of fading channel in order to achieve high spectral efficiencies and performance gains.

2.3 Fading Channels Model

In wireless communications, fading is a deviation of the attenuation that a carrier-modulated telecommunication signal experiences over a certain propagation media. Fading varies with time, geographical position and/or radio frequency. In wireless systems, fading is either due to multipath propagation or Doppler shift. Fading causes a poor performance in a communication system because of its result in a loss of signal power without reducing the power of the noise. This signal loss can be over some or all of the signal bandwidth. Communication systems are often designed to adapt to such impairments. Common diversity schemes that are used to overcome the fading signal include: the techniques that are used in MIMO system which are already mentioned in section 2.2 and multiple access techniques which are going to be explained in section 2.5.

2.3.1 Multipath Propagation

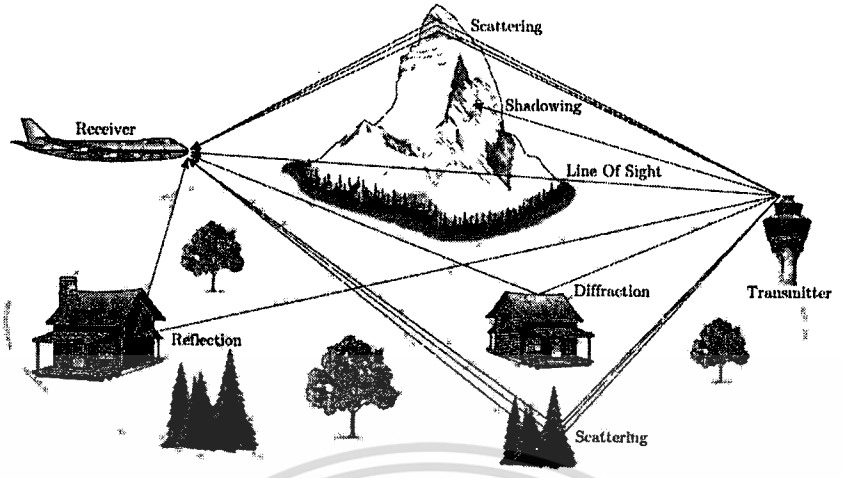

Figure 2.3 Multipath propagation systems.

In wireless communications, the presence of reflectors in the environment surrounding a transmitter and receiver creates multiple paths. Multipath propagation occurs when the electromagnetic field carrying the information signal propagates along more than one "path" connecting the transmitter to the receiver as shown in Figure 2.3 [37]. As a consequence, the receiver will receive the reflected, diffracted and scattered signals from all directions. The direct path between the transmitter and the receiver is called the line of sight (LOS). The corresponding signal received through the LOS is usually the strongest and the dominant signal. Reflection occurs when a propagating electromagnetic wave encounters a surface that is large relative to the wavelength of the propagating wave [37]. This reflected wave may interfere constructively or destructively at the receiver due to the change in phase shift after reflection. Sources for reflections include the surface of the earth, buildings and walls. Diffraction can occur at the edge of an impenetrable body or at a surface with sharp irregularities that is large compared to the wavelength of the radio wave [38]. The waves resulting from such edges or surfaces are partially reflected and retransmitted with a bend of waves around the obstacle. This allows the signal to be transmitted even when there is no LOS path between the transmitter and the receiver. Scattering occurs when the radio path between the transmitter and receiver consists of large amount of objects with dimensions that are small compared to the wavelength of the signal [37]. The scattered waves can be produced by rough surfaces or by other irregularities in the channel such as foliage and traffic signs. Finally, the shadowing is due to the absorption of the radiated signal by scattering structures.

2.3.2 Doppler Shift

Due to the relative motion between the transmitter and the receiver, each multipath wave is subject to a shift in frequency. The frequency shift of the received signal caused by the relative motion is called the Doppler shift [39]. It is proportional to the speed of the mobile unit. Consider a situation when only a single tone of frequency fc is transmitted and a received signal consists of only one wave coming at an incident angle θ with respect to the direction of the vehicle motion. The Doppler shift of the received signal, denoted by *fd*, is given by

$$f_d = \frac{vf_c}{c}\cos\theta \tag{2.5}$$

where v is the vehicle speed and c is the speed of light. The Doppler shift in a multipath propagation environment spreads the bandwidth of the multipath waves within the range of $f_c \pm fd_{\max}$, where $fd_{\max}$ is the maximum Doppler shift, given by

$$f_{d_{\max}} = \frac{vf_c}{c} \tag{2.6}$$

2.3.3 Statistical Model for Fading Channels

The nature of the multipath channel is the amplitude of the delta functions are random. This randomness originates from the multipath and the random location of objects in the environment. Therefore, statistical models are needed to investigate the behavior of the amplitude and power of the received signal. Depending on the nature of the propagation environment, there are different models describing the statistical behavior of the multipath fading envelope. In this section, the Rayleigh and Rician fading models, used to describe signal variations in a multipath environment, are introduced.

2.3.3.1 Rayleigh Fading

Rayleigh fading is the most applicable model that is applied where there is no LOS between the transmitter and receiver and many buildings and other objects attenuate, reflect, refract and diffract the signal [40]. When the number of reflected waves is large, according to the central limit theorem, two quadrature components of the received signal are uncorrelated Gaussian random processes with a zero mean and variance σ_s^2. As a result, the envelope of the received signal at any time instant undergoes a Rayleigh probability distribution and its phase obeys a uniform distribution between $-\pi$ and π. The probability density function (pdf) of the Rayleigh distribution r is given by [41]:

$$p(a) = \begin{cases} \frac{a}{\sigma_s^2} \cdot e^{-a^2/2\sigma_s^2} & a \geq 0 \\ 0 & a < 0 \end{cases} \tag{2.7}$$

The mean value, denoted by m_a, and the variance, denoted by σ_a^2, of the Rayleigh distributed random variable are given by

$$m_a = \sqrt{\frac{\pi}{2}} \cdot \sigma_s = 1.2533\sigma_s$$
$$\sigma_a^2 = (2 - \frac{\pi}{2})\sigma_s^2 = 0.4292\sigma_s^2 \tag{2.8}$$

If the probability density function in (2.7) is normalized so that the average signal power $(E[a^2])$ is unity, then the normalized Rayleigh distribution becomes

$$p(a) = \begin{cases} 2ae^{-a^2} & a \geq 0 \\ 0 & a < 0 \end{cases} \tag{2.9}$$

The mean value and the variance are

$$m_a = 0.8862$$
$$\sigma_a^2 = 0.2146 \tag{2.10}$$

The pdf for a normalized Rayleigh distribution is shown in Figure 2.4.

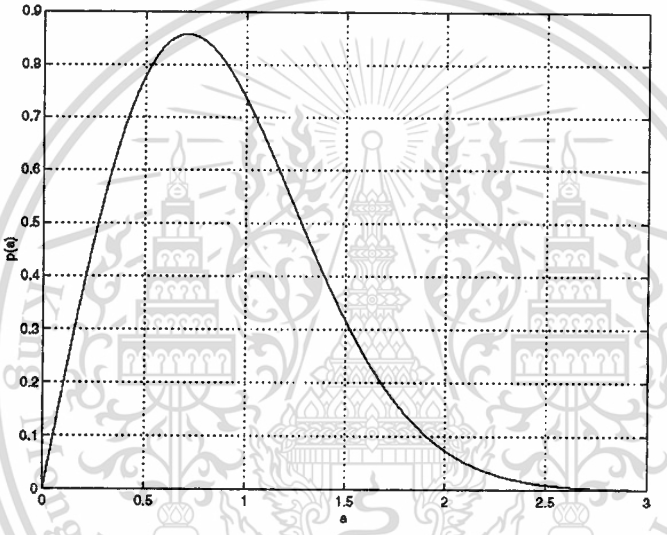

Figure 2.4 The pdf of Rayleigh distribution.

2.3.3.2 Rician Fading

Rician fading is a stochastic model for radio propagation anomaly caused by partial cancelation of a radio signal. Generally, the sum of a constant amplitude direct signal and a Rayleigh distributed scattered signal results in a signal with a Rician envelope distribution. Hence, the pdf of the Rician distribution is given by

$$p(a) = \begin{cases} \frac{a}{\sigma_s^2} \cdot e^{\frac{-(a^2+D^2)}{2\sigma_s^2}} I_0\left(\frac{aD}{\sigma_s^2}\right) & a \geq 0 \\ 0 & a < 0 \end{cases} \tag{2.11}$$

where D^2 is the direct signal power and $I_0(.)$ is the modified Bessel function of the first kind and zero-order. Assuming that the total average signal power is normalized to unity, the pdf in (2.11) becomes

$$p(a)=\begin{cases}2a(1+K)e^{-K-(1+K)a^2}I_0\sqrt{K(K+1)} & a\geq 0\\ 0 & a<0\end{cases} \tag{2.12}$$

where K is the Rician factor, denoting the power ratio of the direct and the scattered signal components.

The Rician factor is given by

$$K=\frac{D^2}{2\sigma_s^2} \tag{2.13}$$

The mean and the variance of the Rician distributed random variable are given by

$$\begin{aligned} m_a &= \frac{1}{2}\sqrt{\frac{\pi}{1+K}}e^{-\frac{K}{2}\left[(1+K)I_0\left(\frac{K}{2}\right)+KI_1\left(\frac{K}{2}\right)\right]} \\ \sigma_a^2 &= 1-m_a^2 \end{aligned} \tag{2.14}$$

where $I_1(.)$ is the first order modified Bessel function of the first kind. Small values of K indicate a severely faded channel. For K = 0, there is no direct signal component and the Rician pdf becomes a Rayleigh pdf. Large values of K indicate a slightly faded channel. For K approaching infinity, there is no fading. The Rician distributions with various K are shown in Figure 2.5.

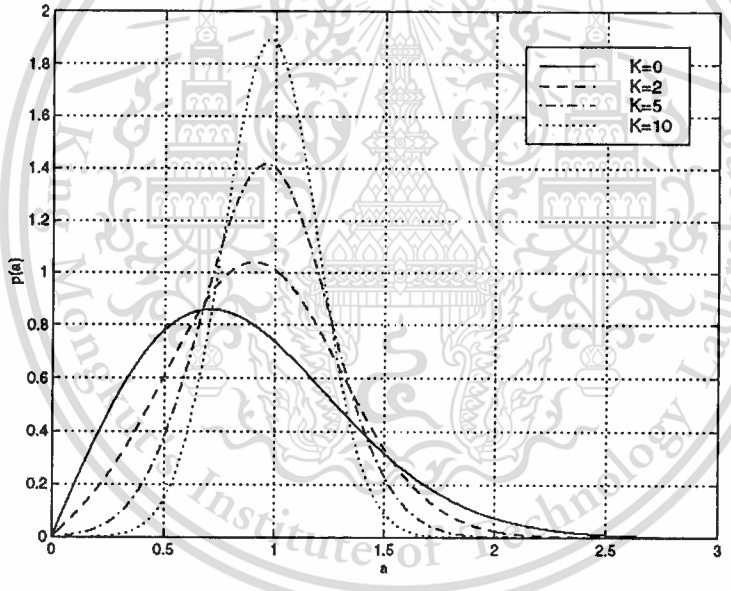

Figure 2.5 The pdf of Rician distributions with various K.

2.4 Interferences in Multiuser Systems

Interference is a fundamental nature of wireless communication systems, in which multiple transmissions often take place simultaneously over a common communication medium. In recent years, there has been a rapidly growing interest in developing reliable and spectral efficient wireless communication systems. One primary challenge in such a development is how to deal with the interference, which may substantially limit the reliability and the throughput of a wireless communication system.

2.4. 1 Intersymbol Interference

Intersymbol interference (ISI) is a form of distortion of a signal in which one symbol interferes with subsequent symbols [42]. The presence of ISI in the system introduces errors in the decision device at the receiver output. Generally, ISI is caused by multipath propagation in which a wireless signal from a transmitter reaches the receiver via many different paths. Since all of these paths are different lengths and some of these effects will slow the signal down. As the result, there are different versions of the signal arriving at different times. This delay means that part or all of a given symbol will be spread into the subsequent symbols, thereby interfering with the correct detection of those symbols.

2.4.2 Co-channel Interference

Generally, wireless systems that employ frequency reuse are affected by co-channel interference (CCI). CCI occurs when two or more independent signals are transmitted simultaneously by the same frequency band. In CDMA system, frequency reuse implies that in a given coverage area, there are several cells that use the same set of frequencies. These cells are called co-channel cells, and the interference between signals from these cells is called co-channel interference. Unlike thermal noise which can be overcome by increasing the signal-to noise ratio (SNR), co-channel interference cannot be combated by simply increasing the carrier power of a transmitter. This is because an increase in carrier transmit power increases the interference to neighboring co-channel cells.

2.4.3 Multiple Access Interference

Multiple Access Interference (MAI) is a type of interference caused by multiple users who are using the same frequency allocation at the same time. This multiple-access interference can present a significant problem if the power level of the desired signal is significantly lower (due to distance) than the power level of the interfering user. The occurrence of MAI remains a limiting factor in CDMA detection, degrading the bit-error rate (BER) performance over wireless channels. However, Interference cancellation and suppression techniques are the effective way to alleviate the adverse impact of multiple-access interference [43-45].

2.5 Multiuser Systems and Multiple Access Techniques

2.5.1 Multiuser Systems

Generally, there are various types of multiple user communication systems, where multiple users can access the channel and transmit information through the channel to the receiver. The multiple user communication scenario is depicted in Figure 2.6.

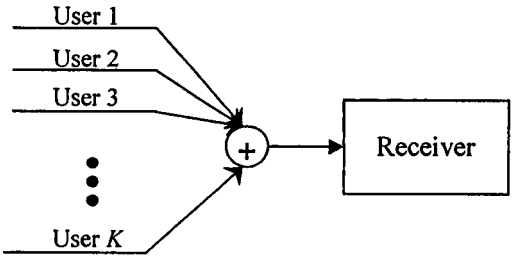

Figure 2.6 Multiple users communication systems.

Two main types of multiuser communication systems are multiple access channel (MAC) and broadcast channel (BC). MAC scenario is often referred to as uplink transmission. A number of users share a common channel to transmit information to a receiver. On the other hand, BC scenario is also known as a downlink transmission. A single transmitter transmits information to a number of receivers.

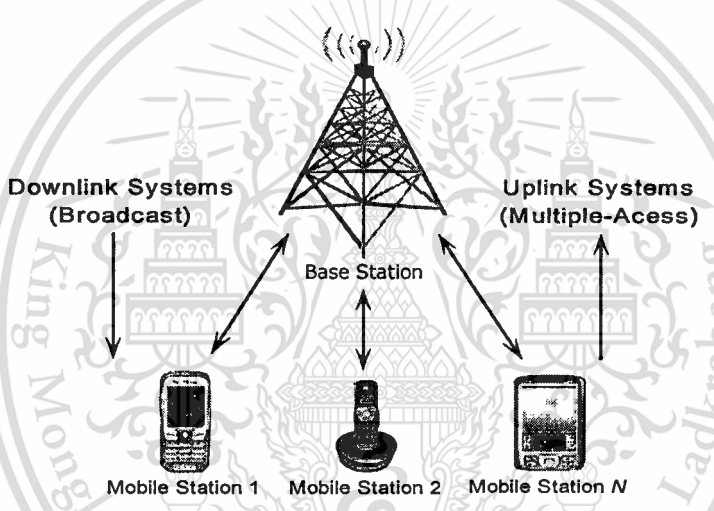

Figure 2.7 Mobile cellular communication systems.

As an example, Figure 2.7 presents two types of multiuser system in a mobile cellular communication, in which there is a single base station and multiple mobile devices. When the base station is transmitting messages to the mobiles, the channel is referred to as a downlink or broadcast channel. Conversely, when the mobiles are transmitting messages to the base station, the channel is referred to as an uplink or multiple access channel.

There are several techniques to accommodate multiple users in a system, whether it is MAC or BC scenarios. The most well-known methods, which have been implemented in current wireless communication systems, are multiple access techniques.

2.5.2 Multiple Access Techniques

The support of parallel transmissions on the uplink and downlink is called multiple access technique. The necessary insulation of this technique is achieved by assigning to each transmission different components of the domains (frequency, time, code) that contain the signals. If the different transmissions are differentiated only for the frequency band, Frequency Division Multiple Access (FDMA) is used. If transmissions are distinguished on the basis of time, the Time Division Multiple Access (TDMA) is applied. Code Division Multiple Access (CDMA) is utilized if a different code is adopted to separate simultaneous transmissions. However, resources can be also differentiated by more than one of the above aspects.

2.5.2.1 FDMA System

In FDMA system, the frequency band available to the system is divided into different portions. Each of them is used for a given channel as shown in Figure 2.8. Then, the different channels are distributed among cells according to a reuse pattern. One disadvantage of FDMA is the lack of flexibility for the support of variable bit-rate transmissions, an essential prerequisite for future mobile multimedia communication systems. With the evolution towards digital communications, TDMA and CDMA access schemes can be implemented.

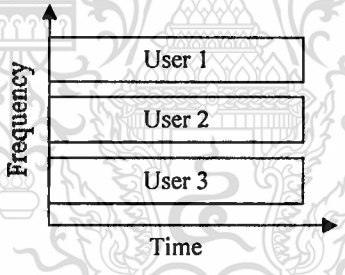

Figure 2.8 FDMA system.

2.5.2.2 TDMA System

In TDMA scheme, each user has assigned the total bandwidth of a carrier for transmission, but only for a short time interval (slot) that is periodically repeated according to a time-organization called frame. Figure 2.9 depicts the TDMA system. Transmission is organized into frames, each of them containing a given number of slot intervals, to transmit *packets* of bits. The main disadvantage of TDMA is that the high peak transmits power that is required to send packets in the assigned slots. Moreover, a fine synchronization must be achieved at the beginning of each transmission for the alignment with the time-frame structure.

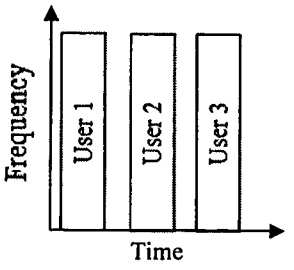

Figure 2.9 TDMA system.

2.5.2.3 CDMA System

Code division multiple access (CDMA) permits to achieve a greater robustness and a higher capacity than other multiple access schemes. CDMA is a multiple access technique where different users share the same physical medium, that is, the same frequency band, at the same time [46]. This opens a third dimension, as can be seen in Figure 2.10.

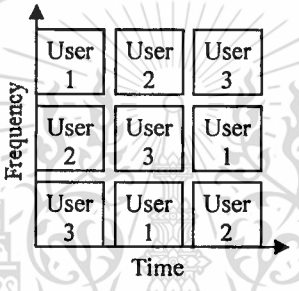

Figure 2.10 CDMA system.

In a CDMA [4] system, each user is assigned a distinct code sequence (signature sequence). Each transmitter sends its data stream by modulating it with their own signature sequence that allows the user to spread the information signal across the available assigned frequency band. Since the signature sequences have fairly low mutual crosscorrelation, a CDMA receiver can detect its own data using the corresponding signature sequence, although the multiple users' signals overlap both in frequency and in time in a random manner. It is clear that the design of the spreading codes strongly influence the performance of CDMA systems. Therefore, the signature sequence should be carefully designed to achieve low crosscorrelation between users [4].

There are three primarily different types of CDMA technologies that have been extensively investigated in the past two decades: direct sequence (DS) CDMA, frequency hopping (FH) CDMA and time hopping (TH) CDMA. However, DS-CDMA is the simplest and most popular CDMA scheme. Each user in a DS-CDMA system uses a particular code to spread its information bit stream directly. The DS-CDMA system is presented in Figure 2.11 where the user signal is spread by a user specific signature sequence, pseudo noise (PN) code, with bits (named chips) whose length is basically processing gain (PG) times smaller than that of the original bits.

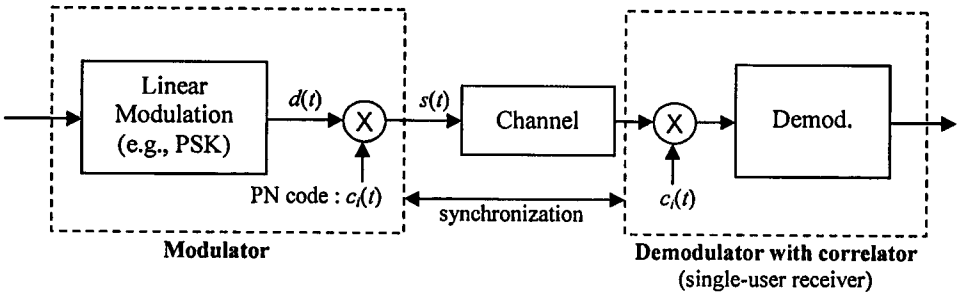

Figure 2.11 Spreading and de-spreading processes for the i-th DS-CDMA user.

2.6 Layered Space-Time Architectures

Layered space-time (LST) architecture was firstly proposed by Foschini [36]. It can attain a tight lower bound on the MIMO channel capacity. The distinguishing feature of this architecture is that it allows processing of multidimensional signals in the space domain by 1-D processing steps, where 1-D refers to one dimension in space. The method relies on powerful signal processing techniques at the receiver and conventional 1-D channel codes. In the originally proposed architecture, n_T information streams are transmitted simultaneously, in the same frequency band, using n_T transmit antennas. The receiver uses $n_R = n_T$ antennas to separate and detect the n_T transmitted signals. The separation process involves a combination of interference suppression and interference cancellation. The separated signals are then decoded by using conventional decoding algorithms developed for (1-D)-component codes, leading to much lower complexity compared to maximum likelihood decoding in space time trellis code. Hence, the complexity of the LST receivers grows linearly with the data rate.

2.6.1 Transmitter Structures

There is a number of various LST architectures, depending on whether error control coding is used or not and on the way that the modulated symbols are assigned to transmit antennas. An uncoded LST structure, known as vertical layered space-time (VLST) or vertical Bell Laboratories layered space-time (VBLAST) scheme [47], is illustrated in Figure 2.12. The input information sequence, denoted by c, is first demultiplexed into n_T sub-streams, called layer. The demultiplexing process can be carried out by using a serial to parallel (S/P). Each of sub-stream is subsequently modulated by an M-level modulation scheme and transmitted from a transmit antenna. This simple transmission process can be combined with conventional block or convolutional one-dimensional codes, to improve the performance of the system. However, the cost of bandwidth efficiency occurs by using this structure [48].

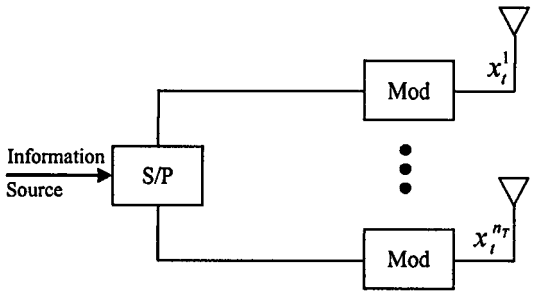

Figure 2.12 A VLST architecture.

Various LST architectures with error control coding were developed, as shown in Figure 2.13(a–c).

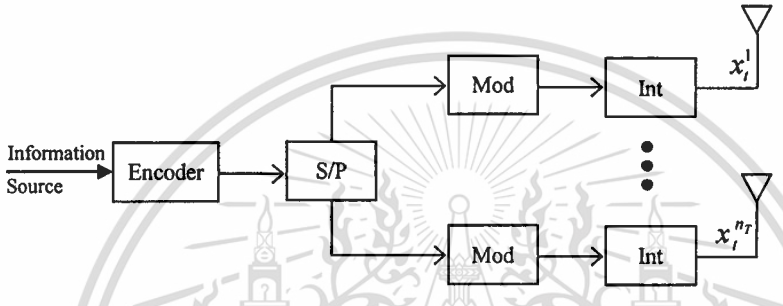

a) An HLST architecture with a single code.

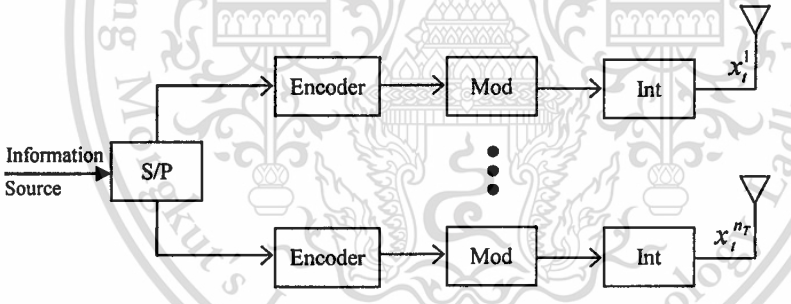

b) An HLST architecture with separate codes in each layer.

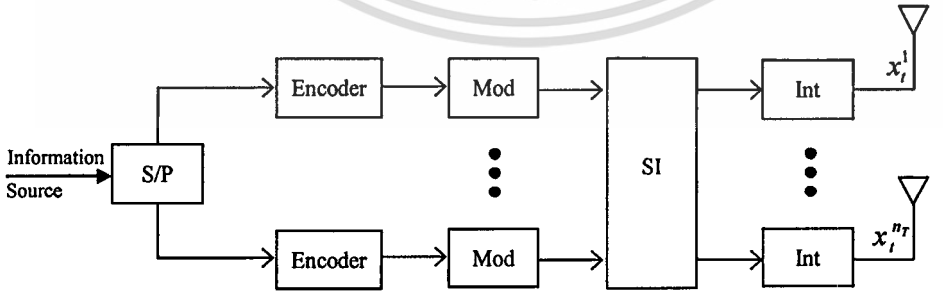

c) DLST and TLST architectures.

Figure 2.13 LST transmitter architectures with error control coding.

In the horizontal layered space-time (HLST) architecture, shown in Figure 2.13(a), the information sequence is first encoded by a channel code and subsequently demultiplexed into n_T sub-streams. Each sub-stream is modulated, interleaved and assigned to a transmit antenna. If the modulator output symbols are denoted by *x(i, t)*, where *i* represents the layer number and *t* is the time interval, the transmission matrix, formed from the modulator outputs, denoted by **X**, is given by

$$\mathbf{X} = \left[x_t^i \right] \tag{2.15}$$

For example, in a system with three transmit antennas, the transmission matrix **X** is given by

$$\mathbf{X} = \begin{bmatrix} x_1^1 & x_2^1 & x_3^1 & x_4^1 & \dots \\ x_1^2 & x_2^2 & x_3^2 & x_4^2 & \dots \\ x_1^3 & x_2^3 & x_3^3 & x_4^3 & \dots \end{bmatrix} \tag{2.16}$$

The sequence $x_1^1, x_2^1, x_3^1, x_4^1, \dots$ is transmitted from antenna 1, the sequence $x_1^2, x_2^2, x_3^2, x_4^2, \dots$ is transmitted from antenna 2 and the sequence $x_1^3, x_2^3, x_3^3, x_4^3, \dots$ is transmitted from antenna 3.

An HLST architecture can also be implemented by splitting the information sequence into n_T sub-streams, as shown in Figure 2.13(b). Each sub-stream is encoded independently by a channel encoder, interleaved, modulated and then transmitted by a particular transmit antenna. It is assumed that channel encoders for various layers are identical. However, utilizing only a 1-D encoder after S/P conversion with time interleaver and simultaneously transmitting the signal by transmit antennas, the HLST scheme will suffer from the presence of sub-channels in deep fade.

A better performance is achieved by a diagonal layered space-time (DLST) architecture [49], in which a modulated codeword of each encoder is distributed among the n_T antennas along the diagonal of the transmission array. For example, the DLST transmission matrix, for a system with three antennas, is formed from matrix **X** in (2.15), by delaying the *i*-th row entries by (*i* - 1) time units, so that the first nonzero entries lie on a diagonal in **X**. The entries below the diagonal are padded by zeros. Then the first diagonal is transmitted from the first antenna, the second diagonal from the second antenna, the third diagonal from the third antenna and then the fourth diagonal from the first antenna etc. Hence the codeword symbols of each encoder are transmitted over different antennas. This can be represented by introducing a spatial interleaver (*SI*) after the modulators, as shown in Figure 2.13(c). The spatial interleaving operation for the DLST scheme can be represented as

$$\begin{bmatrix} x_1^1 & x_2^1 & x_3^1 & x_4^1 & x_5^1 & x_6^1 & \dots \\ 0 & x_1^2 & x_2^2 & x_3^2 & x_4^2 & x_5^2 & \dots \\ 0 & 0 & x_1^3 & x_2^3 & x_3^3 & x_4^3 & \dots \end{bmatrix} \rightarrow \begin{bmatrix} x_1^1 & x_1^2 & x_1^3 & x_4^1 & x_4^2 & x_4^3 & \dots \\ 0 & x_2^1 & x_2^2 & x_2^3 & x_5^1 & x_5^2 & \dots \\ 0 & 0 & x_3^1 & x_3^2 & x_3^3 & x_6^1 & \dots \end{bmatrix} \tag{2.17}$$

The rows of the matrix on the right-hand side of (2.17) are obtained by concatenating the corresponding diagonals of the matrix on the left-hand side. The first row of this matrix is transmitted from the first antenna, the second row from the second antenna and the third row from the third antenna. The diagonal layering introduces space diversity and thus achieves a better performance than the horizontal one. It is important to note that there is a spectral efficiency loss in DLST, since a portion of the transmission matrix on the left-hand side of (2.17) is padded with zeros.

A threaded layered space-time (TLST) structure [50] is obtained from the HLST by introducing a spatial interleaver prior to the time interleavers, in Figure 2.13(c). The transmitter structure differs from DLST in that the transmitted symbols are not periodically cycled among the N antennas and they are first fed into a spatial interleaver, followed by the time interleaver and then transmitted by all the transmit antennas. In a system with $nT = 3$, the operation of spatial interleaver can be expressed as

$$\begin{bmatrix} x_1^1 & x_2^1 & x_3^1 & x_4^1 & \dots \\ x_1^2 & x_2^2 & x_3^2 & x_4^2 & \dots \\ x_1^3 & x_2^3 & x_3^3 & x_4^3 & \dots \end{bmatrix} \rightarrow \begin{bmatrix} x_1^1 & x_2^3 & x_3^2 & x_4^1 & \dots \\ x_1^2 & x_2^1 & x_3^3 & x_4^2 & \dots \\ x_1^3 & x_2^2 & x_3^1 & x_4^3 & \dots \end{bmatrix} \tag{2.18}$$

in which an element of the modulation matrix, shown on the left-hand side of (2.18) denoted by x_t^i, represents the modulated symbol of layer i at time t. The matrix on the right-hand side of (2.18), denoted by $\mathbf{X}'$, is the TLST transmission matrix. That is, the modulated symbols x_1^1, x_2^3, x_3^2, x_4^1, ..., generated by modulators in layers 1, 3, 2 and 4, respectively, are transmitted from antenna 1.

It is shown that the structures of DLST and TLST are very similar. The difference is the spatial interleaving process. The spectral efficiency of both schemes is $RmnT$, where R is the code rate and m is the number of bits in a modulated symbol, while the spectral efficiency of the DLST is slightly reduced due to zero padding in the transmission matrix.

2.6.2 Receiver Structures

For coded LST schemes, the optimum receiver performs a joint detection and decoding algorithm. For many systems, the exponential increase in implementation complexity may make the optimal receiver impractical even for a small number of transmit antennas. There is a number of less complex receiver structures which have good performance and complexity trade-offs which are described in the following sub-sections.

2.6.2.1 Iterative LST Receiver

The iterative receiver is one of the effective receivers, which can efficiently suppress and remove the interference by using suppression and cancellation techniques. Block diagrams of the iterative receivers for LST (a)–(c) architectures are shown in Figure 2.14.

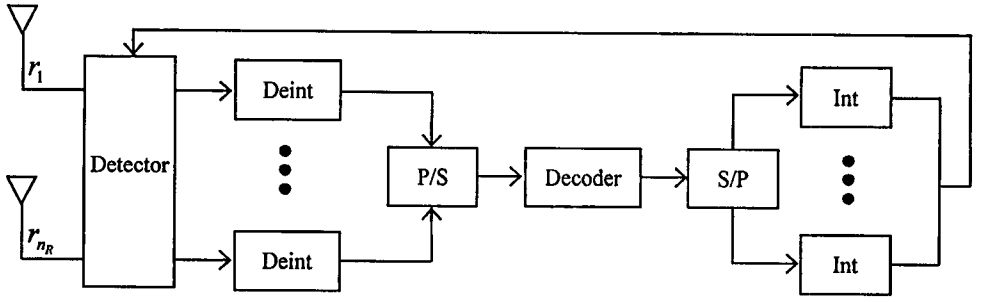

a) HLST with a single code decoder.

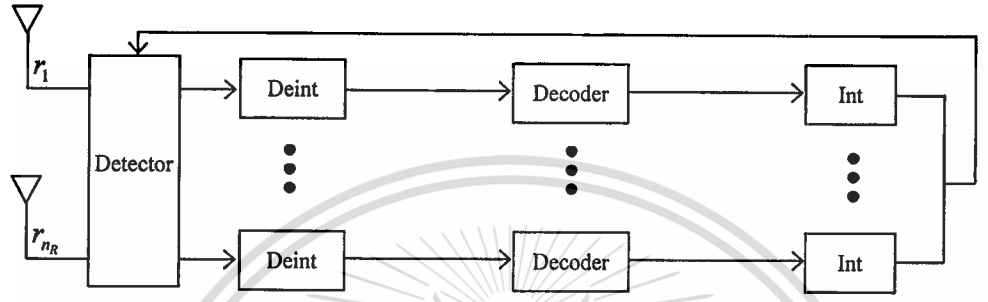

b) HLST with separate decoders.

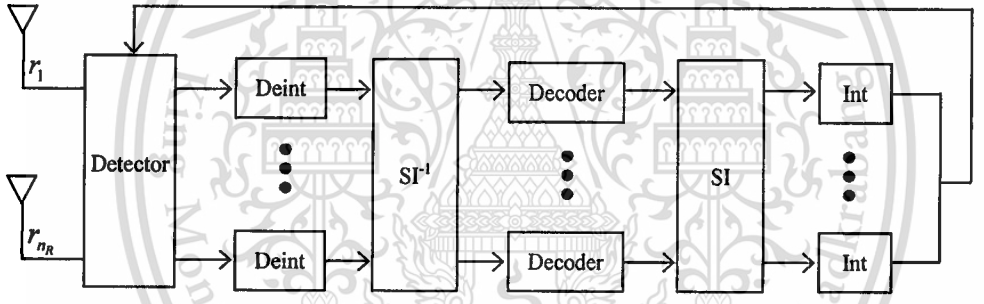

c) DLST and TLST receivers.

Figure 2.14 Block diagrams of iterative LSTC receivers.

In all three receivers, the detector provides joint soft-decision estimates of the n_T transmitted symbol sequences. In LST (a) the detected sequence is decoded by a single decoder with soft inputs/soft outputs, while in LST (b) each of the detected sequences is decoded by a separate channel decoder with soft inputs/soft outputs. At each iteration, the decoder soft outputs are used to update the a priori probabilities of the transmitted signals. These updated probabilities are then used to calculate the symbol estimate in the detector. Each of the coded streams is independently interleaved to enable the receiver convergence. In LST (c), apart from time interleaving/deinterleaving, there is space interleaving/deinterleaving across transmit antennas.

2.6.2.2 Iterative MMSE Receiver

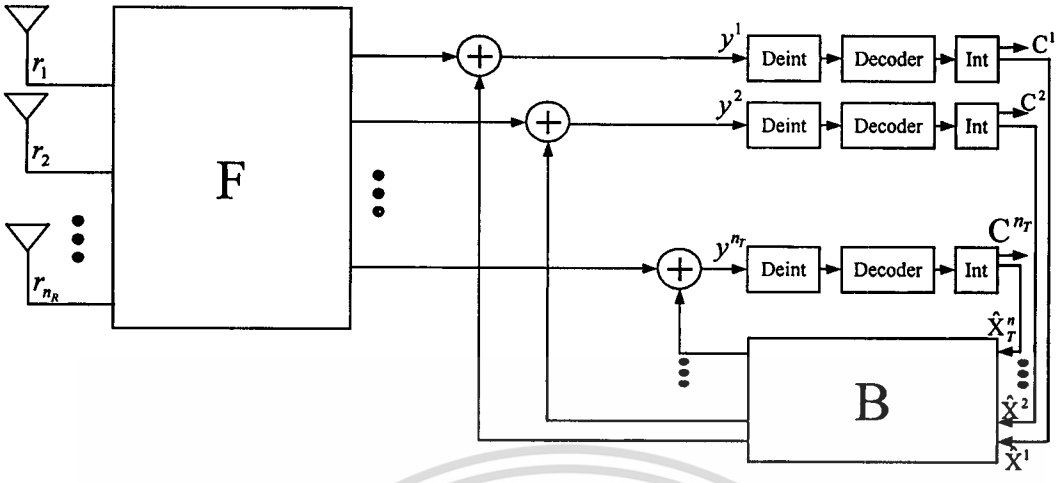

Figure 2.15 Block diagram of an iterative MMSE receiver.

An iterative receiver with a multiuser detector consists of a feed-forward module which performs interference suppression and a feedback module which performs parallel interference cancellation was proposed in [36]. This receiver structure is called an iterative MMSE receiver. A block diagram of the iterative MMSE receiver is shown in Figure 2.15. The iterative MMSE receiver which employs hard decision decoders is equivalent to the receiver which performs linear MMSE suppression in the first iteration and parallel interference cancellation in the following iterations. This filter would be optimal in the MMSE sense if perfect symbol estimates were fed back.

2.6.2.3 Rake Receiver

The RAKE receiver, as shown in Figure 2.16, was first introduced by Price and Green [51]. For frequency selective fading, the signal bandwidth is much greater than the coherence bandwidth of the channel, therefore multipath components are resolvable and independent of each other. RAKE receivers take advantage of the energy present in multipath components by correlating with each path. The RAKE receiver is composed of several fingers which each resemble a single correlator. Each of these fingers has a different time delay and phase rotation that is matched to a multipath component. The crosscorrelation between a spread spectrum signal and a time-delayed version should be low, therefore the RAKE receiver will be able to develop an estimate based on only the multipath component. The resolution of the RAKE is dependent on the chip rate of the system. The multipath components must be separated by at least one chip period for the RAKE to resolve them.

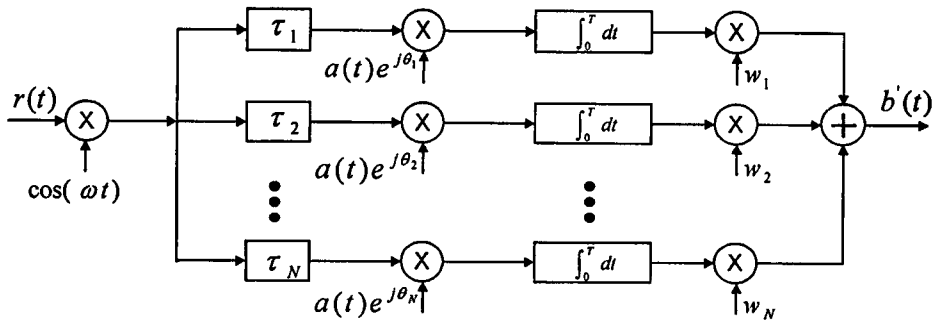

Figure 2.16 RAKE receiver with N fingers.

2.6.3 Channel Coding Principles

During the last few decades, there has been an increasing demand for efficient and reliable digital data transmission and storage systems. To reliably reproduce the data, a major concern of the system design is the control of errors. With his 1948 paper, "A Mathematical Theory of Communication", Shannon [52] demonstrated that, by properly encoding of the information, errors induced by a noisy channel or storage medium can be reduced to any desired level without sacrificing the rate of information transmission or storages, as long as the information rate is less than the capacity of the channel. The fundamental philosophical contribution inspired the research in the error control coding areas.

2.6.3.1 Interleaving

Interleaving plays an important role in many digital communication systems for manifold reasons. In the context of wireless communications, fading channels often lead to bursty errors. Then, several successive symbols may be corrupted by deep fades. This has a crucial impact on the decoding performance, for example, the performance of convolutional codes because of its sensitivity to bursty. In order to overcome this difficulty, interleaving is applied. At the transmitter, an interleaver simply permutes the data stream in a specified manner, so that the symbols are transmitted in a different order. Consequently, a de-interleaver has to be employed at the receiver in order to reorder the symbols back into the original succession.

2.6.3.2 Convolutional Codes

Convolutional codes are used extensively in numerous applications in order to achieve reliable data transfer, including digital video, radio, mobile communication and satellite communication. A convolutional code is described by three integers, which are the number of input symbols, k, the total number of output symbols, n, and memory order, m [31]. The n-tuple emitted by the convolutional encoding procedure is not only a function of an input k-tuple, but is also a function of the previous mk-

input tuples. Figure 2.17 shows a simple convolutional code encoder, which is a linear feed forward shift register. The connection between the shift register elements and the modulo 2 adders can be conveniently described by the following two generator sequences:

$$g^{(1)} = (g_0^{(1)}\, g_1^{(1)}\, g_2^{(1)}) = (101)$$
$$g^{(2)} = (g_0^{(2)}\, g_1^{(2)}\, g_2^{(2)}) = (111) \tag{2.19}$$

If $u = (\ldots, u_{-1}, u_0, u_1, \ldots, u_l, \ldots)$ is the input data stream, then the two output sequences, denoted by $v^{(1)} = (\ldots, v_{-1}^{(1)}, v_0^{(1)}, v_1^{(1)}, \ldots, v_l^{(1)}, \ldots)$ and $v^{(2)} = (\ldots, v_{-1}^{(2)}, v_0^{(2)}, v_1^{(2)}, \ldots, v_l^{(2)}, \ldots)$ can be obtained as

$$v^{(i)} = u * g^{(i)}, \quad i = 1, 2 \tag{2.20}$$

where * denotes the convolutional operator.

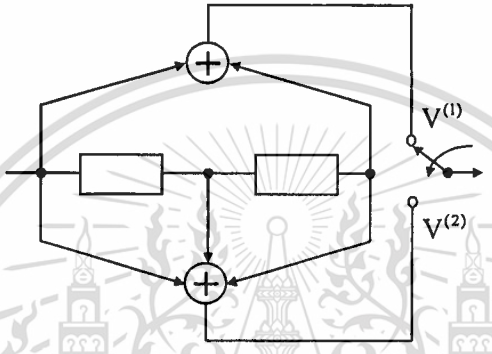

Figure 2.17 A (2,1,2) convolutional encoder.

A convenient and common way of describing encoding and decoding operations is using trellis diagrams. A trellis stage for an input at time t for binary (2,1,2) code is shown in Figure. 2.18. A trellis diagram consists of N stages, where N is the number of input words, each consisting of k input data bits. The stage of the encoder is defined as the content of its shift register. For the encoder with total memory K, the stage number is $2K$. Each new block of k inputs causes the transition to a new stage. That is, there are $2K$ branches leaving each stage. Each branch is labeled the k input causing the transition at time unit t, denoted by $u_t = [u_{t,1}, u_{t,2}, \ldots, u_{t,k}]$ and n corresponding to outputs, denoted by $v_t = [v_{t,0}, v_{t,1}, \ldots, v_{t,n-1}]$.

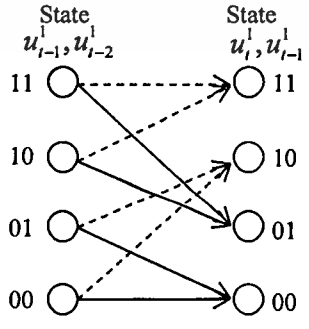

Figure 2.18 One stage in the trellis diagram for binary (2,1,2) convolutional code.

The performance of a convolutional code depends on the decoding algorithm and distance property. If a hard-decision decoding algorithm is used, the code performance is measured by Hamming distance. The minimum free distance of a convolutional code is defined as the minimum Hamming distance between any two code sequences, which is the minimum weight of all non-zero code sequences of any length. If a soft-decision decoding algorithm is used, the code performance is measured by Euclidean distance. The minimum free Euclidean distance is defined as the minimum Euclidean distance between any two code sequences. However, the using of decision decoding algorithms is depends on both the convolutional code trellis and modulation type [53].

2.6.3.3 MAP Decoding Algorithms

The decoder can apply a number of the soft output decoding algorithms. As the overall receiver complexity is mainly dominated by the decoder complexity, the choice of the decoding algorithm depends on the available processing power at the receiver. The maximum a posteriori (MAP) approach [54] is optimum in the sense that it minimizes the bit error probability at the decoder output and is usually implemented by using a forward and backward recursion algorithms. The MAP decoding algorithm operates on a trellis representation of the convolutional code as shown in Figure 2.18.

The conditional error probability of the decoder is defined as:

$$P(E \mid \mathbf{r}) = P(\hat{\mathbf{u}} \neq \mathbf{u}) = P(\hat{\mathbf{v}} \neq \mathbf{v}) \tag{2.21}$$

where – P(E) is the probability of error in the decoder

- **r** is the received where the term P(r) is independent of the decoding algorithms.

P(E) is given by:

$$P(E) = \sum_{\mathbf{r}} P(E \mid \mathbf{r}) P(\mathbf{r}) \tag{2.22}$$

So, the minimum probability of error in equation 2.22 is achieved by minimizing $P(\hat{\mathbf{v}} = \mathbf{v} \mid \mathbf{r})$ for all **r** which is represented by:

$$P(\hat{\mathbf{v}} = \mathbf{v} \mid \mathbf{r}) = \frac{P(\mathbf{r} \mid \mathbf{v}) P(\mathbf{v})}{P(\mathbf{r})} \tag{2.23}$$

If the coded sequences are all likely equal, the probability of optimal decoding for a discrete memories channel is denoted as:

$$P(\mathbf{r} \mid \mathbf{v}) = \prod_{i} P(\mathbf{r}_i \mid \mathbf{v}_i) \tag{2.24}$$

The 2.24 is rewrite in monotone increasing function as:

$$\log P(\mathbf{r} \mid \mathbf{v}) = \sum_{i} \log P(\mathbf{r}_i \mid \mathbf{v}_i) \tag{2.25}$$

where log P(r|v) is known as log-likelihood function.

The soft-output MAP decoder calculates the a posteriori log-likelihood ratio for data bit u_t as:

$$\Lambda(u_t) = \log \frac{p\{u_t = 1 | \mathbf{r}\}}{p\{u_t = 0 | \mathbf{r}\}} \tag{2.26}$$

where $P\{u_t=i|\mathbf{r}\}$ is the a posteriori probability (APP) of the data bit u_t.

Then, the decoder makes the hard decision by:

$$\Lambda(u_t) = \begin{cases} 1, & \text{if } \Lambda(u_t) > 0 \\ 0, & \text{otherwise} \end{cases} \tag{2.27}$$

The APPs in Equation (2.26) can be computed from the trellis diagram as:

$$p\{u_t = 0 | \mathbf{r}\} = \sum_{(m',m)\in B_t^0} P\{S_{t-1} = m', S_t = m | \mathbf{r}\} \tag{2.28}$$

$$p\{u_t = 1 | \mathbf{r}\} = \sum_{(m',m)\in B_t^1} P\{S_{t-1} = m', S_t = m | \mathbf{r}\} \tag{2.29}$$

where S_{t-1} and S_t are the encoder stages at time (t-1) and t, respectively, and B_t^0 and B_t^1 are set of transitions from state m' to stage m caused by u_t=0 and u_t=1, respectively. (2.28) and (2.29) can be written as

$$p\{u_t = 0 | \mathbf{r}\} = \sum_{(m',m)\in B_t^0} \frac{P\{S_{t-1} = m', S_t = m | \mathbf{r}\}}{P(\mathbf{r})} \tag{2.30}$$

$$p\{u_t = 1 | \mathbf{r}\} = \sum_{(m',m)\in B_t^1} \frac{P\{S_{t-1} = m', S_t = m | \mathbf{r}\}}{P(\mathbf{r})} \tag{2.31}$$

where P(r) is a constant.

In order to efficiently calculate the information bits APPs, the following probability functions are defined [31]

$$\alpha_t(m) = P\{S_t = m, \mathbf{r}_1^t\} \tag{2.32}$$

$$\beta_t(m) = P\{\mathbf{r}_{t-1}^N | S_t = m\} \tag{2.33}$$

$$\gamma_t^i(m',m) = P\{u_t = i, S_t = m, \mathbf{r}_t | S_{t-1} = m'\} \tag{2.34}$$

where $$\mathbf{r}_t = (r_{t,0}, \ldots, r_{t,i}, \ldots, r_{t,n-1}) \tag{2.35}$$

and $$\mathbf{r}_t^k = (\mathbf{r}_t, \ldots, \mathbf{r}_{t+1}, \ldots, \mathbf{r}_k) \tag{2.36}$$

The joint transition probability, $P\{S_{t-1} = m', S_1 = m, \mathbf{r}\}$, can be expressed as

$$P\{S_{t-1} = m', S_1 = m, \mathbf{r}\} = \alpha_{t-1}(m) \sum_{i\in 0,1} \gamma_t^i(m',m) \beta_t(m) \tag{2.37}$$

where $\alpha_t(m)$ and $\beta_t(m)$ are obtained recursively as

$$\alpha_t(m) = \sum_{m'} \alpha_{t-1}(m) \sum_{i\in 0,1} \gamma_t^i(m',m) \tag{2.38}$$

$$\beta_t(m) = \sum_{m'} \beta_{t+1}(m) \sum_{i\in 0,1} \gamma_t^i(m',m) \tag{2.39}$$

and $\gamma_t^i(m',m)$ is a channel transition probability weighted by the information bit a priori probability $p_t(u_t = i), i = 0,1$ where u_t is the information symbol associated with transition $S_{t-1} = m' \rightarrow S_1 = m$. Coefficient $\gamma_t^i(m',m)$ can be written as

$$\gamma_t^i(m',m) = p_t(u_t = i)\prod_{j=0}^{j=n-1} P\{r_{t,j} \mid x_{t,j}\} \tag{2.40}$$

$$P\{r_{t,j} \mid x_{t,j}\} = \frac{1}{\sqrt{2\pi\sigma}} e^{\frac{(r_{t,j}-x_{t,j})^2}{2\sigma^2}} \tag{2.41}$$

where $x_{t,j}$, $j = 0,...,n-1$, is a binary phase shift keying (BPSK) modulated symbol in the codeword associated with transition $S_{t-1} = m' \rightarrow S_1 = m$.

If we assume that the encoder starts and ends in a zero stage, the boundary conditions are

$$\alpha_0(0) = 1, \ \alpha_0(m) = 0, \ \text{for } m \neq 0 \tag{2.42}$$

$$\beta_N(0) = 1, \ \beta_N(m) = 0, \ \text{for } m \neq 0 \tag{2.43}$$

The log-likelihood ration now can be written as

$$\Lambda(u_t) = \log \frac{\sum_{(m',m)\in B^1} \alpha_{t-1}(m')\gamma_t^1(m',m)\beta_t(m)}{\sum_{(m',m)\in B^0} \alpha_{t-1}(m')\gamma_t^0(m',m)\beta_t(m)} \tag{2.44}$$

The above algorithm is usually referred to as a forward/backward algorithm, since the coefficients $\alpha_t(m)$ are calculated recursively starting from the beginning of the trellis, and the $\beta_t(m)$ coefficients are calculated recursively starting from the end of the trellis.

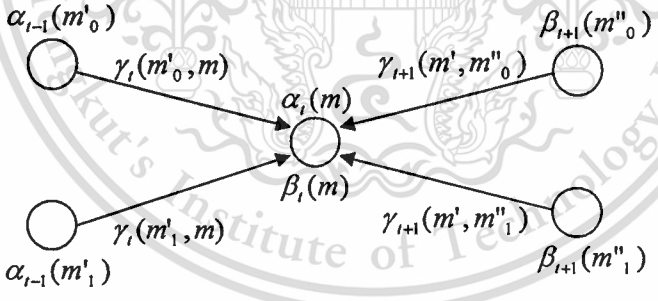

Figure 2.19 Graphical representation of the forward and backwards recursions.

Figure 2.19 shows the graphical representation of the forward and backward recursion. In this figure, $\alpha_{t-1}(m'_t)$ represents α coefficients for state m'_t in the (t-1)th stage which is connected with stage m in t-th trellis stage and where the transition $s_{t-1} = m' \rightarrow S_1 = m$ is caused by the information bit $u_t = i, i = 0,1$. Similarly, the $\beta_{t+1}(m'')$ denotes β coefficient for stage m'' in the (t-1)th trellis stage which is connected with stage m in t-th trellis stage and where the transition $s_{t-1} = m' \rightarrow S_1 = m$ is

caused by the information bit $u_t = i, i = 0,1$ .The a posteriori probabilities of the information bits can be calculates as

$$P\{u_t = 1 \mid \mathbf{r}\} = \frac{e^{\Lambda(u_t)}}{1 + e^{\Lambda(u_t)}} \tag{2.45}$$

$$P\{u_t = 0 \mid \mathbf{r}\} = \frac{1}{1 + e^{\Lambda(u_t)}} \tag{2.46}$$

The a posteriori probabilities of the transmitted bits can be calculated by adding the probabilities of the codeword that contain a particular transmitted, are denoted as

$$P\{x_{t,j} = 1 \mid \mathbf{r}\} = \sum_{u_t = i, x_{t,j} = 1} P\{u_t = i \mid \mathbf{r}\} \tag{2.47}$$

$$P\{x_{t,j} = -1 \mid \mathbf{r}\} = \sum_{u_t = i, x_{t,j} = -1} P\{u_t = i \mid \mathbf{r}\} \tag{2.48}$$

2.7 Multiuser Detection Techniques

Over the past twenty years, a number of sophisticated receiver designs, for example, multiuser detection, have been proposed for interference suppression under various settings. Generally, multiuser detection techniques are applied to joint detection of different signals transmitted over MIMO channel. Multiuser detection [8, 55-57] was first proposed for CDMA systems rather than TDMA systems. The simples approach to demodulate CDMA signals is the single-user matched filter (MF), which was adopted in CDMA receiver. However, conventional single-user receivers are designed to operate in the fading channel without CCI and MAI. Hence, they do not work well in a multiuser system. The studies of multiuser detection techniques for CDMA system was started with the work of verdu [7]. For the AWGN channel, Verdu presented an optimum multiuser receiver based on maximum likelihood (ML) or maximum a posteriori probability (MAP) algorithm. This optimum technique however requires a prior knowledge of the signal amplitudes and phases and involves a high degree of computational complexity. Therefore, some suboptimum multiuser detection, named as linear detection which included zero-forcing (ZF) and minimum mean square error (MMSE) detection have been investigated. They can suppress the interference by means of linear processing in much lower complexity. Other sub-optimal schemes were proposed in hopes of reducing complexity while maintaining good performance, are referred as decision-feedback detection such as successive interference cancellation (SIC) and parallel interference cancellation (PIC). However, in designing a multiuser detector for MIMO channels, the knowledge of MAI characteristics such as the spreading sequences, the availability of the CSI at the receiver, must be jointly take into account in order to mitigate ISI, CCI, and MAI. Another successful technique, named adaptive detector, was introduced, based on an adaptive signal processing scheme

such as recursive solutions. The advantages of using adaptive signal processing techniques are its capacity to track the channel variation without prior knowledge of CSI and its simplicity and robustness to the signal.

2.7.1 Synchronous CDMA Systems

In a *K*-user synchronous CDMA system, the received signal consists of the sum of all users' spread signals embedded in additive white Gaussian noise (AWGN) as shown in Figure 2.20.

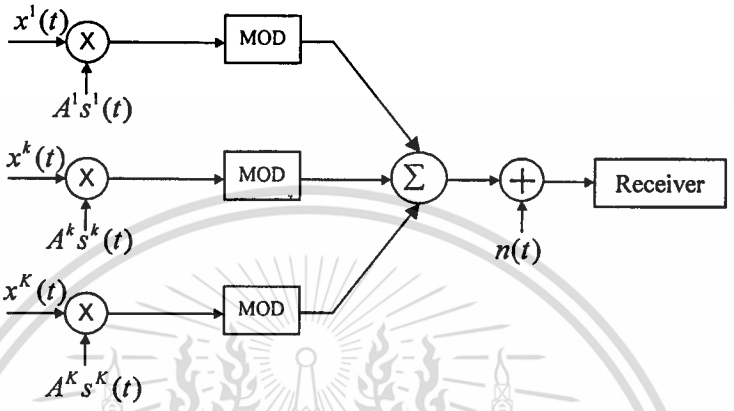

Figure 2.20 DS-CDMA model.

The received signal is represented as:

$$r(t)=\sum_{k=1}^{K}s^k(t)A^kx^k+\sigma n(t)\ ,\qquad t=[0,T] \tag{2.49}$$

where T is the data symbol period. $s^k(t)$ is the signature waveform assigned to the k-th user as:

$$s^k(t)=\sum_{n=1}^{N}s^k(n)q(t-(n-1)T_c) \tag{2.50}$$

where: $s^k(n)$ denotes the n-th chip value of s^k

$q(t)$ is the chip waveform

T_c is the chip interval.

Then, $s^k(t)$ is normalized to have unit energy as given by:

$$\left\|s^k\right\|^2=\int_0^T s^{k^2}(t)dt=1 \tag{2.51}$$

The signature waveforms are assumed to be zero outside the interval [0,T], and hence there is no inter-symbol interference (ISI). A^k is the received amplitude of the k-th user's signal. A^{k^2} is referred to as the energy of the k-th user. $x^k\in[-1,+1]$ is the symbol transmitted by the k-th user and $n(t)$ is additive white Gaussian noise with zero mean and variance σ^2.

Equation (2.49) can be written in a discrete-time form as the following:

$$\mathbf{r} = \mathbf{SAx} + \sigma\mathbf{n} \tag{2.52}$$

where

$$\mathbf{r} = [r(1), r(2), ..., r(N)]^T \tag{2.53}$$

and

$$S = \begin{bmatrix} s^1(1) & s^2(1) & \dots & s^K(1) \\ s^1(2) & s^2(2) & \dots & s^K(2) \\ \vdots & \vdots & \ddots & \vdots \\ s^1(N) & s^2(N) & \dots & s^K(N) \end{bmatrix} \tag{2.54}$$

$$\mathbf{A} = diag[A^1, A^2, ..., A^K] \tag{2.55}$$

$$\mathbf{b} = [b^1, b^2, ..., b^K]^T \tag{2.56}$$

$$\mathbf{n} = [n(1), n(2), ..., n(N)]^T \tag{2.57}$$

where N is number of data frame length.

2.7.2 Matched Filter Detection

The matched filter detector, also known as conventional detector, simply correlates the received signal with the desired user's time reversed spreading waveform, and samples the output at the bit rate. This is the demodulator that was first adopted in CDMA receiver which comes straight from single user designs. Hence, MF is the optimal receiver for single-user CDMA. However, in the multiuser CDMA channel, it does not take into account any other users in the system or channel dynamics. Therefore, this detector is suffer from MAI, and is not robust to asynchronism, fading channels, or *PN* sequences with substantial cross correlation.

The structure of CDMA MF is illustrated in Figure 2.21.

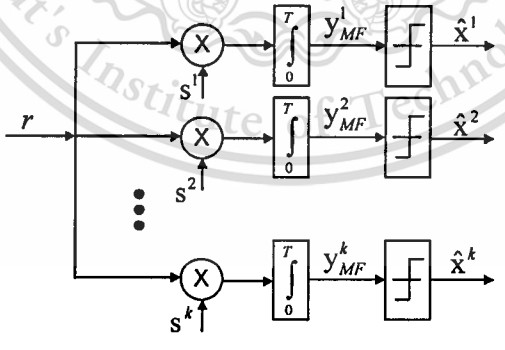

Figure 2.21 Matched filter for CDMA systems.

The filter for a given user is matched to its signature waveform as the follows:

$$y_{MF}^k = \int_0^T s^k(t) r(t) dt = A^k b^k + \sum_{j \neq k} A^k \rho^{j,k} x^j + n^{\prime k} \tag{2.58}$$

where r(t) and $s^k(t)$ are defined in Equation (2.49) and (2.50), respectively.

and

$$n'^k = \int_0^T s^k(t) n(t) dt \tag{2.59}$$

$\rho^{j,k}$ is the crosscorrelation between the j-th and k-th user, given by

$$\rho^{j,k} = \int_0^T s^j(t) s^k(t) dt \tag{2.60}$$

Equation (2.58) can also be expressed in discrete-time form:

$$\mathbf{y}_{MF} = \mathbf{S}^T\mathbf{r} = \mathbf{S}^T\mathbf{S}\mathbf{A}\mathbf{x} + \mathbf{n}' = \mathbf{R}\mathbf{A}\mathbf{x} + \mathbf{n}' \tag{2.61}$$

where

$$\mathbf{y}_{MF} = [y^1_{MF}, y^2_{MF}, \ldots, y^K_{MF}]^T \tag{2.62}$$

$$\mathbf{n}' = [n'^1, n'^2, \ldots, n'^K]^T \tag{2.63}$$

and

$$\mathbf{R} = \mathbf{S}^T\mathbf{S} = \rho^{i,j}, \qquad i, j = 1, 2, \ldots, K \tag{2.64}$$

where: R is a correlation matrix with the autocorrelation factors $\rho^{i,j} = 1$, and crosscorrelation factors $\rho^{i,j} = \rho^{j,i}$.

2.7.3 Optimal Detections

Since the conventional MF is sub-optimal in the multiuser CDMA environment, two optimum multiuser detectors have been proposed. [7,8,58] showed that the maximum likelihood (ML) and Maximum a Posteriori (MAP) detection can achieve the optimum performance in multiuser channels. Although both detectors can nearly eliminate the degradation in performance due to multiuser interferences, they have two main drawbacks: complexity and required side information, which becomes impractical for a CDMA system with much more than ten users per sector.

2.7.3.1 Maximum Likelihood Detection

The introduction of the ML detector for CDMA in [7] essentially launched the field of multiuser detection. The main reason for this is that it was shown that the performance of the ML detector is insensitive to power variations among the users, unlike the matched filter detector.

Referring to (2.4), the ML detectors choose the vector of estimated symbols as:

$$\hat{\mathbf{x}} = \arg\max_b \Pr(\mathbf{r} \text{ received} \mid \mathbf{x} \text{ transmitted}) \tag{2.65}$$

If the addictive noise **n** is Gaussian, then the Equation (2.69) is equivalent to selecting:

$$\hat{\mathbf{x}} = \arg\min_b \|\mathbf{r} - \mathbf{H}\mathbf{x}\| \tag{2.66}$$

where the norm is the regular Euclidean norm and the elements of x are constrained to be constellation points.

2.7.3.2 Maximum A Posteriori Probability Detection

The Maximum a Posteriori (MAP) detector selects:

$$\hat{\mathbf{x}} = \arg\max_{\mathbf{b}} \Pr(\mathbf{x} \text{ transmitted} \mid \mathbf{r} \text{ received}) \tag{2.67}$$

which minimizes the probability of error. This is the same as the ML estimate if the symbols are likely equal. However, when combined with error control coding and iterative soft decoding, the decoder can pass reliability information to the multiuser detector in the form of the a priori distribution or likelihood ratio for each transmitted symbol. Hence, in that scenario the MAP estimate generally differs from the ML estimate. Furthermore, the MAP detector itself computes soft estimates of each symbol, although the final (hard) estimates are obtained from the soft estimates by thresholding. If the receiver detects a subset of the vector **x**, then the MAP estimate maximizes the corresponding marginal distribution. In general, this differs from the estimate in (2.65) and requires less computation.

The MAP detector suffers from the same drawbacks as the ML detector, namely, the complexity grows exponentially with the size of **x**, and it requires knowledge of **H**. However, in some applications where the system size is relatively small, the complexity may be manageable.

2.7.4 Linear Detections

Linear detectors are generally much less complex than the optimal detector, making them practical for most applications. A common property of all linear techniques is that they do not exploit the knowledge of the finite signal alphabet but assume continuously distributed transmit signals. Hence, there is only a polynomial complexity with respect to the number of active users instead of an exponential relationship. The two popular linear detection methods that are used in the design of a MIMO receiver are zero-forcing (ZF) [59] and minimum mean-squared error (MMSE) detection [60].

2.7.4.1 Zero-Forcing Detection

A zero-forcing detection technique uses an inverse filter to compensate for the channel response function. In other words, at the output of the equalizer, it has an overall response function equal to one for the symbol that is being detected and an overall zero response for other symbols. Zero forcing is a linear equalization method that does not consider the effects of noise. However, the noise may be enhanced in the process of eliminating the interference.

The zero-forcing detector multiplies the output of the conventional MF with the inverse of the correlation matrix. The output of the ZF receiver, defined by $\mathbf{y}_{ZF}$, is obtained as:

$$\mathbf{y}_{ZF} = \mathbf{R}^{-1}\mathbf{S}^{T}\mathbf{r} = \mathbf{A}\mathbf{x} + \mathbf{R}^{-1}\mathbf{S}^{T}\mathbf{n} \tag{2.68}$$

where **r** is defined by Equation (2.4) and n is (M x 1) vector of the AWGN noise with zero mean and noise variance of σ^2.

The $\mathbf{y}_{ZF}$ fully decouples the multiuser signal. However, it suffers from the noise enhancement [8] as it is shown in the second term of Equation (2.68). Although, the MAI is perfectly removed, this process increases the noise level. In extreme cases, the additional noise may be higher than the MAI. Therefore, the zero-forcing detector performance deteriorates more than the MF.

2.7.4.1 MMSE Detection

The ZF equalization does not consider the effects of the equalization in enhancing the noise. To address this problem, a mean-square error criterion is minimized. The structure of the MMSE detector [60] can be depicted in Figure 2.22.

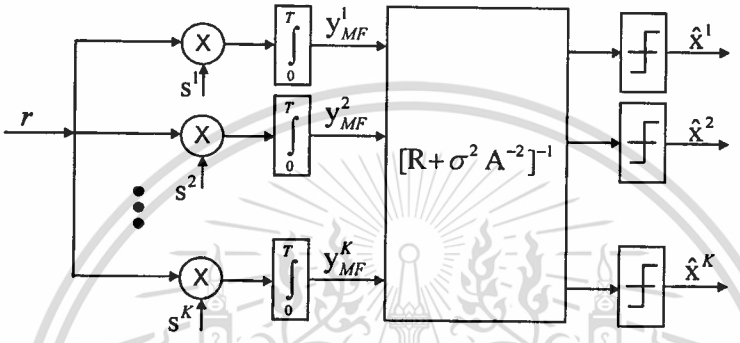

Figure 2.22 MMSE detector for CDMA systems.

The output of the linear MMSE filter [61] for user k-th is:

$$\mathbf{y}^k_{MMSE} = \mathbf{M}^T \mathbf{y}_{MF} \tag{2.69}$$

Where $\mathbf{M}$ is a matrix of MMSE filter coefficients, and $\mathbf{y}_{MF}$ is the matched filter output vector. The problem of MMSE detection is choosing the (K x K) matrix $\mathbf{M}$ to achieve the minimum square-error:

$$\zeta = \min E\left\{\left\|\mathbf{Ax} - \mathbf{M}^T \mathbf{y}_{MF}\right\|^2\right\} \tag{2.70}$$

[8] has proved that the solution is:

$$\mathbf{M} = [\mathbf{R} + \sigma^2 \mathbf{A}^{-2}]^{-1} \tag{2.71}$$

where $\sigma^2 \mathbf{A}^{-2} = diag\{\sigma^2 \mathbf{A}_1^{-2}, \sigma^2 \mathbf{A}_2^{-2}, ..., \sigma^2 \mathbf{A}_K^{-2}\}$ and it is assumed that the receiver has the exact knowledge of σ^2. So, the MMSE detection can be rewritten as:

$$\mathbf{y}_{MMSE} = [\mathbf{R} + \sigma^2 \mathbf{A}^{-2}]^{-1} \mathbf{S}^T \mathbf{r} \tag{2.72}$$

Because the MMSE detector takes the background noise into account, it generally provides better performance than the zero-forcing detector. The consideration of noise also avoids the noise enhancement problem of the decorrelator. However, both detectors require the inversion of the correlation matrix. Hence, with an increasing number of users or large data frame size, the calculation of the inverse may become numerically expensive. In short-code scrambling systems, the inversion can be

implemented with low complexity. On the other hand, the complexity of the inversion can hardly be reduced to a realistic level in long-code systems.

2.7.5 Interference Cancellation Detections

Besides the linear detection schemes, researchers have also proposed non-linear detectors that use the interferers' data to detect that of the desired user. Interference cancellation (IC) [62] detectors employ temporary data estimates to reconstruct the interference, and then subtract it from the received signal. The IC detector includes two classes: successive interference cancellation (SIC) [63-65] and parallel interference cancellation (PIC) [66-69].

2.7.5.1 Successive Interference Cancellation Detection

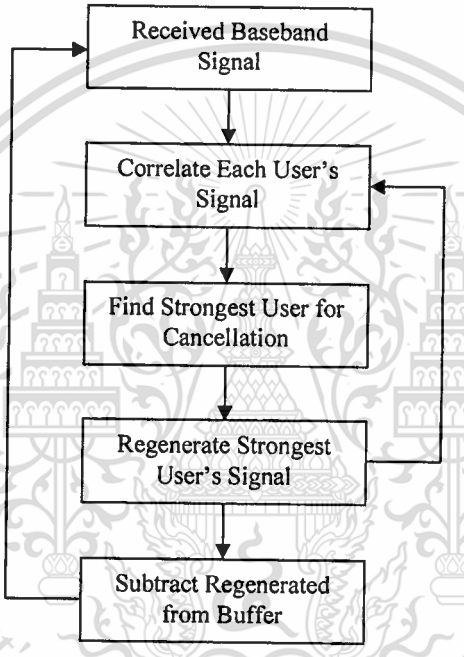

Figure 2.23 Algorithm for successive interference cancellation.

The successive interference cancellation scheme uses the algorithm shown in Figure 2.23. At each iteration of the scheme, all the user's signals are estimated. The signal with the largest power is then regenerated and subtracted from the buffered received signal. The remaining signals are now re-estimated and a new largest user is selected. The process will continue until all the users' signals have been recovered or the maximum allowable number of cancellations is reached.

Successive interference cancellation has been shown to be very robust to imperfect power control in a DS-CDMA system. This comes from the strongest users (and thus best estimated) all having been cancelled from the received waveform. Successive interference cancellation is considered one of the simplest forms of interference cancellation because of the single stage of cancellation. However, the

processor performing the cancellation must perform all the cancellations while maintaining the necessary data rate. As show in [70], this class of detectors has the almost paradoxical feature that interference cancellation can be performed most reliably when the interference is strong relative to the desired signal, i.e. when there is a significant power difference between each of the users signals. However, its performance is poor when power levels are approximately equal. At the same time, the signals need to be sorted by power correctly, and signal reordering is required whenever the power profile changes. This will be a particular risk in a high capacity system with widely variable power levels. Moreover, serial cancellation one by one will lead to a relatively long processing delay.

2.7.5.2 Parallel Interference Cancellation Detection

Parallel interference cancellation detection simultaneously removes from each user the interference produced by the remaining users. In this detector, each user in the system receives equal treatment in the attempt to cancel its MAI. Compared with the SIC, since the IC is performed in parallel for all users, the delay required to complete the process is dramatically reduced. Figure 2.24 illustrates the structure of the PIC detector in a two-user scenario. The PIC performs the estimation for all users' signals separately at first. Then the signal decisions are used to reconstruct the MAI, which is subtracted later. It's clear that the parallel cancellation process should be divided into at least two stages as shown in figure 2.24 and 2.25.

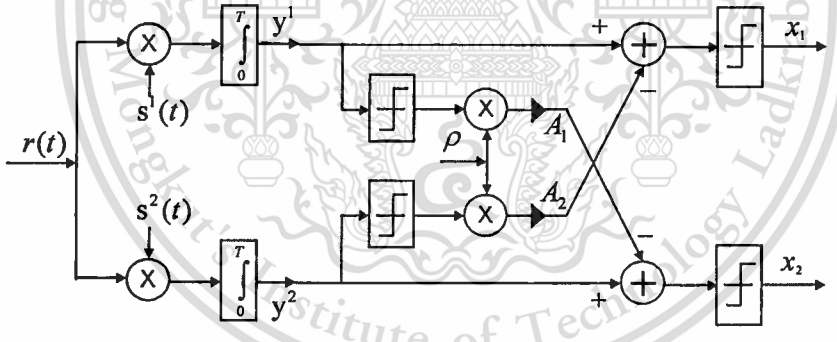

Figure 2.24 Parallel Interference Cancellation for CDMA systems.

In the first stage which can be provided by the MF or linear detectors, the signal from each users are demodulated. Then, the data estimate of the kth user is given by:

$$\tilde{x}_k = \mathrm{sgn}(y_{MF}^k) \tag{2.73}$$

where sgn(.) is the sign of a real number.

For the desired user *k*, remodulating the signal of user *j* with the signature wave, we get the MAI construction $s^j(t)s^k(t)A_j\tilde{x}_j$, which is subtracted from the received signal:

$$y_{PIC}^{k}(t) = y_{MF}^{k}(t) - \sum_{j \neq k} \rho_{jk}(t) A_j \tilde{x}_j^{MF}$$
$$= A_k x_k - \sum_{j \neq k} \rho_{jk}(t) A_j (x_j - \tilde{x}_j) + n'(t) \quad (2.74)$$

Assuming that a hard decision is employed, the output of the two-stage PIC detector is:

$$\tilde{x}_{PIC}^{k} = \mathrm{sgn}(y_{PIC}^{k})$$
$$= \mathrm{sgn}(A_k x_k - \sum_{j \neq k} \rho_{jk}(t) A_j (x_j - \tilde{x}_j) + n'(t)) \quad (2.75)$$

The PIC approach can be further iterated by replacing the conventional MF outputs with the increasingly reliable temporary decisions of the interfering users. It is made by PIC detector in the last iteration as shown in Figure 2.25.

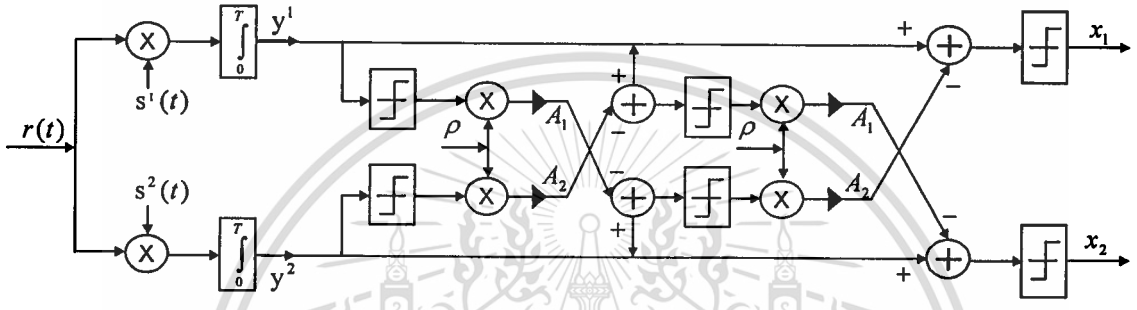

Figure 2.25 Iterative PIC detector.

Then, the received signal is rewritten as:

$$y_{PIC}^{k,l}(t) = y_{MF}^{k}(t) - \sum_{j \neq k} \rho_{jk}(t) A_j \tilde{x}_{PIC}^{j,l-1} \quad (2.76)$$

where $y_{PIC}^{k,l}$ is the l-th iteration PIC detection result and $\tilde{x}_{PIC}^{j,l-1}$ is the data decision made by the PIC detection in the (l-1) th iteration. Moreover, the iteration can be performed as many times as needed. In general, the performance of the detector should continuously improve with increasing number of iterations. However, the disadvantage of PIC is that the risk of error propagation still exists. From Equation (2.80), the MAI can be fully removed if the temporary decision is correct. On the other hand, if the temporary decision is wrong, the error will be doubled after the PIC.

2.7.6 Adaptive Detections

Another alternative detection technique is an adaptive signal processing scheme, based on adaptive filters and adaptive algorithm. The advantages of using adaptive detection are its capacity to track the channel variations without prior knowledge of channel state information and its simplicity and robustness to the signal. The most common adaptive filters, which are used during the adaptation process, are the finite impulse response filters (FIR) types. These are preferable because they are stable, and no special adjustments are needed for their implementation. The adaptation algorithms, which will

be introduced in this thesis, are: Least Means Square (LMS) Algorithm, Partially Filter Gradient Least Means Square (PFGLMS) Algorithm and Recursive Least Squares (RLS) Algorithm.

2.7.6.1 Least Means Square Algorithm

LMS adaptive filter scheme is simple to implement with low computational complexity and capable to track the channel variation by recursively updating the filter tap coefficients without prior knowledge of channel state information. Moreover, the LMS algorithm can be attributed to its simplicity and robustness to the signal statistic without requiring matrix inversion which has a high computational complexity. This technique only requires a training sequence to adapt the filter tap coefficient.

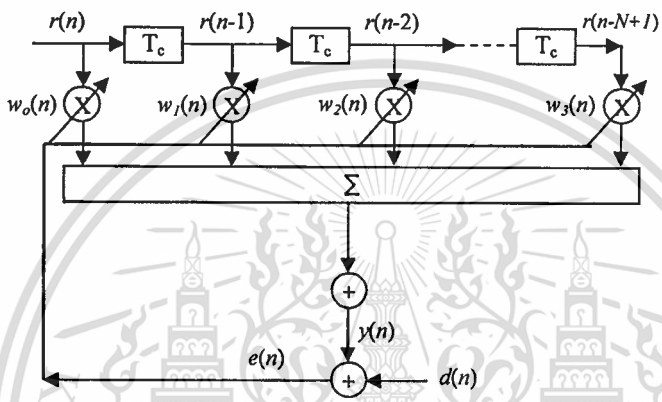

Figure 2.26 An *N*-tap transversal adaptive filter.

The *N*-tap transversal adaptive filter is presented in Figure 2.26. The filter input and tap-weight vector are defined, respectively, by the column vectors [19]:

$$\mathbf{r}(n) = [r(n), r(n-1), \ldots, r(n-N+1)]^T \tag{2.77}$$

$$\mathbf{w}(n) = [w_0(n), w_1(n), \ldots, w_{N-1}(n)]^T \tag{2.78}$$

The filter output [18, 25] is defined by:

$$y(n) = \sum_{i=0}^{N-1} w_i(n) r(n-i) = \mathbf{w}^T \mathbf{r}(n) \tag{2.79}$$

The mean square error function is represented by:

$$\zeta(n) = E[e^2(n)] \tag{2.80}$$

where

$$e(n) = d(n) - y(n) \tag{2.81}$$

To adapt the tap coefficient $\mathbf{w}(n)$, $e(n)$ is minimized in the mean square sense. By using LMS algorithm, the tap coefficient can be obtained by:

$$w(n+1) = w(n) - \mu \nabla e^2(n) \tag{2.82}$$

where μ is the algorithm step-size parameter and ∇ is the gradient operator defined as a column vector [19]:

$$\nabla = \left[\frac{\partial}{\partial w_0}, \frac{\partial}{\partial w_1}, \ldots, \frac{\partial}{\partial w_{N-1}} \right]^T \tag{2.83}$$

The i-th element of the gradient vector $\nabla e^2(n)$ is :

$$\nabla e^2(n) = 2e(n)\frac{\partial e(n)}{\partial w_i} \tag{2.84}$$

Substituting Equation (2.81) with Equation (2.84) and $d(n)$ is independent of w_i, the Equation (2.85) is obtained as:

$$\frac{\partial e^2(n)}{\partial w_i} = -2e(n)\frac{\partial y(n)}{\partial w_i} \tag{2.85}$$

Substituting $y(n)$ from Equation (2.79) in Equation (2.85), the Equation (2.86) is represented as:

$$\frac{\partial e^2(n)}{\partial w_i} = -2e(n)r(n-i) \tag{2.86}$$

Using the gradient operator in Equation (2.83), the Equation (2.87) is represented:

$$\nabla e^2(n) = -2e(n)\mathbf{r}(n) \tag{2.87}$$

where **r**(n) is defined in (2.77). Therefore, the tap coefficient w(n) can be recursively calculated by [19]:

$$\mathbf{w}(n+1) = \mathbf{w}(n) + \mu e(n)\mathbf{r}(n) \tag{2.88}$$

2.7.6.2 Partially Filter Gradient Least Means Square Algorithm

Although, the LMS algorithm is simple to implement with low computational complexity, it has a slow convergence speed. To improve the convergence speed of the LMS algorithm, several adaptive algorithms have been proposed. The partially filter gradient LMS algorithm [20] based on an exponentially weighted least square error is one of these adaptive algorithms.

A more accurate estimate of the minimum error function (2.80) is introduced with exponentially weighted least square errors and defined by [20]:

$$\zeta(n) = \frac{1}{2}\sum_{l=0}^{n} \lambda^{t-l} e^2(l) \tag{2.89}$$

where λ is the forgetting faction $(0 \le \lambda < 1)$. The MSE estimate of (2.89) can be represented as:

$$\zeta(n) = \lambda\zeta(n-1) + \frac{1}{2}e^2(n) \tag{2.90}$$

By taking the derivative of Equation (2.90) with respect to filter tap coefficients, w(t), the negative gradient vector can be represented by [20]:

$$\mathbf{g}(n) = -\nabla\zeta(n) = \lambda\mathbf{g}(n-1) + \frac{1}{2}\mathbf{r}(n)e(n) \tag{2.91}$$

To achieve a more effective estimate of the MSE, the weighted least MSE is modified as:

$$\zeta(n) = \frac{1}{2}\left(e^2(n) + \sum_{l=0}^{n} \lambda^{n-1}\gamma e_l^2 \right) = \frac{1}{2}e^2(n) + \hat{\zeta}(n) \tag{2.92}$$

$$\hat{\zeta}(n) = \frac{\left(\sum_{l=0}^{n} \lambda^{n-1}\gamma\zeta_l^{\,2} \right)}{2} \tag{2.93}$$

where γ is a scaling factor $(0 \le \gamma < 1)$. The negative gradient vector is then given by:

$$\mathbf{g}(t) = -\nabla\zeta(n) = \mathbf{r}(n)e(n) + \hat{\mathbf{g}}(n) \tag{2.94}$$

with

$$\hat{\mathbf{g}}(n) = \lambda\hat{\mathbf{g}}(n-1) + \gamma\mathbf{r}(n)e(n) \tag{2.95}$$

Therefore, the tap coefficient w(n) can be recursively calculated by:

$$\mathbf{w}(n+1) = \mathbf{w}(n) + \mu\mathbf{g}(n) \tag{2.96}$$

2.7.6.3 Recursive Least Squares Algorithm

RLS algorithm has higher computational requirement than LMS and PFGLMS, but behaves much better in terms of steady state MSE and transient time [21]. The RLS algorithm is based on the Least Squares estimate of the filter coefficients $\mathbf{w}(n\text{-}1)$ at iteration $(n\text{-}1)$, by computing its estimate at iteration n using the newly arrive data [71]. Figure 2.27 presents the general RLS block diagram.

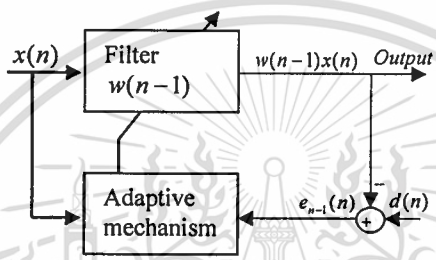

Figure 2.27 RLS block diagram algorithm.

According to the exponentially weight least squares solution, the means square error function in (2.84) is rewrite with the criterion of exponential forgetting factor λ as:

$$\zeta(n) = \sum_{i=i_1}^{n} \lambda^{n-i}[e(i)^2] = \sum_{i=i_1}^{n} \lambda^{n-i}[d(i) - \sum_{k=0}^{M-1} w_k(n)r(i-k)]^2 \tag{2.97}$$

Make the following variable change:

$$\left.\begin{aligned} r'(i) &= \sqrt{\lambda^{n-i}}\, r(i) \\ d'(i) &= \sqrt{\lambda^{n-i}}\, d(i) \end{aligned}\right\} \tag{2.98}$$

Then, (2.97) is rewritten as:

$$\zeta(n) = \sum_{i=i_1}^{n}[d'(i) - \sum_{k=0}^{M-1} w_k(n)r'(i-k)]^2 \tag{2.99}$$

So, the LS solution can be obtained as:

$$w(n) = [\Phi(n)]^{-1} z(n) \tag{2.100}$$

where

$$\Phi(n) = \sum_{i=1}^{n} \lambda^{i-1} r(i) r^T(i) \tag{2.101}$$

$$z(n) = \sum_{i=1}^{n} \lambda^{i-1} r(i) d(i) \tag{2.102}$$

Note that the data before (i=0) is zero. By using the information already available at time $(n\text{-}1)$, (2.103) is defined as:

$$w(n-1) = [\Phi(n-1)]^{-1} z(n-1) \tag{2.103}$$

Rewrite the variable $\Phi(n)$ and $z(n)$ as the functions of $z(n-1)$ and $\Phi(n-1)$:

$$\Phi(n) = \lambda\Phi(n-1) + r(n)r^T(n) \tag{2.104}$$

$$z(n) = \lambda z(n-1) + r(n)d(n) \tag{2.105}$$

By using the matrix inversion formula [71], we have:

$$A = B^{-1} + CD^{-1}C^T \tag{2.106}$$

then,
$$A^{-1} = B - BC(D + C^T BC)^{-1} C^T B \tag{2.107}$$

where,

$$\left.\begin{aligned} A &= \Phi(n) \\ B^{-1} &= \lambda\Phi(n-1) \\ C &= r(n) \\ D &= 1 \end{aligned}\right\} \tag{2.108}$$

By applying the matrix inversion formula to (2.104), we obtain:

$$\Phi^{-1}(n) = \lambda^{-1}\Phi^{-1}(n-1) - \frac{\lambda^{-2}\Phi^{-1}(n-1)r(n)r^T(n)\Phi^{-1}(n-1)}{1+\lambda^{-1}r^T(n)\Phi^{-1}(n-1)r(n)} \tag{2.109}$$

Denoting:

$$U(n) = \Phi^{-1}(n) = \lambda^{-1}U(n-1) - \lambda^{-1}g(n)r^T(n)U(n-1) \tag{2.110}$$

$$g(n) = \frac{\lambda^{-1}U(n-1)r(n)}{1+\lambda^{-1}r^T(n)U(n-1)r(n)} \tag{2.111}$$

$$e(n) = d(n) - r^T(n)w(n-1) \tag{2.112}$$

Therefore, the tap coefficient w(n) can be recursively calculated by:

$$w(n) = w(n-1) + g(n)e(n) \tag{2.113}$$

where $w(0) = 0$ and $U(0) = \delta I$.

2.8 Conclusion

In this chapter, the concept of the MIMO channel is described and it is shown that the presence of multiple transmit antennas is a potential source of interference, i.e., CCI. Two main techniques for realizing a MIMO system, i.e., space-time coding and spatial multiplexing, are introduced. A brief survey of various multiple access techniques is given with particular emphasis on CDMA schemes, where the presence of multiple users introduces MAI at the receiver. This chapter is concluded by introducing some basic multiuser detection schemes, some of which will be briefly described in the remainder of this thesis.

In particular, an adaptive iterative LSTC-CDMA receiver and an adaptive Generalized RAKE LSTC-CDMA receiver are proposed in Chapter 3 and Chapter 4, respectively.

Chapter 3

Adaptive Iterative LSTC-CDMA Receiver

An adaptive iterative receiver for a layered space-time coded CDMA (LSTC-CDMA) system is proposed in this chapter. The proposed receiver is investigated in both time and frequency domain. Moreover, the least means square (LMS), the partially filtered gradient LMS (PFGLMS) and the recursive least squares (RLS) algorithms are used for both feed-forward filter and feedback filters in the adaptive detector. Due to the higher reliability of the co-channel interference (CCI) and multiple access interference (MAI) estimation, the proposed adaptive iterative receivers have an ability to effectively mitigate the CCI and MAI using the interference suppression and cancellation techniques. The system model of LSTC-CDMA system, based on a joint adaptive iterative detection and decoding algorithm, is described. The structure of the transmitter is firstly introduced. Then, the designs of proposed adaptive receiver in both time and frequency domain are presented separately. Finally, the analysis of the system computational complexity is investigated.

3.1 Introduction

With the integration of the internet and multimedia applications in the next generation wireless communications, the huge demand of highly reliable data rate service and the increase in the system capacity are growing very fast. Several broadband wireless communication systems have been widely studied such as CDMA technique and MIMO systems. Direct-Sequence CDMA (DS-CDMA) has emerged as a predominantly multiple-access technique because of its efficient capacity and facility of network planning. At the same time as researchers paid attention to various types of CDMA techniques, a large amount of research also addressed MIMO systems, as shown in Figure 3.1, which are encouraged by the demand for higher link capacity. Therefore, the combination of MIMO and CDMA techniques are proposed [72-74] in order to improve the data rate of CDMA systems.

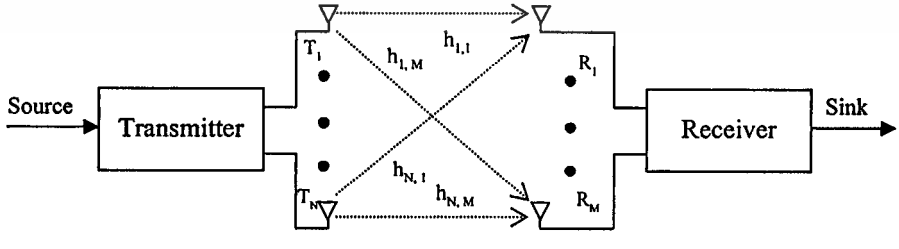

Figure 3.1 MIMO systems.

Later, the layered space-time (LST) architecture is proposed by Foschini in [36] in the purpose of improving the throughput of this wireless system. Then, the combination of Layered Space-Time Coding (LSTC) and CDMA, named as LSTC-CDMA as shown in Figure 3.2, has been intensively studied in [75-78]. This implementation generates Co-Channel Interference (CCI) from the adjacent layers and Multiple Access Interference (MAI) from the users; hence, both will degrade the system performance seriously.

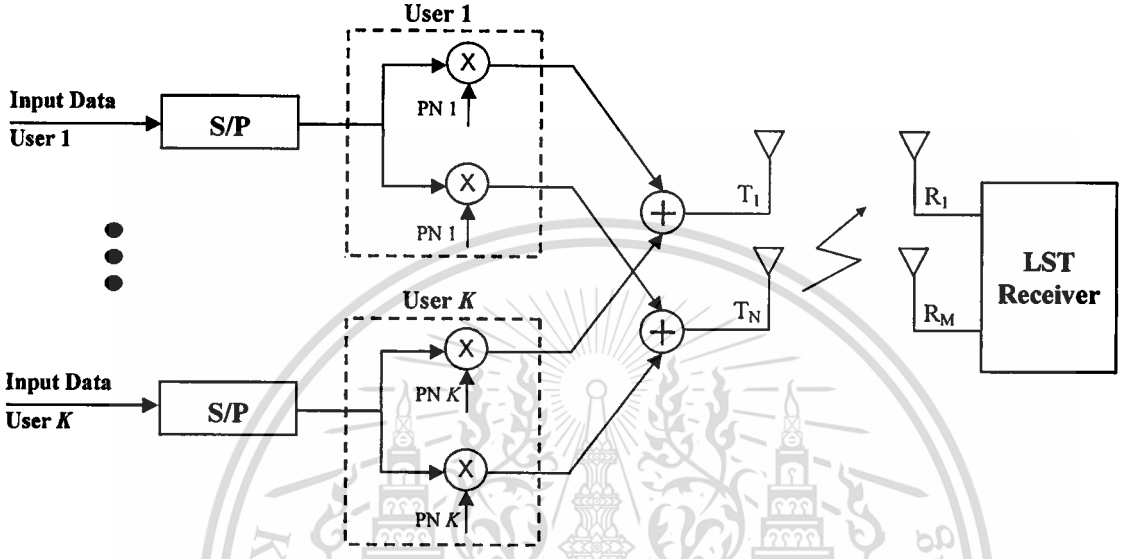

Figure 3.2 LSTC-CDMA system model .

To mitigate the aforementioned interferences, an adaptive Minimum Means Square Error (MMSE) receiver for a LSTC system have been proposed in [16] as in Figure 3.3. In this work, CCI can be reduced. However, MAI is still a huge problem which degraded the system performance and yielding channel estimation inaccurate in a high interference environment.

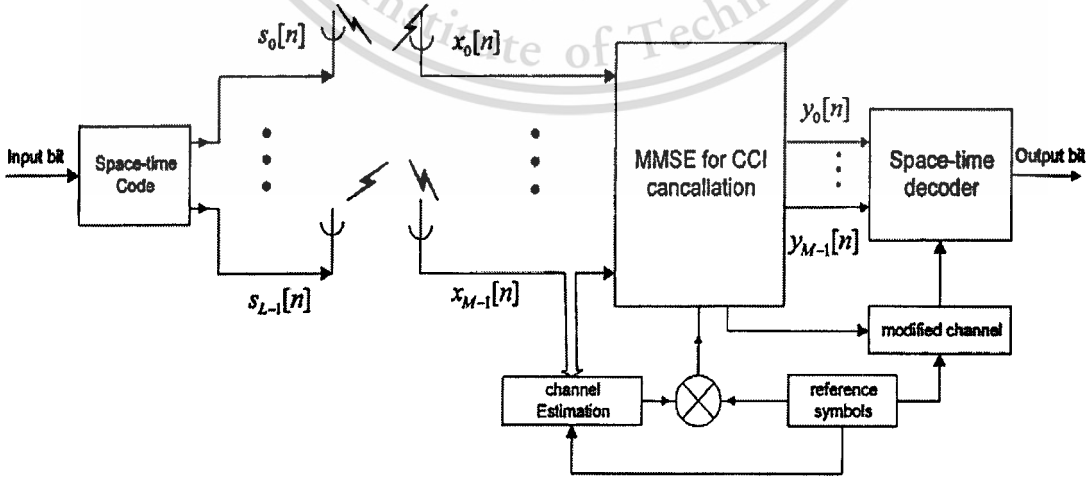

Figure 3.3 Adaptive MMSE receiver.

A non-linear adaptive iterative receiver has been studied in [17, 18], as show in Figure 3.4. This proposed structure contains a feed-forward filter to suppress the system interference and a feedback filter to cancel the interference from adjacent antennas under an iterative format. As the result, the tracking ability of the adaptive detector is improved. Therefore, these proposed receivers have faster convergence speed than a MMSE receiver. However, the complexity is increased because of the feedback filter, compared to the linear system which has only the feed forward filter.

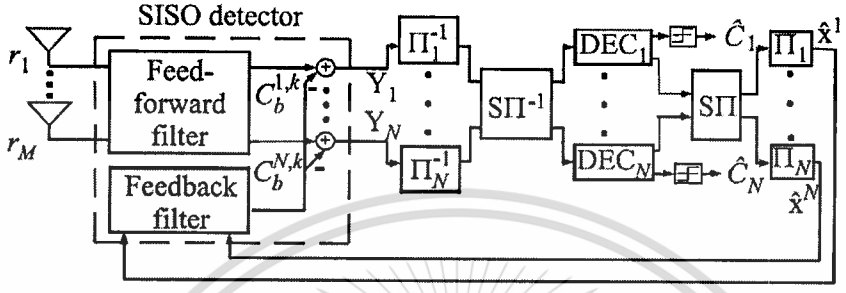

Figure 3.4 Iterative LST receiver.

In order to reduce the computational complexity and to improve the system convergence speed of the above proposed systems, an adaptive iterative LSTC-CDMA receiver for multiuser system has been proposed in this research work. The proposed adaptive receiver is based on a joint adaptive iterative detection and decoding algorithm. The designed detectors consist of M feed forward filters and a feedback iterative parallel interference canceller.

Three main adaptive detection algorithms; namely Least Means Square (LMS), Partially Filtered Gradient LMS (PFGLMS) and Recursive Least Squares (RLS) algorithms; are used in the adaptive filters. The LMS algorithm can be attributed to its simplicity and robustness to the signal statistic and does not require matrix inversion. These advantages make the LMS algorithm become a preferable choice to reduce the system complexity. However, the convergence speed of the adaptive detector is not yet satisfied. For this reason, the adaptive iterative receiver using a Partially Filtered Gradient LMS (PFGLMS) [20] algorithm is proposed to improve convergence speed of LMS based receiver with slightly increase in complexity. Although PFGLMS algorithm has a better convergence speed compared to LMS algorithm, it may not track in a non-stationary environment very well. In reality, Recursive Least Squares algorithm behaves much better in term of steady state Means Square Error (MSE) with a faster convergence speed. Thus, PFGLMS and RLS algorithm are utilized in the adaptation process of the adaptive detector in order to improve the convergence speed of the proposed LMS based receiver. As the result, the computational complexities of the receivers based on these detection algorithms are still high.

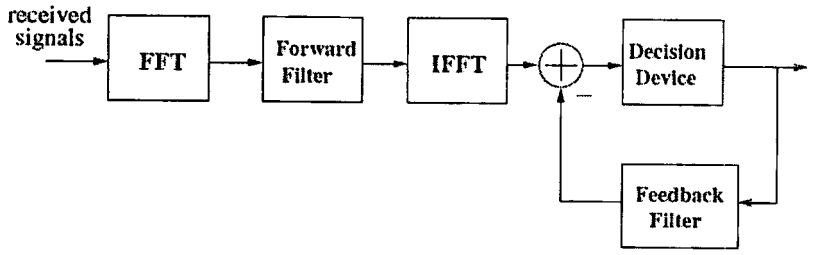

Figure 3.5 Non-iterative FDE-TDDF equalizer.

However, recent researches [79,80] have been proved that frequency domain equalizer (FDE) [81], as in Figure 3.5, offers significant reduction in the computation complexity with performance comparable to time-domain equalizer (TDE) [82]. Consequently, the proposed adaptive receiver in frequency domain is also proposed in this chapter.

Hence, the proposed receiver have the abilities to achieve the spatial diversity, to increase throughput in the high SNR region, to combat the effect of multipath fading channel, to cancel the system interferences such as CCI and MAI by using the interference suppression and cancelation techniques, to reduce the system computational complexity that lead to a decrease in cost of system design and to improve the convergence speed with high quality services of data transmission.

3.2 System Model

A downlink CDMA system as depicted in Figure 3.6 is considered in this study with no a priori knowledge of Channel State Information (CSI), spreading sequences and fading coefficients except the training sequence for each user. Data from different users is modulated by different signature waveforms before being transmitted asynchronously through a wireless channel [83], which is modeled as multipath Rayleigh fading. Then, the entire signals are combined with noises through Addictive White Gaussian Noise (AWGN) Channel. At the receiver, the user data is retrieved adaptively by using the proposed adaptive iterative detector.

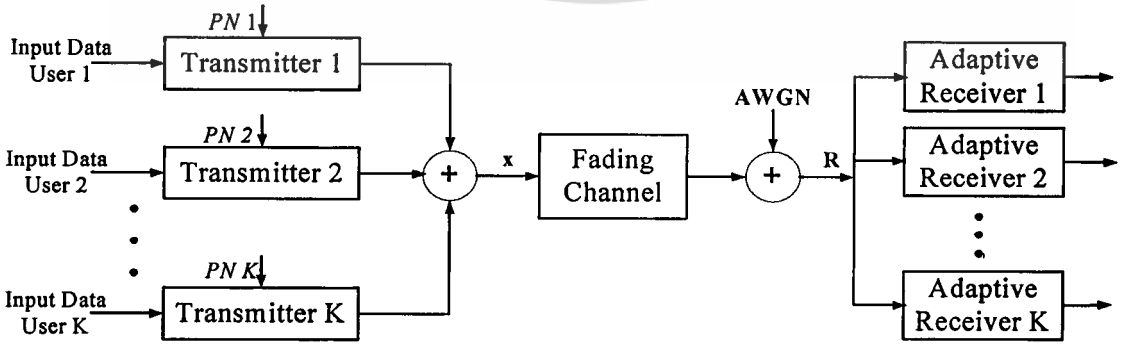

Figure 3.6 An adaptive CDMA system model.

3.2.1 Transmitter Structure

The layered space-time (LST) architecture is used in the proposed transmitter structure. In LST coding algorithm, N data streams are transmitted simultaneously over N antennas over the same frequency band. The receiver uses M receive antennas and interference canceling/suppression techniques to minimize interference caused by simultaneous transmission from N transmit antennas.

There is a number of various LST architectures, depending on whether error control coding is used or not and on the way the modulated symbols are assigned to transmit antennas. The proposed LSTC-CDMA transmitter structure is described in detail as followed.

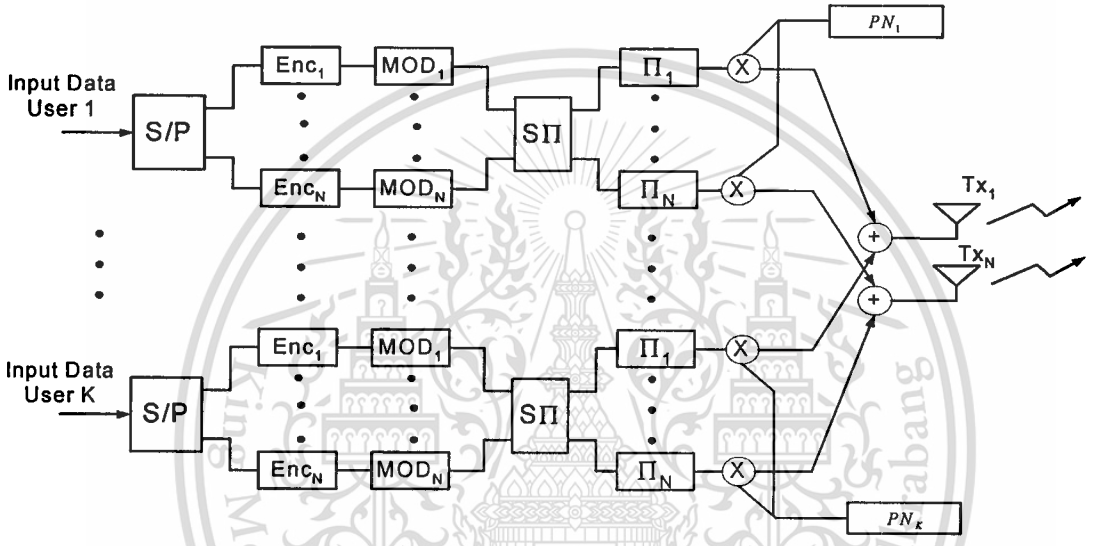

Figure 3.7 Block diagram of LSTC-CDMA transmitter structure.

In a downlink LSTC-CDMA system, all user signals are transmitted simultaneously with N transmitters and M receivers antennas. Figure 3.7 shows the LSTC-CDMA transmitter structure with K users. The binary information of each user is transmitted at a data rate of $r_b = 1/T_b$, where T_b is the bit interval. This data information is first converted into layered data information streams by a serial to parallel (S/P) converter. Before modulating, each information stream is encoded by a convolutional encoder to produce coded data stream for each layer. The layered coded data streams are then fed into a spatial time interleaver ($S\Pi$) and time interleaver (Π). Next, the coded data streams are spread by its signature sequence using a spreading gain of L with $L = T/T_c$, where T is the symbol interval, and T_c is chip duration of spreading sequence. Finally, the spread symbols of all users are then combined together and simultaneously transmitted through N transmit antennas.

Let's **b** is the coded signal vectors transmitted by K users through N transmit antennas and is defined by:

$$\mathbf{b} = [\mathbf{b}_1, \mathbf{b}_2, ..., \mathbf{b}_p, ..., \mathbf{b}_k]^T \tag{3.1}$$

where

$$\mathbf{b}_p = [b_p^1, ..., b_p^n, ..., b_p^N] \tag{3.2}$$

and b_p^n is the information bit of the p-th user for n-th transmit antenna with n=1,..,N and p=1,..,K.

Let **S** represents the L x KN spread transmitted sequences of K users for n transmit antennas, as given by:

$$\mathbf{S} = [\mathbf{s}_1^1, ..., \mathbf{s}_1^N, ..., \mathbf{s}_p^n ... \mathbf{s}_K^1, ... \mathbf{s}_K^N] \tag{3.3}$$

where

$$\mathbf{s}_p^n = [s_p^{n,1}, ..., s_p^{n,q}, ..., s_p^{n,L}]^T \tag{3.4}$$

and $s_p^{n,q}$ is the q-th chip of a spreading sequence for the p-th user and n-th transmit antenna with n =1,..., N; p=1,..,K; and q=1,..,L.

Let's $\mathbf{r}_{t,j}^p$ is the received signal vector for the p-th user at the receiver antenna j, $j = 1, ..., M$, for symbol t, is represented by:

$$\mathbf{r}_{t,j}^p = \mathbf{S}\mathbf{H}_{t,j}^p \mathbf{b} + \mathbf{n}_{t,j}^p \tag{3.5}$$

where

$$\mathbf{r}_{t,j}^p = [r_{t,j}^{p,1}, ... r_{t,j}^{p,q}, ..., r_{t,j}^{p,L}]^T \tag{3.6}$$

and $r_{t,j}^{p,q}$ is the received signal for the p-th user at the q-th chip of the t-th symbol for j-th antenna.

The received signals for all receive antennas of the p-th user are given by

$$\mathbf{R}_t^p = [\mathbf{r}_{t,1}^p, ..., \mathbf{r}_{t,j}^p, ..., \mathbf{r}_{t,M}^p]^T \tag{3.7}$$

$\mathbf{H}_{t,j}^p$ is defined by:

$$\mathbf{H}_{t,j}^p = diag(\mathbf{h}_{t,j}^p, ..., \mathbf{h}_{t,j}^p)_{KNxKN} \tag{3.8}$$

where

$$\mathbf{h}_{t,j}^p = diag\,[h_{j,1}^p(t), ..., h_{j,n}^p(t), ..., h_{j,N}^p(t)]_{NxN} \tag{3.9}$$

and $h_{j,n}^p(t)$ represents the fading coefficient from j-th receive antenna to n-th transmit antenna of the p-th user.

$\mathbf{n}_{t,j}^p$ is defined as an L×1 noise vector at the receive antenna j of the p-th user, given by:

$$\mathbf{n}_{t,j}^p = [n_{j,1}^p(t), ..., n_{j,q}^p(t), ..., n_{j,L}^p(t)]^T \tag{3.10}$$

where $n_{j,q}^p(t)$ is a Gaussian random variable with a zero mean and two sided power spectral density $N_o/2$ per dimension.

3.2.2 Receiver Structure

In downlink LSTC-CDMA system, there is an assumption that the system has no knowledge of Channel State Information (CSI), spreading sequences, and fading coefficients except the training sequence. A block diagram of the proposed adaptive iterative LSTC-CDMA multiuser receiver for the p-th user is shown in Figure 3.8. This structure consists of K adaptive iterative LSTC-CDMA single user receivers, each with an adaptive detector followed by N parallel soft-input soft-output channel decoders. The received signals are first input to the adaptive detector. The detector outputs are then fed to the time and spatial deinterleavers, definded by Π^{-1} and $S\Pi^{-1}$, respectively. The deinterleavers outputs are then decoded by a Maximum A Posteriori (MAP) decoder. The estimated soft symbols of MAP decoders from all users are sent to the spatial and time interleavers, and then fed back to the adaptive detector under iterative technique to cancel the interference from adjacent antennas of the user, called CCI, and the interference from other users, called MAI.

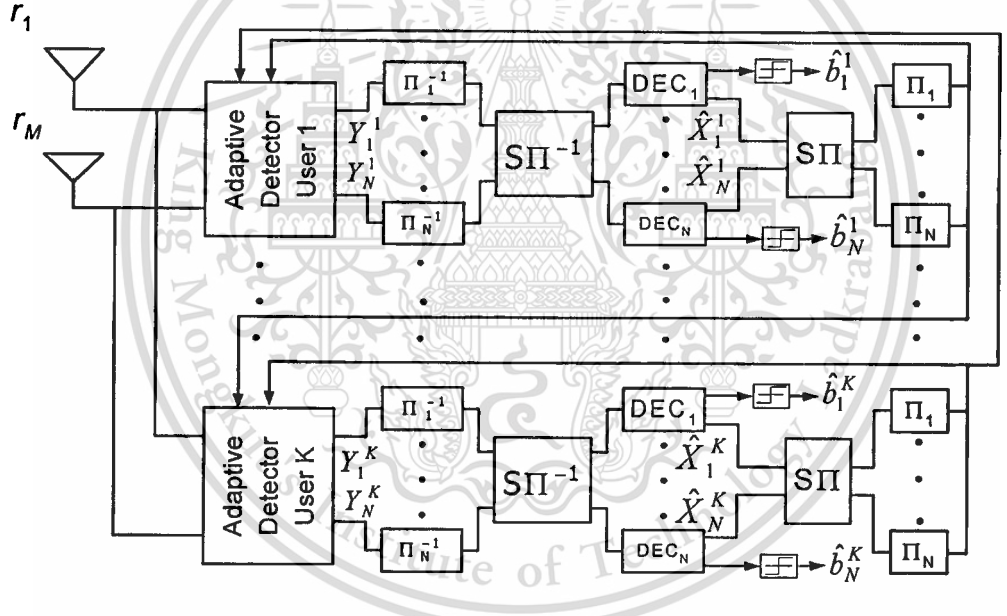

Figure 3.8 Block diagram of LSTC- CDMA receiver structure.

The challenge in detection of space-time signals is to design a low-complexity detector with improving system performance. Hence, two detector structures in time and frequency domain system are investigated in this proposed receiver design. Three main detection algorithms are studied. The MAP approaches [84], which minimizes the big error probability at the decoder output, is employed in this structure.

3.2.2.1 Time Domain Adaptive Iterative LSTC-CDMA receiver

The block diagram of the adaptive iterative LSTC-CDMA receiver for the p-th user in time domain system is shown in Figure 3.9. In the proposed adaptive receiver structure, N sets of adaptive detector consist of M equalizers for the feed-forward filter and an equalizer for the feedback filter modules. An equalizer, employed in the proposed adaptive detector, is based on the LMS, PFGLMS and RLS algorithms. The detector output for each layer is obtained from combining a feed-forward and a feedback filter output. In the iterative process, the feed-forward filter is compensated for the channel estimation error, and the feedback filter is used to cancel the interference from adjacent antennas and other users. In the first iteration, there are no estimated symbols from the decoders and the feedback filter coefficients are zeros; thus, the feedback filter output is also zero. In the feed-forward filter, the M adaptive equalizers are used to estimate the channel coefficients and signature sequence for each layer of each user. The equalizer outputs from all receive antennas are added to obtain a feed-forward filter output signal for each transmit antenna as shown in Figure 3.9.

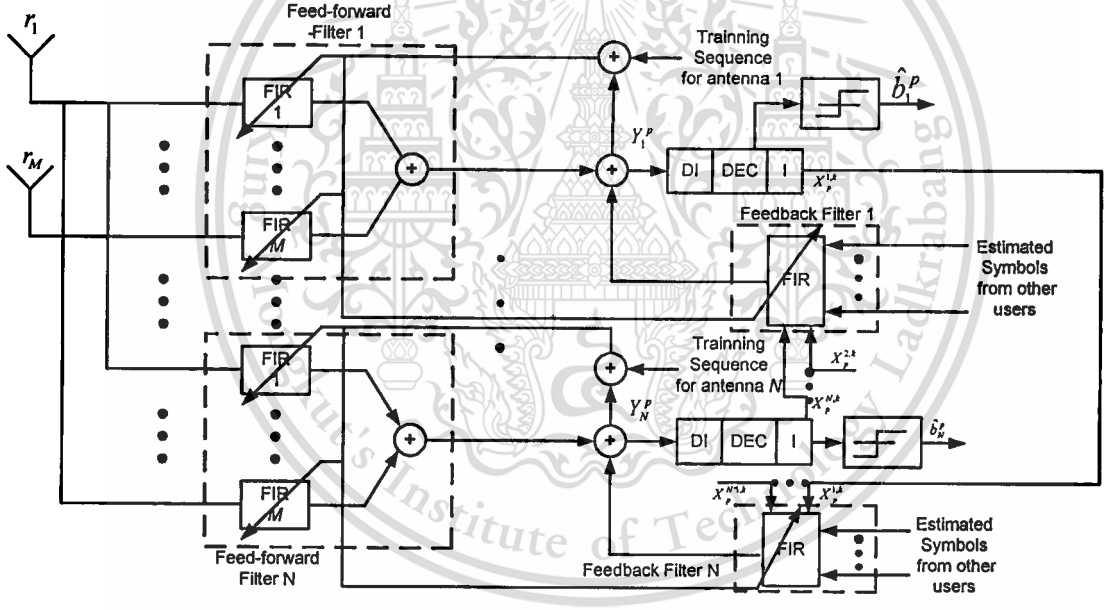

Figure 3.9 Block diagram of the time domain adaptive iterative LSTC-CDMA receiver.

Let $\mathbf{w}_j^{p,k}(t)$ be an Lx1 feed-forward tap coefficients vector for the j-th receive antenna of the p-th user during the k-th iteration at symbol interval t and be given by:

$$\mathbf{w}_j^{p,k}(t)=[w_{t,j}^{p,k}(0),\ldots,w_{t,j}^{p,k}(q),\ldots,w_{t,j}^{p,k}(L\text{-}1)]^T \tag{3.11}$$

where $w_{t,j}^{p,k}(q)$ is the feed-forward tap coefficient corresponding to the q-th chip of the spreading sequence.

$\underline{\hat{\mathbf{x}}}_{t,p}^{i,k}$ is $(KN-1)\times 1$ vector of the estimated soft symbols, at the k-th iteration, from MAP decoders of every antenna of all users, except the i-th antenna of p-th user at symbol interval t, given by:

$$\underline{\hat{\mathbf{x}}}_{t,p}^{i,k} = (\hat{\mathbf{x}}_{t,1}^{1,k},\ldots,\hat{\mathbf{x}}_{t,1}^{N,k},\ldots,\hat{\mathbf{x}}_{t,p}^{i,k},\ldots,\hat{\mathbf{x}}_{t,K}^{1,k},\ldots,\hat{\mathbf{x}}_{t,K}^{N,k})^{\mathrm{T}} \tag{3.12}$$

where
$$\hat{\mathbf{x}}_{t,p}^{i,k} = (\hat{\mathbf{x}}_{t,p}^{1,k},\hat{\mathbf{x}}_{t,p}^{2,k},\ldots,\hat{\mathbf{x}}_{t,p}^{i-1,k},\hat{\mathbf{x}}_{t,p}^{i+1,k},\ldots,\hat{\mathbf{x}}_{t,p}^{N,k}) \tag{3.13}$$

Let $\mathbf{w}_b^{i,k}(t)$ be the feedback filter coefficients of all users, except the i-th antenna of the p-th user, at symbol interval t in time domain, is expressed as:

$$\mathbf{w}_b^{i,k}(t)=[\mathbf{w}_{b,1}^{1,k}(t),\ldots,\mathbf{w}_{b,1}^{N,k}(t),\ldots,\mathbf{w}_{b,p}^{i,k}(t),\ldots,\mathbf{w}_{b,K}^{1,k}(t),\ldots,\mathbf{w}_{b,K}^{N,k}(t)]^T \tag{3.14}$$

where
$$\mathbf{w}_{b,p}^{i,k}(t)=[w_{b,p}^{1,k}(t),\ldots,w_{b,p}^{i-1,k}(t),w_{b,p}^{i+1,k}(t),\ldots,w_{b,p}^{N,k}(t)] \tag{3.15}$$

The detected symbol of the p-th user obtained at the output of the adaptive detector for the i-th antenna during the k-th iteration at symbol interval t, denoted by $y_{t,p}^{i,k}$, is defined as:

$$y_{t,p}^{i,k} = \sum_{j=0}^{M} \mathbf{w}_j^{p,k}(t)^H \mathbf{r}_{t,j}^{p} + \mathbf{w}_b^{i,k}(t)^H \underline{\hat{\mathbf{x}}}_{t,p}^{i,k} \tag{3.16}$$

The detector soft output $y_{t,p}^{i,k}$ in the time domain is then compared to training symbol, denoted by $\mathbf{x}_{t,p}^{i,k}$. The difference between them is calculated as the detection error. The detection error for the p-th user in the k-th iteration at symbol interval t, for i-th antenna, denoted by $e_{t,p}^{i,k}$, is represented by:

$$e_{t,p}^{i,k} = y_{t,p}^{i,k} - x_{t,p}^{i,k} \tag{3.17}$$

The detection error is then used to adapt the feed-forward filter and feedback filter tap coefficients in the time domain. After the Mean Square Error (MSE) approaches a specified value, the training mode is switched to the decision directed mode, in which the training sequence is replaced by the hard decision output of each user detector. In the decision directed mode, the detection error is given by the difference between the detector output and the hard decision of the detector output.

The values tap coefficients, $\mathbf{w}_j^{p,k}(t)$ in (3.11) and feedback filter tap coefficients, $\mathbf{w}_b^{i,k}(t)$ in (3.14) are calculated by minimizing the mean square error, defined as ζ, and given by

$$\zeta = mim\left(E\left|e_{t,p}^{i,k}\right|^2\right) = \min\left(E\left[\left|y_{t,p}^{i,k} - x_{t,p}^{i,k}\right|^2\right]\right) \tag{3.18}$$

Finally, the value of $\mathbf{w}_j^{p,k}(t)$ and $\mathbf{w}_b^{i,k}(t)$ can be calculated recursively by the adaptive detection algorithms such as LMS, PFGLMS and RLS, as shown in section 3.2.2.3.

3.2.2.2 Frequency Domain Adaptive Iterative LSTC-CDMA Receiver

In this section, a new low complexity frequency domain adaptive iterative receiver for LSTC-CDMA system is presented. The proposed frequency domain adaptive receiver is a modified structure of time domain adaptive iterative receiver, presented in section 3.2.2.1, for computational complexity reduction purpose. Therefore, the proposed receiver uses the frequency domain equalizer to replace the time domain equalizer. As the results, both receiver structures receive the signal from same transmitter structure as presented in section 3.2.1.

The block diagram of the proposed frequency domain adaptive iterative receiver for LSTC-CDMA is shown in Figure 3.10. In the proposed system, an adaptive frequency domain equalizer (FDE) is employed in the adaptive detector for both feed-forward and feedback filter. The FDE also uses adaptive detection algorithm for its adaptation process. However, the detector outputs are passed to the time deinterleaver followed by the spatial-deinterleaver after the adaptation process. Then the spatial-deinterleaver outputs are encoded by parallel MAP decoders. If the system performance achieves a satisfactory level, the decoder soft outputs are then passed to a decision device to make a decision for the desired outputs; otherwise the iteration process is needed for further improvement in the interference suppression and cancellation.

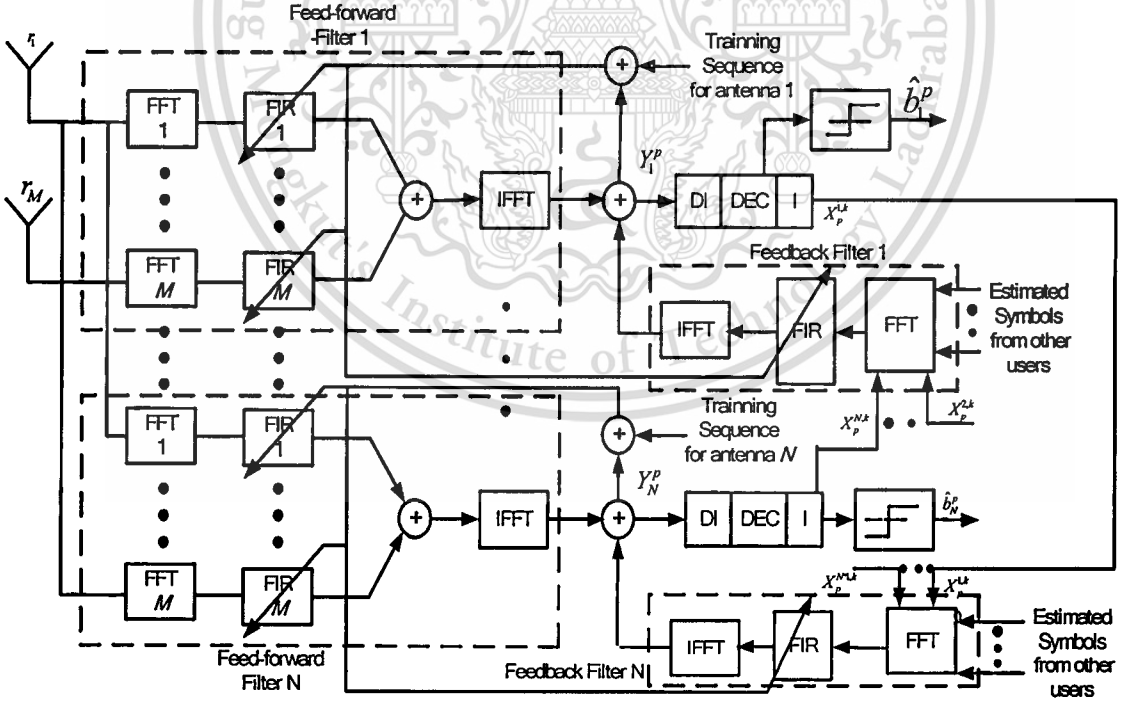

Figure 3.10 Block diagram of the frequency domain adaptive iterative LSTC-CDMA receiver.

The adaptive detector consists of an adaptive feed-forward filter and an adaptive feedback filter. In the feed-forward filter module, the adaptive feed-forward filter of each user is a frequency domain equalizer. It's used to estimate the channel coefficients and signature sequences of each user, as well as to suppress the interference in the system. So, the received signal at each receive antenna is transformed into the frequency domain using the fast Fourier transform (FFT) and the convolution is also performed in the frequency domain. Then, the inverse fast Fourier transform (IFFT) transforms the feed-forward filter output signal from the frequency domain into the time domain.

For the proposed receiver, L chips received signals ($\mathbf{r}_{t,j}^{p}$) of p-th user at the symbol t are transformed by using Fast Fourier transform (FFT) into frequency domain. The output of each FFT is defined by:

$$\Theta_{t,j}^{p} = fft\left(\mathbf{r}_{t,j}^{p}\right) \tag{3.19}$$

where $j = 1,\ldots,M$, $\Theta_{t,j}^{p}$ is the received signal of j-th receive antenna of p-th user at time t in frequency domain, represented by

$$\Theta_{t,j}^{p} = \left[\Theta_{t,j}^{p,1},\ldots,\Theta_{t,j}^{p,q},\ldots,\Theta_{t,j}^{p,L}\right] \tag{3.20}$$

where

$$\Theta_{t,j}^{p,q} = \sum_{l=0}^{L-1} r_{t,j}^{p,l} e^{\frac{-j2\pi ql}{L}} \tag{3.21}$$

and $fft(\cdot)$ is the fast Fourier transform function, and $\Theta_{t,j}^{p,q}$, q=1,…,L, is the FFT transformation of the received signal for the j-th receive antenna of the p-th user at the q-th chip of the t-th symbol.

$\mathbf{w}_{j}^{p,k}(t)$ is $L\times1$ feed-forward tap coefficient vector for the j-th receive antenna of the p-th user during the k-th iteration at symbol interval t, is given by

$$\mathbf{w}_{j}^{p,k}(\mathrm{t}) = [w_{t,j}^{p,k}(0),\ldots,w_{t,j}^{p,k}(q),\ldots,w_{t,j}^{p,k}(L\text{-}1)]^{T} \tag{3.22}$$

Let $\Psi_{t,j}^{p,k}$ represents the FFT of the feed forward filter tap coefficient vector of the p-th user for k-th iteration at the time t, at the receive antenna j, defined by

$$\Psi_{t,j}^{p,k} = fft\left(\mathbf{w}_{j}^{p,k}(t)\right) \tag{3.23}$$

where:

$$\Psi_{t,j}^{p,k} = \left[\Psi_{t,j}^{p,k}(0),\ldots,\Psi_{t,j}^{p,k}(q),\ldots,\Psi_{t,j}^{p,k}(L-1)\right] \tag{3.24}$$

and

$$\Psi_{t,j}^{p,k}(q) = \sum_{l=0}^{L-1} w_{t,j}^{p,k}(t) e^{\frac{-j2\pi lq}{L}} \tag{3.25}$$

$\Theta_{t,j}$ is then sent to the feed forward filter to perform the convolution with the feed forward tap coefficient $\Psi_{t,j}^{p,k}$ in the frequency domain. The output of each feed forward filter is combined together and is denoted by

$$\overline{\mathbf{F}}_{t,p}^{i,k} = \left(\sum_{j=1}^{M} diag\left(\Theta_{t,j}^{p}\right)^{H} \Psi_{t,j}^{p,k} \right) \tag{3.26}$$

where $diag(\cdot)$ and $(\cdot)^{H}$ denoted a diagonal matrix and a conjugate transpose function respectively.

Next, $\overline{\mathbf{F}}_{t,p}^{i,k}$ is transformed back into the time domain by the inverse FFT (IFFT). The feed forward filter output of p-th user in the k-th iteration at time t, for layer i, is given by

$$F_{t,p}^{i,k} = \mathbf{I}_{\mathbf{F}} \cdot \hat{F}_{t,p}^{i,k} \tag{3.27}$$

where $\mathbf{I}_F = [1 \quad \mathbf{0}_{L-1}]$, $\mathbf{0}_{L-1}$ is a row vector of length L-1 containing all zero, and

$$\hat{F}_{t,p}^{i,k} = ifft(\overline{\mathbf{F}}_{t,p}^{i,k}) \tag{3.28}$$

$$\hat{F}_{t,p}^{i,k} = \left[F_{t,p}^{i,k}(0), \ldots, F_{t,p}^{i,k}(q), \ldots, F_{t,p}^{i,k}(L-1) \right] \tag{3.29}$$

$$\hat{F}_{t,p}^{i,k}(q) = \frac{1}{L} \sum_{l=0}^{L-1} \overline{F}_{t,p}^{i,k} e^{\frac{-j2\pi lq}{L}} \tag{3.30}$$

For the feedback filter module, the feedback filter output can be obtained in the same manner as the feed-forward filter process but the input of the feedback filter is the MAP decoder soft output from the previous iteration. The estimated symbols from the decoder outputs are fed back to the feedback filter to cancel the interference from adjacent antennas and from the antennas of other users. The symbol estimates from the output of the decoders are transformed into the frequency domain using the FFT and then passed to the feedback filter. Then, the output signal is converted into time domain system by using IFFT before it is feeded back to feed forward filter.

To cancel MAI and CCI, the estimated symbols from the outputs of the decoders are first input to the feedback filter and transformed into frequency domain by using the FFT. The output of the FFT is represented by

$$\Lambda_{t,p}^{i,k} = fft(\underline{\hat{\mathbf{x}}}_{t,p}^{i,k}) \tag{3.31}$$

where: $$\Lambda_{t,p}^{i,k} = \left[\Lambda_{t,p}^{i,k}(1), \ldots, \Lambda_{t,p}^{i,k}(a), \ldots, \Lambda_{t,p}^{i,k}(KN-1) \right] \tag{3.32}$$

and $$\Lambda_{t,p}^{i,k}(a) = \sum_{m=0}^{KN-2} \hat{x}_{t,p}^{m,k} e^{\frac{-j2\pi am}{KN-1}} \qquad \begin{cases} a \in (1, \ldots, KN-1) \\ p \in (1, \ldots, K) \end{cases} \tag{3.33}$$

$\underline{\hat{\mathbf{x}}}_{t,p}^{i,k}$ is an $(KN-1)\times 1$ vector of the estimated soft symbols, at the k-th iteration, from MAP decoders of all antennas of all users, excluding the j-th antenna of the p-th user, given by

$$\underline{\hat{\mathbf{x}}}_{t,p}^{i,k} = \left(\hat{\mathbf{x}}_{t,1}^{1,k}, \ldots, \hat{\mathbf{x}}_{t,1}^{N,k}, \ldots, \hat{\mathbf{x}}_{t,p}^{i,k}, \ldots, \hat{\mathbf{x}}_{t,K}^{1,k}, \ldots, \hat{\mathbf{x}}_{t,K}^{N,k} \right)^{\mathrm{T}} \tag{3.34}$$

where $$\mathbf{x}_{t,p}^{i,k} = \left(\hat{\mathbf{x}}_{t,p}^{1,k}, \hat{\mathbf{x}}_{t,p}^{2,k}, \ldots, \hat{\mathbf{x}}_{t,p}^{i-1,k}, \hat{\mathbf{x}}_{t,p}^{i+1,k}, \ldots, \hat{\mathbf{x}}_{t,p}^{N,k} \right) \tag{3.35}$$

$\mathbf{w}_b^{i,k}(t)$ is the feedback filter coefficients of all user except the j-th antenna of the p-th user, given by

$$\mathbf{w}_b^{i,k}(t)=[\mathbf{w}_{b,1}^{1,k}(t),...,\mathbf{w}_{b,1}^{N,k}(t),...,\mathbf{w}_{b,p}^{i,k}(t),...,\mathbf{w}_{b,K}^{1,k}(t),...,\mathbf{w}_{b,K}^{N,k}(t)]^T \quad (3.36)$$

where $$\mathbf{w}_{b,p}^{i,k}(t)=\left[\mathbf{w}_{b,p}^{1,k}(t),...,\mathbf{w}_{b,p}^{i-1,k}(t),\mathbf{w}_{b,p}^{i+1,k}(t),\ldots,\mathbf{w}_{b,p}^{N,k}(t)\right] \quad (3.37)$$

Let $\Psi_{t,b,p}^{i,k}$ represents the FFT of $\underline{\hat{w}}_{b,p}^{i,k}(t)$ which is defined by

$$\Psi_{t,b,p}^{i,k} = fft\left(\mathbf{w}_b^{i,k}(t)\right) \quad (3.38)$$

where: $$\Psi_{t,b,p}^{i,k}=\left[\Psi_{t,b,p}^{i,k}(1),...,\Psi_{t,b,p}^{i,k}(a),...,\Psi_{t,b,p}^{i,k}(KN-1)\right] \quad (3.39)$$

and $$\Psi_{t,b,p}^{i,k}(a)=\sum_{m=0}^{KN-2} w_{t,b,p}^{m,k} e^{\frac{-j2\pi am}{KN-1}} \quad (3.40)$$

The output of the FFT, as denoted as $\Lambda_{t,p}^{i,k}$ in (3.31), is then input to the feedback filter to perform convolution with the feedback tap coefficients $\Psi_{t,b}^{k}$ in (3.38) in frequency domain. Hence, the feedback filter output signals, defined by

$$\overline{\mathbf{F}}_{t,b,p}^{i,k} = \left(diag\left(\Lambda_{t,p}^{i,k\ H}\right)\cdot\Psi_{t,b,p}^{i,k}\right) \quad (3.41)$$

and then transformed back into time domain by IFFT. The feedback filter output is given by

$$F_{t,b,p}^{i,k} = \mathbf{I}_B \cdot ifft(\overline{\mathbf{F}}_{t,b,p}^{i,k}) \quad (3.41)$$

where $\mathbf{I}_B=[1\ \mathbf{0}_{KN-1}]$ and $\mathbf{0}_{KN-1}$ is a zero row vector with length of KN-1, and

$$\hat{F}_{t,b,p}^{i,k} = ifft(\overline{\mathbf{F}}_{t,b,p}^{i,k}) \quad (3.42)$$

where $$\hat{F}_{t,b,p}^{i,k}=\left[F_{t,b,p}^{i,k}(1),...,F_{t,b,p}^{i,k}(a),...,F_{t,b,p}^{i,k}(KN-1)\right] \quad (3.43)$$

and $$\hat{F}_{t,b,p}^{i,k}(a)=\frac{1}{KN-1}\sum_{m=0}^{KN-2}\overline{F}_{t,b,p}^{m,k} e^{\frac{-j2\pi am}{KN-1}} \quad (3.44)$$

The detected symbol of the p-th user obtained in the k-th iteration at time t, for layer i, denoted by

$$y_{t,p}^{i,k} = F_{t,p}^{i,k} + F_{t,b,p}^{i,k} \quad (3.45)$$

where $F_{t,p}^{i,k}$ and $F_{t,b,p}^{i,k}$ represent feed forward and feedback filter output in time domain, given in (3.27) and (3.41) respectively. Note that the output of the feedback filter is zero at the first iteration.

The values of $\mathbf{w}_j^{p,k}(t)$ in (3.22) and $\mathbf{w}_b^{i,k}(t)$ in (3.36) are calculated by minimizing the mean square error, defined as

$$\zeta = \mathrm{M\,in}\left(E\left[\left|y_{t,p}^{i,k} - x_{t,p}^{i,k}\right|^2\right]\right) \quad (3.46)$$

and they can be determined recursively by the adaptive detection algorithms as show in section 3.2.2.3.

3.2.2.3 Adaptive Detection Algorithms

In the adaptation process of both proposed receiver structure, the adaptive detection algorithms are used in order to compute the value of feed forward and feedback tap coefficients. It is obvious that the LMS adaptive filter scheme is simple to implement with low computational complexity and capable to track the channel variation by recursively updating the filter tap coefficients.

So, the values of feed forward tap coefficients in (3.11 and 3.22) and the values of feedback tap coefficients in (3.14 and 3.36) can be determined recursively by LMS algorithm as follows [21]:

$$\mathbf{w}_j^{p,k}(t+1) = \mathbf{w}_j^{p,k}(t) + \mu_f e_{t,p}^{i,k} \mathbf{r}_{t,j}^{p} \tag{3.47}$$

$$\mathbf{w}_b^{i,k}(t+1) = \mathbf{w}_b^{i,k}(t) + \mu_b e_{t,p}^{i,k} \underline{\hat{\mathbf{x}}}_{t,p}^{i,k} \tag{3.48}$$

where μ_f and μ_b are the step sizes for the feed-forward and feedback adaptation.

As the LMS algorithm has slow convergence and may not track in a non-stationary environment very well, the partially filtered gradient LMS (PFGLMS) algorithm [20] based on an exponentially weighted least square error is utilized to improve the convergence speed with a slight increase in complexity. The modified feed-forward and feedback coefficients of the PFGLMS algorithm can be expressed as:

$$\mathbf{w}_f^{i,k}(t+1) = \mathbf{w}_f^{i,k}(t) + \mu_f \mathbf{g}_f^{i,k}(t) \tag{3.49}$$

$$\mathbf{w}_b^{i,k}(t+1) = \mathbf{w}_b^{i,k}(t) + \mu_b \mathbf{g}_b^{i,k}(t) \tag{3.50}$$

where

$$\begin{aligned} \mathbf{g}_f^{i,k}(t) &= e(t)\mathbf{r}_{t,j}^{p} + \hat{\mathbf{g}}_f^{i,k}(t) \\ \hat{\mathbf{g}}_f^{i,k}(t) &= \lambda_f \hat{\mathbf{g}}_f^{i,k}(t-1) + \gamma_f e(t)\mathbf{r}_{t,j}^{p} \end{aligned} \tag{3.51}$$

and

$$\begin{aligned} \mathbf{g}_b^{i,k}(t) &= e(t)\underline{\hat{\mathbf{x}}}_{t,p}^{i,k} + \hat{\mathbf{g}}_b^{i,k}(t) \\ \hat{\mathbf{g}}_b^{i,k}(t) &= \lambda_b \hat{\mathbf{g}}_b^{i,k}(t-1) + \gamma_b e(t)\underline{\hat{\mathbf{x}}}_{t,p}^{i,k} \end{aligned} \tag{3.52}$$

where (λ_f, λ_b) and (γ_f, γ_b) are the forgetting factors and the scaling factors of feed-forward and feedback adaptation respectively, and $\hat{\mathbf{g}}_f^{i,k}(0) = \hat{\mathbf{g}}_b^{i,k}(0) = 0$.

Although PFGLMS algorithm has a better convergence speed compared to conventional LMS algorithm, it may not track in a non-stationary environment very well. In reality, Recursive Least Squares algorithm behaves much better in term of steady state Means Square Error (MSE) and transient time with a faster convergence speed. So, tap coefficients of feed forward and feedback filter, can be determined recursively by Recursive Least Squares (RLS) algorithms as the following equations [21]:

Feed-Forward tap coefficients

$$\mathbf{w}_f^{p,k}(t+1) = \mathbf{w}_f^{p,k}(t) + \mathbf{g}_f^{p,k}(t+1)e(t) \tag{3.53}$$

where

$$\mathbf{g}_f^{p,k}(t+1) = \frac{\mathbf{U}_f^{p,k}(t)\mathbf{r}_{t,f}^{p}}{\lambda_f + \mathbf{r}_{t,f}^{p\,T}\mathbf{U}_f^{p,k}(t)\mathbf{r}_{t,f}^{p}} \tag{3.54}$$

$$\mathbf{U}_f^{p,k}(t) = \lambda_f^{-1}[\mathbf{U}_f^{p,k}(t-1) - \mathbf{g}_f^{p,k}(t)\mathbf{r}_{t,f}^{p\,T}\mathbf{U}_f^{p,k}(t-1)]$$

Feedback tap coefficients

$$\mathbf{w}_b^{p,k}(t+1) = \mathbf{w}_b^{p,k}(t) + \mathbf{g}_b^{p,k}(t+1)e(t) \tag{3.55}$$

where

$$\mathbf{g}_b^{p,k}(t+1) = \frac{\mathbf{U}_b^{p,k}(t)\hat{\underline{\mathbf{x}}}_{t,p}^{i,k}}{\lambda_b + \hat{\underline{\mathbf{x}}}_{t,p}^{i,k\,T}\mathbf{U}_b^{p,k}(t)\hat{\underline{\mathbf{x}}}_{t,p}^{i,k}} \tag{3.56}$$

$$\mathbf{U}_b^{p,k}(t) = \lambda_b^{-1}[\mathbf{U}_b^{p,k}(t-1) - \mathbf{g}_b^{p,k}(t)\hat{\underline{\mathbf{x}}}_{t,p}^{i,k\,T}\mathbf{U}_b^{p,k}(t-1)]$$

where $\mathbf{r}_{t,f}^{p}$ and $\hat{\underline{\mathbf{x}}}_{t,p}^{i,k}$ are defined in (3.6) and (3.12), (λ_f, λ_b) are the forgetting factor of feed-forward and feedback adaptation respectively. The initializations of RLS algorithm are:

- $\mathbf{w}(0) = 0$
- $\mathbf{U}(0) = \delta^{-1}I$

where δ is the inverse of the input signal power estimate and the recommended value is $\delta > 100\sigma^2$, I is the $(p+1)$ by $(p+1)$ identity matrix and p is the filter order.

3.2.2.4 MAP Decoder

In the proposed receiver structure, detector output for user p, denoted by $y_{t,p}^{i,k}$, is decoded by Maximum A Posteriori (MAP) Decoder. The soft-output from the decoder is used to suppress the interference in the feedback filter in the next iteration. The process of this adaptive iterative detection/decoding is performed until the symbol estimation can converge to the optimal performance. The soft-output from the decoder in the last iteration is then fed into a decision device to produce a decision. For a Binary Phase Shift Keying (BPSK), the functions for the transmitted modulated symbols 1 and –1 can be written as:

$$P\left(y_{t,p}^{i,k} \middle| x_{t,p}^{i,k} = \pm 1\right) = \frac{1}{\sqrt{2\pi\sigma^2}} \exp \frac{-\left(y_{t,p}^{i,k} \mp 1\right)^2}{2\sigma^2} \tag{3.57}$$

The Log-Likelihood Ratios (LLR) is determined in the k-th iteration for the i-th transmit layer of p-th user, denoted by $\lambda_{t,p}^{i,k}$:

$$\lambda_{t,p}^{i,k} = \log\left(\frac{P\left(x_{t,p}^{i,k}=1\middle|y_{t,p}^{i,k}\right)}{P\left(x_{t,p}^{i,k}=-1\middle|y_{t,p}^{i,k}\right)}\right) \tag{3.58}$$

The symbol A Posteriori Probabilities (APP) $P(x_{t,p}^{i,k} = q| y_{t,p}^{i,k})$, with q equal 1 and -1, conditioned on the output variable which is defined as $\lambda_{t,p}^{i,k}$ for p-th user, can be obtained as:

$$P\left(x_{t,p}^{i,k}=1\middle|y_{t,p}^{i,k}\right) = \frac{e^{\lambda_{t,p}^{i,k}}}{e^{\lambda_{t,p}^{i,k}}+1} \tag{3.59}$$

and

$$P\left(x_{t,p}^{i,k}=-1\middle|y_{t,p}^{i,k}\right) = \frac{1}{e^{\lambda_{t,p}^{i,k}}+1} \tag{3.60}$$

The soft-output symbols are estimated in the i-th layer and k-th iteration for p-th user, calculated as:

$$\hat{x}_{t,p}^{i,k} = \frac{e^{\lambda_{t,p}^{i,k}}-1}{e^{\lambda_{t,p}^{i,k}}+1} \tag{3.61}$$

3.3 Complexity Analysis

In order to calculate the number of complexity of the proposed receiver structure, the receiver computational complexity are defined as the required number of signal processing operations per coded symbol and per layer. Both multiplications and addition are calculated for each coded symbol with K users, N transmit antennas, M receive antennas, I iterations and L spreading sequence length. Moreover, the purpose of complexity calculation is to compare the cost between the time domain receiver and frequency domain receiver by using different types of adaptive detection algorithms. So, the complexity of the detector is only considered since the decoder is the same for both implementations.

3.3.1 Time domain

In time domain system, the computation requirement for each feed forward filter parameters require L multiplier and (KN-1) multiplier for those of the feedback filter.

The time domain detector soft output $y_{t,p}^{i,k}$ in (3.16) is given as the follows:

$$y_{t,p}^{i,k} = \sum_{j=0}^{M} \mathbf{w}_j^{p,k}(t)^H \mathbf{r}_{t,j}^{p} + \mathbf{w}_b^{i,k}(t)^H \underline{\hat{\mathbf{x}}}_{t,p}^{i,k}$$

So, the total number of computational complexity, $CC_{detector}$, of the detector is defined as:

$$CC_{detector} = KI\,[M\,(CC_f + L) + (CC_b + (KN\text{-}1))] \tag{3.62}$$

LMS Algorithms

By using LMS algorithm, the total number of CC_f and CC_b can be defined base on the Equation (3.47) and (3.48) as the follows:

$$CC_f = L + 1$$

$$CC_f = (KN\text{-}1) + 1 = KN$$

So, the total number of computational complexity of the detector by using LMS algorithm is defined as:

$$CC_{\text{detector}}^{LMS} = KI\,[M\,(2L+1) + (2KN - 1)] \tag{3.63}$$

PFGLMS Algorithms

The total number of CC_f and CC_b can also be calculated according to the Equation (3.49-3.52) as the follows:

$$CC_f = 3L + 1$$

$$CC_f = 3(KN\text{-}1) + 1 = 3KN - 2$$

So, the total number of computational complexity of the detector by using PFGLMS algorithm is defined as:

$$CC_{\text{detector}}^{PFGLMS} = KI\,[M\,(4L+1) + (4KN - 3)] \tag{3.64}$$

RLS Algorithms

According to equation (3.53-3.56), the CC_f and CC_b are given as:

$$CC_f = 5L + 1$$

$$CC_f = 5(KN\text{-}1) + 1 = 5KN - 2$$

So, the total number of computational complexity of the detector by using RLS algorithm is defined as:

$$CC_{\text{detector}}^{RLS} = KI\,[M\,(6L+1) + (6KN - 5)] \tag{3.65}$$

3.3.2 Frequency domain

The frequency domain adaptive detector soft output $y_{t,p}^{i,k}$ in (3.45) is given as follows:

$$y_{t,p}^{i,k} = F_{t,p}^{i,k} + F_{t,b,p}^{i,k}$$

In principle, the computation requirement for frequency domain adaptive detector requires $\text{Log}_2 L$ of multiplier for each feed forward filter as well as $\text{Log}_2(KN\text{-}1)$ for feedback filter. Therefore, the total numbers of complexity of the adaptive detector by using different algorithms are defined as the follows:

$$CC^{LMS}_{\text{detector, frequency}} = KI[M\log_2(2L + 1) + \log_2(2KN - 1)] \quad (3.66)$$

$$CC^{PFGLMS}_{\text{detector, frequency}} = KI[M\log_2(4L + 1) + \log_2(4KN - 3)] \quad (3.67)$$

$$CC^{RLS}_{\text{detector, frequency}} = KI[M\log_2(6L + 1) + \log_2(6KN - 5)] \quad (3.68)$$

The summary of the complexity comparison between time domain and frequency domain filter and its example are listed in Table 3.1 and Table 3.2 respectively. It can be observed that the computational complexity in the frequency domain is significantly lower than that of the time domain approach. Moreover, the complexity of the detector base on RLS algorithm is higher than that of PFGLMS and LMS algorithm respectively. Although RLS and PFGLMS algorithm have higher complexity compared to the LMS algorithm, their convergence speed, which is going to be presented in Chapter 5, is much faster than that of the LMS. Moreover, the numbers of multiplications of the proposed adaptive iterative LSTC-CDMA receiver are much lower than that of the non-adaptive MMSE receiver which was proposed in [17, 18].

Table 3.1. Complexity comparison between time and frequency domain receivers.

Algorithms	LMS	PFGLMS	RLS
Time Domain	$KI\,[\,M(2L+1) + 2KN\text{-}1\,]$	$KI\,[\,M(4L+1) + 4KN\text{-}3\,]$	$KI\,[\,M(6L+1) + (6KN\text{–}5)\,]$
Frequency Domain	$KI\,[\,M\log_2(2L+1) + \log_2(2KN\text{-}1)\,]$	$KI\,[\,M\log_2(4L+1) + \log_2(4KN\text{-}3)\,]$	$KI\,[\,M\log_2(6L+1) + \log_2(6KN\text{-}5)\,]$
[17, 18] Non-adaptive MMSE receiver (Time domain) = $KI[M^3(L+1) + 5M(L+1) + 4(KN\text{-}1)]$			

N= number of transmit antennas, M= number of receive antennas,

K= number of users, L= processing gain, I= number of iteration

Table 3.2. Complexity comparison in number of multiplications.

Algorithms (Number of multiplications)	LMS	PFGLMS	RLS
Time Domain	**4900**	**9500**	**14100**
Frequency Domain	**1206.17**	**1492.50**	**1663.40**
[17, 18] Non-adaptive MMSE receiver (Time domain) = **18000**			

N= 2, M= 2, K= 5, L= 7, I= 20

3.4 Conclusion

An adaptive iterative LSTC-CDMA receiver for MIMO systems in Rayleigh fading channels is presented in this chapter. The proposed receiver is investigated in both time and frequency domain base on three main adaptive detection algorithms such as LMS, PFGLMS and RLS. As the result, the proposed receiver can suppress the system interference, such as the CCI and MAI, from the received signal with a number of iterations by using the design of interference suppression and cancellation techniques. Moreover, the use of a decoding stage at each iteration allows for a greater performance improvement over multistage detectors, due to the higher reliability of the co-channel interference and multiple access interference estimation. The comparison of the complexity is considered only the complexity of the detector since the MAP decoder has been used with all detectors in the receiver structures. It is shown that the proposed frequency domain receiver has a significant reduction in computation complexity and achieves the same performance compared to the time domain system. The system performance of adaptive iterative LSTC-CDMA system in both time and frequency domain are quantified through the simulation results which are going to be presented in Chapter 5.

However, it is a difficult task to enlarge the network capacity and improve the quality of service due to the multipath fading of wireless channel. By comparing to adaptive CDMA receiver, G-RAKE receiver can theoretically provide significant gains in performance by suppressing interference and combat the effect of multipath channels. Hence, the design of the combination between G-RAKE receiver and LSTC-CDMA receiver will be discussed in the next chapter.

Chapter 4

Adaptive Generalized RAKE LSTC-CDMA Receiver

The design of system model of a Generalized RAKE LSTC-CDMA receiver in both time and frequency domain systems are presented in this chapter. The least means square (LMS), the partially filtered gradient LMS (PFGLMS) and the recursive least squares (RLS) algorithms are used for both feed-forward filter and feedback filter in the adaptive detection in order to determine the weight coefficient of each finger element. Moreover, the proposed adaptive G-RAKE receiver is based on a joint adaptive iterative detection and decoding algorithm same as the adaptive iterative receiver that was proposed in Chapter 3. However, this receiver has the ability not only to effectively cancel the system interferences but also adaptively mitigate the effect of multipath fading. Chapter 4 is organized as follows. Firstly, there is an explanation of the motivation of this proposed research work. Then, system model is demonstrated, which is mainly focus on proposed transmitter and receiver structure. The detail description of the receiver's design in both time and frequency domain is presented and followed by the explanation of the adaptive detection algorithms. Finally, there is a conclusion of this work.

4.1 Introduction

The development of communication systems over the past decade has had a significant impact on the modern life of people in today's society. As the results, wireless technology is experiencing spectacular developments according to the emergence of interactive and digital multimedia applications as well as rapid advance in the highly integrated systems. Code division multiple access (CDMA) is an access scheme that shows a promising to meet these ever growing capacity demands of wireless services [85]. At the same time, a large amount of research also addressed MIMO systems which are encouraged by the demand for higher link capacity. In order to reduce the computational complexity and improve the system performance of these evolving systems, the recent research works on the combination of MIMO and CDMA systems were proposed [16-18, 72-78]. Moreover, an adaptive iterative receiver for LSTC-CDMA system has also been investigated in Chapter 3 in both time and frequency domain, in order to improve the quality service of data transmission and reduce the cost of system design.

However, it is a difficult task to enlarge the network capacity and improve the quality of service due to the multipath fading channels. Furthermore, system capacity is limited by multiuser interference in the downlink of DS-CDMA systems. This interference can be suppressed at the receiver by interference whitening approaches such as chip equalization and generalized RAKE (G-RAKE)

reception [86]. The generalized RAKE (G-RAKE) receivers for interference suppression and multipath mitigation have been developed in [87-89] as shown in Figure 4.1. The G-RAKE receiver scheme is based on the RAKE receiver structure but with different finger placement and combining coefficients than used in the conventional RAKE receiver. Therefore, the conventional RAKE receiver is a special case of G-RAKE receiver when the number of fingers is equal to the number of multipath. The combining coefficients are developed according to the maximum likelihood criterion and take into account the spectral coloration of the interference and noise introduced by the combined effect of multipath channel and the pulse shaping filter. The G-RAKE scheme can improve the performance by using more fingers than channel multipath, as some of the fingers are used for whitening the colored interference plus noise term. This scheme is capable of taking into account also interference caused by neighboring cells and is not restricted to dealing only with own cell interference. It was shown that significant improvement over conventional RAKE can be achieved both in system performance and system capacity. Furthermore, G-RAKE receiver can theoretically provide significant gains in performance, by suppressing interference and combat the effect of multipath channels [89], than that of the adaptive iterative receiver.

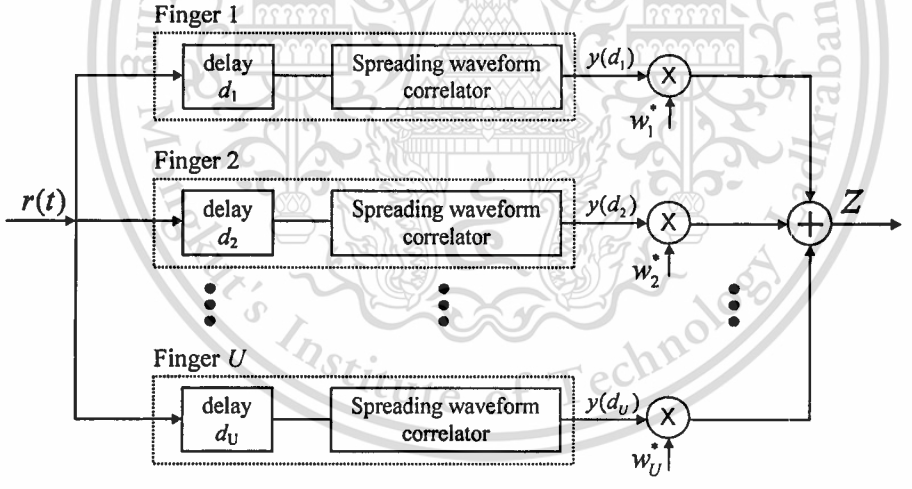

Figure 4.1 G-RAKE receiver structure.

In this chapter, a generalized RAKE receiver for LSTC-CDMA systems in multipath fading channel has been proposed in both time and frequency domain. The proposed receiver is the result of the combination between the existing system model, which is proposed in Chapter 3, and the G-RAKE receiver structure. The G-RAKE LSTC-CDMA receiver has the ability to combat the effect of multipath fading channel, cancel the system interferences by using the interference suppression and cancelation

techniques, to reduce the system computational complexity that lead to a decrease in cost of system design and to improve the convergence speed with high quality services of data transmission. Consequently, the proposed adaptive detectors; based on the LMS [21], PFGLMS [20], and RLS algorithms [71]; were investigated. Moreover, how interference suppression at the receiver can significantly improve downlink system capacity for the LSTC-CDMA systems is also presented.

4.2 System Model

4.2.1 Transmitter Structure

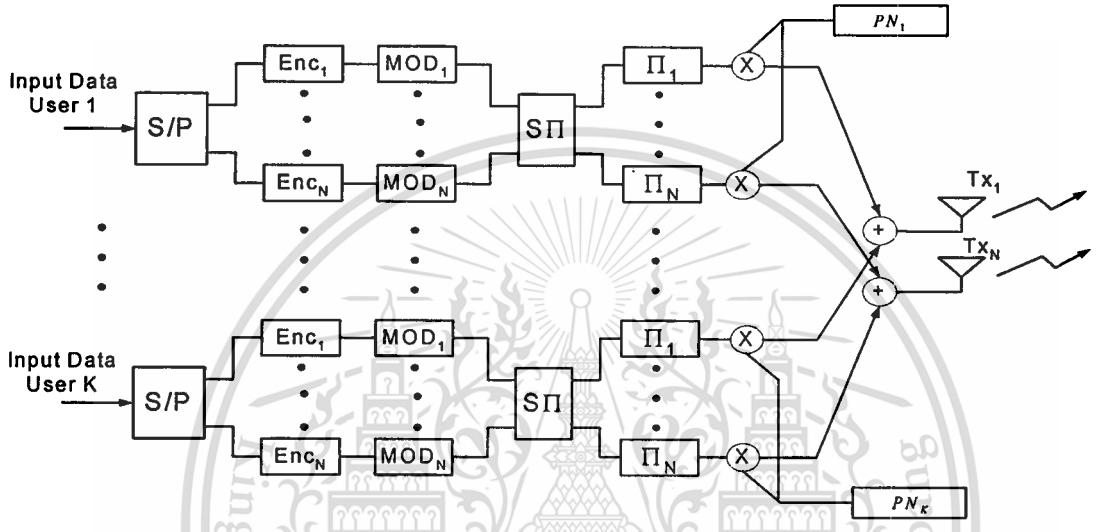

Figure 4.2 LSTC-CDMA transmitter structure.

The layered space-time coded transmitter structure for multiuser systems in downlink wireless communications, as shown in Figure 4.2, is utilized in the proposed system model. However, the system performance design and the system performance comparisons are considered only at the receiver end. Therefore, the transmitted signals of all N transmit antennas are the same transmitted signals as given in Chapter 3.

The equations represent the transmitted signals from input data users to the receiver end are presented as the follows:

$$\mathbf{b}=[\mathbf{b}_1,\mathbf{b}_2,...,\mathbf{b}_p,...,\mathbf{b}_k]^T \tag{4.1}$$

where $\mathbf{b}$ is the coded signal vectors transmitted by K users through N transmit antennas, $\mathbf{b}_p = [b_p^1,..., b_p^n,..., b_p^N]$ and b_p^n is the information bit of the p-th user for n-th transmit antenna with n=1,..,N and p=1,..,K.

$$\mathbf{S} = [\mathbf{s}_1^1, \ldots, \mathbf{s}_1^N, \ldots, \mathbf{s}_p^n \ldots \mathbf{s}_K^1, \ldots \mathbf{s}_K^N] \tag{4.2}$$

where $\mathbf{S}$ represents the L x KN spread transmitted sequences of K users for n transmit antennas, $\mathbf{s}_p^n = [s_p^{n,1}, \ldots, s_p^{n,q}, \ldots, s_p^{n,L}]^T$ and $s_p^{n,q}$ is the q-th chip of a spreading sequence for the p-th user and n-th transmit antenna with n =1,..., N; p=1,..,K; and q=1,..,L.

$$\mathbf{H}_{t,j}^p = diag(\mathbf{h}_{t,j}^p, \ldots, \mathbf{h}_{t,j}^p)_{KNxKN} \tag{4.3}$$

where $\mathbf{H}_{t,j}^p$ represents the fading coefficient from j-th receive antenna to n-th transmit antenna of the p-th user, $\mathbf{h}_{t,j}^p = diag[h_{j,1}^p(t), \ldots, h_{j,n}^p(t), \ldots, h_{j,N}^p(t)]_{NxN}$ and $h_{j,n}^p(t)$ represents the fading coefficient from j-th receive antenna to n-th transmit antenna of the p-th user.

$$\mathbf{n}_{t,j}^p = [n_{j,1}^p(t), \ldots, n_{j,q}^p(t), \ldots, n_{j,L}^p(t)]^T \tag{4.4}$$

where $\mathbf{n}_{t,j}^p$ is defined as an L×1 noise vector at the receive antenna j of the p-th user and $n_{j,q}^p(t)$ is a Gaussian random variable with a zero mean and two sided power spectral density $N_o/2$ per dimension.

$$\mathbf{r}_{t,j}^p = \mathbf{S}\mathbf{H}_{t,j}^p \mathbf{b} + \mathbf{n}_{t,j}^p \tag{4.5}$$

where $\mathbf{r}_{t,j}^p$ is the received signal vector for the p-th user at the receiver antenna j, $j = 1, \ldots, M$, for symbol t, $\mathbf{r}_{t,j}^p = [r_{t,j}^{p,1}, \ldots r_{t,j}^{p,q}, \ldots, r_{t,j}^{p,L}]^T$ and $r_{t,j}^{p,q}$ is the received signal for the p-th user at the q-th chip of the t-th symbol for j-th antenna.

4.2.2 Receiver Structure

In a downlink CDMA system, it was assumed that all the users have the same number of antennas and each user can detect all other user's information and suppress them in its receiver, just like a conventional multi-user detection. A block diagram of the proposed adaptive G-RAKE LSTC-CDMA receiver is shown in Figure 4.3. It consists of M receive antennas with K adaptive detector followed by N parallel soft-input soft output channel decoders. The received signals are first processed by the adaptive detector. The detector outputs, corresponding to the N transmitted antennas for each user, are then fed to the time and spatial deinterleavers, denoted by π^{-1} and $s\pi^{-1}$, respectively. The outputs of the deinterleavers are decoded by parallel MAP decoders. CCI and MAI interferences are cancelled by an iterative technique. The soft output of the MAP decoders, which have the same algorithm as the one in Chapter3, from all users are sent to the spatial and time interleavers, and then fed back to the adaptive MMSE detector. A soft estimate of a particular user's signals transmitted from a given antenna is obtained by cancelling the interference from other antennas and other users.

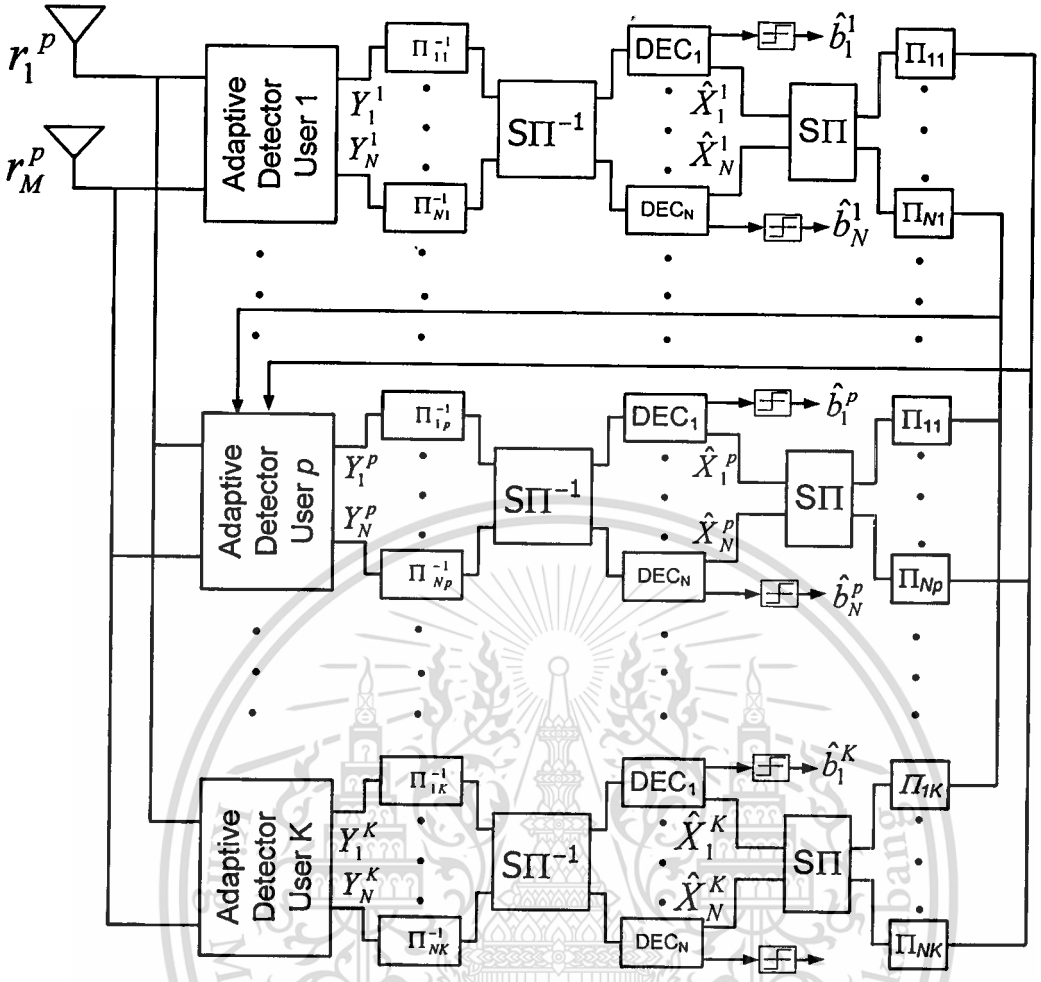

Figure 4.3 LSTC-CDMA receiver structure.

4.2.2.1 Time Domain Adaptive Generalized RAKE LSTC-CDMA Receiver

The block diagram of the adaptive iterative generalized RAKE LSTC-CDMA receiver for the p-th user is shown in Figure 4.4. In the proposed adaptive receiver structure, N sets of adaptive detector consist of M equalizers for the feed-forward filter and an equalizer for the feedback filter modules. An equalizer, employed in the proposed adaptive detector, is based on the adaptive detection algorithms such as: LMS, PFGLMS and RLS algorithms.

In order to determine a weight coefficient of each finger element, the proposed detector employs an adaptive G-RAKE structure and antenna array processing. The structure consists of a bank of U RAKE fingers, each correlating to a different delay of the received signal. Unlike the conventional RAKE receiver, the G-RAKE receiver benefits from using more fingers than the number of multipath.

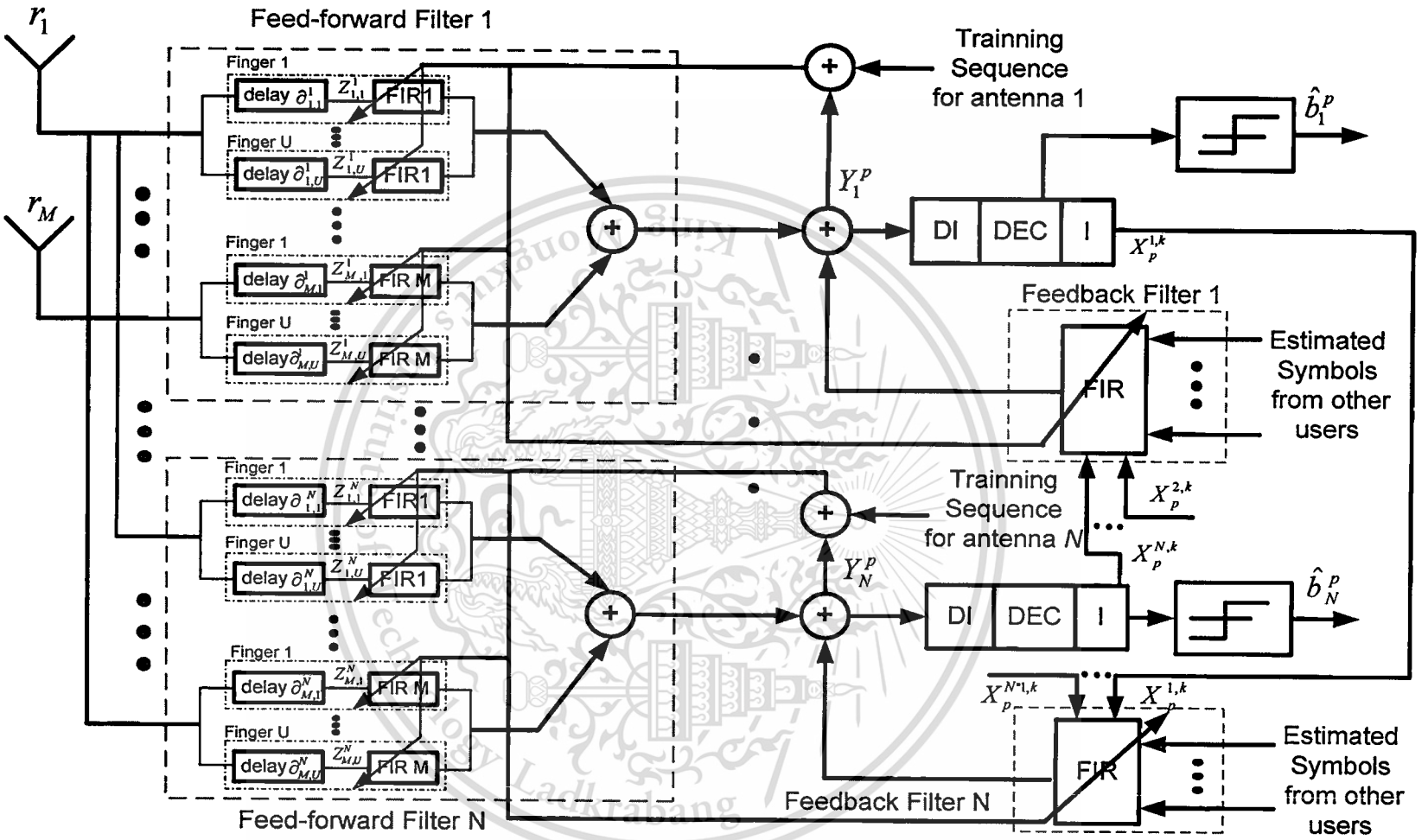

Figure 4.4 Block diagram of the time domain adaptive iterative G-RAKE LSTC-CDMA receiver.

The detector output for each layer is obtained from combining a feed-forward and a feedback filter output. In the iterative process, the feed-forward filter is compensated for the channel estimation error, and the feedback filter is used to cancel the interference from adjacent antennas and other users. In the first iteration, there are no estimated symbols from the decoders, and the feedback filter coefficients are zeros; thus, the feedback filter output is also zero. In the feed-forward filter, the M adaptive equalizers are used to estimate the channel coefficients and signature sequence for each layer of each user. The fingers outputs are used to combine with the signal from all receive antennas to form a decision statistic. Then, the equalizer outputs from all receive antennas are added to obtain a feed-forward filter output signal for each transmit antenna as shown in Fig. 4.4.

Let $\mathbf{w}_j^{p,k}(t)$ be an Lx1 feed-forward tap coefficients vector for the j-th receive antenna of the p-th user during the k-th iteration at symbol interval t and be given by:

$$\mathbf{w}_j^{p,k}(\mathrm{t})=[w_{t,j}^{p,k}(0),\ldots,w_{t,j}^{p,k}(q),\ldots,w_{t,j}^{p,k}(L\text{-}1)]^T \tag{4.6}$$

where $w_{t,j}^{p,k}(q)$ is the feed-forward tap coefficient corresponding to the q-th chip of the spreading sequence.

Let $\mathbf{w}_b^{i,k}(t)$ be the feedback filter coefficients of all users, except the i-th antenna of the p-th user, at symbol interval t in time domain, is expressed as:

$$\mathbf{w}_b^{i,k}(t)=[\mathbf{w}_{b,1}^{1,k}(t),\ldots,\mathbf{w}_{b,1}^{N,k}(t),\ldots,\mathbf{w}_{b,p}^{i,k}(t),\ldots,\mathbf{w}_{b,K}^{1,k}(t),\ldots,\mathbf{w}_{b,K}^{N,k}(t)]^T \tag{4.7}$$

where
$$\mathbf{w}_{b,p}^{i,k}(t)=[w_{b,p}^{1,k}(t),\ldots,w_{b,p}^{i-1,k}(t),w_{b,p}^{i+1,k}(t),\ldots,w_{b,p}^{N,k}(t)] \tag{4.8}$$

$\underline{\hat{\mathbf{x}}}_{t,p}^{i,k}$ is $(KN-1)\times 1$ vector of the estimated soft symbols, at the k-th iteration, from MAP decoders of every antenna of all users, except the i-th antenna of p-th user at symbol interval t, given by:

$$\underline{\hat{\mathbf{x}}}_{t,p}^{i,k}=(\hat{\mathbf{x}}_{t,1}^{1,k},\ldots,\hat{\mathbf{x}}_{t,1}^{N,k},\ldots,\hat{\mathbf{x}}_{t,p}^{i,k},\ldots,\hat{\mathbf{x}}_{t,K}^{1,k},\ldots,\hat{\mathbf{x}}_{t,K}^{N,k})^{\mathrm{T}} \tag{4.9}$$

where
$$\hat{\mathbf{x}}_{t,p}^{i,k}=(\hat{\mathbf{x}}_{t,p}^{1,k},\hat{\mathbf{x}}_{t,p}^{2,k},\ldots,\hat{\mathbf{x}}_{t,p}^{i\text{-}1,k},\hat{\mathbf{x}}_{t,p}^{i+1,k},\ldots,\hat{\mathbf{x}}_{t,p}^{N,k}) \tag{4.10}$$

The finger outputs are then combined to form a decision statistic. $\mathbf{z}_{t,j}^{p}$ is the finger outputs for u-th finger of p-th user at the receive antenna j and transmit antenna i for symbol t and be represented by:

$$\mathbf{z}_{t,j}^{p}=\mathrm{r}_{t,j}^{p}\,\delta(t-\partial_{j,u}^{i}) \tag{4.11}$$

The detected symbol of the p-th user obtained at the output of the adaptive detector for the i-th antenna during the k-th iteration at symbol interval t, denoted by $y_{t,p}^{i,k}$, is defined as:

$$y_{t,p,RAKE}^{i,k} = \sum_{j=0}^{M} \mathbf{w}_j^{i,k}(t)^H \mathbf{z}_{t,j}^{p} + \mathbf{w}_b^{i,k}(t)^H \hat{\underline{\mathbf{x}}}_{t,p}^{i,k} \tag{4.12}$$

The detector soft output $y_{t,p}^{i,k}$ in the time domain is then compared to training symbol, denoted by $\mathbf{x}_{t,p}^{i,k}$. The difference between them is calculated as the detection error. The detection error for the p-th user in the k-th iteration at symbol interval t, for i-th antenna, denoted by $e_{t,p}^{i,k}$, is represented by:

$$e_{t,p}^{i,k} = y_{t,p}^{i,k} - x_{t,p}^{i,k} \tag{4.13}$$

The detection error is then used to adapt the feed-forward filter and feedback filter tap coefficients in the time domain. After the Mean Square Error (MSE) approaches a specified value, the training mode is switched to the decision directed mode, in which the training sequence is replaced by the hard decision output of each user detector.

The values tap coefficients, $\mathbf{w}_b^{i,k}(t)$ in (4.6) and feedback filter tap coefficients, $\mathbf{w}_j^{p,k}(t)$ in (4.7) are calculated by minimizing the mean square error, defined as ζ, and given by

$$\zeta = mim\left(E\left|e_{t,p}^{i,k}\right|^2\right) = \min\left(E\left[\left|y_{t,p,RAKE}^{i,k} - x_{t,p}^{i,k}\right|^2\right]\right) \tag{4.14}$$

4.2.2.3 Frequency Domain Adaptive Generalized RAKE LSTC-CDMA Receiver

The block diagram of the adaptive G-RAKE LSTC-CDMA receiver for the p-th user in frequency domain system is shown in Figure 4.5 In the proposed adaptive receiver structure, N sets of adaptive detector consist of M equalizers for the feed-forward filter and an equalizer for the feedback filter modules. In the iterative process, the feed-forward filter is compensated for the channel estimation error, and the feedback filter is used to cancel the interference from adjacent antennas and other users. A frequency domain equalizer (FDE) is employed in the adaptive detector for both feed-forward and feedback filter. The FDE also uses adaptive detection algorithms for its adaptation process.

In order to determine a weight coefficient of each finger element, the proposed detector employs a G-RAKE structure. Unlike the conventional RAKE receiver, the G-RAKE receiver benefits from using more fingers than the number of multipath. Therefore, the structure also consists of a bank of U RAKE fingers, each correlating to a different delay of the received signal.

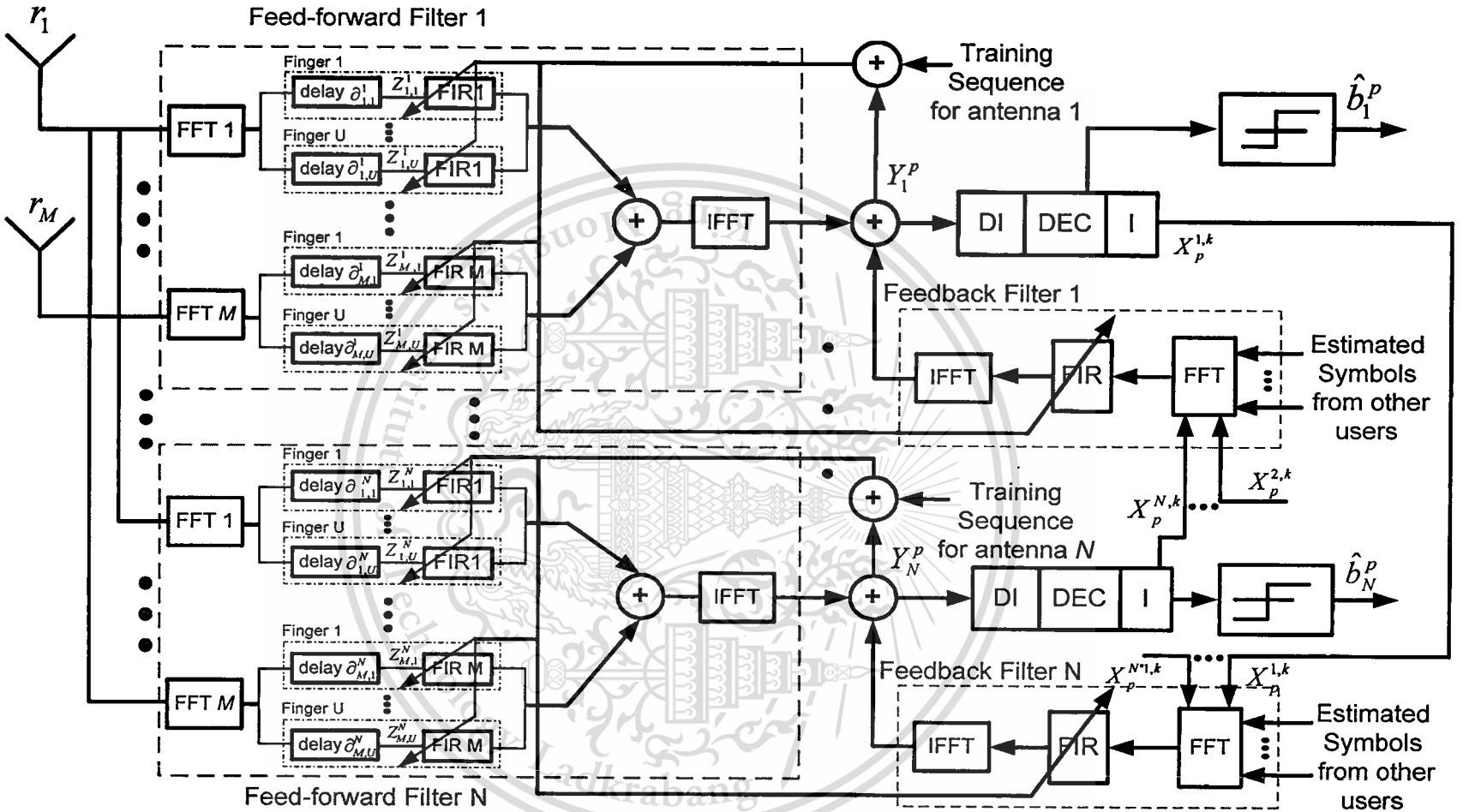

Figure 4.5 Block diagram of the frequency domain adaptive iterative G-RAKE LSTC-CDMA receiver.

Next, the detector outputs are passed to the time deinterleaver followed by the spatial-deinterleaver after the adaptation process. Then the spatial-deinterleaver outputs are encoded by parallel MAP decoders. If the system performance achieves a satisfactory level, the decoder soft outputs are then passed to a decision device to make a decision for the desired outputs; otherwise the iteration process is needed for further improvement in the interference suppression and cancellation. In the first iteration, there are no estimated symbols from the decoders, and the feedback filter coefficients are zeros; thus, the feedback filter output is also zero.

$\mathbf{z}_{t,j}^{p}$ is the finger outputs for u-th finger of p-th user at the receive antenna j and transmit antenna i for symbol t and be represented by:

$$\mathbf{z}_{t,j}^{p} = \mathbf{r}_{t,j}^{p}\delta(t-\partial_{j,u}^{i}) \tag{4.15}$$

where $\partial_{j,u}^{i}$ represents the delay of each finger u at receive antenna j and transmit antenna i and the received signals $\mathbf{r}_{t,j}^{p}$ is defined in (4.5).

Then, the outputs are transformed by using Fast Fourier transform (FFT) into frequency domain. The output of each FFT is defined by:

$$\Theta_{t,j}^{p} = fft\left(\mathbf{z}_{t,j}^{p}\right) \tag{4.16}$$

where $j = 1,\ldots,M$, $\Theta_{t,j}^{p}$ is the received signal of j-th receive antenna of p-th user in frequency domain, represented by

$$\Theta_{t,j}^{p} = \left[\Theta_{t,j}^{p,1},\ldots,\Theta_{t,j}^{p,q},\ldots,\Theta_{t,j}^{p,L}\right] \tag{4.17}$$

where

$$\Theta_{t,j}^{p,q} = \sum_{l=0}^{L-1} z_{t,j}^{p,l} e^{\frac{-j2\pi ql}{L}} \tag{4.18}$$

,and $fft(\cdot)$ is the fast Fourier transform function, and $\Theta_{t,j}^{p,q}$, q=1,…,L, is the FFT transformation of the received signal for the j-th receive antenna of the p-th user at the q-th chip of the t-th symbol.

$\mathbf{w}_{j}^{p,k}(t)$ is $L\times1$ feed-forward tap coefficient vector for the j-th receive antenna of the p-th user during the k-th iteration at symbol interval t, is given by

$$\mathbf{w}_{j}^{p,k}(\mathrm{t}) = [w_{t,j}^{p,k}(0),\ldots,w_{t,j}^{p,k}(q),\ldots,w_{t,j}^{p,k}(L\text{-}1)]^{T} \tag{4.19}$$

Let $\Psi_{t,j}^{p,k}$ represents the FFT of the feed forward filter tap coefficient vector of the p-th user for k-th iteration at the time t, at the receive antenna j, defined by

$$\Psi_{t,j}^{p,k} = fft\left(\mathbf{w}_{j}^{p,k}(t)\right) \tag{4.20}$$

$\Theta_{t,j}$ is then sent to the feed forward filter to perform the convolution with the feed forward tap coefficient $\Psi_{t,j}^{p,k}$ in the frequency domain. The output of each feed forward filter is combined together and is denoted by

$$\overline{\mathbf{F}}_{t,p}^{i,k} = \left(\sum_{j=1}^{M} diag\left(\Theta_{t,j}^{p}\right)^{H} \Psi_{t,j}^{p,k} \right) \tag{4.21}$$

where $diag(\cdot)$ and $(\cdot)^{H}$ denoted a diagonal matrix and a conjugate transpose function respectively.

Next, $\overline{\mathbf{F}}_{t,p}^{i,k}$ is transformed back into the time domain by the inverse FFT (IFFT). The feed forward filter output of p-th user in the k-th iteration at time t, for layer i, is given by

$$F_{t,p}^{i,k} = \mathbf{I}_{\mathbf{F}} \cdot \hat{F}_{t,p}^{i,k} \tag{4.22}$$

where $\mathbf{I}_F = [1 \ \mathbf{0}_{L-1}]$, $\mathbf{0}_{L-1}$ is a row vector of length L-1 containing all zero, and $\hat{F}_{t,p}^{i,k} = ifft(\overline{\mathbf{F}}_{t,p}^{i,k})$.

To cancel MAI and CCI, the estimated symbols from the outputs of the decoders are first input to the feedback filter and transformed into frequency domain by using the FFT. The output of the FFT is represented by

$$\Lambda_{t,p}^{i,k} = fft(\underline{\hat{\mathbf{x}}}_{t,p}^{i,k}) \tag{4.23}$$

$\underline{\hat{\mathbf{x}}}_{t,p}^{i,k}$ is an $(KN-1)\times 1$ vector of the estimated soft symbols, at the k-th iteration, from MAP decoders of all antennas of all users, excluding the j-th antenna of the p-th user, given by

$$\underline{\hat{\mathbf{x}}}_{t,p}^{i,k} = \left(\hat{\mathbf{x}}_{t,1}^{1,k}, \ldots, \hat{\mathbf{x}}_{t,1}^{N,k}, \ldots, \hat{\mathbf{x}}_{t,p}^{i,k}, \ldots, \hat{\mathbf{x}}_{t,K}^{1,k}, \ldots, \hat{\mathbf{x}}_{t,K}^{N,k} \right)^{\mathrm{T}} \tag{4.24}$$

$\mathbf{w}_{b}^{i,k}(t)$ is the feedback filter coefficients of all user except the j-th antenna of the p-th user, given by

$$\mathbf{w}_{b}^{i,k}(t) = [\mathbf{w}_{b,1}^{1,k}(t), \ldots, \mathbf{w}_{b,1}^{N,k}(t), \ldots, \mathbf{w}_{b,p}^{i,k}(t), \ldots, \mathbf{w}_{b,K}^{1,k}(t), \ldots, \mathbf{w}_{b,K}^{N,k}(t)]^{T} \tag{4.25}$$

Let $\Psi_{t,b,p}^{i,k}$ represents the FFT of $\underline{\hat{w}}_{b,p}^{i,k}(t)$, is defined by

$$\Psi_{t,b,p}^{i,k} = fft\left(\mathbf{w}_{b}^{i,k}(t)\right) \tag{4.26}$$

The output of the FFT, as denoted as $\Lambda_{t,p}^{i,k}$ in (4.23), is then input to the feedback filter to perform convolution with the feedback tap coefficients $\Psi_{t,b,p}^{k}$ in (4.26) in frequency domain. Hence, the feedback filter output signals, defined by

$$\overline{\mathbf{F}}_{t,b,p}^{i,k} = \left(diag\left(\Lambda_{t,p}^{i,k\ H}\right) \cdot \Psi_{t,b,p}^{i,k} \right) \tag{4.27}$$

and then transformed back into time domain by IFFT. The feedback filter output is given by

$$F_{t,b,p}^{i,k} = \mathbf{I}_B \cdot ifft(\overline{\mathbf{F}}_{t,b,p}^{i,k}) \tag{4.28}$$

where $\mathbf{I}_B$ =[1 $\mathbf{0}_{KN-1}$] and $\mathbf{0}_{KN-1}$ is a zero row vector with length of KN-1, and $\hat{F}_{t,b,p}^{i,k} = ifft(\overline{\mathbf{F}}_{t,b,p}^{i,k})$.

The detected symbol of the p-th user obtained in the k-th iteration at time t, for layer i, denoted by

$$y_{t,p,RAKE}^{i,k} = F_{t,p}^{i,k} + F_{t,b,p}^{i,k} \tag{4.29}$$

where $F_{t,p}^{i,k}$ and $F_{t,b,p}^{i,k}$ represent feed forward and feedback filter output in time domain, given in (4.22) and (4.28) respectively. Note that the output of the feedback filter is zero at the first iteration.

The values of $\mathbf{w}_j^{p,k}(t)$ in (4.19) and $\mathbf{w}_b^{i,k}(t)$ in (4.25) are calculated by minimizing the mean square error, defined as

$$\zeta = \mathrm{Min}\left(E\left[\left|y_{t,p,RAKE}^{i,k} - x_{t,p}^{i,k}\right|^2\right]\right) \tag{4.30}$$

4.2.2.3 Adaptive Detection Algorithms

The modified feed-forward in (4.19) and feedback (4.25) tap coefficients of the LMS, PFGLMS, and RLS algorithm for frequency domain adaptive G-RAKE CDMA detector can be expressed as:

LMS algorithm

$$\begin{aligned}\mathbf{w}_j^{p,k}(t+1) &= \mathbf{w}_j^{p,k}(t) + \mu_f e_{t,p}^{i,k}\mathbf{z}_{t,j}^{p} \\ \mathbf{w}_b^{i,k}(t+1) &= \mathbf{w}_b^{i,k}(t) + \mu_b e_{t,p}^{i,k}\underline{\hat{\mathbf{x}}}_{t,p}^{i,k}\end{aligned} \tag{4.31}$$

where μ_f and μ_b are the step sizes for the feed-forward and feedback adaptation.

PFGLMS algorithm

$$\begin{aligned}\mathbf{w}_f^{i,k}(t+1) &= \mathbf{w}_f^{i,k}(t) + \mu_f \mathbf{g}_f^{i,k}(t) \\ \mathbf{g}_f^{i,k}(t) &= e(t)\mathbf{z}_{t,j}^{p} + \hat{\mathbf{g}}_f^{i,k}(t) \\ \hat{\mathbf{g}}_f^{i,k}(t) &= \lambda_f \hat{\mathbf{g}}_f^{i,k}(t-1) + \gamma_f e(t)\mathbf{z}_{t,J}^{p}\end{aligned} \tag{4.32}$$

$$\begin{aligned}\mathbf{w}_b^{i,k}(t+1) &= \mathbf{w}_b^{i,k}(t) + \mu_b \mathbf{g}_b^{i,k}(t) \\ \mathbf{g}_b^{i,k}(t) &= e(t)\underline{\hat{\mathbf{x}}}_{t,p}^{i,k} + \hat{\mathbf{g}}_b^{i,k}(t) \\ \hat{\mathbf{g}}_b^{i,k}(t) &= \lambda_b \hat{\mathbf{g}}_b^{i,k}(t-1) + \gamma_b e(t)\underline{\hat{\mathbf{x}}}_{t,p}^{i,k}\end{aligned} \tag{4.33}$$

where (λ_f, λ_b) and (γ_f, γ_b) are the forgetting factors and the scaling factors of feed-forward and feedback adaptation respectively, and $\hat{\mathbf{g}}_f^{i,k}(0) = \hat{\mathbf{g}}_b^{i,k}(0) = 0$.

RLS algorithm

$$\begin{aligned}
\mathbf{w}_j^{p,k}(t+1) &= \mathbf{w}_j^{p,k}(t) + \mathbf{g}_j^{p,k}(t+1)e(t) \\
\mathbf{g}_j^{p,k}(t+1) &= \frac{\mathbf{U}_j^{p,k}(t)\mathbf{z}_{t,j}^{p}}{\lambda_f + \mathbf{z}_{t,j}^{p\,T}\mathbf{U}_j^{p,k}(t)\mathbf{z}_{t,j}^{p}} \\
\mathbf{U}_j^{p,k}(t) &= \lambda_f^{-1}[\mathbf{U}_j^{p,k}(t-1) - \mathbf{g}_j^{p,k}(t)\mathbf{z}_{t,j}^{p\,T}\mathbf{U}_j^{p,k}(t-1)]
\end{aligned} \tag{4.34}$$

$$\begin{aligned}
\mathbf{w}_b^{p,k}(t+1) &= \mathbf{w}_b^{p,k}(t) + \mathbf{g}_b^{p,k}(t+1)e(t) \\
\mathbf{g}_b^{p,k}(t+1) &= \frac{\mathbf{U}_b^{p,k}(t)\hat{\underline{\mathbf{x}}}_{t,p}^{i,k}}{\lambda_b + \hat{\underline{\mathbf{x}}}_{t,p}^{i,k\,T}\mathbf{U}_b^{p,k}(t)\hat{\underline{\mathbf{x}}}_{t,p}^{i,k}} \\
\mathbf{U}_b^{p,k}(t) &= \lambda_b^{-1}[\mathbf{U}_b^{p,k}(t-1) - \mathbf{g}_b^{p,k}(t)\hat{\underline{\mathbf{x}}}_{t,p}^{i,k\,T}\mathbf{U}_b^{p,k}(t-1)]
\end{aligned} \tag{4.35}$$

where (λ_f, λ_b) are the forgetting factor of feed-forward and feedback adaptation respectively. The initializations of RLS algorithm are:

- $\mathbf{w}(0) = 0$
- $\mathbf{U}(0) = \delta^{-1} I$

where δ is the inverse of the input signal power estimate and the recommended value is $\delta > 100\sigma^2$, I is the $(p+1)$ by $(p+1)$ identity matrix and p is the filter order.

4.3 Conclusion

In order to improve the network capacity and cancel the interferences of wireless communications systems, the adaptive Generalized RAKE receiver for LSTC-CDMA systems in both time and frequency domain is presented in this chapter. The proposed receiver is based on the Least Means Square (LMS), the Partially Filtered Gradient LMS (PFGLMS) and the Recursive Least Squares (RLS) algorithms. Due to the higher reliability of the Co-Channel Interference (CCI) and Multiple Access Interference (MAI) estimation, the G-RAKE LSTC-CDMA receiver can effectively not only suppress the CCI and MAI using the interference suppression and cancellation techniques but also mitigate the effect of multipath of fading channel. The system performances of the proposed receivers are investigated in multipath Rayleigh fading channels, which are presented in Chapter 5.

Chapter 5

Simulation Results and Performance Analysis

In this chapter, the system performances of adaptive iterative LSTC-CDMA receiver and adaptive G-RAKE LSTC-CDMA receiver are quantified through the simulation results whereby the performances results have been compared to each other. The performances of the systems are evaluated in not only slow but also fast multipath Rayleigh fading channels. Consequently, the proposed adaptive detectors; based on the least means square (LMS), the partially filtered gradient LMS (PFGLMS), and the recursive least squares (RLS) algorithms; were investigated in both time and frequency domain. The results show that the system performances of adaptive G-RAKE receiver outperformed to the one of adaptive iterative receiver. Moreover, the RLS based receiver yields much faster convergence speed and has better tracking ability than that of PFGLMS and LMS. The simulation results also prove that the performance results of the proposed receiver in frequency domain system achieve the same performance as the one in time domain system. The simulation systems and parameters are firstly presented. Then, the performance results of adaptive iterative LSTC-CDMA receiver are described and followed by the simulation results of adaptive G-RAKE LSTC-CDMA receiver. Finally, the performance of both proposed receivers are compared to each other.

5.1 Simulation Systems and Parameters

The system models of both adaptive iterative LSTC-CDMA receiver and adaptive G-RAKE LSTC-CDMA receiver utilize the layered space-time coding (LSTC) system structure with the selected components as show in Table 5.1.

Table 5.1 Simulation systems.

Components	**Selected Components**
Encoder	Convolutional Code
Decoder	MAP
Modulator	BPSK
Spreading Codes	Gold sequence
Interleaver	Random Interleaving
Channels Model	Rayleigh Fading Channels
Noise Channels	AWGN

Table 5.2 Simulation parameters.

Number of transmit antenna (N)	**2, 4**
Number of receive antenna (M)	**2, 4**
Number of users (K)	**5**
Number of iteration (I)	**20**
Number of multipath fading (NM)	**3**
Number of Spreading sequences (L)	**7**

The simulation parameters are summarized in Table 5.2. The constituent codes are nonsystematic convolutional codes with the code rate R of 1/2 and memory order of 3. The spreading sequence is a gold sequence with processing gain of 7. The proposed system is simulated with 2 and 4 transmit and receive antennas with multipath fading of 3 and with 130 information bits in each frame per layer for each user. Each layer consists of 266 encoded symbols per frame. The data rate is 1 Mb/s at the carrier frequency, f_c, of 2 GH_z. The simulation results are represented in terms of average BER versus the ratio of averaged energy per bit, denoted by *Eb*, to the power spectral density of the AWGN, denoted by *No*.

5.2 System Performances Results

5.2.1 Adaptive Iterative LSTC-CDMA Receiver

The simulation results for the adaptive iterative LSTC-CDMA receiver with BPSK modulation in both time and frequency domain systems are presented in this section. The system operates in the training mode until the mean square error (MSE) approaches the minimum mean square error (MMSE), then it switches to the decision directed mode.

5.2.1.1 Time Domain Systems

In this section, the simulation results of the proposed adaptive iterative receiver in time domain systems are depicted in slow and fast Rayleigh fading channels.

a. Slow and Quasi Static Fading Channel

The slow fading channel is modeled as a quasi-static fading channel, where each fading coefficients is constant within a frame but changes from one frame to another.

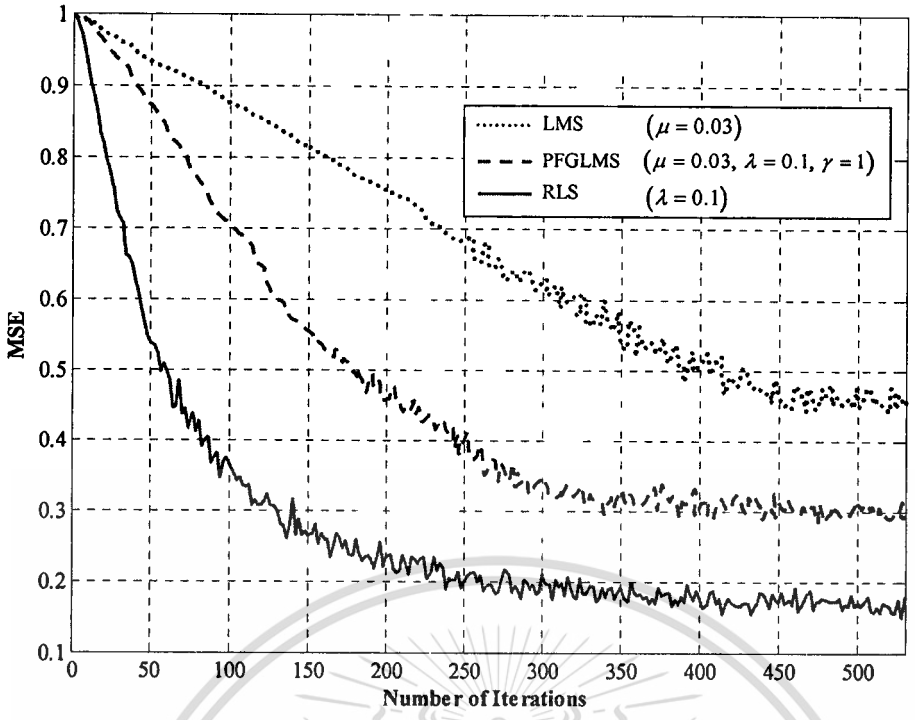

Figure 5.1 The convergence speed comparisons of time domain adaptive iterative LSTC-CDMA receiver in a quasi-static Rayleigh fading channel with a 2x2 antennas system.

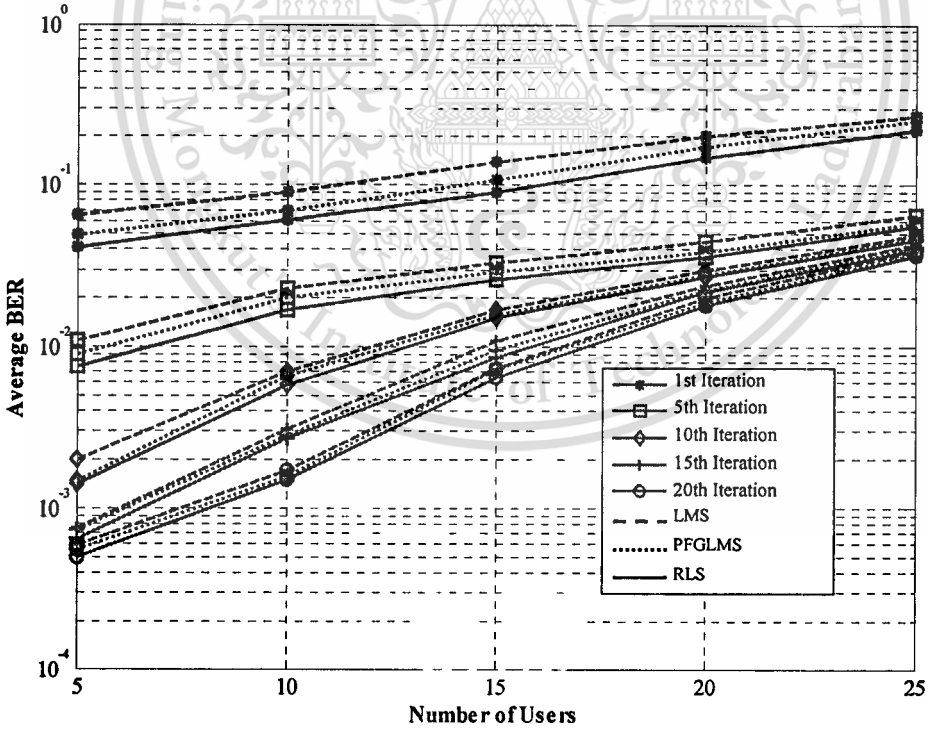

Figure 5.2 Number of users of time domain adaptive iterative LSTC-CDMA receiver in a quasi-static Rayleigh fading channel with a 2x2 antennas system.

The convergence speed comparison of the proposed adaptive iterative LSTC-CDMA receiver for 2x2 antenna sytems, based on LMS, PFGLMS, and RLS detection algorithms, is showed in Figure 5.1. The figure shows that the convergence speed of RLS algorithm is about two times faster than that of PFGLMS and four times faster than that of LMS algorithms.

The number of users of the time domain adaptive iterative LSTC-CDMA receiver for 2x2 antennas system at E_b/N_o equal to 16 dB is shown in Figure 5.2. The proposed adaptive detector is based on LMS, PFGLMS and RLS algorithms. The simulation results show that at the number of users equal to 15 and iterations equal to 5, the BER of LMS based receiver is 3.40×10^{-2}, the BER of PFGLMS based receiver is 3.00×10^{-2} and the BER of RLS based receiver is 2.70×10^{-2}. These results also show that when the number of users increases, a higher number of iteration is required to achieve the same BER. For example, the RLS based receiver requires 5 iterations to achieve a BER of 2.70×10^{-2} for 15 users while it requires 10 iterations to achieve the same BER for 20 users.

The performances of 2x2, 2x4, 4x2 and 4x4 antennas systems of adaptive iterative LSTC-CDMA receiver for 5 users under time domain approach are depicted in Figure 5.3, Figure 5.4, Figure 5.5 and Figure 5.6 as below respectively. The result shows that the performances of the proposed receiver have a significant improvement in the first iteration and gradually improves for the higher iterations. These four BER curves also show that the proposed RLS iterative receiver has an excellent tracking ability in the scattering environment than that of PFGLMS and LMS.

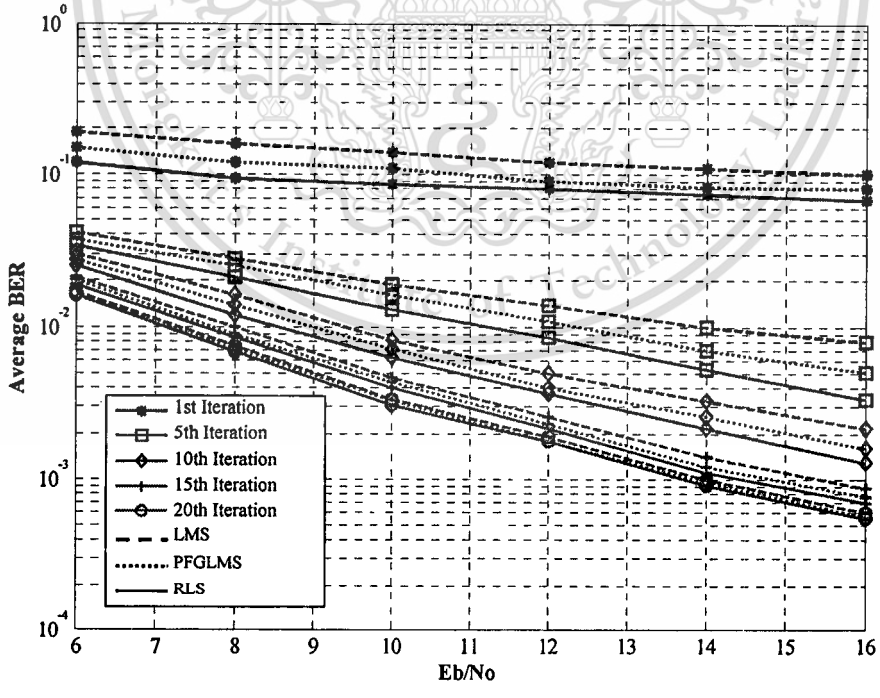

Figure 5.3 The BER performance of time domain adaptive iterative LSTC-CDMA receiver in a quasi-static Rayleigh fading channel with a 2x2 antennas system.

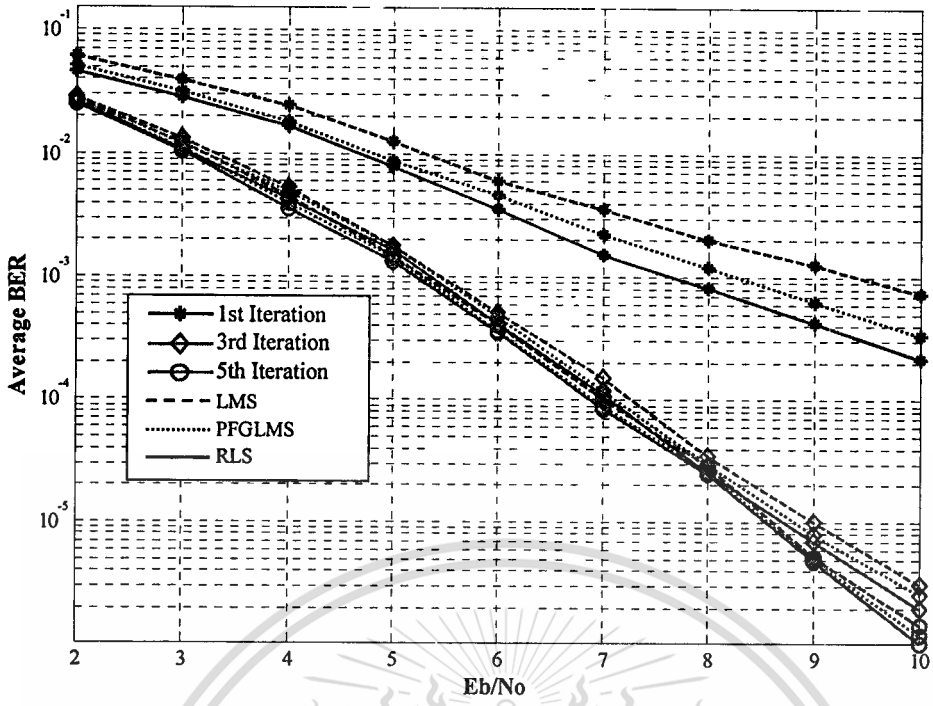

Figure 5.4 The BER performance of time domain adaptive iterative LSTC-CDMA receiver in a quasi-static Rayleigh fading channel with a 2x4 antennas system.

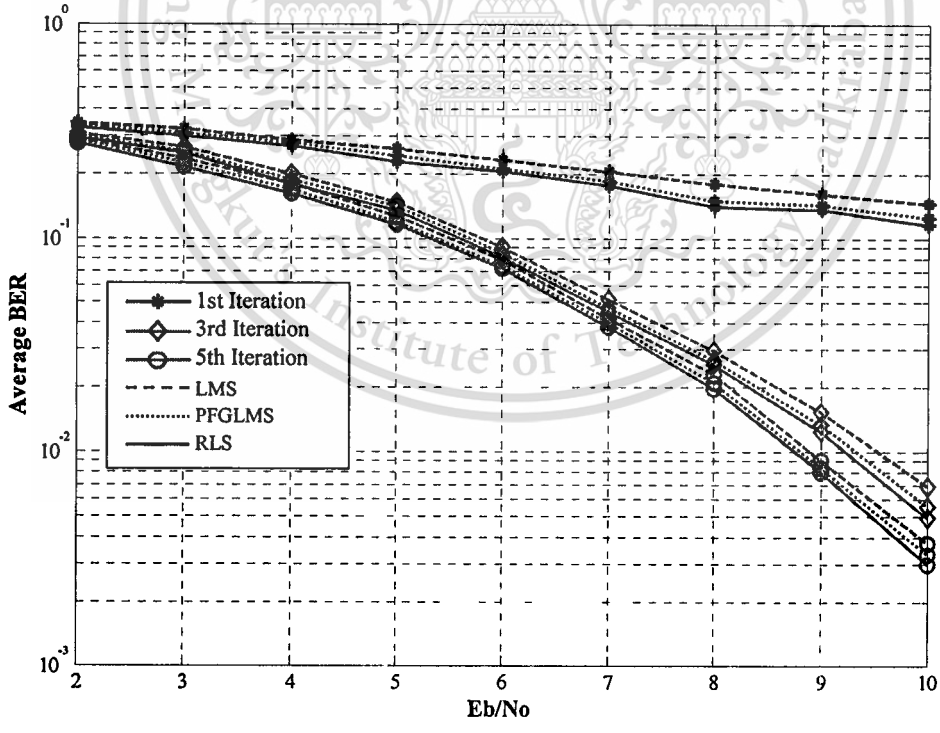

Figure 5.5 The BER performance of time domain adaptive iterative LSTC-CDMA receiver in a quasi-static Rayleigh fading channel with a 4x2 antennas system.

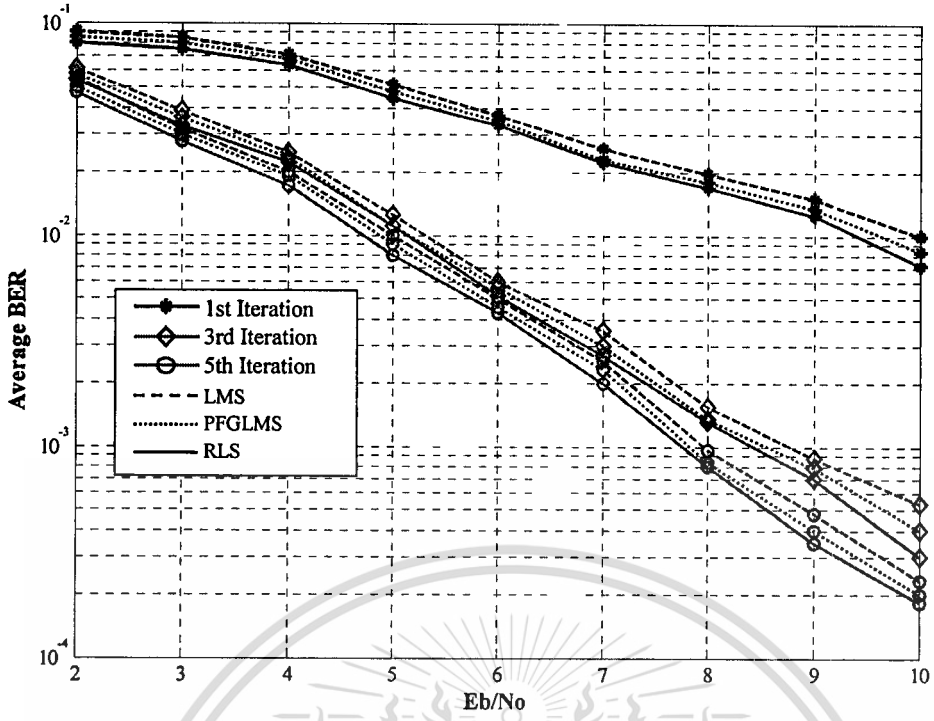

Figure 5.6 The BER performance of time domain adaptive iterative LSTC-CDMA receiver in a quasi-static Rayleigh fading channel with a 4x4 antennas system.

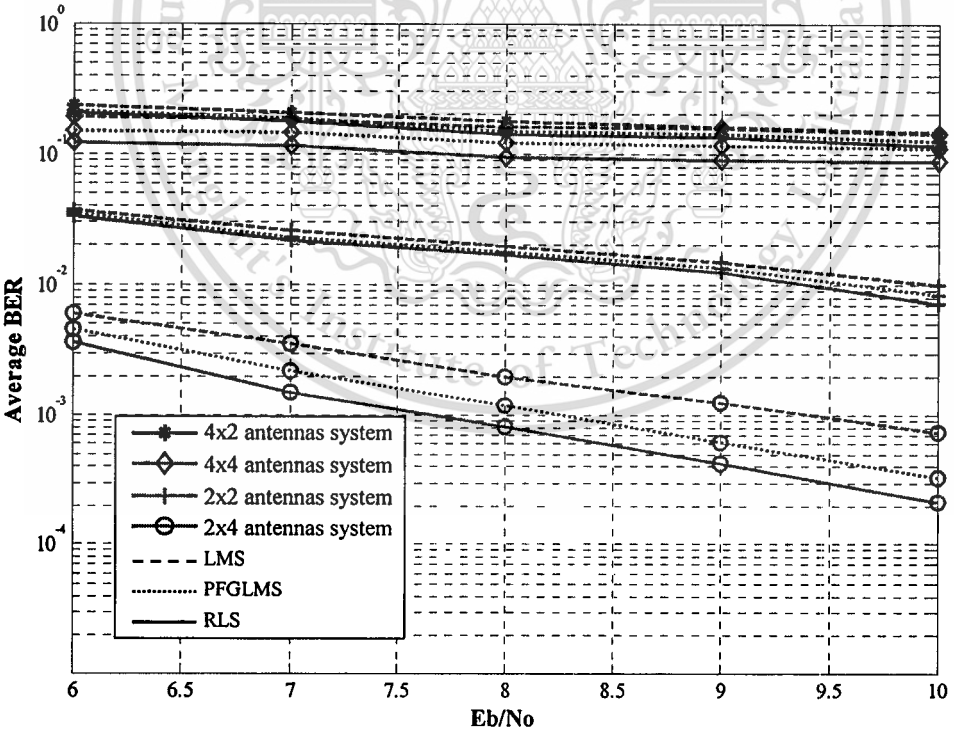

Figure 5.7 The BER performances comparisons of time domain adaptive iterative LSTC-CDMA receiver in a quasi-static Rayleigh fading channel at 1st iteration.

Figure 5.7 presents the comparisons of BER performances between 2x2, 2x4, 4x2 and 4x4 antennas systems of proposed adaptive iterative LSTC-CDMA system in a time domain quasi-static Rayleigh fading channel at the first Iteration. Since the system with 4x2 antennas utilizes more transmit antennas, the interference caused by other transmit antennas is increased corresponding to the number of transmit antennas in use. Consequently, the performance of the system of 4x2 antennas is decreased compared to other three antennas system. On the other hand, when the number of receive antennas are increased more than the transmit antennas; the ability to track errors and cancel interference is also increase. Hence, the 2x4 antennas system achieve the best performance.

b. Fast Fading

In the fast fading channel, the fading coefficients are constant within each symbol period and vary from one symbol to another. The performance of the 2x2 adaptive iterative LSTC-CDMA receiver at various fading rates based on LMS, PFGLMS and RLS algorithms are shown in Figure 5.8, Figure 5.9 and Figure 5.10 respectively. The results show that the average BER decreases when the fading rate is increased. When the fading rate is increased, the inputs to the MAP decoder are less correlated and the decoder has a better performance. However, the adaptive LSTC-CDMA detector is sensitive to the channel estimation accuracy [32]. Therefore, the average BER of the proposed adaptive iterative receiver is increased because of inaccurate channel estimation in the fast fading channel.

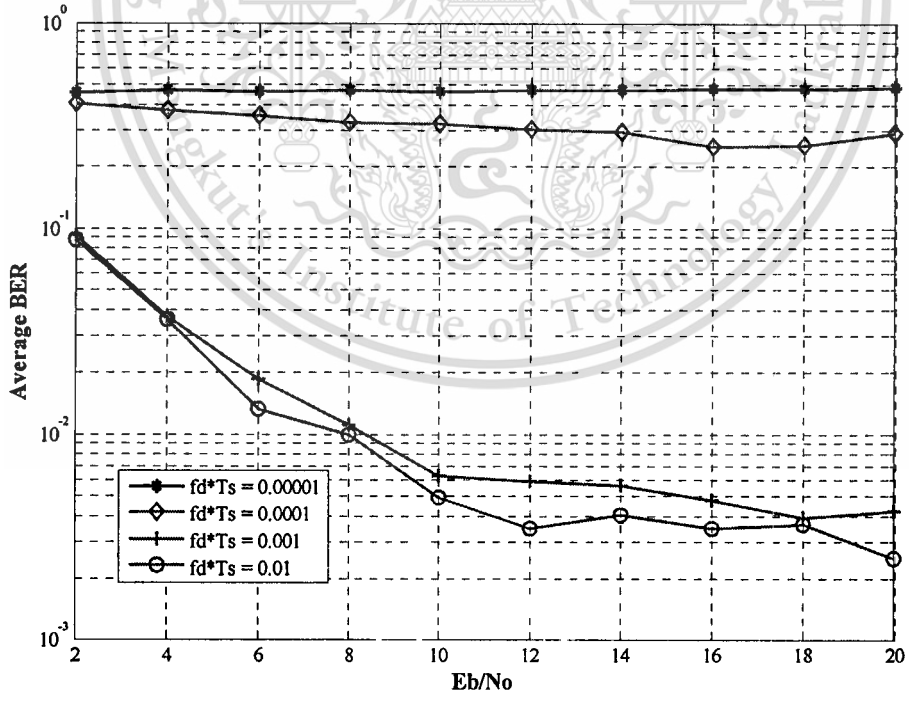

Figure 5.8 Performances of the time domain adaptive iterative LSTC-CDMA receiver in various normalized fading rates based on LMS algorithms.

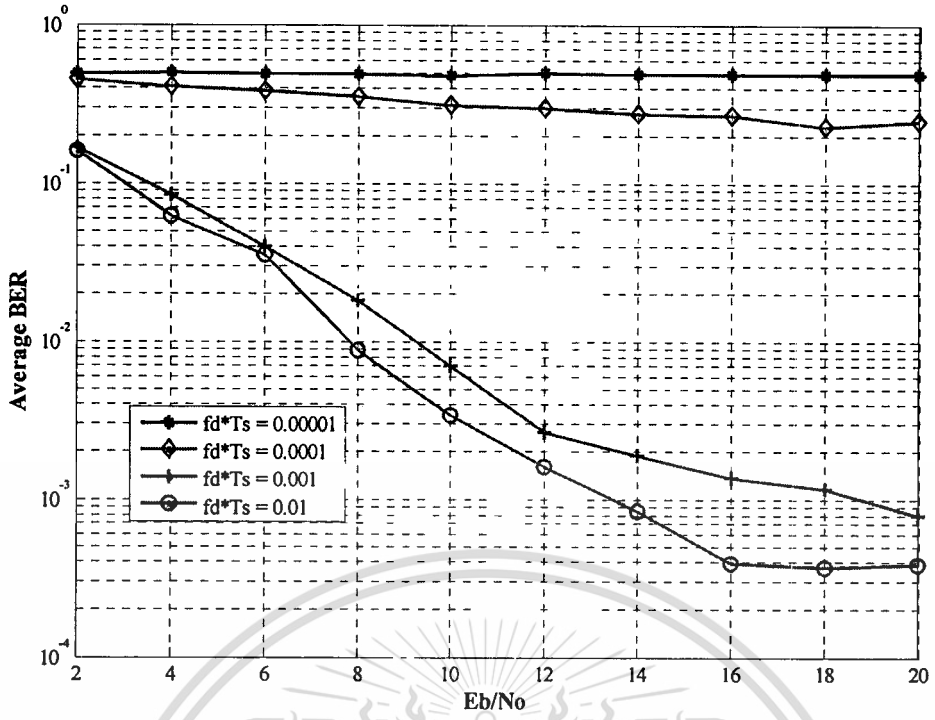

Figure 5.9 Performances of the time domain adaptive iterative LSTC-CDMA receiver in various normalized fading rates based on PFGLMS algorithms.

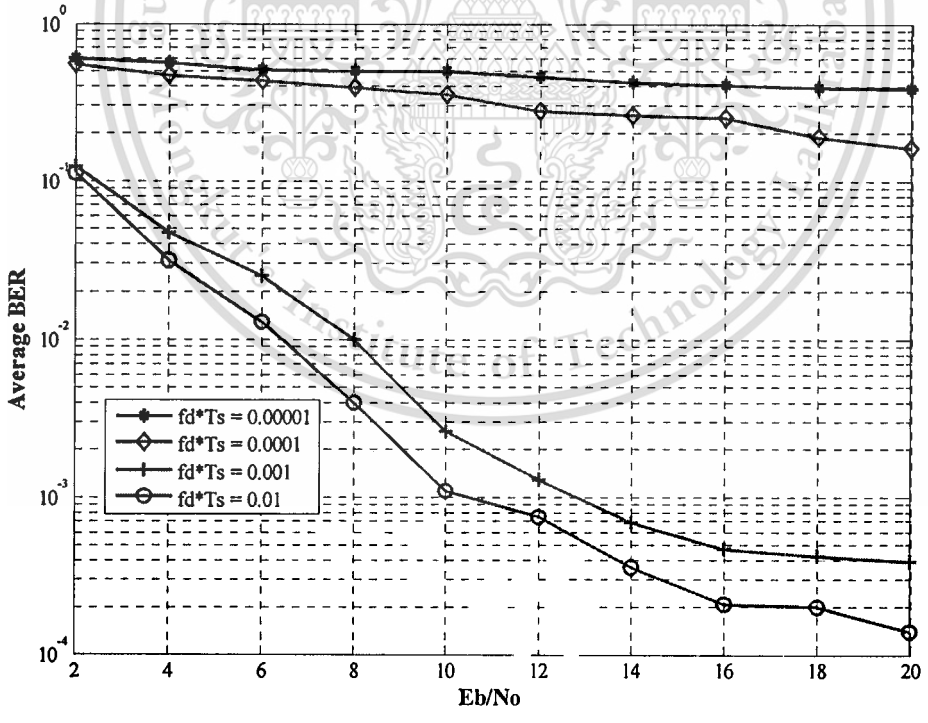

Figure 5.10 Performances of the time domain adaptive iterative LSTC-CDMA receiver in various normalized fading rates based on RLS algorithms.

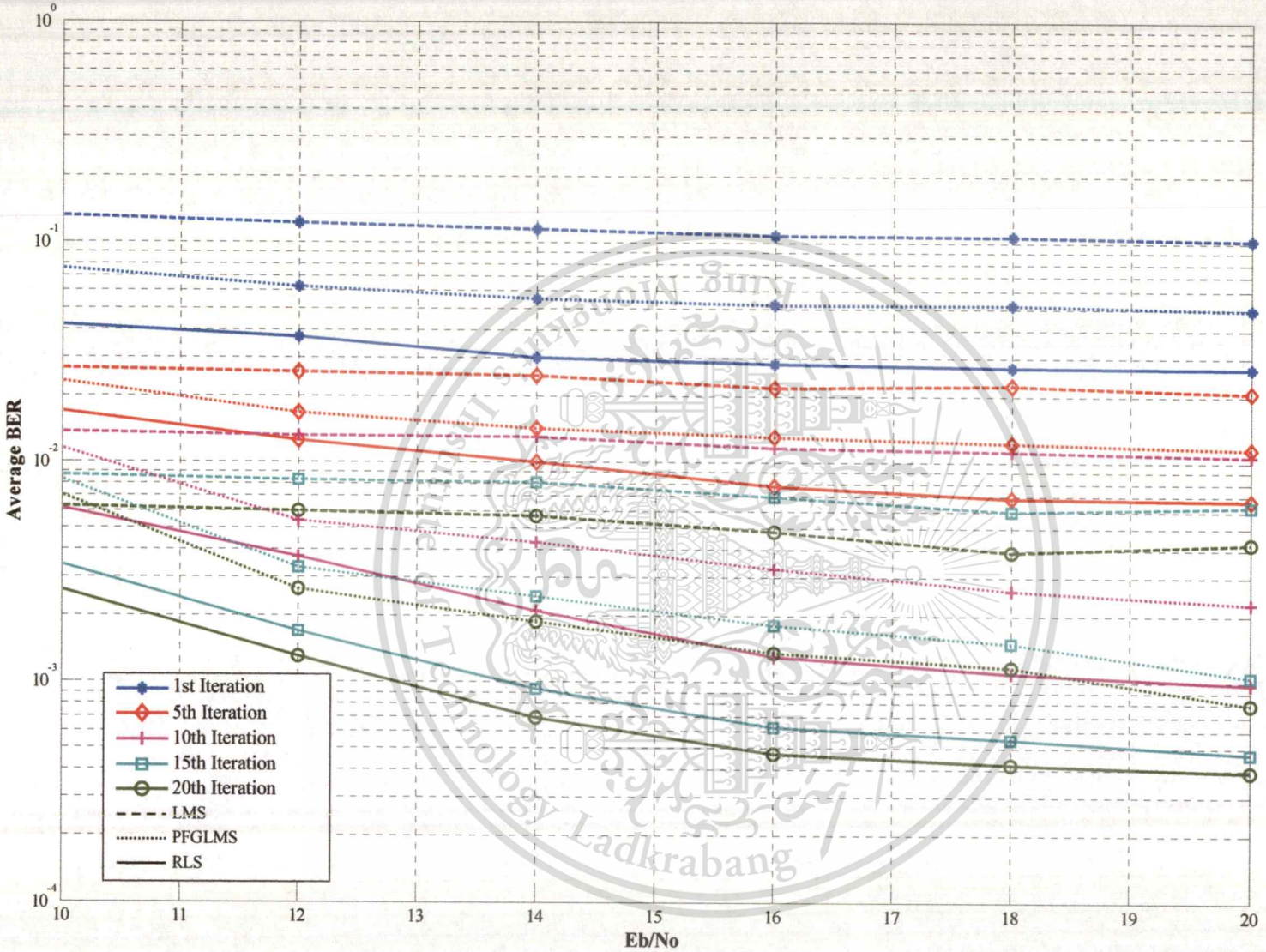

Figure 5.11 Performances comparisons of the time domain adaptive iterative LSTC-CDMA receiver at 0.001 normalized fading rates.

Figure 5.11 presents the comparison of the LMS, PFGLMS and RLS receivers at the normalized fading rate of 0.001 for 2x2 antennas sytem. The result shows that the RLS algorithm has good tracking ability compared to the PFGLMS and LMS algorithms on a fast fading channel. The average BER of the RLS receiver is the smallest since the first iteration until 20th Iteration. Therefore, the RLS receiver is more convenient for the fast fading channels.

5.2.1.2 Frequency Domain Systems

The performances comparisons of the proposed adaptive iterative LSTC-CDMA receiver in frequency domain by comparing to those of time domain system are presented in this section. The average BER of the time and frequency domain LMS, PFGLMS and RLS adaptive iterative LSTC-CDMA receiver of a 2 x2 MIMO system for various numbers of iterations is shown in Figure 5.12, Figure 5.13 and Figure 5.14 respectively. The results show that the performances of the time and frequency domain approach are identical. The system performance is significantly improved for the second iteration compared to the first iteration and gradually increases for higher iterations. The BER curves also show that the performances of both time and frequency domain system converge to a steady state after the fifth iteration and can achieve the interference free single user performance for a high signal to noise ratio (SNR).

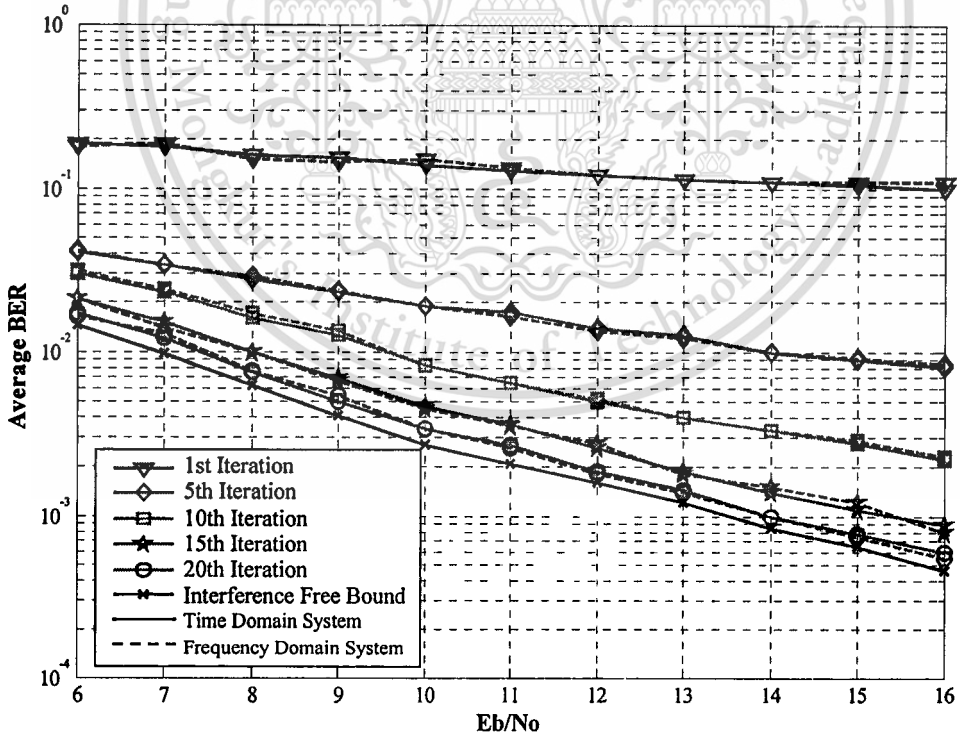

Figure 5.12 The BER Comparison of the adaptive iterative LSTC-CDMA receiver in time and frequency domain system, based on LMS algorithm.

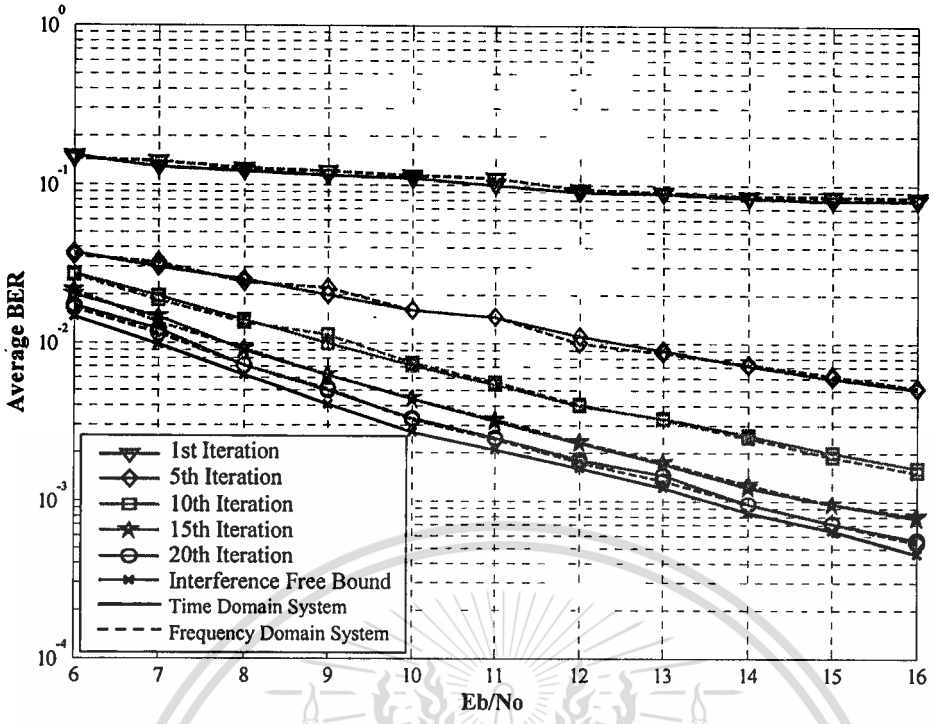

Figure 5.13 The BER comparison of the adaptive iterative LSTC-CDMA receiver in time and frequency domain system, based on PFGLMS algorithm.

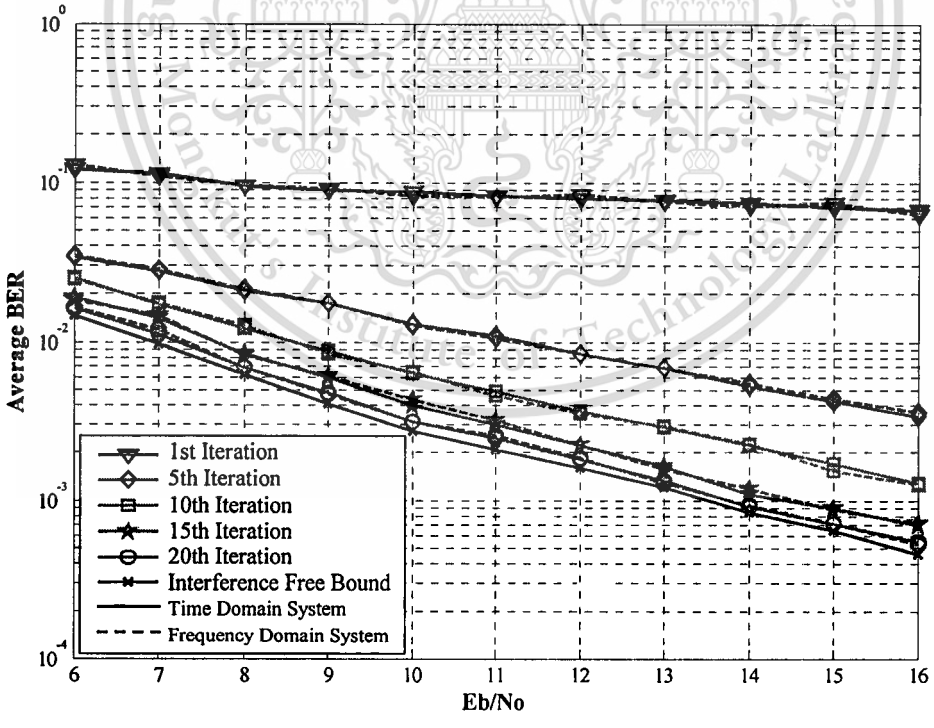

Figure 5.14 The BER comparison of the adaptive iterative LSTC-CDMA receiver in time and frequency domain system, based on RLS algorithm.

5.2.2 Adaptive Generalized RAKE LSTC-CDMA Receiver

The simulation results of the proposed adaptive G-RAKE LSTC-CDMA receiver in both time and frequency quasi-static Rayleigh fading channel for 2x2 antennas system are presented in detail in this section. Moreover, the 3 fingers and 6 finger RAKE receivers are simulated and compared to each other. The proposed G-RAKE receiver is also based on LMS, PFGLMS and RLS algorithm same as the adaptive iterative receiver.

5.2.2.1 Time Domain Systems

The performance of 2x2 adaptive G-RAKE LSTC-CDMA receiver, with 3 multipaths for 5 users, based on LMS, PFGLMS and RLS are depicted in Figure 5.15, Figure 5.16 and Figure 5.17. The BER curves show that the proposed G-RAKE receiver using 6 fingers outperforms the one using 3 fingers. This proves that the system performance improves when additional finger is placed at a delay; which is corresponds to no multipath component.

The number of users for adaptive G-RAKE receivers is shown in Figure 5.18, Figure 5.19 and Figure 5.20. These results also show that when the number of users increases, a higher number of iteration is required to achieve the same BER.

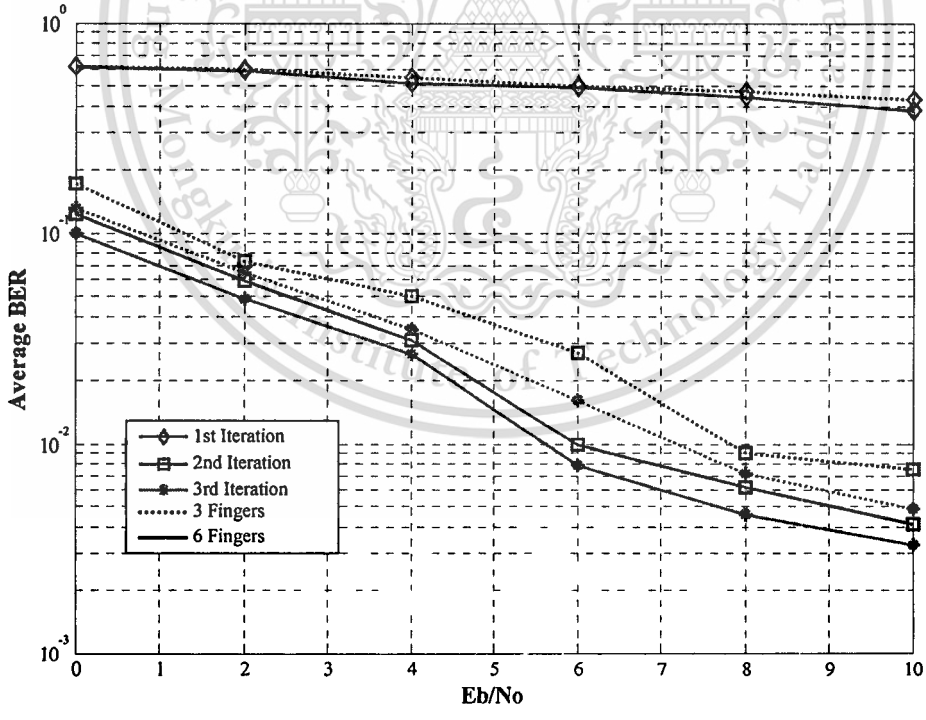

Figure 5.15 BER of time domain adaptive G-RAKE LSTC-CDMA receiver based on LMS algorithms.

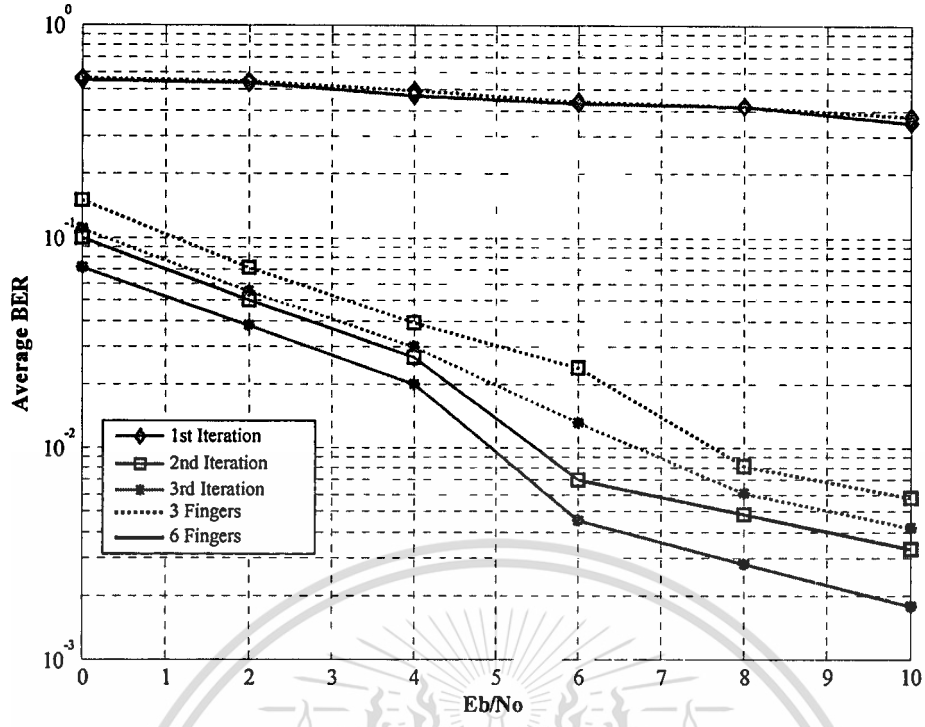

Figure 5.16 BER of time domain adaptive G-RAKE LSTC-CDMA receiver based on PFGLMS algorithms.

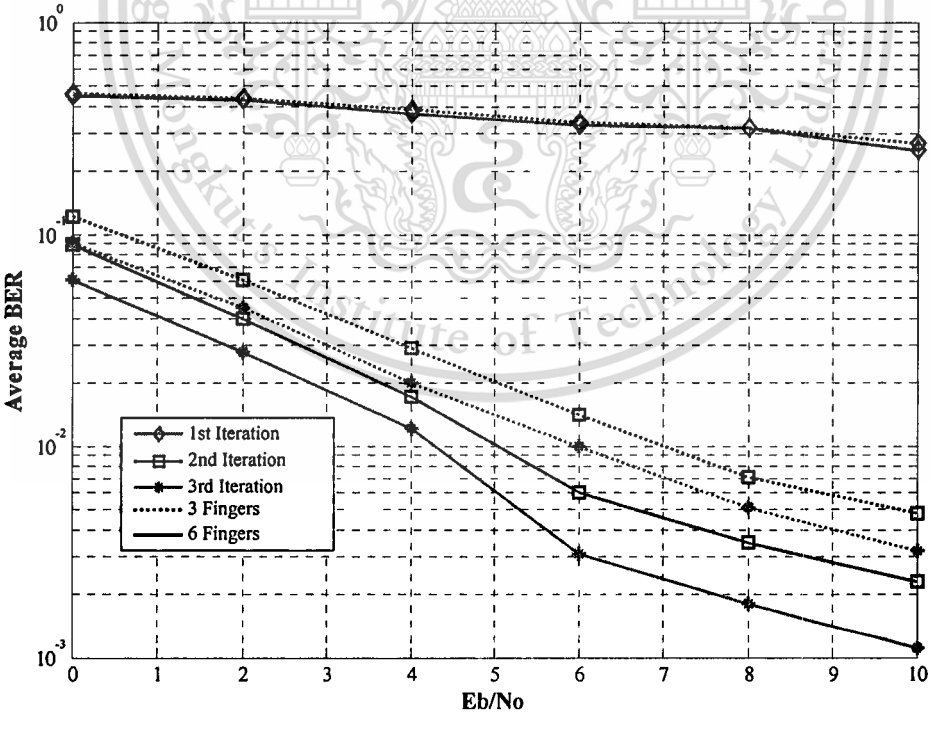

Figure 5.17 BER of time domain adaptive G-RAKE LSTC-CDMA receiver based on RLS algorithms.

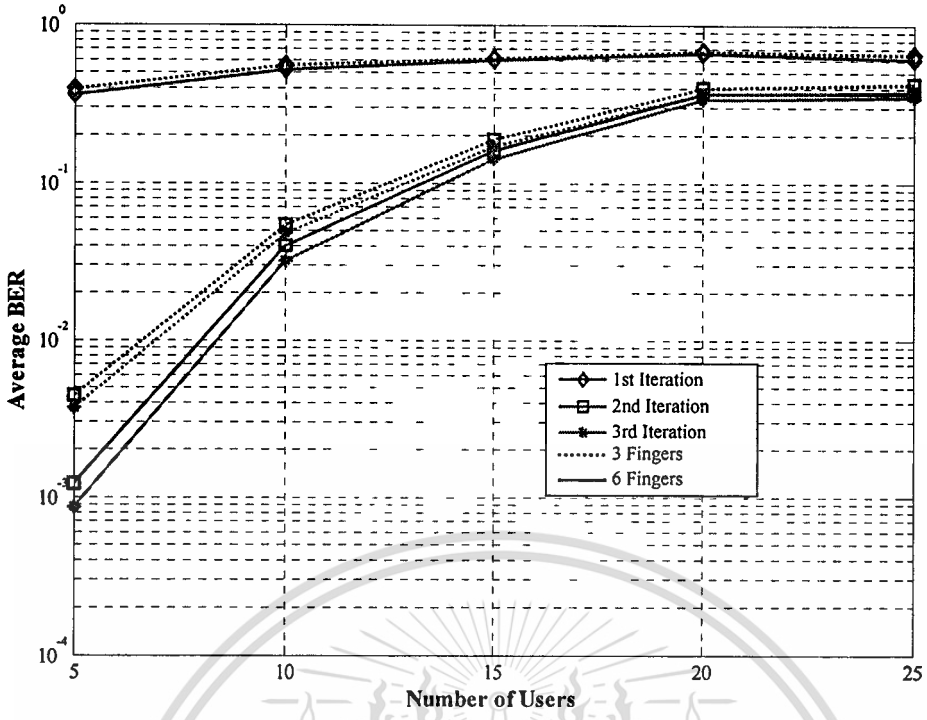

Figure 5.18 Number of users for time domain adaptive G-RAKE LSTC-CDMA receiver based on LMS algorithms.

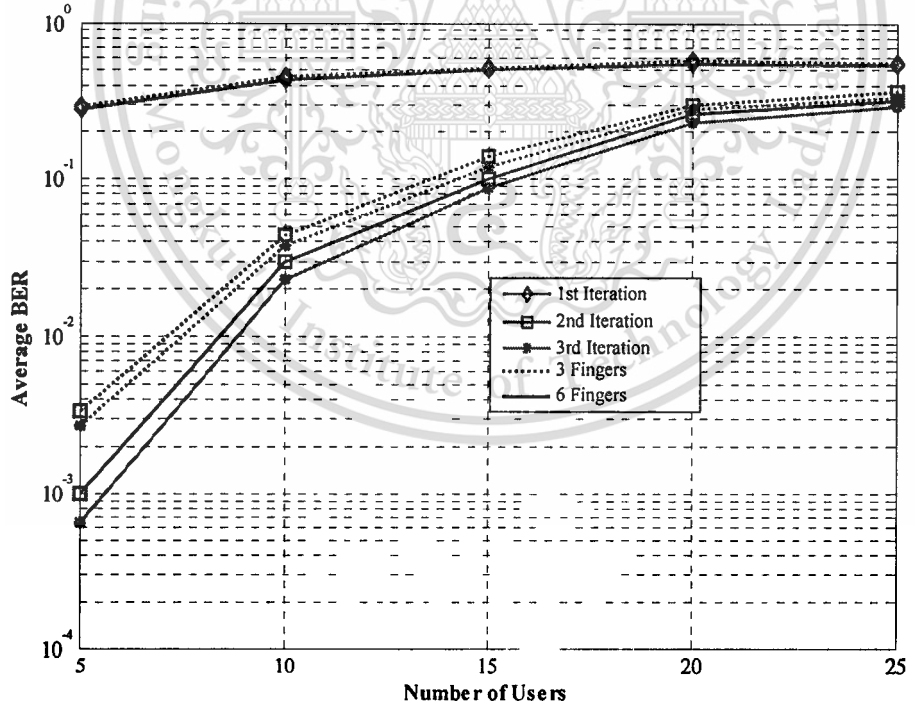

Figure 5.19 Number of users for time domain adaptive G-RAKE LSTC-CDMA receiver based on PFGLMS algorithms.

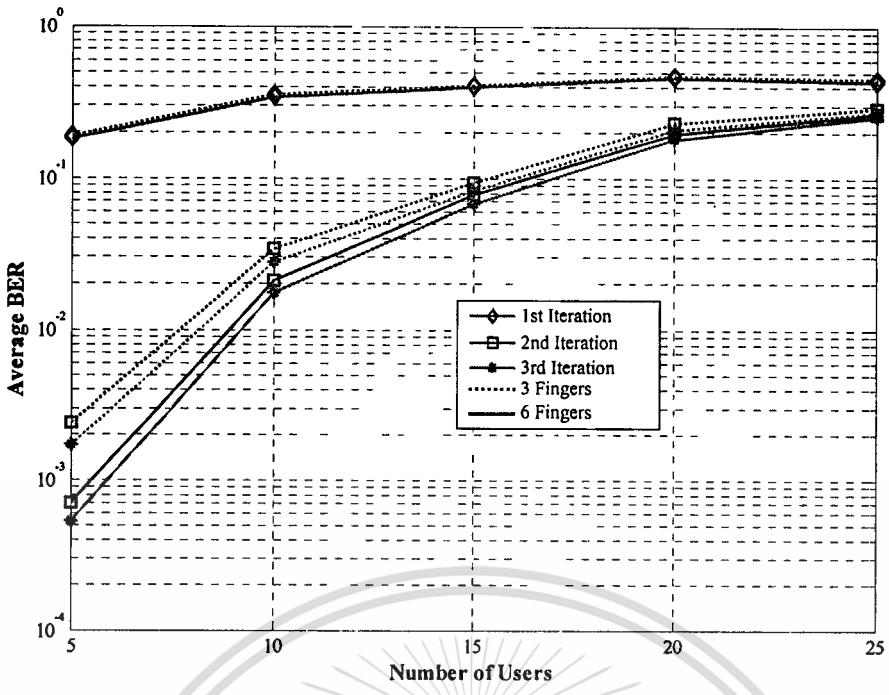

Figure 5.20 Number of users for time domain adaptive G-RAKE LSTC-CDMA receiver based on RLS algorithms.

Figure 5.21 shows the BER curve and Figure 5.22 depicts the number of 3 fingers adaptive G-RAKE receiver. The simulations results are simulated based on three main detection algorithms such as LMS, PFGLMS and RLS algorithms. It can be clearly seen that the system performance of the receiver that based on RLS algorithm outperforms to that of PFGLMS and LMS algorithms.

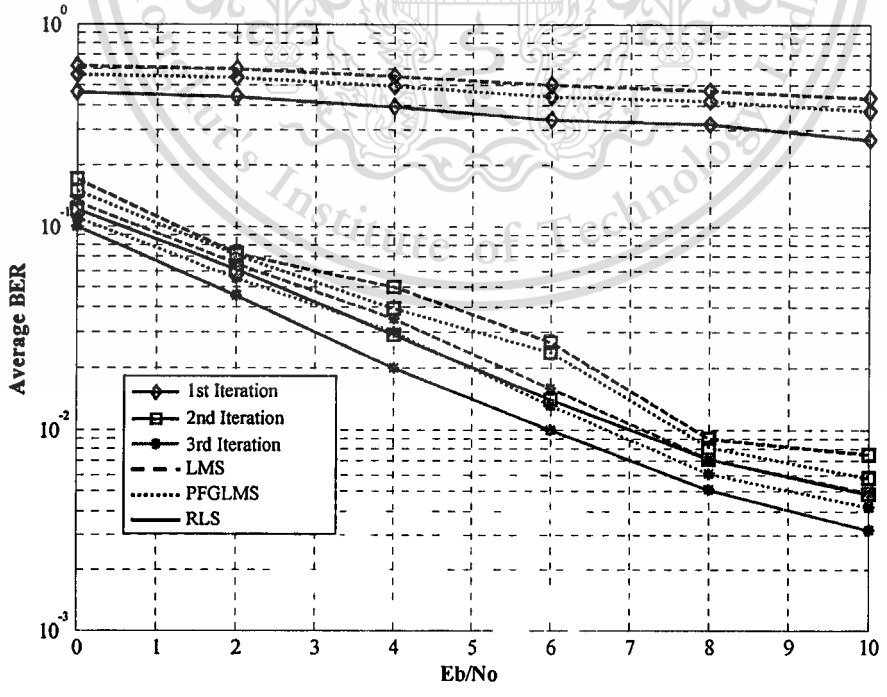

Figure 5.21 BER comparisons of 3 fingers adaptive G-RAKE LSTC-CDMA receiver.

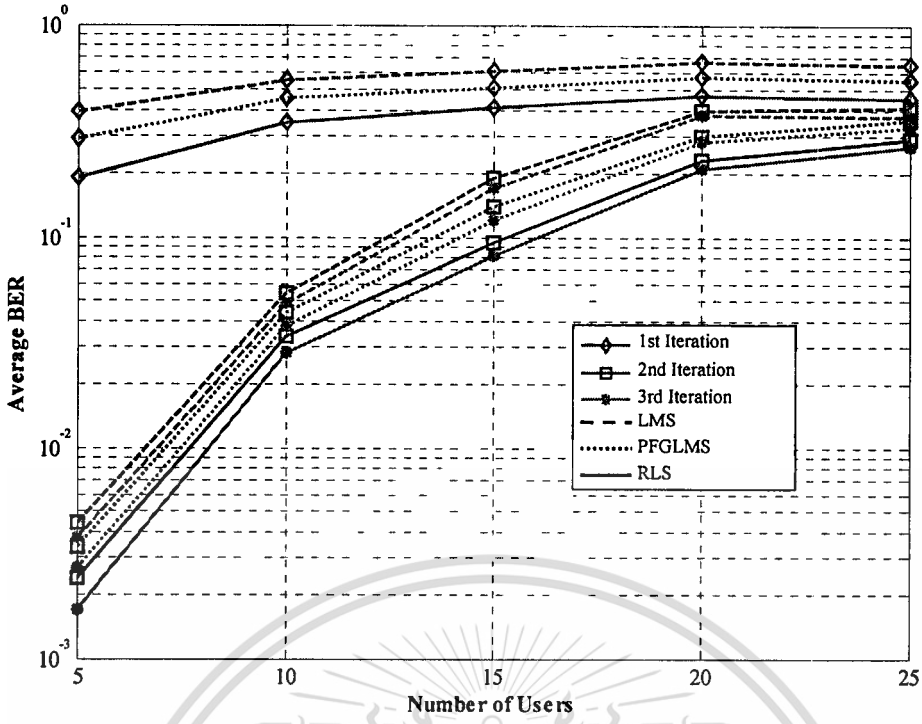

Figure 5.22 Number of users for 3 fingers adaptive G-RAKE LSTC-CDMA receiver in time domain systems.

5.2.2.2 Frequency Domain Systems

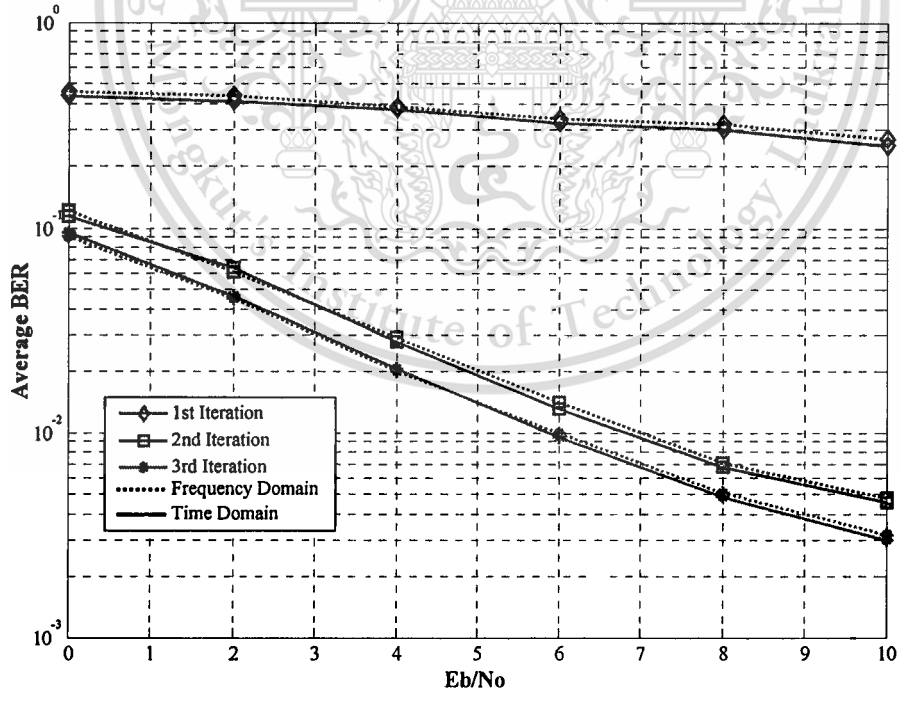

Figure 5.23 BER comparisons of 3 fingers adaptive G-RAKE LSTC-CDMA receiver in time and frequency domain systems, based on RLS algorithm.

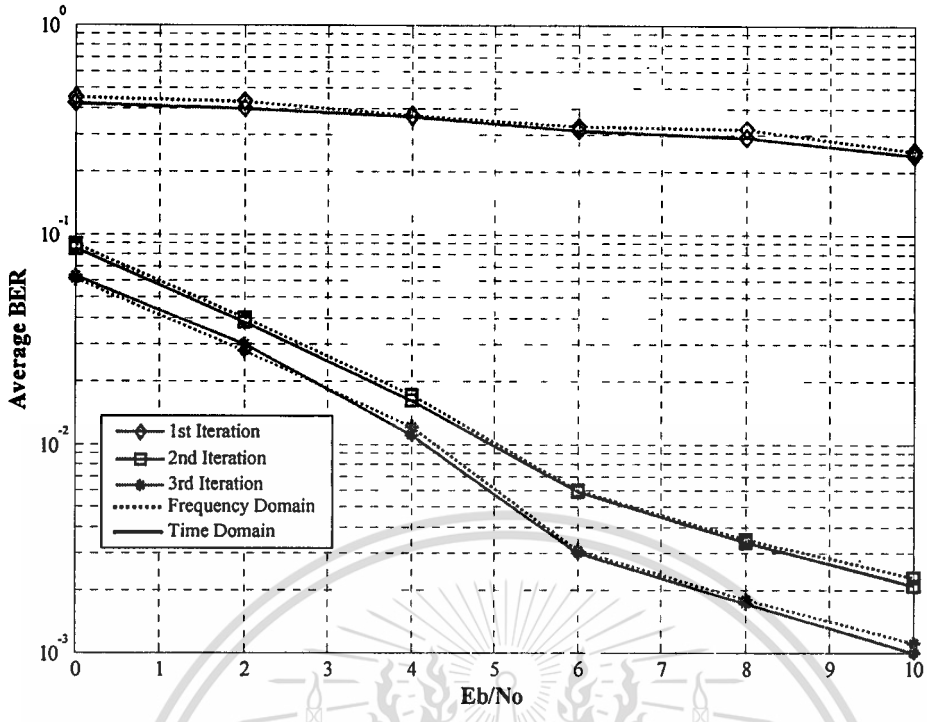

Figure 5.24 BER comparisons of 6 fingers adaptive G-RAKE LSTC-CDMA receiver in time and frequency domain systems, based on RLS algorithm.

According the simulation results which are presented in previous sections, RLS algorithm achieves the best performance among LMS and PFGLMS algorithms. So, the comparison of the proposed receivers that based on RLS algorithms are only presented in this section. The comparison of performance results between the frequency domain and time domain adaptive G-RAKE LSTC-CDMA receiver for 3 fingers and 6 fingers are shown in Figure 5.23 and Figure 5.24. The simulation results show that the proposed receiver in frequency domain system have the same performances as the one in time domain system with less computational complexity.

5.2.3 Systems Performances Comparisons

In this section, the performance comparisons between an adaptive iterative LSTC-CDMA receiver and a 3 fingers adaptive G-RAKE LSTC-CDMA receiver, based on LMS, PFGLMS and RLS algorithm, are presented. The BER performance comparisons are depicted in Figure 5.25, Figure 5.26 and Figure 5.27. These curves clearly show that adaptive iterative receiver only performs better than adaptive G-RAKE receiver in the first iteration. This means that the proposed adaptive G-RAKE receiver have a better performance from second up to higher iteration.

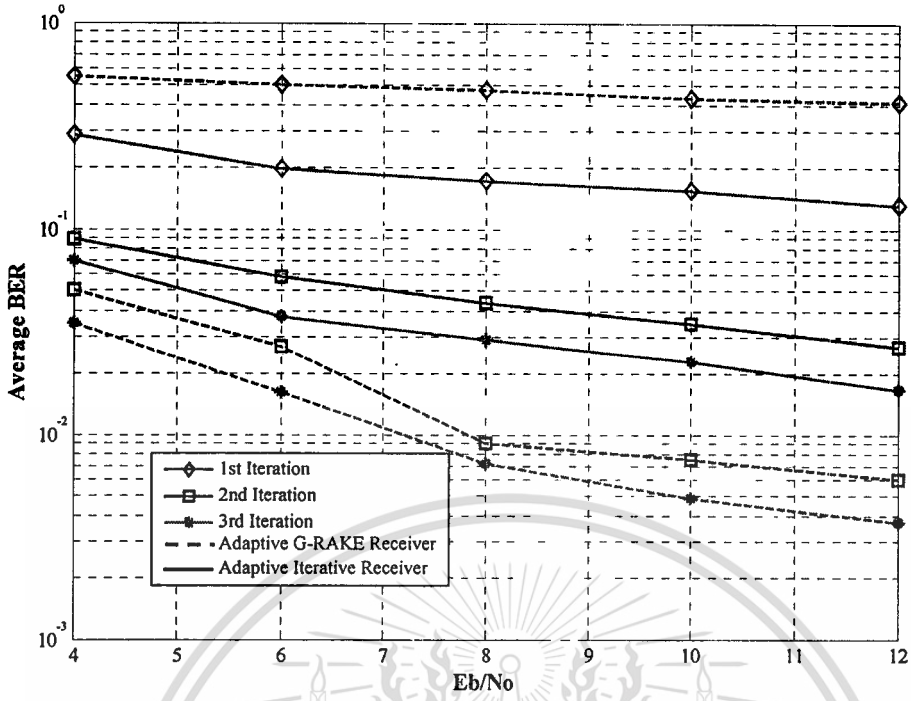

Figure 5.25 BER comparisons of adaptive iterative receiver and 3 fingers adaptive G-RAKE receiver in time domain LSTC-CDMA system, based on LMS algorithm.

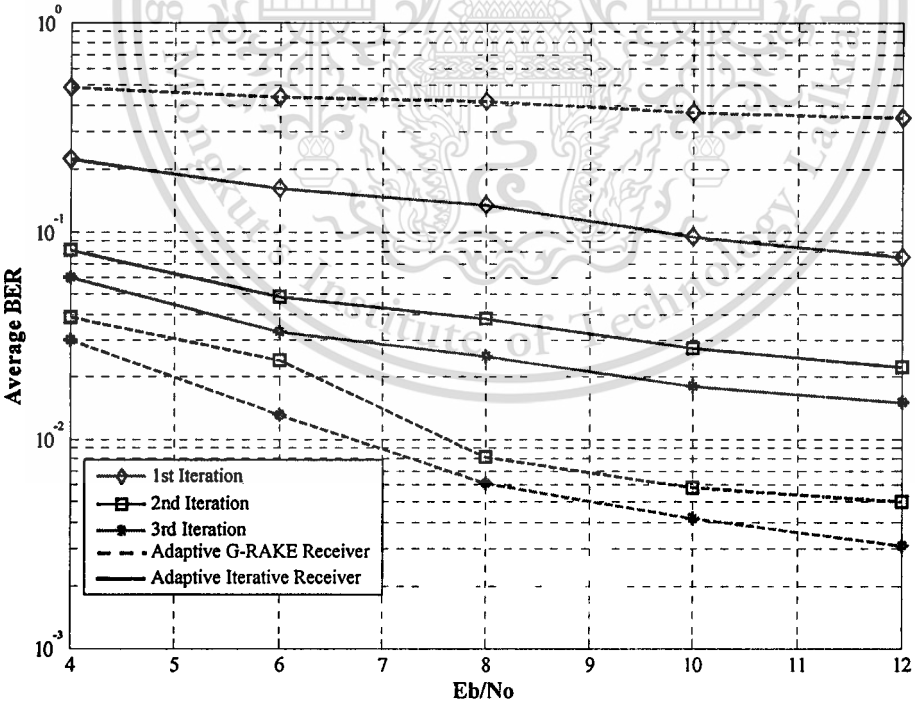

Figure 5.26 BER comparisons of adaptive iterative receiver and 3 fingers adaptive G-RAKE receiver in time domain LSTC-CDMA system, based on PFGLMS algorithm.

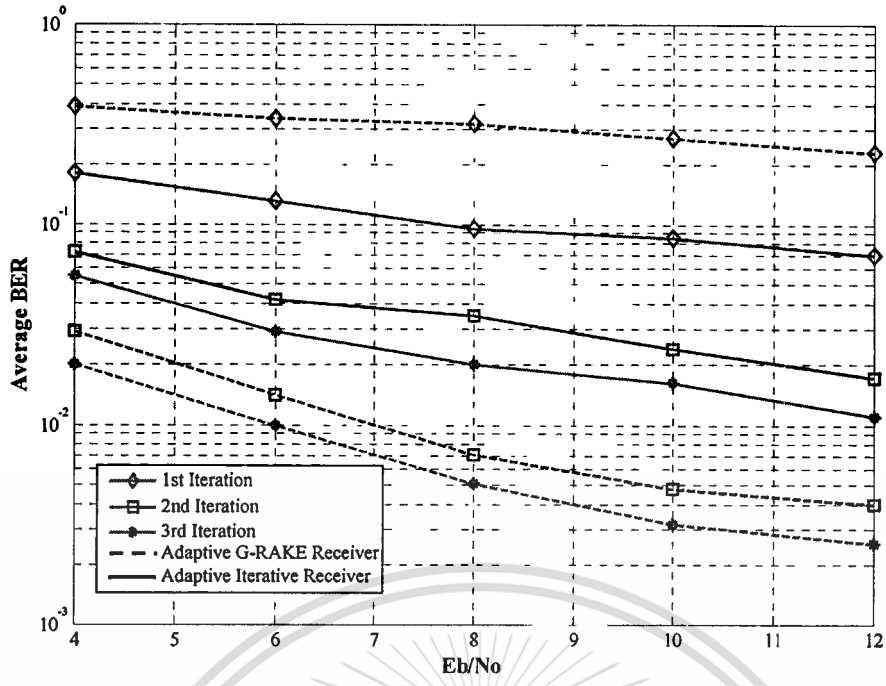

Figure 5.27 BER comparisons of adaptive iterative receiver and 3 fingers adaptive G-RAKE receiver in time domain LSTC-CDMA system, based on RLS algorithm.

5.3 Conclusion

In this chapter, the simulation results of the proposed adaptive receivers for LSTC-CDMA system in time and frequency domain are given. The receivers are based on LMS, PFGLMS and RLS algorithm and are compared to each other in Rayleigh fading channel. The system performance of adaptive iterative LSTC-CDMA receiver is investigated in both slow and fast fading channel for various antennas systems. The results show that the average BER of the adaptive receiver increases when the fade rate is increased. The performance results also show that the 2x4 antennas system achieves the best performance among 4x4, 2x2 and 4x2 antennas systems. The 3 fingers and 6 fingers RAKE receiver structures are investigated in the proposed adaptive G-RAKE LSTC-CDMA receiver. The performance results prove that the adaptive G-RAKE receiver improves when the number of fingers is increased beyond the number of resolvable multipath.

Moreover, both proposed receivers based on the RLS algorithm has a faster convergence speed and better tracking ability compared to the PFGLMS and LMS receiver in both rich scattering environment and fast fading channels with a slight increase in the complexity. Furthermore, the proposed frequency domain receiver has a significantly lower computational complexity and achieves the same performance in comparison to the time domain receiver. Finally, the simulation results show that the adaptive G-RAKE receiver outperforms the adaptive iterative receiver. The conclusion of the thesis and the discussion of the potential future work are concluded in Chapter 6.

Chapter 6

Conclusions

6.1 Conclusions

The development of communications systems over the past decades has had a significant impact on the modern life of people in today's society. Demand for faster and easier ways to communicate and transfer information worldwide with real time processing is a basic requirement for current communications systems. However, at high transmission rates, wireless communications links become unreliable and have fundamentally low capacity due to multipath fading channels and the systems interferences such as co-channel interferences (CCI) and multiple access interferences (MAI).

In this thesis, two new structure receivers in layered space-time coding (LSTC) and MIMO DS-CDMA systems for applications in downlink wireless communication, as discussed in Chapter 2, are presented. The proposed receivers are investigated in both time and frequency domain systems. Specifically, adaptive detection algorithms such as least means square (LMS), partially filtered gradient LMS (PFGLMS) and recursive least squares (RLS) algorithm play an important role in designing these downlink LSTC-CDMA receivers. The purposes of these designs are to cancel the system interferences and combat the effect of multipath fading with a low computational complexity and a fast convergence speeds. Both proposed adaptive receivers are named as adaptive iterative LSTC-CDMA receiver and adaptive G-RAKE LSTC-CDMA receiver.

Due to the high computational complexity in the non-adaptive MMSE receivers, an adaptive iterative LSTC-CDMA receiver is proposed in Chapter 3. The system model of LSTC-CDMA system, based on a joint adaptive iterative detection and decoding algorithm, is described. Based on the designed system models of both transmitter and receiver, the proposed adaptive iterative receiver has the ability to effectively suppress and cancel the CCI and MAI by performing interference suppression and cancelation techniques. LMS, PFGLMS and RLS algorithm are utilized in the adaptation process of the proposed adaptive detector in time and frequency domain. Firstly, the LMS algorithm is used in the purpose of reducing the computational complexity of the existing systems. However, the convergence speeds of this proposed structure are not satisfied yet. Hence, the PFGLMS algorithm is introduced in order to improve the convergence speeds with a slightly increase in the system complexity. Moreover, it has been shown that the RLS algorithm behaves much better in the scattering environments. Then, it is also used in the proposed adaptive detection process. Therefore, the computational complexities of the

three adaptive detection algorithms in time and frequency domain are investigated. It is shown that the number of complexity of the proposed receiver in frequency domain system is significantly reduced in comparison with the one in time domain system. The table of complexity comparisons, as shown in Chapter 3, shows that both RLS and PFGLMS based receivers have slightly more number of complexities than the LMS based receivers.

Generally, it is a difficult task to enlarge the network capacity and improve the quality of service due to the multipath fading of wireless channel. Therefore, an adaptive G-RAKE LSTC-CDMA receiver is proposed in Chapter 4. The proposed receiver can effectively not only suppress the CCI and MAI using the interference suppression and cancellation techniques but also mitigate the effect of multipath of fading channel. The design of the proposed system models are presented in detail in both time and frequency domain. More importantly, LMS, PFGLMS, and RLS algorithm are utilized in the adaptive detection process in order to determine the weight coefficient of each finger element.

The simulation systems of both proposed receivers are presented in detail in Chapter 5. The Raleigh fading channels and additive white Gaussian noise (AWGN) channels are taken into account. The proposed adaptive iterative LSTC-CDMA receiver is investigated in both fast and slow fading channels and it is shown that the average BER of the adaptive receiver decreases when the fading rate is increased. Moreover, a number of various antennas systems are simulated for the proposed adaptive iterative receiver. The simulations results also show that the 2x4 antennas system achieve the best performances based on the increasing of the ability to track the errors at the receiver end when the number of receive antennas is increased.

The adaptive G-RAKE LSTC-CDMA receiver is simulated in both time and frequency domain with 3 and 6 fingers RAKE structure. The adaptive G-RAKE receiver improves when the number of fingers is increased beyond the number of resolvable multipath. Furthermore, the performances of the both proposed frequency receivers achieve the same performances compared to those of the time domain system. The performances results show that the RLS based receivers outperform the PFGLMS and LMS based receivers and has a better tracking ability in the rich scattering environment. Finally, the simulation results prove that the adaptive G-RAKE LSTC-CDMA receiver has the ability to combat the effect of multipath fading channels and also to cancel the system interferences than the adaptive iterative LSTC-CDMA receiver with a better performance.

6.2 Future Research Works

Nowadays, Cooperative Diversity (CD) technology is a promising solution for future wireless communications systems to achieve broader coverage and to mitigate wireless channels' impairments

without the need to use high power at the transmitter. Nevertheless, problems in cooperative communication continue to intrigue researchers by their difficulty and the potential for faster and more reliable communication. Hence, "Adaptive iterative detections for LSTC receivers in cooperative communication systems" is going to be the next research topic.

This potential future research are going to be proposed in the field of cooperative communications networks by integrating the techniques in CD technology with the existing systems model that were already proposed in this thesis. Consequently, the main objectives of doing this research are to achieve diversity through independent channels; to obtain broadcast nature of CD technology and to improve communication capacity, speed, and performance of the existing system. Main techniques and designs are going to be proposed such as: a study on the cooperative protocols and designs which are good over a wide range of channels, an efficient bandwidth approach design, a design of a cooperative diversity system on an effective and suitable multiple access platform which have the ability to demonstrate the cooperative diversity gains in practical wireless systems and a new cooperative communication protocol that increases Signal-to-Noise Ratio (SNR) range.

In order to achieve the objectives of these proposed techniques and designs, some advanced techniques in two main areas of cooperative communication such as: cooperative beamforming and cooperative MIMO relay channel are going to be studied and investigated. Beamforming with antenna arrays is a well studied technology. It provides Space-Division Multiple Access (SDMA) which enables significant increases in communication rate. Indeed, a key aspect of the cooperative MIMO relay channel is the processing of the signal received from the source node done by the relay. It is a new paradigm that draws from the ideas of using the broadcast nature of the wireless channels to make communicating nodes help each other. Furthermore, it implements the communication process in a distribution fashion and gain the same advantages as those found in MIMO systems.

The outcomes of this future research works on the integration between the CD technology and the LSTC systems would be a design of a various types of receiver structures in cooperative wireless communication systems. Therefore, these receivers will have the abilities to achieve the spatial diversity, to increase throughput in the high SNR region, to deal with the effect of multipath fading channel, cancel the system interferences by using the interference suppression and cancelation techniques, to reduce the system computational complexity that lead to a decrease in cost of system design and to improve the convergence speed with high quality services of data transmission.

References

[1] H. Weingarten, Y. Steinberg and S. Shamai, "On the capacity region of the multi-antennas broadcast channel with common messages," *IEEE International Symposium on Information Theory*, pp. 2195–2199, 2006.

[2] R. Rui and V.K. Lau, "Cross layer design of downlink multi antennas OFDMA systems with imperfect CSIT for slow fading channel," *IEEE Transaction on Wireless Communications*, vol. 6, no. 7, pp. 2417-2421, 2007.

[3] S. Lin and D. Costello, "Error control coding: fundamentals and applications," *2nd Ed.*, Pearson Education, 2004.

[4] H. Chen, "The next generation CDMA technologies," England: John Wiley & Sons Ltd, 2007.

[5] V. Kuhn, "Wireless communications over MIMO channels," England: John Wiley & Sons Ltd, 2006.

[6] J. Shen, "Iterative multiuser detection," *Thesis (Ph.D.) Communication Research Group,* Department of Electronics, University of York, 2004.

[7] S. Verdu, "Minimum probability of error for asynchronous Gaussian multiple-access channels," *IEEE Transactions on Information Theory*, pp.85–96, January 1986.

[8] S. Verdu, "Multiuser detection," Cambridge University Press, 1998.

[9] M. L. Honig, "Advances in multiuser detection," United States: John Wiley & Sons Ltd, 2009.

[10] F. B. Ueng, H. F. Wang, R. Chang and L.D. Jeng, "Zero forcing and minimum mean-square-error equalization for OFDMA-CDMA multiuser detection in multipath fading channels" *IEEE ISPACS 06,* pp. 505-509, 2006.

[11] S. Marinkovic, B. Vucetic and A. Ushirokawa, "Space-time iterative and multistage receiver structures for CDMA mobile communication systems," *IEEE Journal on Selected Areas in Communications*, vol. 19, pp. 1594-1604, 2001.

[12] M. Frikel, B. Targui, M. M'saad and S. Safi, "BER analysis of parallel and successive interference cancelation employing MMSE equalizer for CDMA systems," *IEEE International Conference on Multimedia Computing and Systems*, pp. 158-161, 2009.

[13] H. El Gamal and E. Geraniotis, "Iterative multiuser detection for coded CDMA signals in AWGN and fading channels," *IEEE Journal on Selected Areas in Communications*, vol. 18, pp. 30-41, 2000.

[14] L. Fang and L.B. Milstein, "Performance of successive interference cancellation in convolutionally coded multicarrier DS-CDMA systems," *IEEE Transactions on Communications*, vol. 49, pp. 2062-2067, 2001.

[15] K. Shahtaleb, G. R. Bakhshi and H. S. Rad, "Interference cancellation in non-coherent CDMA system using parallel iterative algorithms," *IEEE International Conference on Wireless Communications and Networking*, pp. 392-396, 2008.

[16] J. Li, K. B. Letaief and Z. Cao, "Adaptive cochannel interference cancellation in space-time coded communication systems," *IEEE Trans. on Communication*, vol. 50, pp. 1580-1583, October 2002.

[17] C. Teekapakvisit, V. D. Pham and B. Vucetic, "An adaptive iterative receiver for space-time coding MIMO systems," *3rd Workshop on the Internet, Telecommunications and Signal Processing*, 2004.

[18] Y. Sun, M. L. Honig and V. Tripathi, "Adaptive, iterative, reduced-rank equalization for MIMO channels," *IEEE Proc. of MILCOM*, vol.2, pp.1029-1033, October 2002.

[19] S. F. Boroujeny, "Adaptive filters: theory and applications", *2nd ed.*, England: John Wiley & Sons Ltd, 2004.

[20] J. S. Lim, "Fast adaptive filtering algorithm based on exponentially weighted least-square errors," *Electronics Letters*, vol.35, pp. 1913-1915, October 1999.

[21] S. S. Haykin, "Adaptive filter theory," *4th ed.*, Printice Hall, 2002.

[22] T.S. Rappaport, "Wireless communications: principles and practice," Prentice Hall, 2002.

[23] G.E. Bottomley, T. Ottosson and Y.P. Eric Wang, "A generalized RAKE receiver for interference suppression," *IEEE Journal on Selected Areas in Communications*, vol. 18, pp.1536-1545, 2000.

[24] G. E. Bottomley and C. Cozzo, "RAKE reception with channel estimation error," *IEEE Transactions on Vehicular Technology*, vol. 55, pp. 1923-1926, 2006.

[25] J. Yi and J. Lee, "RAKE receiver with adaptive interference cancellers for a DS-CDMA system in multipath fading channels," *IEEE VTS-Fall VTC*, vol. 3, pp.1216-1220, 2000.

[26] T. L. Fulghum, D. A. Cairns, C. Cozzo, Y. P. Eric Wang and G. E. Bottomley, "Adaptive generalized RAKE reception in DS-CDMA systems," *IEEE Trans. On Wireless Communications*, vol.8, pp. 3464-3474, 2009.

[27] D. Gesbert, M. Shafi, D. Shiu, P.J. Smith and A. Naguib, "From theory to practice: an overview of MIMO space–time coded wireless systems," *IEEE Journal on Selected Areas in Communications*, vol.21, pp.281–302, 2003.

[28] A. Paulraj, R. Nabar and D. Gore, "Introduction to space–time wireless communications," UK: Cambridge University Press, 2003.

[29] G. Tsoulos, "MIMO system technology for wireless communications," Taylor and Francis Group, 2006.

[30] Q. H. Spencer, C. B. Peel, A. L. Swindlehurst and M. Haardt, "An introduction to the multi-user MIMO downlink," *IEEE Communication Magazine*, vol. 42, pp. 60–67, 2004.

[31] B. Vucetic and J. Yuan, "Turbo codes : principles and applications." Boston: Kluwer Academic Publishers, 2000.

[32] H. Jafarkhani, "Space-time coding : theory and practice," Cambridge: Cambridge University Press, 2005.

[33] V. Tarokh, N. Seshadri and A. R. Calderbank, "Space-time codes for high data rate wireless communication: performance criterion and code construction," *IEEE Transactions on Information Theory*, vol. 44, pp. 744-765, 1998.

[34] V. Tarokh, H. Jafarkhani and A. R. Calderbank, "Space-time block codes from orthogonal designs," *IEEE Transactions on Information Theory*, vol. 45, pp. 1456-1467, 1999.

[35] S. M. Alamouti, "A simple transmit diversity technique for wireless communications," *IEEE Journal on Selected Areas in Communication*, vol. 16, no. 8, pp. 1451–1458, 1998.

[36] G. Foschini, "Layered space-time architecture for wireless communication in a fading environment when using multi-element antennas," *Bell Labs Technical Journal*, pp. 41–59, 1999.

[37] W. Webb, "Wireless communications: the future," John Wiley & Sons Ltd, 2007.

[38] W. Stallings, "Wireless communications and networks," Prentice Hall, 2004.

[39] B. Vucetice and J. Yuan, "Space-time coding", England: John Wiley & Sons Ltd, 2003.

[40] D. Chizhik, J. Ling, P. W. Wolniansky, R. A. Valenzuela, N. Costa and K. Huber, "Multiple-input-multiple-output measurements and modeling in Manhattan," *IEEE Journal on Selected Areas in Communication*, vol. 21, pp. 321–331, Apr. 2003.

[41] J. G. Proakis, "Digital communications," *4th ed.*, New York: McGraw-Hill, 2001.

[42] D. Popescu and C. Rose, "Interference avoidance methods for wireless systems," Springer, 2004.

[43] K. Slattery and H. Skinner, "Platform interference in wireless systems," UK: Elsevier Inc., 2008.

[44] R. H. Mahadevappa and J. G. Proakis, "Mitigation multiple access interference and intersymbol interference in uncoded CDMA systems with chip-level interleaving," *IEEE Transactions on Wireless Communications*, vol.1, pp.781-792, 2002.

[45] H. Marouane, A. Benabdennabi, A. Kachouri and L. Kamoun, "Performance of adaptive filter in CDMA system for multiple access interference suppressing," *IEEE International Conference on Design and Test of Integrated Systems in Nanoscale Technology*, pp. 424-426, 2006.

[46] M. A. A. Rgheff, "Introduction to wireless communications," UK: Elsevier Inc., 2007.

[47] M. Sellathurai and S. Haykin, "Space-time layered information processing for wireless communications," Wiley-IEEE Press, 2009.

[48] G. J. Foschini, D. Chizhik, M. J. Gans, C. Papadias and R. A. Valenzuela, "Analysis and performance of some basic space-time architectures," *IEEE Journal on Selected Areas in Communications,* vol. 21, pp. 303-320, 2003.

[49] M. Sellathurai and S. Haykin, "Further results on diagonal layered space-time architecture," *IEEE International Conference on Vehicular Technology*, vol.3, pp. 1958-1962, 2001.

[50] H. E. Gamal, "On the design of layered space-time systems for autocoding," *IEEE Transactions on Communications*, vol.50, pp. 1451-1461.

[51] R. Price and P. E. Green, "A communication technique for multipath channels," *Proceeding of the IRE*, vol. 46, pp. 55-570, 1958.

[52] C. E. Shannon, "A mathematical theory of communication," *Bell System Technology Journal*, vol. 27, pp. 379–423, 1948.

[53] K. Peng, "Collaborative HARQ Schemes for cooperative diversity communications in wireless networks," *Master of Philosophy Thesis*, School of Electrical and Information Engineering, The University of Sydney, 2008.

[54] R. G. Gallager, "Principle of digital communications," Cambridge University Press, 2008.

[55] J. Schiller, "Mobile communications," *2nd Ed.*, Pearson Education Limited, 2003.

[56] D. xu, Y. Xiao and H. Du, "An improve algorithm of MMSE multiuser detection for CDMA systems," *IEEE International Conference on Communication and Information Technology*, vol.1, pp. 552-555, 2005.

[57] Y. Xiao and M. H. Lee, "MIMO multiuser detection for CDMA systems," *IEEE International Conference on Signal Processing*, vol.1, pp. 1566-1570, 2006.

[58] P. Castoldi, "Multiuser detection in CDMA mobile terminals," Artech House Publishers, 2003.

[59] R. Lupas and S. Verdu, "Linear multiuser detectors for synchronous code-division multiple-access channels," *IEEE Transactions on Information Theory,* vol. 35, pp. 123-136, 1989.

[60] U. Madhow and M. L. Honig, "MMSE interference suppression for directsequence spread-spectrum CDMA," *IEEE Transactions on Communications*, vol. 42, pp. 3178-3188, 1994.

[61] J. M. Holzman, "DS-CDMA successive interference cancellation," *IEEE International Symposium on Spread Spectrum Techniques and Applications*, pp. 69-78, 1994.

[62] M. K. Varanasi and B. Aazhang, "Multistage detection in asynchronous code division multiple-access communications," *IEEE Transactions on Communications*, vol. 38, pp. 509-519, 1990.

[63] F. Berggren and S. B. Slimane, "Successive interference cancellation in multi-rate DS-CDMA systems, " *IEEE Proceeding on Personal Indoor and Mobile Radio Communications*, vol.2, pp. 1756-1756, 2003.

[64] T. Huovinen and T. Ristaniemi, "Blind source separation based successive interference cancellation in the DS-CDMA uplink," *IEEE International Symposium on Control Communications and Signal Processing*, pp. 775-778, 2004.

[65] M. F. Madkour, S. C. Gupta and Y. P. E. Wang, "Successive interference cancellation algorithms for downlink CDMA communications," *IEEE Transactions on Wireless Communications*, vol.1, pp. 169-177, 2002.

[66] L. G. F. Trichard, J. S. Evans and I. B. Collings, "Large system analysis of linear parallel interference cancellation," *IEEE International Conference on Communications*, vol.1, 26-30, 2001.

[67] M. Ghotbi and M. R. Soleymani, "Multistage parallel interference cancellation with power and phase estimation," *IEEE Proceeding on Vehicular Technology*, vol.3, pp. 1716-1719, 2002.

[68] S. Liang and W. Wu, "The performance analysis of a receiver with combing multistage parallel interference cancellation and antenna array," *IEEE Proceeding on Communication Technology*, vol.2, pp. 1887-1890, 2003.

[69] L. T. Tie, Y. H. Chaw and A. Nallanathan, "On the performance improvement through the use of parallel interference cancellation in channel estimation for multipath CDMA systems," *IEEE International conference on Global Telecommunications*, vol.4, pp. 2339-2343, 2004.

[70] S. J. Baines, "Linear multi-user detection in CDMA cellular systems," *Ph.D Thesis*, Department of Electronics, University of York, 2000.

[71] A. D. Poularikas and Z. M. Ramadan, "Adaptive Filtering," Taylor and Francis Group, 2006.

[72] E. Biglieri, B. Calderbank, A. Constantinides, A. goldsmith, A. Paulraj, and H.V. Poor, "MIMO Wireless Communications," 2nd ed., Cambridge University Press, 2007.

[73] C. Oestges and B. Clerckx, "MIMO wireless communications: from real-world propagation to space-time code design," London: Academic Press, 2007.

[74] C. Schlegel and A. Grant, "Coordinated multiuser communications," Springer, 2006.

[75] R. L.-U. Choi, K. B. Letaief and R. D. Murch, "MIMO CDMA antenna systems," *Proceeding of IEEE ICC*, vol. 2, pp. 990-994, 2000.

[76] L. Mailaender, "Linear MIMO Chip Equalization for CDMA Downlink," *Procedding of IEEE SPAWC,* June 2003.

[77] S. Marinkovic, "Interference mitigation in CDMA and space-time coded MIMO systems," *Ph.D Thesis*, Telecommunications Laboratory, Department of Electrical and Information Engineering, University of Sydney, 2002.

[78] C. Teekapakvisit ,"Low complexity adaptive iterative receivers for layered space-time coded and CDMA system," *Ph.D Thesis*, The University of Sydney, 2006.

[79] D. Falconer, S. L. Ariyavisitakul, A. Benyamin-Seeyar and B. Eidson, "Frequency domain equalization for single-carrier broadband wireless systems," *IEEE Magazine on Communiations*, vol. 40, pp. 58-66, 2002.

[80] X. Zhu and R. D. Murch, "Layered space-frequency equalization in a single-carrier MIMO system for frequency-selective channels," *IEEE Transactions on Wireless Communications,* vol. 3, pp. 701-708, 2004.

[81] Y. Park and F. Adachi, "Enhanced radio access technology for next generation mobile communications," Springer, 2007.

[82] C. L. Borgman, "Scholarship in the digital age," The MIT Press, 2007.

[83] P. Lin, P. Rapajic and Z. Krusevac, "On the tracking performance of LMS and RLS algorithms in an adaptive MMSE CDMA Receiver," *IEEE Proceeding on Communications Theory*, pp.175-178, 2005.

[84] C. F. Leanderson and C. E. W. Sundberg, "Performance evaluation of list sequence MAP decoding," *IEEE Transactions on Communications*, vol.53, pp. 422-432, 2005.

[85] A. Yener, "Efficient access and interference management for CDMA wireless systems," Thesis (Ph. D.), Graduate Program in Electrical and Computer Engineering, The State University of New Jersey, 2000.

[86] Y. P. E. Wang and G. E. Bottomley, "DS-CDMA downlink system capacity enhancement through interference suppression," *IEEE Transactions on Wireless Communications*, vol.5, pp. 1767-1774, 2006.

[87] G.E. Bottomley, T. Ottosson and Y.P. Eric Wang, "A generalized RAKE receiver for interference suppression," *IEEE Journal on Selected Areas in Communications*, vol. 18, pp.1536-1545, 2000.

[88] J. Yi and J. Lee, "RAKE receiver with adaptive interference cancellers for a DS-CDMA system in multipath fading channels," *IEEE VTS-Fall VTC*, vol. 3, pp.1216-1220, 2000.

[89] T. L. Fulghum, D. A. Cairns, C. Cozzo, Y. P. Eric Wang and G. E. Bottomley, "Adaptive generalized RAKE reception in DS-CDMA systems," *IEEE Transactions on Wireless Communications*, vol.8, pp. 3464-3474, 2009.

Author Biography

Personal Information

Name	TEAV KEOV KOLYAN
Nationality	Cambodian
Date of birth	June 06, 1986
Place of birth	Kampong Thom Province, Cambodia

Education

Bachelor degree

Field	Computer and Communication Engineering
Duration	2003-2008
Department	Department of Computer Science
University	Institute of Technology of Cambodia (ITC), Cambodia

Master degree

Field	Information Engineering
Duration	2008-2010
Department	School of Computer Engineering
Faculty	Engineering
University	King Mongkut's Institute of Technology Ladkrabang (KMITL), Thailand

Research Interests

Wireless Communication Systems: MIMO systems, CDMA systems, OFDMA systems, cooperative communications, multiuser detections and channels coding algorithms.

List of International Conferences

Proceeding Papers

1- **Teav Keov Kolyan**, Chakree Teekapakvisit, Dewi Nugrahani, Pitak Thumwarin, and Takenobu Matsuura, "*An Adaptive Generalized RAKE CDMA Receiver for Layered Space Time Coded Systems in Multipath Fading Channels,*" ECTI-CON 2010 International Conference on Electrical Engineering/Electronics Computer Telecommunications and Information Technology, 19-21 May 2010, Chiang Mai, Thailand, pp. 56-60.

2- **Teav Keov Kolyan** and Chakree Teekapakvisit, "*Low Complexity LMS Based Adaptive Iterative Receiver for CDMA Systems,*" ICROS-SICE International Joint Conference (ICCAS-SICE 2009), 18-21 August 2009, Fukuoka, Japan, pp. 2339-2343.

3- **Teav Keov Kolyan** and Chakree Teekapakvisit, "*Adaptive Iterative Receiver for CDMA Systems in Rayleigh Fading Channels,*" IEEE-RIVF 2009 International Conference on Computing and Communication Technologies , 13-17 July 2009, Da Nang, Vietnam, pp. 249-252.

4- **Teav Keov Kolyan**, Chakree Teekapavisit, and Kanok Janchitrapongvej, "*Adaptive Iterative Receiver for Layered Space-Time coding CDMA Systems,*" ECIT-CON 2009 International Conference on Electrical Engineering/Electronics Computer Telecommunications and Information Technology, 06-09 May 2009, Pattaya, Thailand, pp. 852-855.

ECTI-CON 2010

The 2010 ECTI International Conference on Electrical Engineering/Electronics, Computer, Telecommunications and Information Technology

Empress Convention Centre
Chiang Mai, Thailand
19-21 May 2010

IEEE Catalog Number: CFP1006E-CDR
ISBN: 978-974-672-491-3
Organized by ...

ECTI Association
IEEE THAILAND SECTION

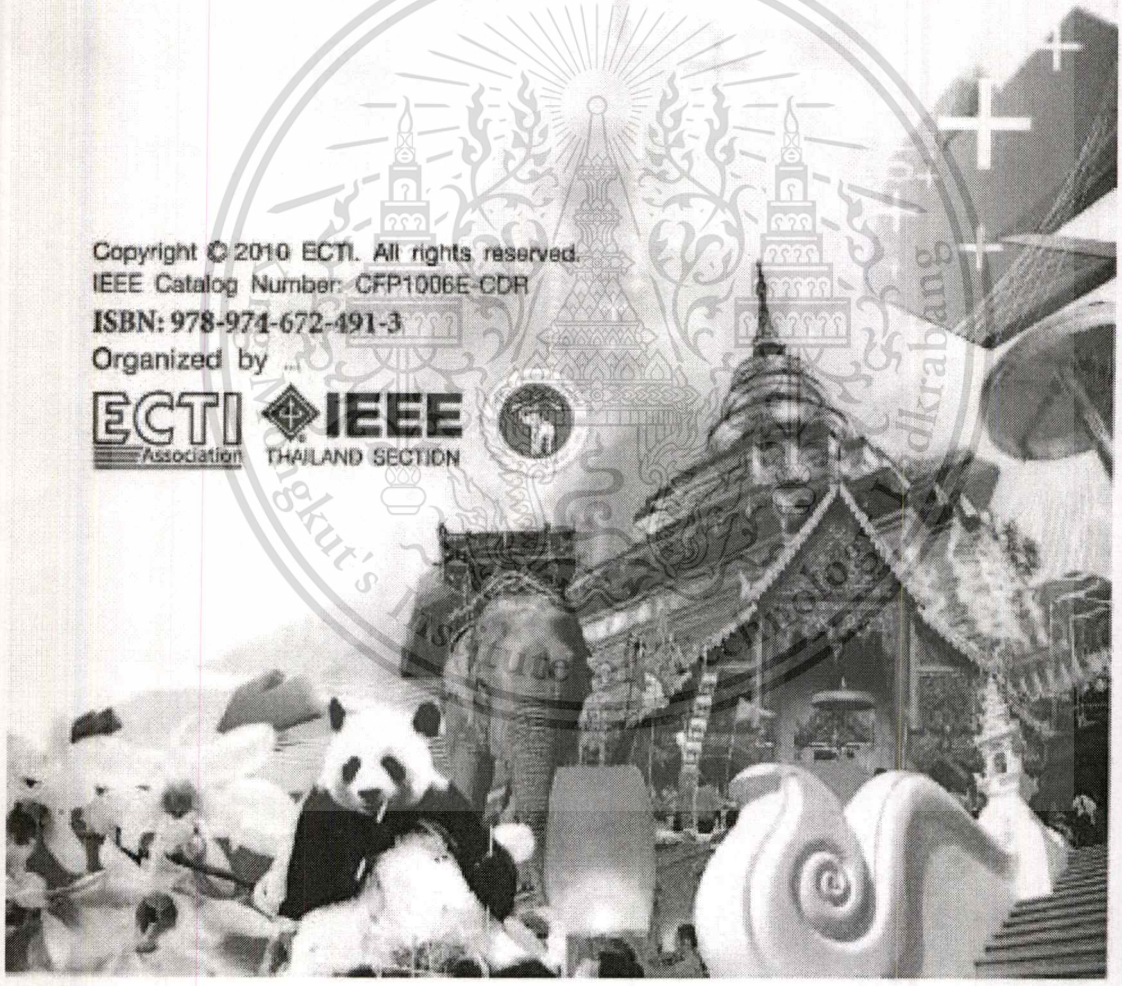

An Adaptive Generalized RAKE CDMA Receiver for Layered Space Time Coded Systems in Multipath Fading Channels

T. Keovkolyan[1], D. Nugrahani[1], P. Thumwarin[1], C. Teekapakvisit[2], and T. Matsuura[3]
[1]Faculty of Engineering, King Mongkut's Institute of Technology Ladkrabang (KMITL),
Chalongkrung Rd, Bangkok 10520, Thailand
[2]Department of Electronics Engineering, KMITL, Chumphon Campus Chumko, Pathiu, Chumphon 86160, Thailand
[3]Department of Electrical and Electronic Engineering, Tokai University, 259-1292, Japan
teav_keovkolyan@yahoo.com, dewi_en12@yahoo.com, ktpitak@kmitl.ac.th, ktchakre@kmitl.ac.th, and matsuura@tokai.ac.jp

***Abstract*- An adaptive generalized RAKE receiver for Layered Space Time Coded CDMA (LSTC-CDMA) system has been proposed in this paper. The proposed Generalized RAKE receiver, based on a joint adaptive iterative detection and decoding algorithm, adaptively mitigates the effect of multipath fading and cancels the system interferences such as Co-Channel Interference (CCI) and Multiple Access Interference (MAI). The Partially Filtered Gradient Least Means Square (PFGLMS) algorithm is used for both feed-forward filter and feedback filter in the adaptive detection in order to determine the weight coefficient of each finger element. The performance of the system is evaluated by simulation results for the various numbers of RAKE fingers in multipath Rayleigh fading channels.**

I. Introduction

Wireless technology is experiencing spectacular developments according to the emergence of interactive and digital multimedia applications as well as rapid advances in the highly integrated systems. The MIMO technique proposed in recent years makes a full use of the space resources by employing multiple antennas at the transmitting and receiving terminal, thus largely increasing the channel capacity. Moreover, Direct-Sequence CDMA (DS-CDMA) has emerged as a predominantly multiple-access technique for 3G systems because of its efficient capacity and facility of network planning in a cellular environment.

To improve the throughput of this cellular system, the combination of Layered Space-Time Coding (LSTC) and CDMA, named as LSTC-CDMA, has been intensively studied in [1-3]. This implementation generates Co-Channel Interference (CCI) from the adjacent layers and Multiple Access Interference (MAI) from the users; hence, both will degrade the system performance seriously. To mitigate the aforementioned interferences controlled by Channel State Information (CSI), an adaptive Minimum Means Square Error (MMSE) receiver for a LSTC system have been proposed in [4]. In this work, CCI can be reduced, but MAI is still a huge problem, degrading the performance and yielding channel estimation inaccurate in a high interference environment. A non-linear adaptive iterative receiver has been studied in [5, 6], containing a feed-forward filter to suppress the system interference and a feedback filter to cancel the interference from adjacent antennas under an iterative format. In order to reduce the computational complexity of the feedback filter and improve the convergence speed of the above proposed systems, an adaptive iterative receiver for multiuser LSTC-CDMA system based on LMS and PFGLMS algorithms have been investigated in [7].

Due to the multipath fading of wireless channel, it is a difficult task to enlarge the network capacity and improve the quality of service. As the results, the generalized RAKE (G-RAKE) receivers for interference suppression and multipath mitigation have been developed in [8,9]. Compared to the conventional RAKE receiver, this generalized RAKE receiver has more fingers and has different combining weights.

In this paper, an adaptive iterative generalized RAKE LSTC-CDMA receiver for interference suppression and multipath mitigation has been proposed. Consequently, the proposed adaptive detector, based on the PFGLMS algorithm [10], was investigated in multipath Rayleigh fading channels. Moreover, the performance results show that the systems performances have been improved by increasing the number of RAKE fingers beyond the number of multipath components. The paper is organized as follows. System model is demonstrated in Section II which is mainly focus on proposed transmitter and receiver structure. The system performance is quantified through the Performance results from the computer simulation which is presented in Section III. Finally, section IV gives a conclusion of this work.

II. System Model

A CDMA system as depicted in Fig.1 is considered in this paper. Data from different users is modulated by different signature waveforms before being transmitted asynchronously through a wireless channel [11], which is modeled as multipath Rayleigh fading. At the receiver, the user data is retrieved adaptively base on the minimum mean square error criterion (MMSE).

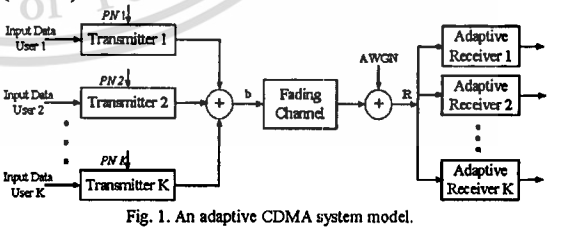

Fig. 1. An adaptive CDMA system model.

978-1-4244-5607-9/10/$25.00 ©2010 ECTI

A. Transmitter Structure

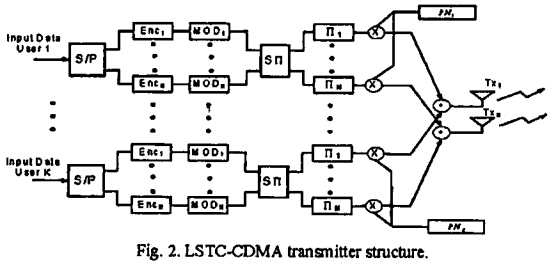

Fig. 2. LSTC-CDMA transmitter structure.

In a downlink LSTC-CDMA system, all user signals are transmitted simultaneously with N transmitters and M receivers antennas. Fig. 2 shows the LSTC-CDMA transmitter structure with K users. The binary information of each user is transmitted at a data rate of $r_b = 1/T_b$, where T_b is the bit interval. This data information is first converted into layered data information streams by a serial to parallel (S/P) converter. Before modulated, each information stream was encoded by a convolutional encoder to produce coded data stream for each layer. The layered coded data streams are then fed into a spatial time interleaver ($S\Pi$) and time interleaver (Π). Next, the coded data streams are spread by its signature sequence using a spreading gain of L with $L = T/T_c$, where T is the symbol interval, and T_c is chip duration of spreading sequence. Finally, the spread symbols of all users are then combined together and simultaneously transmitted through N transmit antennas in a multipath Rayleigh Fading channels.

Let $\mathbf{b}$ be the coded signal vectors transmitted by K users through N transmit antennas and be defined by:

$$\mathbf{b}=[\mathbf{b}_1,\mathbf{b}_2,...,\mathbf{b}_p,...,\mathbf{b}_K]^T \quad (1)$$

where $\mathbf{b}_p = [b_p^1,..., b_p^n,..., b_p^N]$, and b_p^n is the information bit of the p-th user for n-th transmit antenna with n=1,..,N and p=1,..,K.

Let $\mathbf{S}$ represents the L x KN spread transmitted sequences of K users for n transmit antennas, as given by:

$$\mathbf{S}=[\mathbf{s}_1^1,...,\mathbf{s}_1^N,...,\mathbf{s}_p^n...\mathbf{s}_K^1,...\mathbf{s}_K^N] \quad (2)$$

where $\mathbf{s}_p^n=[s_p^{n,1},...,s_p^{n,q},...,s_p^{n,L}]^T$, and $s_p^{n,q}$ is the q-th chip of a spreading sequence for the p-th user and n-th transmit antenna with n =1,...., N; p=1,..,K; and q=1,..,L.

Let $\mathbf{A}$ is the received amplitude of the p-th user's signal for n-th transmit antenna with n=1,..,N and p=1,..,K; which is represented by:

$$\mathbf{A}=\text{diag}(A_{1,1},...,A_{1,N},...,A_{p,n},...,A_{K,1},...,A_{K,N}) \quad (3)$$

Let $\mathbf{r}_{t,j}^p$ is the received signal vector for the p-th user at the receiver antenna j, $j=1,...,M$, for symbol t and delay time τ, is represented by:

$$r(t) = s(t-\tau)hAb + n(t)$$
$$\text{and is equivalently by:} \quad \mathbf{r}_{t,j}^p = \mathbf{S}\mathbf{H}_{t,j}^p\mathbf{A}\mathbf{b}+\mathbf{n}_{t,j}^p \quad (4)$$

where $\mathbf{r}_{t,j}^p=[r_{t,j}^{p,1},...r_{t,j}^{p,q},...,r_{t,j}^{p,L}]^T$, and $r_{t,j}^{p,q}$ is the received signal for the p-th user at the q-th chip of the t-th symbol for j-th antenna. $\mathbf{H}_{t,j}^p$ is defined by $\mathbf{H}_{t,j}^p = diag(\mathbf{h}_{t,j}^p,...,\mathbf{h}_{t,j}^p)_{KN\times KN}$ where $\mathbf{h}_{t,j}^p = diag[h_{j,1}^p(t),...,h_{j,n}^p(t),...,h_{j,N}^p(t)]_{N\times N}$, and $h_{j,n}^p(t)$ represents the fading coefficient from j-th receive antenna to n-th transmit antenna of the p-th user. $\mathbf{n}_{t,j}^p$ is defined as an $L\times1$ noise vector at the receive antenna j of the p-th user, given by $\mathbf{n}_{t,j}^p=[n_{j,1}^p(t),...,n_{j,q}^p(t),...,n_{j,L}^p(t)]^T$ where $n_{j,q}^p(t)$ is a Gaussian random variable with a zero mean and two sided power spectral density $N_o/2$ per dimension. The received signals for all receive antennas of the p-th user are given by $\mathbf{R}_t^p=[\mathbf{r}_{t,1}^p,...,\mathbf{r}_{t,j}^p,...,\mathbf{r}_{t,M}^p]^T$.

B. Receiver Structure

In downlink LSTC-CDMA system, we assume that the system has no knowledge of Channel State Information (CSI), spreading sequences, and fading coefficients except the training sequence. A block diagram of the proposed adaptive iterative generalized RAKE CDMA multiuser receiver for Layered Space Time Coded systems in multipath fading channels is shown in Fig. 3.

This structure consists of K adaptive iterative G-RAKE LSTC-CDMA single user receivers, each with an adaptive detector that followed by N parallel soft-input soft-output channel decoders. The received signals are first input to the adaptive detector in order to mitigate the effect of multipath fading. The detector outputs are then fed to the time and spatial deinterleavers, defined by Π^{-1} and $S\Pi^{-1}$, respectively. The deinterleavers outputs are then decoded by a Maximum A Posteriori (MAP) decoder. Next, the estimated soft symbols of MAP decoders from all users are sent to the spatial and time interleavers, and then fed back to the adaptive detector under iterative technique to cancel the interference from adjacent antennas of the user, called CCI, and the interference from other users, called MAI.

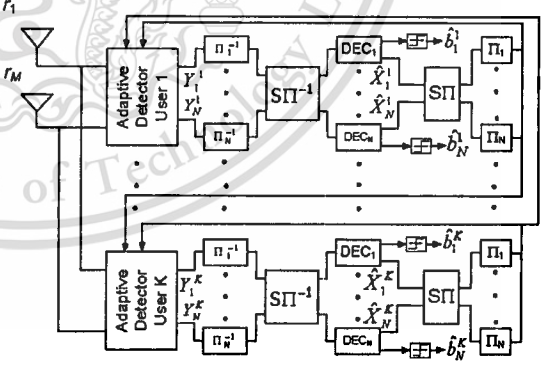

Fig. 3. Block diagram of G-RAKE LST- CDMA receiver.

1. Proposed Adaptive Iterative Detector

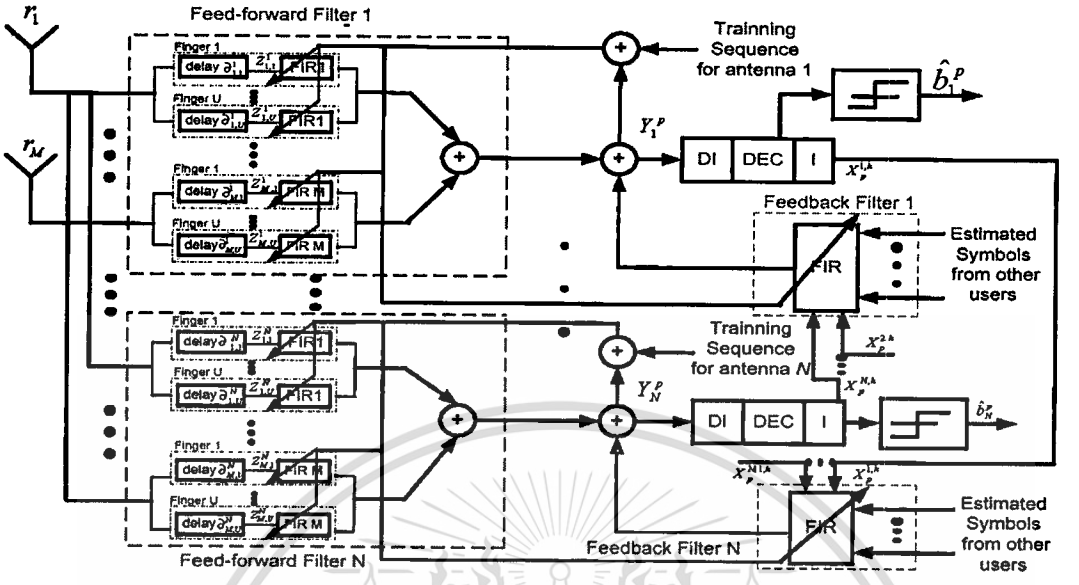

Fig. 4. Block diagram of the adaptive iterative G-RAKE LSTC-CDMA receiver.

The block diagram of the adaptive iterative generalized RAKE LSTC-CDMA receiver for the p-th user is shown in Fig. 4. In order to determine a weight coefficient of each finger element, the proposed detector employs an adaptive G-RAKE structure and antenna array processing. Unlike the conventional RAKE receiver, the G-RAKE receiver benefits from using more fingers than the number of multipath. In the proposed adaptive receiver structure, N sets of adaptive detector consist of M equalizers for the feed-forward filter and an equalizer for the feedback filter modules. An equalizer, employed in the proposed adaptive detector, is based on the PFGLMS algorithm. Moreover, the structure consists of a bank of U RAKE fingers, each correlating to a different delay of the received signal. The finger outputs are then combined to form a decision statistic. Importantly, the detector output for each layer is obtained from combining a feed-forward and a feedback filter output. In the iterative process, the feed-forward filter is compensated for the channel estimation error, and the feedback filter is used to cancel the interference from adjacent antennas and other users. In the first iteration, there are no estimated symbols from the decoders, and the feedback filter coefficients are zeros; thus, the feedback filter output is also zero. In the feed-forward filter, the M adaptive equalizers are used to estimate the channel coefficients and signature sequence for each layer of each user. The equalizer outputs from all receive antennas are added to obtain a feed-forward filter output signal for each transmit antenna as shown in Fig. 4.

Let $\mathbf{w}_j^{p,k}(t)$ be an Lx1 feed-forward tap coefficients vector for the j-th receive antenna of the p-th user during the k-th iteration at symbol interval t and be given by:

$$\mathbf{w}_j^{p,k}(t) = [w_{t,j}^{p,k}(0),\ldots, w_{t,j}^{p,k}(q),\ldots, w_{t,j}^{p,k}(L-1)]^T \quad (5)$$

where $w_{t,j}^{p,k}(q)$ is the feed-forward tap coefficient corresponding to the q-th chip of the spreading sequence.

Let $\mathbf{w}_b^{i,k}(t)$ be the feedback filter coefficients of all users, except the i-th antenna of the p-th user, at symbol interval t in time domain, is expressed as:

$$\mathbf{w}_b^{i,k}(t)=[\mathbf{w}_{b,1}^{1,k}(t),\ldots,\mathbf{w}_{b,1}^{N,k}(t),\ldots,\mathbf{w}_{b,p}^{i,k}(t),\ldots,\mathbf{w}_{b,K}^{1,k}(t),\ldots,\mathbf{w}_{b,K}^{N,k}(t)]^T \quad (6)$$

where $$\mathbf{w}_{b,p}^{i,k}(t) = [w_{b,p}^{1,k}(t),\ldots, w_{b,p}^{i-1,k}(t), w_{b,p}^{i+1,k}(t),\ldots, w_{b,p}^{N,k}(t)] \quad (7)$$

$\hat{\underline{\mathbf{x}}}_{t,p}^{i,k}$ is $(KN-1)$×1 vector of the estimated soft symbols, at the k-th iteration, from MAP decoders of every antenna of all users, except the i-th antenna of p-th user at symbol interval t, given by:

$$\hat{\underline{\mathbf{x}}}_{t,p}^{i,k} = (\hat{\mathbf{x}}_{t,1}^{1,k},\ldots,\hat{\mathbf{x}}_{t,1}^{N,k},\ldots,\hat{\mathbf{x}}_{t,p}^{i,k},\ldots,\hat{\mathbf{x}}_{t,K}^{1,k},\ldots,\hat{\mathbf{x}}_{t,K}^{N,k})^T \quad (8)$$

where $$\hat{\mathbf{x}}_{t,p}^{i,k} = (\hat{\mathbf{x}}_{t,p}^{1,k}, \hat{\mathbf{x}}_{t,p}^{2,k},\ldots, \hat{\mathbf{x}}_{t,p}^{i-1,k}, \hat{\mathbf{x}}_{t,p}^{i+1,k},\ldots, \hat{\mathbf{x}}_{t,p}^{N,k}) \quad (9)$$

$\mathbf{z}_{t,j}^{p}$ is the finger outputs for u-th finger of p-th user at the receive antenna j and transmit antenna i for symbol t and be represented by:

$$\mathbf{z}_{t,j}^{p} = \mathrm{r}_{t,j}^{p}\,\delta(t-\partial_{j,u}^{i}) \quad (10)$$

The detected symbol of the p-th user obtained at the output of the adaptive detector for the i-th antenna during the k-th iteration at symbol interval t, denoted by $y_{t,p}^{i,k}$, is defined as:

$$y_{t,p}^{i,k} = \sum_{j=0}^{M} \mathbf{w}_j^{i,k}(t)^H \mathbf{z}_{t,j}^{p} + \mathbf{w}_b^{i,k}(t)^H \hat{\underline{\mathbf{x}}}_{t,p}^{i,k} \qquad (11)$$

The detector soft output $y_{t,p}^{i,k}$ in the time domain is then compared to training symbol, denoted by $\mathbf{x}_{t,p}^{i,k}$ The difference between them is calculated as the detection error. The detection error for the p-th user in the k-th iteration at symbol interval t, for i-th antenna, denoted by $e_{t,p}^{i,k}$, is represented by:

$$e_{t,p}^{i,k} = y_{t,p}^{i,k} - x_{t,p}^{i,k} \qquad (12)$$

The detection error is then used to adapt the feed-forward filter and feedback filter tap coefficients in the time domain. After the Mean Square Error (MSE) approaches a specified value, the training mode is switched to the decision directed mode, in which the training sequence is replaced by the hard decision output of each user detector.

The values tap coefficients, $\mathbf{w}_j^{p,k}(t)$ in (5) and feedback filter tap coefficients, $\mathbf{w}_b^{i,k}(t)$ in (6) are calculated by minimizing the mean square error, defined as ζ , and given by

$$\zeta = mim\left(E\left|e_{t,p}^{i,k}\right|^2 \right) = \min\left(E\left[\left|y_{t,p}^{i,k} - x_{t,p}^{i,k}\right|^2\right] \right) \qquad (13)$$

And they can be determined recursively by partially filtered gradient LMS (PFGLMS) algorithm. PFGLMS algorithm based on an exponentially weighted least square error is utilized to improve the convergence speed with a slight increase in complexity [10].

The modified feed-forward and feedback coefficients of the PFGLMS algorithm can be expressed as:

$$\mathbf{w}_f^{i,k}(t+1) = \mathbf{w}_f^{i,k}(t) + \mu_f \mathbf{g}_f^{i,k}(t) \qquad (14)$$

and

$$\mathbf{w}_b^{i,k}(t+1) = \mathbf{w}_b^{i,k}(t) + \mu_b \mathbf{g}_b^{i,k}(t) \qquad (15)$$

where

$$\left.\begin{aligned} \mathbf{g}_f^{i,k}(t) &= e(t)\mathbf{z}_{t,j}^{p} + \hat{\mathbf{g}}_f^{i,k}(t) \\ \hat{\mathbf{g}}_f^{i,k}(t) &= \lambda_f \hat{\mathbf{g}}_f^{i,k}(t-1) + \gamma_f e(t)\mathbf{z}_{t,j}^{p} \end{aligned}\right\} \qquad (16)$$

and

$$\left.\begin{aligned} \mathbf{g}_b^{i,k}(t) &= e(t)\hat{\underline{\mathbf{x}}}_{t,p}^{i,k} + \hat{\mathbf{g}}_b^{i,k}(t) \\ \hat{\mathbf{g}}_b^{i,k}(t) &= \lambda_b \hat{\mathbf{g}}_b^{i,k}(t-1) + \gamma_b e(t)\hat{\underline{\mathbf{x}}}_{t,p}^{i,k} \end{aligned}\right\} \qquad (17)$$

where $\hat{\underline{\mathbf{x}}}_{t,p}^{i,k}$ and $\mathbf{z}_{t,j}^{p}$ are defined in (8) and (10), respectively. μ_f and μ_b are the step sizes for feed-forward and feedback adaptation. (γ_f, γ_b) and (λ_f, λ_b) are the forgetting factors and the scaling factors respectively, and $\hat{\mathbf{g}}_f^{i,k}(0) = \hat{\mathbf{g}}_b^{i,k}(0) = 0$.

2. *Maximum A Posteriori Decoder*

In the proposed receiver structure, detector output for user p, denoted by $y_{t,p}^{i,k}$ is decoded by Maximum A Posteriori (MAP) Decoder. The soft-output from the decoder is used to suppress the interference in the feedback filter in the next iteration. The process of this adaptive iterative detection/decoding is performed until the symbol estimation can converge to the optimal performance. The soft-output from the decoder in the last iteration is then fed into a decision device to produce a decision. For a Binary Phase Shift Keying (BPSK), the functions for the transmitted modulated symbols 1 and –1 can be written as [12]:

$$P\left(y_{t,p}^{i,k} \middle| x_{t,p}^{i,k} = \pm 1\right) = \frac{1}{\sqrt{2\pi\sigma^2}} \exp\frac{-\left(y_{t,p}^{i,k} \mp 1\right)^2}{2\sigma^2} \qquad (18)$$

The Log-Likelihood Ratios (LLR) is determined in the k-th iteration for the i-th transmit layer of p-th user, denoted by $\lambda_{t,p}^{i,k}$:

$$\lambda_{t,p}^{i,k} = \log\left(\frac{P\left(x_{t,p}^{i,k} = 1 \middle| y_{t,p}^{i,k}\right)}{P\left(x_{t,p}^{i,k} = -1 \middle| y_{t,p}^{i,k}\right)} \right) \qquad (19)$$

The symbol A Posteriori Probabilities (APP) $P(x_{t,p}^{i,k} = q | y_{t,p}^{i,k})$, with q equal to 1 and -1, conditioned on the output variable which is defined as $y_{t,p}^{i,k}$ for p-th user, can be obtained as:

$$P\left(x_{t,p}^{i,k} = 1 \middle| y_{t,p}^{i,k}\right) = \frac{e^{\lambda_{t,p}^{i,k}}}{e^{\lambda_{t,p}^{i,k}} + 1}, \qquad P\left(x_{t,p}^{i,k} = -1 \middle| y_{t,p}^{i,k}\right) = \frac{1}{e^{\lambda_{t,p}^{i,k}} + 1} \qquad (20)$$

The soft-output symbols are estimated in the i-th layer and k-th iteration for p-th user, calculated as:

$$\hat{x}_{t,p}^{i,k} = \frac{e^{\lambda_{t,p}^{i,k}} - 1}{e^{\lambda_{t,p}^{i,k}} + 1} \qquad (21)$$

III. Performance Results

This section presents simulation results of the adaptive G-RAKE receiver for downlink LSTC-CDMA systems over a quasi-static Rayleigh fading channel whereby the fading coefficient is constant within a frame, but changes independently from one frame to another. The constituent codes are nonsystematic convolutional codes with the code rate R of 1/2 and memory order of 3. The spreading sequence is a gold sequence with processing gain of 7. The proposed system is simulated with 2 transmit and 2 receive antennas with multipath fading of 3 and with 130 information bits in each frame per layer for each user. Each layer consists of 266 encoded symbols per frame. The data rate is 1 Mb/s at the carrier frequency, f_c, of 2 GH_z.

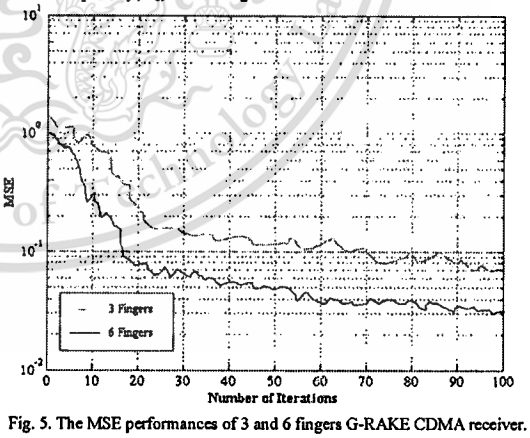

Fig. 5. The MSE performances of 3 and 6 fingers G-RAKE CDMA receiver.

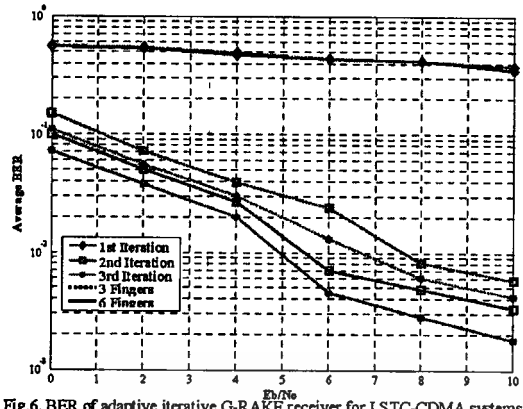

Fig.6. BER of adaptive iterative G-RAKE receiver for LSTC-CDMA systems.

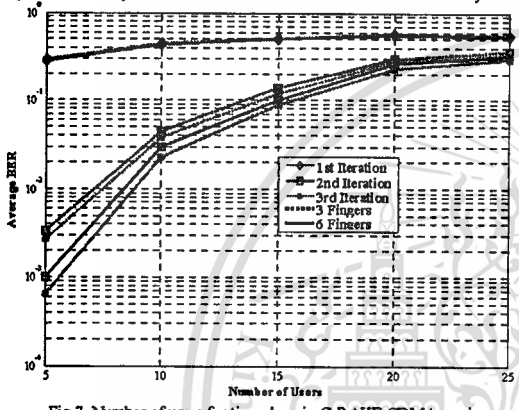

Fig.7. Number of users for time domain G-RAKE CDMA receiver.

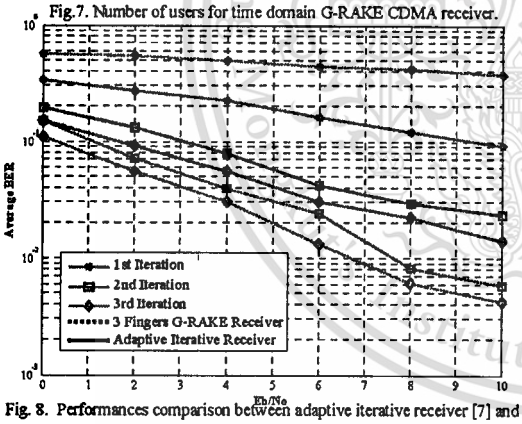

Fig. 8. Performances comparison between adaptive iterative receiver [7] and G-RAKE LSTC-CDMA receiver based on PFGLMS adaptive algorithm.

A comparison of MSE performances of adaptive G-Rake CDMA receiver for 3 and 6 fingers is shown in Fig. 5, whereby the MSE curve of 6 fingers RAKE receiver is lower than that of 3 fingers. This shows that the system performance improves when additional finger is placed at a delay. The performance of the 2 transmit and 2 receive antennas for 5 users under time domain approach is depicted in Fig. 6. The result shows that the performance of the G-RAKE receiver, based on PFGLMS algorithm, has a significant improvement in the first iteration and gradually improves for the higher iterations. The number of users for adaptive CDMA G-RAKE receiver is shown in Fig. 7. The simulation results show that the number of users is 15 at 3 iterations for a BER of 8.5×10^{-2}. These results also show that when the number of users increases, a higher number of iteration is required to achieve the same BER. In Fig. 8, we present the performance comparison between an adaptive LSTC-CDMA receiver [7] and a 3 fingers G-RAKE LSTC-CDMA receiver. The BER curves show that adaptive iterative receiver only performs better then G-RAKE receiver in the first iteration. This means that the proposed G-RAKE receiver have a better performance from second up to higher iteration.

IV. Conclusion

In this paper, we present an adaptive iterative generalized RAKE receiver for Layered Space-Time Coded CDMA systems, based on the Partially Filtered Gradient LMS algorithm, in order to mitigate the effect of multipath and suppress the interferences of the systems. Moreover, the system performance improved when the number of fingers was increased beyond the number of resolvable multipath. Due to the higher reliability of the Co-Channel Interference (CCI) and Multiple Access Interference (MAI) estimation, this performance results prove that the proposed G-RAKE CDMA receiver can effectively mitigate the CCI and MAI using the interference suppression and cancellation techniques.

References

[1] R. L.-U. Choi, K. B. Letaief, and R. D. Murch, "MIMO CDMA antenna systems," *Proc. of IEEE ICC*, vol. 2, pp. 990-994, 2000.

[2] L. Mailaender, "Linear MIMO Chip Equalization for CDMA Downlink," *Proc. of IEEE SPAWC*, pp.299-303, June 2003.

[3] S. Marinkovic, "Interference mitigation in CDMA and space-time coded MIMO systems," Thesis (Ph. D.) Telecommunications Laboratory, Dept. of Electrical and Information Engineering, University of Sydney, 2002 .

[4] J. Li, K. B. Letaief, and Z. Cao, "Adaptive cochannel interference cancellation in space-time coded communication systems," *IEEE Trans. on Communication*, vol. 50, pp. 1580-1583, October 2002.

[5] C. Teekapakvisit, V. D. Pham, and B. Vucetic, "An Adaptive Iterative Receiver for Space-time coding MIMO Systems," *3rd Workshop on the Internet, Telecommunications and Signal Processing*, pp. 54-59, 2004.

[6] Y. Sun, M. L. Honig, and V. Tripathi, "Adaptive, iterative, reduced-rank equalization for MIMO channels," *Proc. of MILCOM*, vol.2, pp.1029-1033, October 2002.

[7] T. Keovkolyan, C. Teekapakvisit, and K. Janchitrapongvej, "Adaptive Iterative Receiver for Layered Space-Time Coding CDMA System," *Proc. of IEEE-ECTI-CON*, vol. 2, pp.852-855, May 2009.

[8] G.E. Bottomley, T. Ottosson, and Y.P. Eric Wang, "A Generalized RAKE Receiver for Interference Suppression," *IEEE Journal on Selected Areas in Communications*, vol. 18, pp.1536-1545, 2000.

[9] J. Yi and J. Lee, "RAKE Receiver with Adaptive Interference Cancellers for a DS-CDMA System in Multipath Fading Channels," *IEEE VTS-Fall VTC*, vol. 3, pp.1216-1220, 2000.

[10] J. S. Lim, "Fast adaptive filtering algorithm based on exponentially weighted least-square errors," *Electronics Letters*, vol.35, pp. 1913-1915, October 1999.

[11] P. Lin, P. Rapajic, and Z. Krusevac, "On the tracking performance of LMS and RLS algorithms in an adaptive MMSE CDMA Receiver," *Proc. of IEEE-Communications Theory Workshop*, pp.175-178, 2005.

[12] B Vucetic and J. Yuan, "Turbo Codes: Principle and Application,", Boston: Kluwer Academic Publisher, 2000.

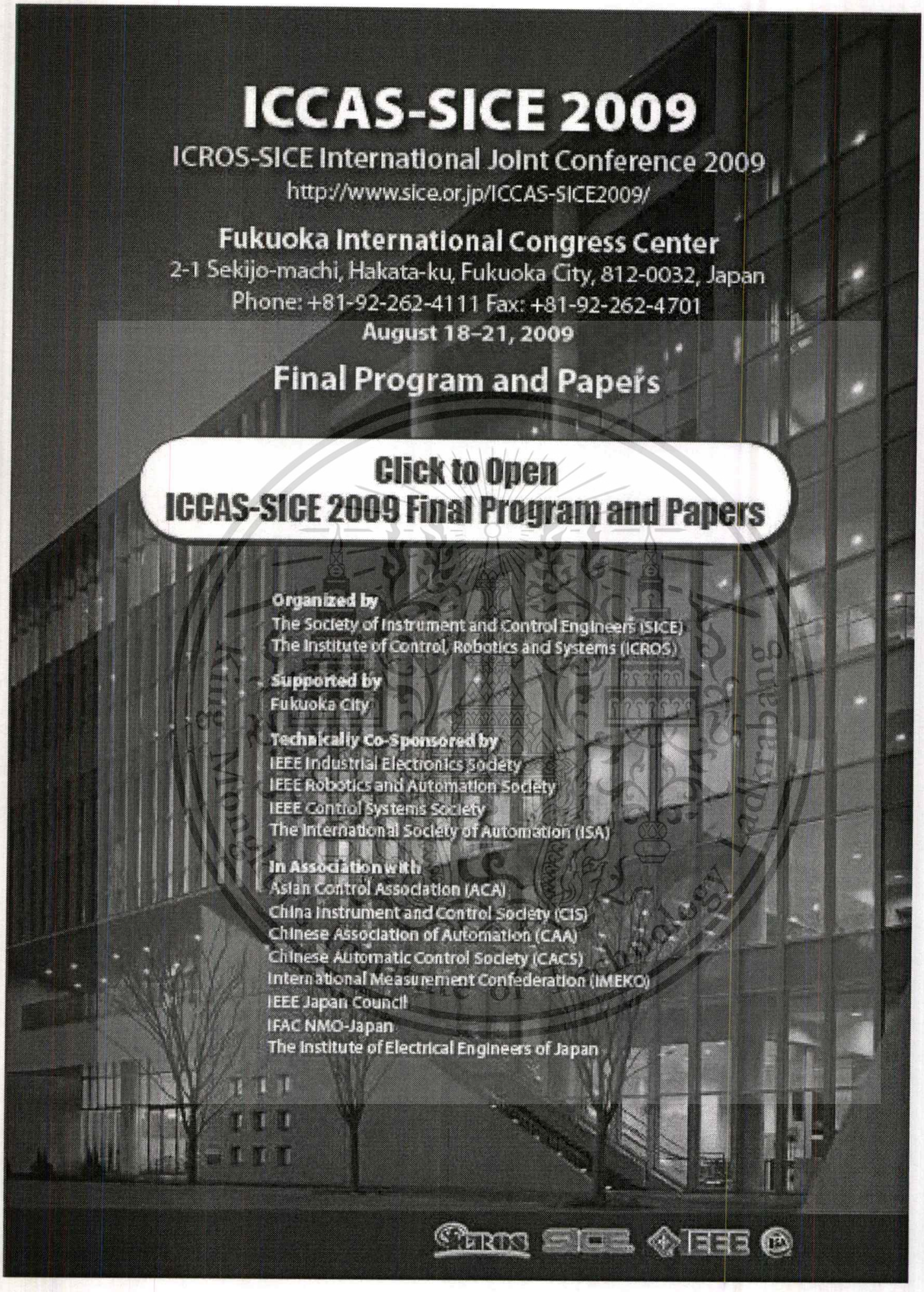

ICROS-SICE International Joint Conference 2009
August 18-21, 2009, Fukuoka International Congress Center, Japan

Low Complexity LMS Based Adaptive Iterative Receiver for CDMA Systems

Teav Keovkolyan[1] and Chakree Teekapavisit[2]

[1,2]Department of Information Engineering, Faculty of Engineering, King Mongkut's Institute of Technology Ladkrabang (KMITL), Chalongkrung Rd, Bangkok 1520, Thailand
[1](Tel : +66-8-0450-3025; E-mail: teav_keovkolyan@yahoo.com)
[2](Tel : +66-8-4093-2354; E-mail: ktchakre@kmitl.ac.th)

Abstract: An adaptive iterative frequency domain receiver for a Layered Space-Time Coded CDMA (LSTC-CDMA) system has been proposed in this paper. The proposed receiver, based on a joint adaptive iterative detection and decoding algorithm, adaptively cancels Co-Channel Interference (CCI) and mitigates Multiple Access Interference (MAI), and also has a significant reduction in computation complexity with the same performance compared to a time domain receiver. The Least Means Square (LMS) algorithm is used for both feed-forward filter and feedback filter in the adaptive detection. A Partially Filtered Gradient LMS (PFGLMS) algorithm is also proposed to improve the convergence speed of the adaptive detector. The performance results show that the proposed adaptive receiver can approach the interference-free single user performance for a certain range of the signal to noise ratio (SNR).

Keywords: Code Division Multiple Access, Layered Space Time Coding, Frequency domain equalizer, Least Mean Square, Partially Gradient LMS.

1. INTRODUCTION

With the integration of the internet and multimedia applications in the next generation wireless communications, the huge demand of highly reliable data rate service and the increase in the system capacity are growing very fast. Several broadband wireless communication systems have been widely studied such as Code Division Multiple Access (CDMA) and Multi-Input-Multi-Output (MIMO) systems.

Direct-Sequence CDMA (DS-CDMA) has emerged as a predominantly multiple-access technique for 3G systems, compared to the 2G TDMA systems. To improve the throughput of this system, the combination of Layered Space-Time Coding (LSTC) and CDMA, named as LSTC-CDMA, has been studied in [1-3]. This implementation generates Co-Channel Interference (CCI) and Multiple Access Interference (MAI). To mitigate these, an adaptive MMSE receiver for a LSTC system have been proposed in [4]. A non-linear adaptive iterative receiver has been studied in [5, 6], containing a feed-forward filter and a feedback filter. By using this algorithm, the convergence speed can be improved; however, the complexity of the system is still high because of the feedback filter. Moreover, the adaptive iterative receiver for LSTC CDMA system was proposed in [7], which can improve the performance of the system but still have high complexity. Recently, frequency domain equalizer (FDE) has been proposed for SISO system in [8]. In [9], the FDE has been extended to MIMO system. Such technique offers significant reduction in the computation complexity.

In this paper, an adaptive iterative frequency domain receiver for multiuser LSTC-CDMA system under quasi-static fading channel was proposed. Such receiver can effectively mitigate the MAI, thus improve the multiuser system performance with low complexity, compared to that in time domain approach. The proposed low complexity receiver consists of a feed forward filter and a feedback iterative parallel interference canceller. Consequently, the proposed adaptive detector was investigated, based on the Adaptive Least Mean Square (LMS) algorithm [10], whereby the performance, i.e. complexity, has been improved. However, the convergence speed of the adaptive detector is not satisfied. For this reason, the adaptive iterative receiver using a Partially Filtered Gradient LMS (PFGLMS) [11] algorithm was proposed to improve convergence speed with slightly increase in complexity, compared to LMS algorithm. The simulation results show that the adaptive iterative receiver in frequency domain can also approach the interference-free single user performance for a certain range of the signal to noise ratio (SNR).

2. SYSTEM MODEL

2.1 Transmitter Structure

In a downlink LSTC-CDMA system, all user signals are transmitted simultaneously with N transmitters and M receivers antennas. Fig. 1 shows the LSTC-CDMA transmitter structure with K users. The binary information of each user is transmitted at a data rate of $r_b = 1/T_b$, where T_b is the bit interval. This data information is first converted into layered data information streams by a serial to parallel (S/P) converter. Before modulating, each information stream is encoded by a convolutional encoder to produce coded data stream for each layer. The layered coded data streams are then fed into a spatial time interleaver ($S\Pi$) and time interleaver (Π). Next, the coded data streams are spread by its signature sequence using a spreading gain of L with $L = T/T_c$, where T is the symbol interval, and T_c is chip duration of spreading sequence. Finally, the spread symbols of all users are then combined together and simultaneously transmitted through N transmit antennas.

PR0002/09/0000-2339 ¥400 ©

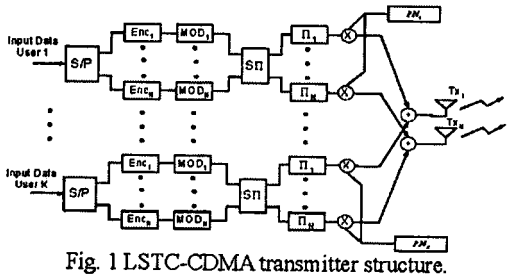

Fig. 1 LSTC-CDMA transmitter structure.

Let $\mathbf{b}$ be the coded signal vectors transmitted by K users through N transmit antennas and be defined by:

$$\mathbf{b}=[\mathbf{b}_1,\mathbf{b}_2,...,\mathbf{b}_p,...,\mathbf{b}_k]^T \quad (1)$$

where $\mathbf{b}_p=[b_p^1,...,b_p^n,...,b_p^N]$, and b_p^n is the information bit of the p-th user for n-th transmit antenna with n=1,..,N and p=1,..,K.

Let $\mathbf{S}$ represents the L x KN spread transmitted sequences of K users for n transmit antennas, as given by:

$$\mathbf{S}=[\mathbf{s}_1^1,...,\mathbf{s}_1^N,...,\mathbf{s}_p^n...\mathbf{s}_K^1,...\mathbf{s}_K^N] \quad (2)$$

where $\mathbf{s}_p^n=[s_p^{n,1},...,s_p^{n,q},...,s_p^{n,L}]^T$, and $s_p^{n,q}$ is the q-th chip of a spreading sequence for the p-th user and n-th transmit antenna with n =1,..., N; p=1,..,K; and q=1,..,L.

Let $\mathbf{r}_{t,j}^p$ is the received signal vector for the p-th user at the receiver antenna j, $j=1,...,M$, for symbol t, is represented by:

$$\mathbf{r}_{t,j}^p=\mathbf{S}\mathbf{H}_{t,j}^p\mathbf{b}+\mathbf{n}_{t,j}^p \quad (3)$$

where $\mathbf{r}_{t,j}^p=[r_{t,j}^{p,1},...r_{t,j}^{p,q},...,r_{t,j}^{p,L}]^T$, and $r_{t,j}^{p,q}$ is the received signal for the p-th user at the q-th chip of the t-th symbol for j-th antenna. $\mathbf{H}_{t,j}^p$ is defined by:

$$\mathbf{H}_{t,j}^p=diag(\mathbf{h}_{t,j}^p,...,\mathbf{h}_{t,j}^p)_{KN\&KN} \quad (4)$$

where $\mathbf{h}_{t,j}^p=diag[h_{j,1}^p(t),...,h_{j,n}^p(t),...,h_{j,N}^p(t)]_{N\&N}$, and $h_{j,n}^p(t)$ represents the fading coefficient from j-th receive antenna to n-th transmit antenna of the p-th user. $\mathbf{n}_{t,j}^p$ is defined as an $L\times1$ noise vector at the receive antenna j of the p-th user, given by $\mathbf{n}_{t,j}^p=[n_{j,1}^p(t),...,n_{j,q}^p(t),...,n_{j,L}^p(t)]^T$ where $n_{j,q}^p(t)$ is a Gaussian random variable with a zero mean and two sided power spectral density $N_o/2$ per dimension. The received signals for all receive antennas of the p-th user are given by $\mathbf{R}_t^p=[\mathbf{r}_{t,1}^p,...,\mathbf{r}_{t,j}^p,...,\mathbf{r}_{t,M}^p]^T$.

2.2 Receiver Structure

In downlink LSTC-CDMA system, we assume that the system has no knowledge of Channel State Information (CSI), spreading sequences, and fading coefficients except the training sequence. A block diagram of the proposed adaptive iterative LSTC-CDMA multiuser receiver for the p-th user is shown in Fig. 2.

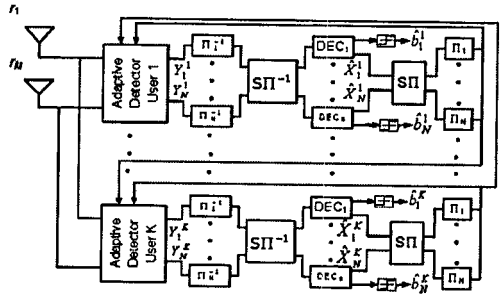

Fig. 2 Block diagram of iterative LST- CDMA Receiver.

This structure consists of K adaptive iterative LSTC-CDMA single user receivers, each with an adaptive detector followed by N parallel soft-input soft-output channel decoders. The received signals are first input to the adaptive detector. The detector outputs are then fed to the time and spatial deinterleavers, definded by Π^{-1} and $S\Pi^{-1}$, respectively. The deinterleavers outputs are then decoded by a Maximum A Posteriori (MAP) decoder. The estimated soft symbols of MAP decoders from all users are sent to the spatial and time interleavers, and then fed back to the adaptive detector under iterative technique to cancel the interference from adjacent antennas of the user, called CCI, and the interference from other users, called MAI.

2.2.1 Proposed Adaptive Iterative Detector

In this study, we assume that downlink LSTC-CDMA system has no knowledge of Channel State Information (CSI), spreading sequences, and fading coefficients except the training sequence. The block diagram of the proposed frequency domain adaptive iterative receiver for LSTC-CDMA is shown in Fig 3.

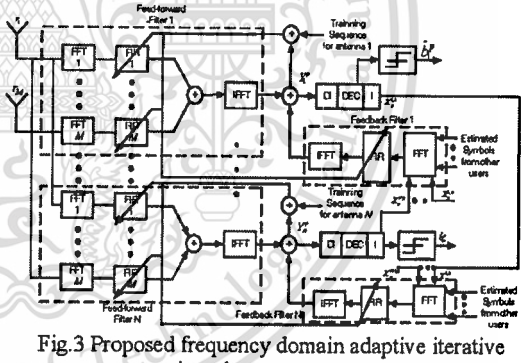

Fig.3 Proposed frequency domain adaptive iterative receiver detector structure.

The adaptive detector consists of an adaptive LMS feed-forward filter and an adaptive LMS feedback filter. For the proposed receiver, L chips received signals ($\mathbf{r}_{t,j}^p$) of p-th user at the symbol t are transformed by using Fast Fourier transform (FFT) into frequency domain. The output of each FFT is defined by, $\Theta_{t,j}^p=fft(\mathbf{r}_{t,j}^p)$ where $j=1,...,M$, $\Theta_{t,j}^p$ is the received signal of j-th receive antenna of p-th user at time t in frequency domain, represented by $\Theta_{t,j}^p=[\Theta_{t,j}^{p,1},...,\Theta_{t,j}^{p,q},...,\Theta_{t,j}^{p,L}]$, $\Theta_{t,j}^{p,q}=\sum_{l=0}^{L-1}r_{t,j}^{p,l}e^{\frac{-j2\pi ql}{L}}$

,and $fft(\cdot)$ is the fast Fourier transform function, and $\Theta_{t,j}^{p,q}$, q=1,...,L, is the FFT transformation of the received signal for the j-th receive antenna of the p-th user at the q-th chip of the t-th symbol.

Let $\Psi_{t,j}^{p,k}$ represents the FFT of the feed forward filter tap coefficient vector of the p-th user for k-th iteration at the time t, at the receive antenna j, defined by $\Psi_{t,j}^{p,k} = fft\left(\mathbf{w}_{t,j}^{p,k}\right)$ where:

$\Psi_{t,j}^{p,k} = \left[\Psi_{t,j}^{p,k}(0),..., \Psi_{t,j}^{p,k}(q),..., \Psi_{t,j}^{p,k}(L-1)\right]$

, $\Psi_{t,j}^{p,k}(q) = \sum_{l=0}^{L-1} w_{t,j}^{p,k}(t) e^{\frac{-j2\pi lq}{L}}$, and $\mathbf{w}_{t,j}^{p,k}$ is L×1 feed-forward tap coefficient vector given by

$$\mathbf{w}_{t,j}^{p,k} = \left[w_{t,j}^{p,k}(0),..., w_{t,j}^{p,k}(q),..., w_{t,j}^{p,k}(L-1)\right]^T \quad (5)$$

$\Theta_{t,j}$ is sent to the feed forward filter to perform the convolution with the feed forward tap coefficient $\Psi_{t,j}^{p,k}$. The output of each feed forward filter is combined together, denoted by

$$\overline{\mathbf{F}}_{t,p}^{i,k} = \left(\sum_{j=1}^{M} diag\left(\Theta_{t,j}^{p}\right)^H \cdot \Psi_{t,j}^{p,k}\right) \quad (6)$$

where $diag(\cdot)$ and $(\cdot)^H$denoted a diagonal matrix and a conjugate transpose function. $\overline{\mathbf{F}}_{t,p}^{i,k}$ is then transformed back into the time domain by the inverse FFT (IFFT). The feed forward filter output of p-th user in the k-th iteration at time t, for layer i, is given by

$$F_{t,p}^{i,k} = \mathbf{I}_F \cdot ifft\left(\overline{\mathbf{F}}_{t,p}^{i,k}\right) \quad (7)$$

where $\mathbf{I}_F = [1\ \mathbf{0}_{L-1}]$,$\mathbf{0}_{L-1}$ is a row vector of length L-1 containing all zero, and $\hat{F}_{t,p}^{i,k} = ifft\left(\overline{\mathbf{F}}_{t,p}^{i,k}\right)$ where

$\hat{F}_{t,p}^{i,k} = \left[F_{t,p}^{i,k}(0),..., F_{t,p}^{i,k}(q),..., F_{t,p}^{i,k}(L-1)\right]$

and $\hat{F}_{t,p}^{i,k}(q) = \frac{1}{L}\sum_{l=0}^{L-1} \overline{F}_{t,p}^{i,k} e^{\frac{-j2\pi lq}{L}}$.

To cancel MAI and CCI, the estimated symbols from the outputs of the decoders are first input to the feedback filter and transformed into frequency domain by using the FFT. The output of the FFT is represented by $\Lambda_{t,p}^{i,k} = fft(\underline{\hat{\mathbf{x}}}_{t,p}^{i,k})$ where: $\Lambda_{t,p}^{i,k} = \left[\Lambda_{t,p}^{i,k}(1),...\Lambda_{t,p}^{i,k}(a),...\Lambda_{t,p}^{i,k}(KN-1)\right]$

, and $\Lambda_{t,p}^{i,k}(a) = \sum_{m=0}^{KN-2} \hat{x}_{t,p}^{m,k} e^{\frac{-j2\pi am}{KN-1}}$ $\begin{cases} a \in (1...KN-1) \\ p \in (1...K) \end{cases}$

$\underline{\hat{\mathbf{x}}}_{t,p}^{i,k}$ is an $(KN-1)$×1 vector of the estimated soft symbols, at the k-th iteration, from MAP decoders of all antennas of all users, excluding the j-th antenna of the p-th user, given by

$$\underline{\hat{\mathbf{x}}}_{t,p}^{i,k} = \left(\hat{\mathbf{x}}_{t,1}^{1,k},..., \hat{\mathbf{x}}_{t,1}^{N,k},..., \hat{\mathbf{x}}_{t,p}^{i,k},..., \hat{\mathbf{x}}_{t,K}^{1,k},..., \hat{\mathbf{x}}_{t,K}^{N,k}\right)^T \quad (8)$$

$\underline{\hat{w}}_{b,p}^{i,k}(t)$ is the feedback filter coefficients of all user except the j-th antenna of the p-th user, given by

$$\underline{\hat{w}}_{b,p}^{i,k}(t) = \left[\mathbf{w}_{b,1}^{1,k}(t),..,\mathbf{w}_{b,1}^{N,k}(t),..,\mathbf{w}_{b,p}^{i,k}(t),..,\mathbf{w}_{b,K}^{1,k}(t),..,\mathbf{w}_{b,K}^{N,k}(t)\right]^T \quad (9)$$

Let $\Psi_{t,b,p}^{i,k}$ represents the FFT of $\underline{\hat{w}}_{b,p}^{i,k}(t)$ which is defined by $\Psi_{t,b,p}^{i,k} = fft\left(\underline{\hat{w}}_{b,p}^{i,k}(t)\right)$ where:

$\Psi_{t,b,p}^{i,k} = \left[\Psi_{t,b,p}^{i,k}(1),..., \Psi_{t,b,p}^{i,k}(a),..., \Psi_{t,b,p}^{i,k}(KN-1)\right]$ and

$\Psi_{t,b,p}^{i,k}(a) = \sum_{m=0}^{KN-2} w_{t,b,p}^{m,k} e^{\frac{-j2\pi am}{KN-1}}$.

The output of the FFT, as denoted as $\Lambda_{t,p}^{i,k}$, is then input to the feedback filter to perform convolution with the feedback tap coefficients $\Psi_{t,b}^{k}$ in frequency domain. Hence, the feedback filter output signals, defined by $\overline{\mathbf{F}}_{t,b,p}^{i,k} = \left(diag\left(\Lambda_{t,p}^{i,k\ H}\right) \cdot \Psi_{t,b,p}^{i,k}\right)$ and then transformed back into time domain by IFFT. The feedback filter output is given by

$$F_{t,b,p}^{i,k} = \mathbf{I}_B \cdot ifft\left(\overline{\mathbf{F}}_{t,b,p}^{i,k}\right) \quad (10)$$

where $\mathbf{I}_B = [1\ \mathbf{0}_{KN-1}]$ and $\mathbf{0}_{KN-1}$ is a zero row vector with length of KN-1, and $\hat{F}_{t,b,p}^{i,k} = ifft\left(\overline{\mathbf{F}}_{t,b,p}^{i,k}\right)$ where $\hat{F}_{t,b,p}^{i,k} = \left[F_{t,b,p}^{i,k}(1),..., F_{t,b,p}^{i,k}(a),..., F_{t,b,p}^{i,k}(KN-1)\right]$

, and $\hat{F}_{t,b,p}^{i,k}(a) = \frac{1}{KN-1}\sum_{m=0}^{KN-2} \overline{F}_{t,b,p}^{m,k} e^{\frac{-j2\pi am}{KN-1}}$

The detected symbol of the p-th user obtained in the k-th iteration at time t, for layer i, denoted by

$$y_{t,p}^{i,k} = F_{t,p}^{i,k} + F_{t,b,p}^{i,k} \quad (11)$$

where $F_{t,p}^{i,k}$ and $F_{t,b,p}^{i,k}$ represent feed forward and feedback filter output in time domain, given in (7) and (10) respectively. Note that the output of the feedback filter is zero at the first iteration.

The values of $\mathbf{w}_f^{p,k}(t)$ and $\mathbf{w}_b^{i,k}(t)$ are calculated by minimizing the mean square error, defined as

$$\zeta = \text{Min}\left(E\left[\left|y_{t,p}^{i,k} - x_{t,p}^{i,k}\right|^2\right]\right) \quad (12)$$

where $x_{t,p}^{i,k}$ is the training sequence of p-th user in the k-th iteration at time t, for layer i and then can be calculated recursively by an adaptive LMS algorithm as the following:

$$\mathbf{w}_f^{p,k}(t+1) = \mathbf{w}_f^{p,k}(t) + \mu_f e_{t,p}^{i,k} \mathbf{r}_{t,j}^{p} \quad (13)$$

$$\mathbf{w}_b^{i,k}(t+1) = \mathbf{w}_b^{i,k}(t) + \mu_b e_{t,p}^{i,k} \underline{\hat{\mathbf{x}}}_{t,p}^{i,k} \quad (14)$$

where $\mathbf{r}_{t,j}^{p}$ is the received signal vector for the p-th user which is defined in (3), and $\underline{\hat{\mathbf{x}}}_{t,p}^{i,k}$ is defined in (8). μ_f and μ_b are the step sizes for the feed-forward and feedback adaptation.

As the LMS algorithm has slow convergence and may not track in a non-stationary environment very well, the partially filtered gradient LMS (PFGLMS) algorithm [11] is utilized to improve the convergence speed. To apply the PFGLMS algorithm to the adaptive iterative receiver, the detected symbol of the p-th user i-th antenna during the k-th iteration at time t , defined in (11), is denoted by [10]:

$$y_{t,PFGLMS}^{i,k} = F_{t,p}^{i,k} + F_{t,b,p}^{i,k} \quad (15)$$

The modified feed-forward and feedback coefficients of the PFGLMS algorithm can be expressed as [10]:

$$\mathbf{w}_f^{i,k}(t+1) = \mathbf{w}_f^{i,k}(t) + \mu_f \mathbf{g}_f^{i,k}(t) \quad (16)$$

and

$$\mathbf{w}_b^{i,k}(t+1) = \mathbf{w}_b^{i,k}(t) + \mu_b \mathbf{g}_b^{i,k}(t) \quad (17)$$

where
$$\left.\begin{aligned} \mathbf{g}_f^{i,k}(t) &= e(t)\mathbf{r}_t + \hat{\mathbf{g}}_f^{i,k}(t) \\ \mathbf{g}_b^{i,k}(t) &= e(t)\hat{\underline{\mathbf{x}}}_t^{i,k} + \hat{\mathbf{g}}_b^{i,k}(t) \end{aligned}\right\} \quad (18)$$

and
$$\left.\begin{aligned} \hat{\mathbf{g}}_f^{i,k}(t) &= \lambda_f \hat{\mathbf{g}}_f^{i,k}(t-1) + \gamma_f e(t)\mathbf{r}_t \\ \hat{\mathbf{g}}_b^{i,k}(t) &= \lambda_b \hat{\mathbf{g}}_b^{i,k}(t-1) + \gamma_b e(t)\hat{\underline{\mathbf{x}}}_t^{i,k} \end{aligned}\right\} \quad (19)$$

where μ_f and μ_b are the step sizes for feed-forward and feedback adaptation. (λ_f, λ_b) and (γ_f, γ_b) are the forgetting factors and the scaling factors respectively, and $\hat{\mathbf{g}}_f^{i,k}(0) = \hat{\mathbf{g}}_b^{i,k}(0) = 0$.

2.2.2 Complexity Analysis

In time domain adaptive detector, each feed-forward filter requires $M(2L+1)$ multiplications while feedback filter uses $(2KN-1)$ by using LMS algorithm. Hence, the total number of operation is $KI[M(2L+1)+2KN-1]$ multiplications. Otherwise, the PFGLMS algorithm requires $M(4L+1)$ multiplications for feed-forward filter and $4(KN-1)+1$ multiplications for feedback filter. Thus, the total number is $KI[M(4L+1)+4KN-3]$ multiplications. On the other hand, the computation requirement for frequency domain adaptive detector requires $\text{Log}_2 L$ of multiplier for each feed forward filter as well as $\text{Log}_2(KN-1)$ for feedback filter. The summary of the complexity comparison between time domain and frequency domain filter is listed in table 1.

Table1. Complexity Comparison between Time and Frequency Domain Filter.

Algorithm	Conventional-LMS	PFGLMS
Time Domain	$KI[M(2L+1)$ $+2KN-1]$	$KI[M(4L+1)$ $+4KN-3]$
Frequency Domain	$KI[M(\log_2 L+L+1)$ $+\log_2(KN-1)+KN]$	$KI[M(\log_2 L+3L+1)$ $+\log_2(KN-1)+3KN-2]$

K= number of users, L= processing gain, N= number of transmit antennas, M= number of receive antennas, I= number of iteration

3. PERFORMANCE RESULTS

This section presents simulation results for the adaptive iterative LSTC-CDMA receiver operating in the frequency domain with Binary Phase Shift Keying (BPSK) modulation over a quasi-static fading channel, for which the fading coefficient is constant within a frame but changes independently from one frame to another. The system operates in the training mode until the MSE reaches the minimum, at which point switches to the decision mode. The constituent codes are non-systematic convolutional codes with the code rate of ½, memory order of 3 and the generating polynomials $g_1=15_8$ and $g_2=17_8$. The spreading sequences used are Gold sequences with the processing gain of 7. The proposed system is simulated with 2 transmit and 2 receive antennas with 130 information symbols in each frame per layer for each user. Therefore, each layers of the LSTC-CDMA system consists of 266 encoded symbols per frame.

A comparison of the convergence speeds of LMS and PFGLMS algorithm in frequency domain is shown in Fig.4, whereby the convergence speeds of PFGLMS adaptive iterative receiver is about seven times faster than that of LMS. The average Mean Square Error (MSE) of adaptive PFGLMS detector is lower than that of LMS detector. This means that the detector that the PFGLMS adaptive iterative receiver have better performance that the one of LMS.

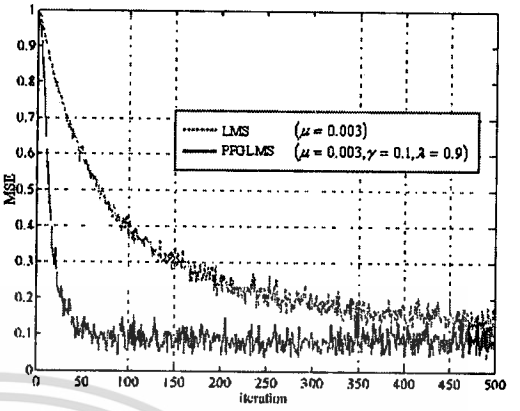

Fig. 4 The Comparison of convergence speeds of LMS and PFGLMS algorithm in frequency domain.

The performance of the 2 transmits and 2 receive antennas for 5 users under frequency domain approach is depicted in Fig.5. The result shows that the performance of the adaptive iterative receiver based on PFGLMS algorithm has a significant improvement in the first iteration and gradually improves for the higher iterations, compared to that of the receiver based on LMS algorithm. The BER curves also show that the PFGLMS iterative receiver approaches the interference free bound and has an excellent tracking ability in the scattering environment.

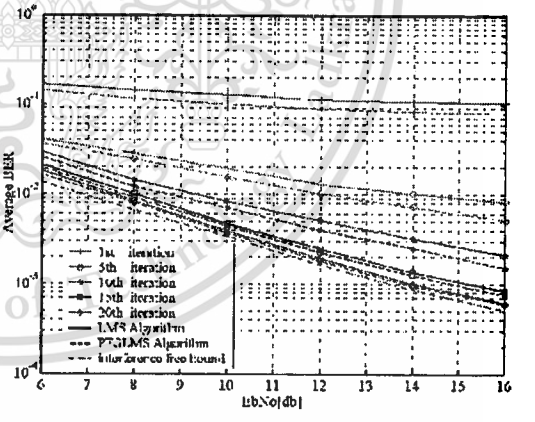

Fig.5 The Comparison between LMS and PFGLMS iterative algorithm for 5 users.

The bite error rate (BER) of the adaptive iterative PFGLMS receiver for five users in time domain and frequency domain is shown in Fig. 6. It can be observed that the system performance is significantly improved

for the second iteration compared to the first iteration and approaches the interference free bound in the 20th iteration. The results also show that performance of the time domain and frequency domain structures are approximately identity.

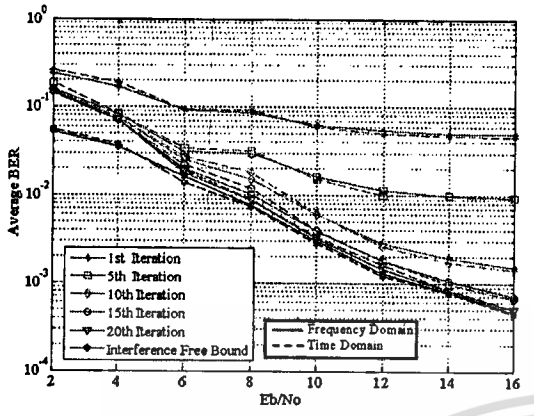

Fig. 6 The Comparison of BER of the adaptive iterative PFGLMS receiver for five users in time domain and frequency domain.

The maximum number of users for the frequency domain adaptive iterative PFGLMS receiver in a target BER at E_b/N_o equal to 16 dB is shown in Fig. 7. The simulation results show that the number of users is 15 after 20 iterations for a BER of 7×10^{-3}. These results also show that when the number of users increases, a higher number of iteration is required to achieve the same BER. For example, the receiver requires 10 iterations to achieve a BER of 1.95×10^{-2} for 15 users while it requires 20 iterations to achieve the same BER for 20 users.

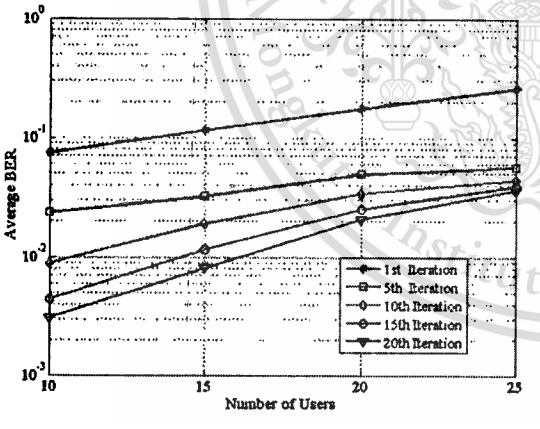

Fig. 7 Number of users for frequency domain adaptive iterative PFGLMS receiver at E_b/N_o 16dB.

4. CONCLUSION

In this paper, we present the low complexity frequency domain adaptive iterative receiver for a LSTC-CDMA based on the PFGLMS algorithm, compared to LMS algorithm. The proposed frequency domain receiver has a significant reduction in computation complexity and achieves the same performance compared to the time domain system. The simulations results show that the proposed receiver based on PFGLMS algorithm yields a faster convergence speed, obtains better tracking ability, and effectively mitigate the CCI and MAI by using the interference suppression and cancellation techniques.

REFERENCES

[1] R. L.-U. Choi, K. B. Letaief, and R. D. Murch, "MIMO CDMA antenna systems," *Proc. of IEEE ICC*, vol. 2, pp. 990-994, 2000.

[2] L. Mailaender, "Linear MIMO Chip Equalization for CDMA Downlink," *Proc. of IEEE SPAWC*, June 2003.

[3] S. Marinkovic, "Interference mitigation in CDMA and space-time coded MIMO systems," Thesis (Ph. D.) Telecommunications Laboratory, Dept. of Electrical and Information Engineering, University of Sydney, 2002 .

[4] J. Li, K. B. Letaief, and Z. Cao, "Adaptive cochannel interference cancellation in space-time coded communication systems," *IEEE Trans. on Communication*, vol. 50, pp. 1580-1583, October 2002.

[5] C. Teekapakvisit, V. D. Pham, and B. Vucetic, "An Adaptive Iterative Receiver for Space-time coding MIMO Systems," *3rd Workshop on the Internet, Telecommunications and Signal Processing*, 2004.

[6] Y. Sun, M. L. Honig, and V. Tripathi, "Adaptive, iterative, reduced-rank equalization for MIMO channels," *Proc. of MILCOM*, October 2002.

[7] T. Keovkolyan, C. Teekapakvisit, and K. Janchitrapongvej, "Adaptive Iterative Receiver for Layered Space-Time Coding CDMA System," Presented at IEEE-ECTI-CON, May 2009.

[8] D. Falconer, S. L. Ariyavisitakul, A. Benyamin-Seeyar, and B. Eidson, "Frequency domain equalization for single-carrier broadband wireless systems," *Communications Magazine, IEEE*, vol. 40, pp. 58-66, 2002.

[9] X. Zhu and R. D. Murch, "Layered space-frequency equalization in a single-carrier MIMO system for frequency-selective channels," *Wireless Communications, IEEE Transactions on*, vol. 3, pp. 701-708, 2004.

[10] S. S. Haykin, *Adaptive filter theory*, 4th ed., Prentice Hall, 2002.

[11] J. S. Lim, "Fast adaptive filtering algorithm based on exponentially weighted least-square errors," *Electronics Letters*, October 1999.

2009 IEEE-RIVF International Conference on Computing and Communication Technologies

Research, Innovation and Vision for the Future

Da Nang University of Technology
Vietnam, July 13 17, 2009

Organized by
IEEE Vietnam Section
In cooperation with IEEE Region 10 Asia Pacific
Da Nang University of Technology

Technically co-sponsored by
IEEE Communications Society
IEEE Computational Intelligence Society
Télécom ParisTech
EPITA

Supported by
RDCOM – International Technology Center – Pacific
Asian Office of Aerospace R&D
IFI Solution JSC
Institut Télécom

Editors
Tru Cao, Ralf-Detlef Kutsche, Akim Demaille

Adaptive Iterative Receiver for CDMA Systems in Rayleigh Fading Channels

T. Keovkolyan[1] and C. Teekapakvisit[2]
Telecommunication Laboratory, Department of Information Engineering, Faculty of Engineering,
King Monkut's Institute of Technology Ladkrabang (KMITL)
Chalongkrung Rd, Bangkok 10520, Thailand

***Abstract*—An adaptive iterative receiver for a Layered Space-Time Coded CDMA (LSTC-CDMA) system has been proposed in this paper. The LSTC-CDMA system, based on a joint adaptive iterative detection and decoding algorithm, adaptively cancels Co-Channel Interference (CCI) and mitigates Multiple Access Interference (MAI). The Least Means Square (LMS) algorithm is used for both feed-forward filter and feedback filter in the adaptive detection. A Partially Filtered Gradient LMS (PFGLMS) algorithm is also proposed to improve the convergence speed of the adaptive detector. The performance results show that the receiver, based on PFGLMS algorithm, yields much faster convergence speed and tracking ability with a slightly increase in complexity. The proposed receiver is analyzed in the slow and fast Rayleigh fading channels.**

***Keywords*- CDMA; Layered Space-Time Coding; Least Mean Square; Partially Filtered Gradient LMS; iterative detection.**

I. INTRODUCTION

Direct-Sequence CDMA (DS-CDMA) has emerged as a predominantly multiple-access technique for 3G systems compared to the 2G of TDMA systems. To improve the throughput of this cellular system, the combination of LSTC and CDMA has been intensively studied in [1-3]. This implementation generates Co-Channel Interference (CCI) from the adjacent layers and Multiple Access Interference (MAI) from the users. To mitigate the aforementioned interferences, an adaptive Minimum Means Square Error (MMSE) receiver for a LSTC system have been proposed in [4]. In this work, CCI can be reduced, but MAI is still a huge problem, degrading the performance and yielding channel estimation inaccurate in a high interference environment. A non-linear adaptive iterative receiver has been studied in [5, 6], containing a feed-forward filter to suppress the system interference and a feedback filter to cancel the interference from adjacent antennas under an iterative format. By using this algorithm, the convergence speed can be improved; however, the feedback filter still has high complexity.

An adaptive iterative receiver for multiuser LSTC-CDMA system has been proposed. The proposed adaptive detector was investigated based on the LMS algorithm [7], whereby the performance has been improved. However, the convergence speed of the adaptive detector is not satisfied. For this reason, the adaptive iterative receiver using a PFGLMS [8] algorithm was proposed to improve convergence speed with slightly increase in complexity. This paper presents adaptive iterative receiver for LSTC-CDMA systems using PFGLMS algorithm which organized as follows. System model is demonstrated in Section II. Performance results are presented in Section III. Finally, section IV gives a conclusion of this work.

1. teav_keovkolyan@yahoo.com
2. ktchakre@kmitl.ac.th

II. SYSTEM MODEL

A. Transmitter Structure

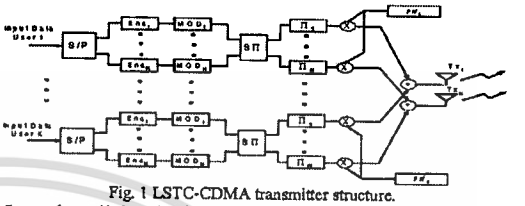

Fig. 1 LSTC-CDMA transmitter structure.

In a downlink LSTC-CDMA system, all user signals are transmitted simultaneously with N transmitters and M receivers antennas. Fig. 1 shows the LSTC-CDMA transmitter structure with K users. The binary information of each user is transmitted at a data rate of $r_b = 1/T_b$, where T_b is the bit interval. This data information is first converted into layered data information streams by a serial to parallel (S/P) converter. Before modulated, each information stream was encoded by a convolutional encoder to produce coded data stream for each layer. The layered coded data streams are then fed into a spatial time interleaver ($S\Pi$) and time interleaver (Π). Next, the coded data streams are spread by its signature sequence using a spreading gain of L with $L = T/T_c$, where T is the symbol interval, and T_c is chip duration of spreading sequence. Finally, the spread symbols of all users are then combined together and transmitted through N transmit antennas.

Let $\mathbf{b}$ be the coded signal vectors transmitted by K users through N transmit antennas and be defined by:

$$\mathbf{b} = [\mathbf{b}_1, \mathbf{b}_2, ..., \mathbf{b}_p, ..., \mathbf{b}_k]^T \quad (1)$$

where $\mathbf{b}_p = [b_p^1, ..., b_p^n, ..., b_p^N]$, and b_p^n is the information bit of the p-th user for n-th transmit antenna with $n=1,..,N$ and $p=1,..,K$.

Let $\mathbf{S}$ represents the L x KN spread transmitted sequences of K users for n transmit antennas, as given by:

$$\mathbf{S} = [\mathbf{s}_1^1, ..., \mathbf{s}_1^N, ..., \mathbf{s}_p^n ... \mathbf{s}_K^1, ... \mathbf{s}_K^N] \quad (2)$$

where $\mathbf{s}_p^n = [s_p^{n1}, .., s_p^{nq}, .., s_p^{nL}]^T$ is the q-th chip of a spreading sequence for the p-th user and n-th transmit antenna with $q=1,..,L$.

Let $\mathbf{r}_{t,j}^p$ is the received signal vector for the p-th user at the receiver antenna j, $j = 1,..., M$, for symbol t, is represented by:

$$\mathbf{r}_{t,j}^p = \mathbf{S}\mathbf{H}_{t,j}^p \mathbf{b} + \mathbf{n}_{t,j}^p \quad (3)$$

where $\mathbf{r}_{t,j}^p = [r_{t,j}^{p,1}, ... r_{t,j}^{p,q}, ..., r_{t,j}^{p,L}]^T$, and $r_{t,j}^{p,q}$ is the received signal for the p-th user at the q-th chip of the t-th symbol for j-th antenna. $\mathbf{H}_{t,j}^p$ is defined by $\mathbf{H}_{t,j}^p = diag(\mathbf{h}_{t,j}^p, ..., \mathbf{h}_{t,j}^p)_{KN \times KN}$.

978-1-4244-4568-4/09/$25.00 ©2009 IEEE

$\mathbf{n}_{t,j}^{p}$ is defined as an $L\times1$ noise vector at the receive antenna j of the p-th user, given by $\mathbf{n}_{t,j}^{p}=[n_{j,1}^{p}(t),\ldots,n_{j,q}^{p}(t),\ldots,n_{j,L}^{p}(t)]^{T}$ where $n_{j,q}^{p}(t)$ is a Gaussian random variable with a zero mean and two sided power spectral density $N_0/2$ per dimension.

B. Receiver Structure

In downlink LSTC-CDMA system, we assume that the system has no knowledge of Channel State Information (CSI), spreading sequences, and fading coefficients except the training sequence. A block diagram of the proposed adaptive iterative LSTC-CDMA multiuser receiver for the p-th user is shown in Fig. 2.

This structure consists of K adaptive iterative LSTC-CDMA single user receivers, each with an adaptive detector followed by N parallel soft-input soft-output channel decoders. The received signals are first input to the adaptive detector. The detector outputs are then fed to the time and spatial deinterleavers, definded by Π^{-1} and $S\Pi^{-1}$, respectively. The deinterleavers outputs are then decoded by a Maximum A Posteriori (MAP) decoder. The estimated soft symbols of MAP decoders from all users are sent to the spatial and time interleavers, and then fed back to the adaptive detector under iterative technique to cancel the interference from adjacent antennas of the user, called CCI, and the interference from other users, called MAI.

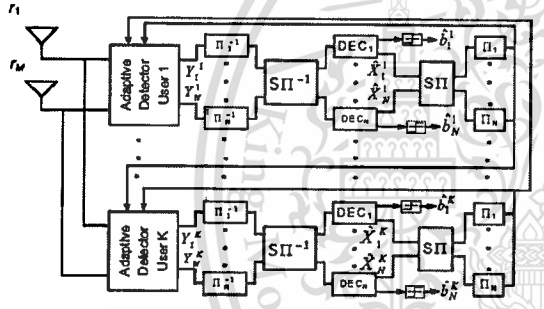

Fig. 2 Block diagram of iterative LST- CDMA Receiver.

1. Proposed Adaptive Iterative Detector

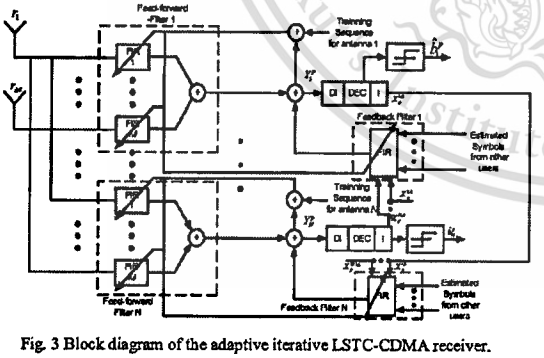

Fig. 3 Block diagram of the adaptive iterative LSTC-CDMA receiver.

The block diagram of the adaptive iterative LSTC-CDMA receiver for the p-th user is shown in Fig. 3. In the proposed adaptive receiver structure, N sets of adaptive detector consist of M equalizers for the feed-forward filter and an equalizer for the feedback filter modules. In the iterative process, the feed-forward filter is compensated for the channel estimation error, and the feedback filter is used to cancel the interference from adjacent antennas and other users. In the first iteration, there are no estimated symbols from the decoders, and the feedback filter coefficients are zeros; thus, the feedback filter output is also zero. In the feed-forward filter, the M adaptive equalizers are used to estimate the channel coefficients and signature sequence for each layer of each user. Finally, the equalizer outputs from all receive antennas are added to obtain a feed-forward filter output signal for each transmit antenna as shown in Fig. 3.

Let $\mathbf{w}_{j}^{p,k}(t)$ be an Lx1 feed-forward tap coefficients vector for the j-th receive antenna of the p-th user during the k-th iteration at symbol interval t and be given by:

$$\mathbf{w}_{j}^{p,k}(t)=[w_{t,j}^{p,k}(0),\ldots,w_{t,j}^{p,k}(q),\ldots,w_{t,j}^{p,k}(L-1)]^{T} \quad (4)$$

where $w_{t,j}^{p,k}(q)$ is the feed-forward tap coefficient corresponding to the q-th chip of the spreading sequence.

$\hat{\underline{\mathbf{x}}}_{t,p}^{t,k}$ is $(KN-1)\times1$ vector of the estimated soft symbols, at the k-th iteration, from MAP decoders of every antenna of all users, except the i-th antenna of p-th user at symbol interval t, given by:

$$\hat{\underline{\mathbf{x}}}_{t,p}^{i,k}=(\hat{\mathbf{x}}_{t,1}^{1,k},\ldots,\hat{\mathbf{x}}_{t,1}^{N,k},\ldots,\hat{\mathbf{x}}_{t,p}^{i,k},\ldots,\hat{\mathbf{x}}_{t,K}^{1,k},\ldots,\hat{\mathbf{x}}_{t,K}^{N,k})^{T} \quad (5)$$

where $\hat{\mathbf{x}}_{t,p}^{i,k}=(\hat{\mathbf{x}}_{t,p}^{1,k},\hat{\mathbf{x}}_{t,p}^{2,k},\ldots,\hat{\mathbf{x}}_{t,p}^{i-1,k},\hat{\mathbf{x}}_{t,p}^{i+1,k},\ldots,\hat{\mathbf{x}}_{t,p}^{N,k})$ (6)

Let $\mathbf{w}_{b}^{i,k}(t)$ be the feedback filter coefficients of all users, except the i-th antenna of the p-th user, at symbol interval t in time domain, is expressed as:

$$\mathbf{w}_{b}^{i,k}(t)=[\mathbf{w}_{b1}^{1,k}(t),\ldots,\mathbf{w}_{b1}^{N,k}(t),\ldots,\mathbf{w}_{b,p}^{1,k}(t),\ldots,\mathbf{w}_{b,K}^{1,k}(t),\ldots,\mathbf{w}_{b,K}^{N,k}(t)]^{T} \quad (7)$$

where $\mathbf{w}_{b,p}^{i,k}(t)=[w_{b,p}^{1,k}(t),\ldots,w_{b,p}^{i-1,k}(t),w_{b,p}^{i+1,k}(t),\ldots,w_{b,p}^{N,k}(t)]$ (8)

The detected symbol of the p-th user obtained at the output of the adaptive detector for the i-th antenna during the k-th iteration at symbol interval t, denoted by $y_{t,p}^{i,k}$, is defined as:

$$y_{t,p}^{i,k}=\sum_{j=0}^{M}\mathbf{w}_{j}^{p,k}(t)^{H}\mathbf{r}_{t,j}^{p}+\mathbf{w}_{b}^{i,k}(t)^{H}\hat{\underline{\mathbf{x}}}_{t,p}^{i,k} \quad (9)$$

The detector soft output $y_{t,p}^{i,k}$ is then compared to training symbol, denoted by $\mathbf{x}_{t,p}^{i,k}$. The difference between them is calculated as the detection error which is denoted by:

$$e_{t,p}^{i,k}=y_{t,p}^{i,k}-x_{t,p}^{i,k} \quad (10)$$

The detection error is then used to adapt the feed-forward filter and feedback filter tap coefficients in the time domain. After the Mean Square Error (MSE) approaches a specified value, the training mode is switched to the decision directed mode, in which the training sequence is replaced by the hard decision output of each user detector.

The values tap coefficients, $\mathbf{w}_{j}^{p,k}(t)$ in (4) and feedback filter tap coefficients, $\mathbf{w}_{b}^{i,k}(t)$ in (7) are calculated by minimizing the mean square error, defined as ζ, and given by

978-1-4244-4568-4/09/$25.00 ©2009 IEEE

$$\zeta = mim\left(E\left|e_{t,p}^{i,k}\right|^2\right) = \min\left(E\left[\left|y_{t,p}^{i,k} - x_{t,p}^{i,k}\right|^2\right]\right) \quad (11)$$

And they can be determined recursively by adaptive LMS algorithm [7] as follows:

$$\mathbf{w}_f^{p,k}(t+1) = \mathbf{w}_f^{p,k}(t) + \mu_f e_{t,p}^{i,k} \mathbf{r}_{t,j}^{p} \quad (12)$$

$$\mathbf{w}_b^{i,k}(t+1) = \mathbf{w}_b^{i,k}(t) + \mu_b e_{t,p}^{i,k} \hat{\underline{\mathbf{x}}}_{t,p}^{i,k} \quad (13)$$

where $\mathbf{r}_{t,j}^{p}$ and $\hat{\underline{\mathbf{x}}}_{t,p}^{i,k}$ are defined in (3) and (5). μ_f and μ_b are the step sizes for the feed-forward and feedback adaptation.

As the LMS algorithm has slow convergence and may not track in a non-stationary environment very well, the PFGLMS algorithm [8] based on an exponentially weighted least square error is utilized to improve the convergence speed. To apply the PFGLMS algorithm to the adaptive iterative receiver, the detected symbol of the p-th user i-th antenna during the k-th iteration at time t, defined in (9), is denoted by [7]:

$$y_{t,PFGLMS}^{i,k} \quad \sum_{j=0}^{M} \mathbf{w}_f^{i,k^H}(t)\mathbf{r}_t + \mathbf{w}_b^{i,k^H}(t)\hat{\underline{\mathbf{x}}}_t^{i,k} \quad (14)$$

The modified feed-forward and feedback coefficients of the PFGLMS algorithm can be expressed as [7]:

$$\mathbf{w}_f^{i,k}(t+1) = \mathbf{w}_f^{i,k}(t) + \mu_f \mathbf{g}_f^{i,k}(t) \quad (15)$$

and

$$\mathbf{w}_b^{i,k}(t+1) = \mathbf{w}_b^{i,k}(t) + \mu_b \mathbf{g}_b^{i,k}(t) \quad (16)$$

where

$$\left.\begin{aligned} \mathbf{g}_f^{i,k}(t) &= e(t)\mathbf{r}_t + \hat{\mathbf{g}}_f^{i,k}(t) \\ \hat{\mathbf{g}}_f^{i,k}(t) &= \lambda_f \hat{\mathbf{g}}_f^{i,k}(t-1) + \gamma_f e(t)\mathbf{r}_t \end{aligned}\right\} \quad (17)$$

and

$$\left.\begin{aligned} \mathbf{g}_b^{i,k}(t) &= e(t)\hat{\underline{\mathbf{x}}}_t^{i,k} + \hat{\mathbf{g}}_b^{i,k}(t) \\ \hat{\mathbf{g}}_b^{i,k}(t) &= \lambda_b \hat{\mathbf{g}}_b^{i,k}(t-1) + \gamma_b e(t)\hat{\underline{\mathbf{x}}}_t^{i,k} \end{aligned}\right\} \quad (18)$$

where μ_f and μ_b are the step sizes for feed-forward and feedback adaptation. (λ_f, λ_b) and (γ_f, γ_b) are the forgetting and scaling factors respectively, and $\hat{\mathbf{g}}_f^{i,k}(0) = \hat{\mathbf{g}}_b^{i,k}(0) = 0$.

2. Complexity Analysis

By using LMS algorithm, each feed-forward filter requires $M(2L+1)$ multiplications while feedback filter uses $(2KN-1)$ multiplications. Hence, the total number of operation is $KI[M(2L+1)+2KN-1]$ multiplications and the same number of additions. Otherwise, the PFGLMS algorithm requires $M(4L+1)$ multiplications for feed-forward filter and $4(KN-1)+1$ multiplications for feedback filter. Thus, the total number of operation is $KI[M(4L+1)+4KN-3]$ multiplications and the same number of additions. Both multiplications and addition are calculated for each coded symbol with K users, N transmit antennas, M receive antennas, I iterations, and L spreading sequence length. The summary of the complexity comparison between LMS and PFGLMS algorithm is listed in TABLE I.

TABLE I
COMPLEXITY COMPARISON BETWEEN LMS AND PFGLMS ALGORITHM

Algorithm	Number of multiplications	Computational Complexity (K=5, I=20, M=2, N=2, L=7)
Conventional-LMS	$KI[M(2L+1)+2KN-1]$	4900
PFGLMS	$KI[M(4L+1)+4KN-3]$	9500

III. PERFORMANCE RESULTS

This section presents simulation results for the adaptive iterative downlink LSTC-CDMA receiver with BPSK modulation Rayleigh fading channels. The slow fading channel is modeled as a quasi-static fading channel whereby the fading coefficient is constant within a frame, but changes independently from one frame to another. The constituent codes are nonsystematic convolutional codes with the code rate R of 1/2, memory order of 3, and the generating polynomial g_1 15_8 and g_2 17_8. The spreading sequence is a gold sequence with processing gain of 7. The proposed system is simulated with 2 transmit and 2 receive antennas with 130 information bits in each frame per layer for each user. Each layer consists of 266 encoded symbols per frame. The data rate is 1 Mb/s at the carrier frequency, f_c, of 2 GH_z. The simulation results are represented in terms of average BER versus the ratio of averaged energy per bit, denoted by Eb, to the power spectral density of the AWGN, denoted by No.

A. Slow Fading Channel

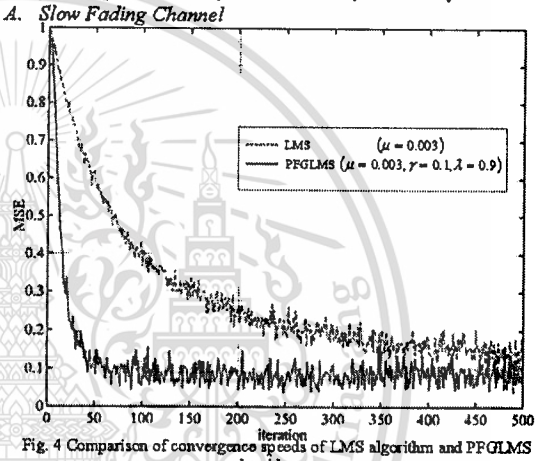

Fig. 4 Comparison of convergence speeds of LMS algorithm and PFGLMS algorithm.

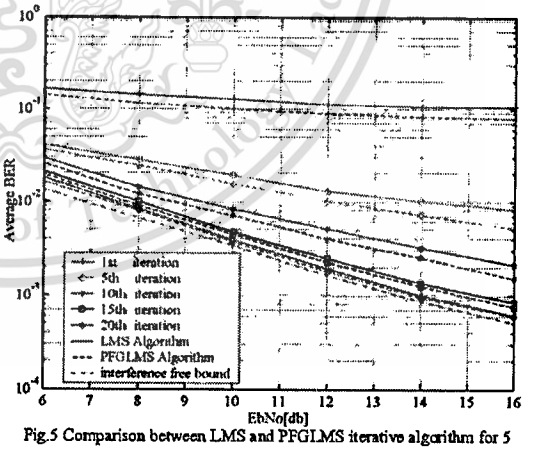

Fig.5 Comparison between LMS and PFGLMS iterative algorithm for 5 users.

978-1-4244-4568-4/09/$25.00 ©2009 IEEE

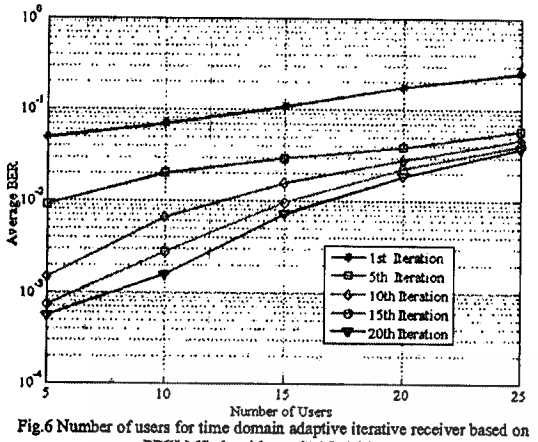

Fig.6 Number of users for time domain adaptive iterative receiver based on PFGLMS algorithm at E_b/N_o 16dB.

A comparison of the convergence speeds of LMS and PFGLMS algorithm is shown in Fig. 4, whereby the convergence speeds of PFGLMS adaptive iterative receiver is about seven times faster than that of LMS.

The performance of the 2 transmit and 2 receive antennas for 5 users under time domain approach is depicted in Fig. 5. The result shows that the performance of the adaptive iterative receiver for LSTC-CDMA systems based on PFGLMS algorithm has a significant improvement in the first iteration and gradually improves for the higher iterations. The BER curves also show that the proposed PFGLMS iterative receiver approaches the interference free bound and has an excellent tracking ability in the scattering environment.

The number of users for the time domain adaptive iterative receiver based on PFGLMS algorithm at E_b/N_o equal to 16 dB is shown in Fig. 6. The simulation results show that the number of users is 15 after 20 iterations for a BER of 7×10^{-3}. These results also show that when the number of users increases, a higher number of iteration is required to achieve the same BER. For example, the receiver requires 10 iterations to achieve a BER of 1.6×10^{-3} for 5 users while it requires 20 iterations to achieve the same BER for 10 users.

B. Fast Fading Channel

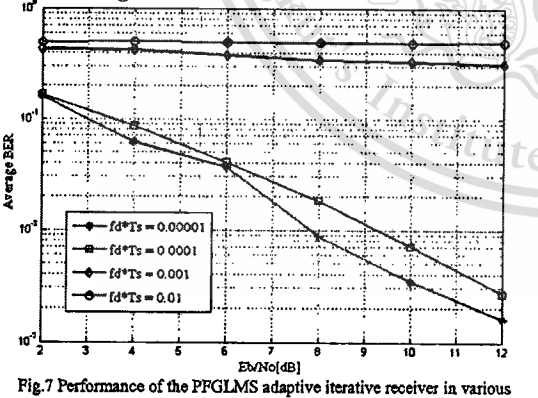

Fig.7 Performance of the PFGLMS adaptive iterative receiver in various normalized fading rate

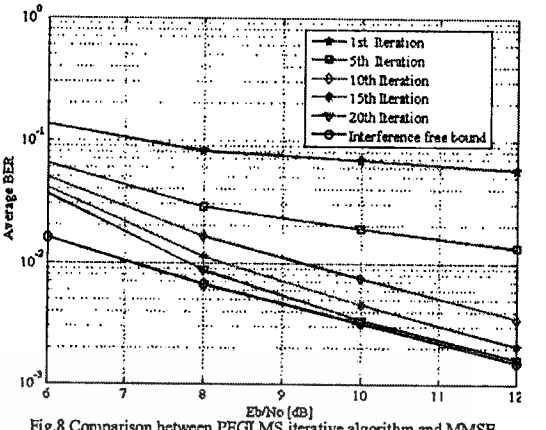

Fig.8 Comparison between PFGLMS iterative algorithm and MMSE algorithm interference free bound at the 0.00001 normalize fading rate.

The performance of the proposed receiver at various fading rates is shown in Fig.7. The results show that the average BER decreases when the fading rate is increased. When the fading rate is increased, the inputs to the MAP decoder are less correlated and the decoder has a better performance. Figure 8 presents the comparison of the performance between the PFGLMS and MMSE algorithm at the fd*Ts = 0.00001. The result show that the PFGLMS has a good tracking ability by approaching the interference free bound at the 20 iterations.

IV. Conclusion

In this paper, we present an adaptive iterative receiver for Layered Space-Time Coded CDMA based on the Partially Filtered Gradient LMS algorithm, compared to LMS algorithm. The simulation results show that the proposed receiver based on PFGLMS algorithm yields a faster convergence speed and better tracking ability with a slightly increase in the complexity in term of multiplication and addition. Due to the higher reliability of the Co-Channel Interference (CCI) and Multiple Access Interference (MAI) estimation, this performance results prove that the proposed adaptive receiver can effectively mitigate the CCI and MAI using the interference suppression and cancellation techniques.

References

[1] R. L-U. Choi, K. B. Letaief, and R. D. Murch, "MIMO CDMA antenna systems," *Proc. of IEEE ICC*, vol. 2, pp. 990-994, 2000.

[2] L. Mailaender, "Linear MIMO Chip Equalization for CDMA Downlink," *Proc. of IEEE SPAWC*, June 2003.

[3] S. Marinkovic, "Interference mitigation in CDMA and space-time coded MIMO systems," Thesis (Ph. D.) Telecommunications Laboratory, Dept. of Electrical and Information Engineering, University of Sydney, 2002 .

[4] J. Li, K. B. Letaief, and Z. Cao, "Adaptive cochannel interference cancellation in space-time coded communication systems," *IEEE Trans. on Communication*, vol. 50, pp. 1580-1583, October 2002.

[5] C. Teekapakvisit, V. D. Pham, and B. Vucetic, "An Adaptive Iterative Receiver for Space-time coding MIMO Systems," *3rd Workshop on the Internet, Telecommunications and Signal Processing*, 2004.

[6] Y. Sun, M. L. Honig, and V. Tripathi, "Adaptive, iterative, reduced-rank equalization for MIMO channels," *Proc. of MILCOM*, October 2002.

[7] S. S. Haykin, *Adaptive filter theory*, 4th ed., Prentice Hall, 2002.

[8] J. S. Lim, "Fast adaptive filtering algorithm based on exponentially weighted least-square errors," *Electronics Letters*, October 1999.

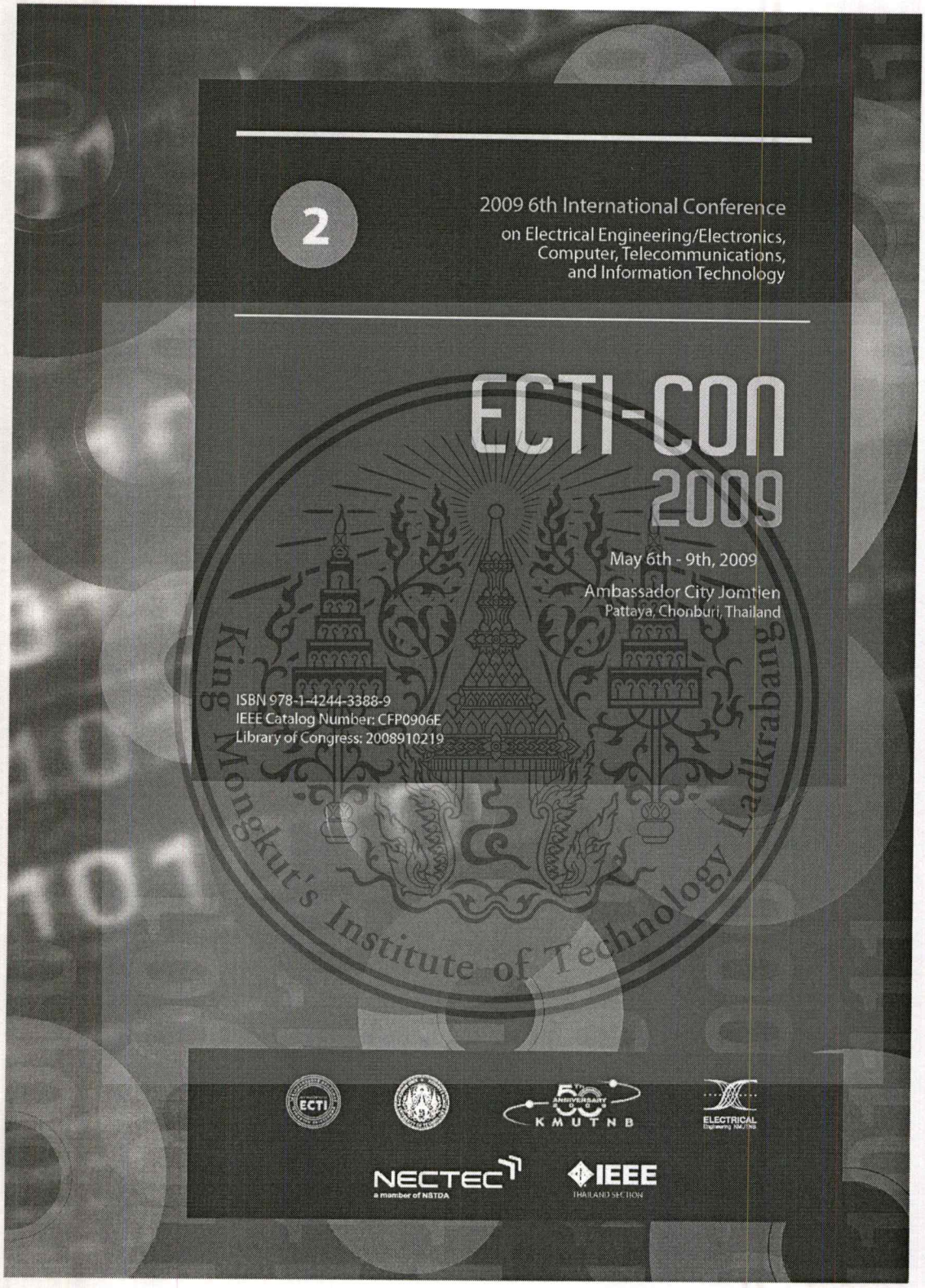

Adaptive Iterative Receiver for Layered Space-Time Coding CDMA Systems

T. Keovkolyan, C. Teekapakvisit, and K. Janchitrapongvej
Faculty of Engineering, King Mongkut's Institute of Technology Ladkrabang (KMITL),
Chalongkrung Rd, Bangkok 10520, Thailand
teav_keovkolyan@yahoo.com, ktchakre@kmitl.ac.th, and kjkanok@kmitl.ac.th

***Abstract*- An adaptive iterative receiver for a Layered Space-Time Coded CDMA (LSTC-CDMA) system has been proposed in this paper. The LSTC-CDMA system, based on a joint adaptive iterative detection and decoding algorithm, adaptively cancels Co-Channel Interference (CCI) and mitigates Multiple Access Interference (MAI). The Least Means Square (LMS) algorithm is used for both feed-forward filter and feedback filter in the adaptive detection. A Partially Filtered Gradient LMS (PFGLMS) algorithm is also proposed to improve the convergence speed of the adaptive detector. The performance results show that the adaptive iterative receiver, based on PFGLMS algorithm, yields much faster convergence speed and tracking ability with a slightly increase in complexity, compared to that of the receiver based on LMS algorithm.**

I. Introduction

With the integration of the internet and multimedia applications in the next generation wireless communications, the huge demand of highly reliable data rate service and the increase in the system capacity are growing very fast. Several broadband wireless communication systems have been widely studied such as Code Division Multiple Access (CDMA) and Multi-Input-Multi-Output (MIMO) systems.

Direct-Sequence CDMA (DS-CDMA) has emerged as a predominantly multiple-access technique for 3G systems because of its efficient capacity and facility of network planning in a cellular environment, compared to the 2G Time Division Multiple Access (TDMA) systems. To improve the throughput of this cellular system, the combination of Layered Space-Time Coding (LSTC) and CDMA, named as LSTC-CDMA, has been intensively studied in [1-3]. This implementation generates Co-Channel Interference (CCI) from the adjacent layers and Multiple Access Interference (MAI) from the users; hence, both will degrade the system performance seriously. To mitigate the aforementioned interferences controlled by Channel State Information (CSI), an adaptive Minimum Means Square Error (MMSE) receiver for a LSTC system have been proposed in [4]. In this work, CCI can be reduced, but MAI is still a huge problem, degrading the performance and yielding channel estimation inaccurate in a high interference environment. A non-linear adaptive iterative receiver has been studied in [5, 6], containing a feed-forward filter to suppress the system interference and a feedback filter to cancel the interference from adjacent antennas under an iterative format. By using this algorithm, the convergence speed can be improved; however, the complexity of the feedback filter still utilizes much computation.

An adaptive iterative receiver for multiuser LSTC-CDMA system has been proposed. Consequently, the proposed adaptive detector was investigated, based on the Adaptive Least Mean Square (LMS) algorithm [7], whereby the performance, i.e. complexity, has been improved. However, the convergence speed of the adaptive detector is not satisfied. For this reason, the adaptive iterative receiver using a Partially Filtered Gradient LMS (PFGLMS) [8] algorithm was proposed to improve convergence speed with slightly increase in complexity, compared to LMS algorithm. This paper presents adaptive iterative receiver for LSTC-CDMA systems using PFGLMS algorithm. The paper is organized as follows. System model is demonstrated in Section II. Performance results are presented in Section III. Finally, section IV gives a conclusion of this work.

II. System Model

A. Transmitter Structure

In a downlink LSTC-CDMA system, all user signals are transmitted simultaneously with N transmitters and M receivers antennas. Fig. 1 shows the LSTC-CDMA transmitter structure with K users. The binary information of each user is transmitted at a data rate of $r_b = 1/T_b$, where T_b is the bit interval. This data information is first converted into layered data information streams by a serial to parallel (S/P) converter. Before modulated, each information stream was encoded by a convolutional encoder to produce coded data stream for each layer. The layered coded data streams are then fed into a spatial time interleaver ($S\Pi$) and time interleaver (Π). Next, the coded data streams are spread by its signature sequence using a spreading gain of L with $L = T/T_c$, where T is the symbol interval, and T_c is chip duration of spreading sequence. Finally, the spread symbols of all users are then combined together and simultaneously transmitted through N transmit antennas.

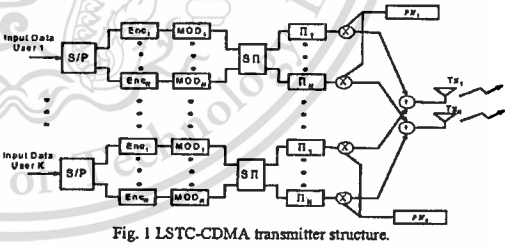

Fig. 1 LSTC-CDMA transmitter structure.

978-1-4244-3388-9/09/$25.00 ©2009 IEEE

Let $\mathbf{b}$ be the coded signal vectors transmitted by K users through N transmit antennas and be defined by:

$$\mathbf{b} = [\mathbf{b}_1, \mathbf{b}_2, ..., \mathbf{b}_p, ..., \mathbf{b}_k]^T \quad (1)$$

where $\mathbf{b}_p = [b_p^1, ..., b_p^n, ..., b_p^N]$, and b_p^n is the information bit of the p-th user for n-th transmit anterna with n=1,..,N and p=1,..,K.

Let $\mathbf{S}$ represents the L x KN spread transmitted sequences of K users for n transmit antennas, as given by:

$$\mathbf{S} = [\mathbf{s}_1^1, ..., \mathbf{s}_1^N, ..., \mathbf{s}_p^n ... \mathbf{s}_K^1, ... \mathbf{s}_K^N] \quad (2)$$

where $\mathbf{s}_p^n = [s_p^{n,1}, ..., s_p^{n,q}, ..., s_p^{n,L}]^T$, and $s_p^{n,q}$ is the q-th chip of a spreading sequence for the p-th user and n-th transmit antenna with n=1,..., N; p=1,..,K; and q=1,..,L.

Let $\mathbf{r}_{t,j}^p$ is the received signal vector for the p-th user at the receiver antenna j, j = 1,..., M, for symbol t, is represented by:

$$\mathbf{r}_{t,j}^p = \mathbf{S}\mathbf{H}_{t,j}^p \mathbf{b} + \mathbf{n}_{t,j}^p \quad (3)$$

where $\mathbf{r}_{t,j}^p = [r_{t,j}^{p,1}, ... r_{t,j}^{p,q}, ..., r_{t,j}^{p,L}]^T$, and $r_{t,j}^{p,q}$ is the received signal for the p-th user at the q-th chip of the t-th symbol for j-th antenna. $\mathbf{H}_{t,j}^p$ is defined by $\mathbf{H}_{t,j}^p = diag(\mathbf{h}_{t,j}^p, ..., \mathbf{h}_{t,j}^p)_{KNxKN}$ where $\mathbf{h}_{t,j}^p = diag[h_{j,1}^p(t), ..., h_{j,n}^p(t), ..., h_{j,N}^p(t)]_{NxN}$, and $h_{j,n}^p(t)$ represents the fading coefficient from j-th receive antenna to n-th transmit antenna of the p-th user. $\mathbf{n}_{t,j}^p$ is defined as an L×1 noise vector at the receive antenna j of the p-th user, given by $\mathbf{n}_{t,j}^p = [n_{j,1}^p(t), ..., n_{j,q}^p(t), ..., n_{j,L}^p(t)]^T$ where $n_{j,q}^p(t)$ is a Gaussian random variable with a zero mean and two sided power spectral density $N_o/2$ per dimension. The received signals for all receive antennas of the p-th user are given by $\mathbf{R}_t^p = [\mathbf{r}_{t,1}^p, ..., \mathbf{r}_{t,j}^p, ..., \mathbf{r}_{t,M}^p]^T$.

B. *Receiver Structure*

In downlink LSTC-CDMA system, we assume that the system has no knowledge of Channel State Information (CSI), spreading sequences, and fading coefficients except the training sequence. A block diagram of the proposed adaptive iterative LSTC-CDMA multiuser receiver for the p-th user is shown in Fig. 2.

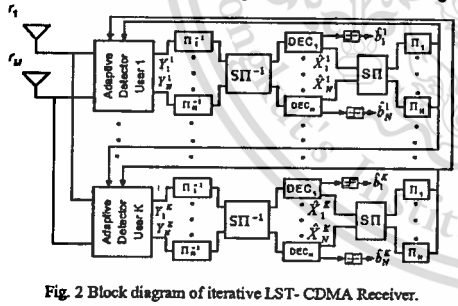

Fig. 2 Block diagram of iterative LST- CDMA Receiver.

This structure consists of K adaptive iterative LSTC-CDMA single user receivers, each with an adaptive detector followed by N parallel soft-input soft-output channel decoders. The received signals are first input to the adaptive detector. The detector outputs are then fed to the time and spatial deinterleavers, definded by Π^{-1} and $S\Pi^{-1}$, respectively. The deinterleavers outputs are then decoded by a Maximum A Posteriori (MAP) decoder. The estimated soft symbols of MAP decoders from all users are sent to the spatial and time interleavers, and then fed back to the adaptive detector under iterative technique to cancel the interference from adjacent antennas of the user, called CCI, and the interference from other users, called MAI.

1. Proposed Adaptive Iterative Detector

The block diagram of the adaptive iterative LSTC-CDMA receiver for the p-th user is shown in Fig. 3. In the proposed adaptive receiver structure, N sets of adaptive detector consist of M equalizers for the feed-forward filter and an equalizer for the feedback filter modules. An equalizer, employed in the proposed adaptive detector, is based on the LMS and PFGLMS algorithm. The detector output for each layer is obtained from combining a feed-forward and a feedback filter output. In the iterative process, the feed-forward filter is compensated for the channel estimation error, and the feedback filter is used to cancel the interference from adjacent antennas and other users. In the first iteration, there are no estimated symbols from the decoders, and the feedback filter coefficients are zeros; thus, the feedback filter output is also zero. In the feed-forward filter, the M adaptive equalizers are used to estimate the channel coefficients and signature sequence for each layer of each user. The equalizer outputs from all receive antennas are added to obtain a feed-forward filter output signal for each transmit antenna as shown in Fig. 3.

Let $\mathbf{w}_j^{p,k}(t)$ be an Lx1 feed-forward tap coefficients vector for the j-th receive antenna of the p-th user during the k-th iteration at symbol interval t and be given by:

$$\mathbf{w}_j^{p,k}(t) = [w_{t,j}^{p,k}(0), ..., w_{t,j}^{p,k}(q), ..., w_{t,j}^{p,k}(L-1)]^T \quad (4)$$

where $w_{t,j}^{p,k}(q)$ is the feed-forward tap coefficient corresponding to the q-th chip of the spreading sequence.

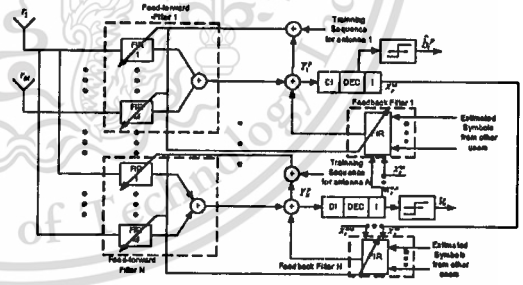

Fig. 3 Block diagram of the adaptive iterative LSTC-CDMA receiver.

$\hat{\underline{x}}_{t,p}^{i,k}$ is $(KN-1)\times 1$ vector of the estimated soft symbols, at the k-th iteration, from MAP decoders of every antenna of all users, except the i-th antenna of p-th user at symbol interval t, given by:

$$\hat{\underline{x}}_{t,p}^{i,k} = (\hat{x}_{t,1}^{1,k},...,\hat{x}_{t,1}^{N,k},...,\hat{x}_{t,p}^{1,k},...,\hat{x}_{t,K}^{1,k},...,\hat{x}_{t,K}^{N,k})^T \quad (5)$$

where $$\hat{x}_{t,p}^{i,k} = (\hat{x}_{t,p}^{1,k}, \hat{x}_{t,p}^{2,k},..., \hat{x}_{t,p}^{i-1,k}, \hat{x}_{t,p}^{i+1,k},..., \hat{x}_{t,p}^{N,k}) \quad (6)$$

Let $\mathbf{w}_b^{i,k}(t)$ be the feedback filter coefficients of all users, except the i-th antenna of the p-th user, at symbol interval t in time domain, is expressed as:

$$\mathbf{w}_b^{i,k}(t) = [w_{b,1}^{1,k}(t),...,w_{b,1}^{N,k}(t),...,w_{b,p}^{i,k}(t),...,w_{b,K}^{1,k}(t),...,w_{b,K}^{N,k}(t)]^T \quad (7)$$

where $$w_{b,p}^{i,k}(t) = [w_{b,p}^{1,k}(t),..., w_{b,p}^{i-1,k}(t), w_{b,p}^{i+1,k}(t),..., w_{b,p}^{N,k}(t)] \quad (8)$$

The detected symbol of the p-th user obtained at the output of the adaptive detector for the i-th antenna during the k-th iteration at symbol interval t, denoted by $y_{t,p}^{i,k}$, is defined as:

$$y_{t,p}^{i,k} = \sum_{j=0}^{M} \mathbf{w}_{ij}^{p,k}(t)^H \mathbf{r}_{t,j}^{p} + \mathbf{w}_b^{i,k}(t)^H \hat{\underline{x}}_{t,p}^{i,k} \quad (9)$$

The detector soft output $y_{t,p}^{i,k}$ in the time domain is then compared to training symbol, denoted by $x_{t,p}^{i,k}$. The difference between them is calculated as the detection error. The detection error for the p-th user in the k-th iteration at symbol interval t, for i-th antenna, denoted by $e_{t,p}^{i,k}$, is represented by:

$$e_{t,p}^{i,k} = y_{t,p}^{i,k} - x_{t,p}^{i,k} \quad (10)$$

The detection error is then used to adapt the feed-forward filter and feedback filter tap coefficients in the time domain. After the Mean Square Error (MSE) approaches a specified value, the training mode is switched to the decision directed mode, in which the training sequence is replaced by the hard decision output of each user detector.

The values tap coefficients, $\mathbf{w}_f^{p,k}(t)$ in (4) and feedback filter tap coefficients, $\mathbf{w}_b^{i,k}(t)$ in (7) are calculated by minimizing the mean square error, defined as ζ, and given by

$$\zeta = mim\left(E\left|e_{t,p}^{i,k}\right|^2\right) = \min\left(E\left[\left|y_{t,p}^{i,k} - x_{t,p}^{i,k}\right|^2\right]\right) \quad (11)$$

And they can be determined recursively by adaptive LMS algorithm [7] as follows:

$$\mathbf{w}_f^{p,k}(t+1) = \mathbf{w}_f^{p,k}(t) + \mu_f e_{t,p}^{i,k} \mathbf{r}_{t,j}^{p} \quad (12)$$

$$\mathbf{w}_b^{i,k}(t+1) = \mathbf{w}_b^{i,k}(t) + \mu_b e_{t,p}^{i,k} \hat{\underline{x}}_{t,p}^{i,k} \quad (13)$$

where $\mathbf{r}_{t,j}^{p}$ and $\hat{\underline{x}}_{t,p}^{i,k}$ are defined in (3) and (5), respectively. μ_f and μ_b are the step sizes for the feed-forward and feedback adaptation.

As the LMS algorithm has slow convergence and may not track in a non-stationary environment very well, the partially filtered gradient LMS (PFGLMS) algorithm [8] based on an exponentially weighted least square error is utilized to improve the convergence speed with a slight increase in complexity. To apply the PFGLMS algorithm to the adaptive iterative receiver, the detected symbol of the p-th user i-th antenna during the k-th iteration at time t, defined in (9), is denoted by [7]:

$$y_{t,PFGLMS}^{i,k} = \sum_{j=0}^{M} \mathbf{w}_f^{i,k^R}(t)\mathbf{r}_t + \mathbf{w}_b^{i,k^R}(t)\hat{\underline{x}}_t^{i,k} \quad (14)$$

The modified feed-forward and feedback coefficients of the PFGLMS algorithm can be expressed as [7]:

$$\mathbf{w}_f^{i,k}(t+1) = \mathbf{w}_f^{i,k}(t) + \mu_f \mathbf{g}_f^{i,k}(t) \quad (15)$$

and

$$\mathbf{w}_b^{i,k}(t+1) = \mathbf{w}_b^{i,k}(t) + \mu_b \mathbf{g}_b^{i,k}(t) \quad (16)$$

where

$$\left.\begin{aligned} \mathbf{g}_f^{i,k}(t) &= e(t)\mathbf{r}_t + \hat{\mathbf{g}}_f^{i,k}(t) \\ \hat{\mathbf{g}}_f^{i,k}(t) &= \lambda_f \hat{\mathbf{g}}_f^{i,k}(t-1) + \gamma_f e(t)\mathbf{r}_t \end{aligned}\right\} \quad (17)$$

and

$$\left.\begin{aligned} \mathbf{g}_b^{i,k}(t) &= e(t)\hat{\underline{x}}_t^{i,k} + \hat{\mathbf{g}}_b^{i,k}(t) \\ \hat{\mathbf{g}}_b^{i,k}(t) &= \lambda_b \hat{\mathbf{g}}_b^{i,k}(t-1) + \gamma_b e(t)\hat{\underline{x}}_t^{i,k} \end{aligned}\right\} \quad (18)$$

where μ_f and μ_b are the step sizes for feed-forward and feedback adaptation. (λ_f, λ_b) and (γ_f, γ_b) are the forgetting factors and the scaling factors respectively, and $\hat{\mathbf{g}}_f^{i,k}(0) = \hat{\mathbf{g}}_b^{i,k}(0) = 0$.

In the proposed receiver structure, detector output for user p, denoted by $y_{t,p}^{i,k}$, is decoded by Maximum A Posteriori (MAP) Decoder. The soft-output from the decoder is used to suppress the interference in the feedback filter in the next iteration. The process of this adaptive iterative detection/decoding is performed until the symbol estimation can converge to the optimal performance. The soft-output from the decoder in the last iteration is then fed into a decision device to produce a decision. For a Binary Phase Shift Keying (BPSK), the functions for the transmitted modulated symbols 1 and −1 can be written as [3]:

$$P\left(y_{t,p}^{i,k} \middle| x_{t,p}^{i,k} = \pm 1\right) = \frac{1}{\sqrt{2\pi\sigma^2}} \exp\frac{-\left(y_{t,p}^{i,k} \mp 1\right)^2}{2\sigma^2} \quad (19)$$

The Log-Likelihood Ratios (LLR) is determined in the k-th iteration for the i-th transmit layer of p-th user, denoted by $\lambda_{t,p}^{i,k}$:

$$\lambda_{t,p}^{i,k} = \log\left(\frac{P\left(x_{t,p}^{i,k} = 1 \middle| y_{t,p}^{i,k}\right)}{P\left(x_{t,p}^{i,k} = -1 \middle| y_{t,p}^{i,k}\right)}\right) \quad (20)$$

The symbol A Posteriori Probabilities (APP) $P(x_{t,p}^{i,k} = q | y_{t,p}^{i,k})$, with q equal 1 and -1, conditioned on the output variable which is defined as $y_{t,p}^{i,k}$ for p-th user, can be obtained as:

$$P\left(x_{t,p}^{i,k} = 1 \middle| y_{t,p}^{i,k}\right) = \frac{e^{\lambda_{t,p}^{i,k}}}{e^{\lambda_{t,p}^{i,k}} + 1} \quad (21)$$

and

$$P\left(x_{t,p}^{i,k} = -1 \middle| y_{t,p}^{i,k}\right) = \frac{1}{e^{\lambda_{t,p}^{i,k}} + 1} \quad (22)$$

The soft-output symbols are estimated in the i-th layer and k-th iteration for p-th user, calculated as:

$$\hat{x}_{t,p}^{i,k} = \frac{e^{\lambda_{t,p}^{i,k}} - 1}{e^{\lambda_{t,p}^{i,k}} + 1} \quad (23)$$

2. *Complexity Analysis*

By using LMS algorithm, each feed-forward filter requires $M(2L+1)$ multiplications while feedback filter uses $(2KN-1)$ multiplications. Hence, the total number of operation is $KI[M(2L+1)+2KN-1]$ multiplications and the same number of additions. Otherwise, the PFGLMS algorithm requires $M(4L+1)$ multiplications for feed-forward filter and $4(KN-1)+1$ multiplications for feedback filter. Thus, the total number of operation is $KI[M(4L+1)+4KN-3]$ multiplications and the same number of additions. Both multiplications and addition are calculated for each coded symbol with K users, N transmit antennas, M receive antennas, I iterations, and L spreading sequence length. The summary of the complexity comparison between LMS and PFGLMS algorithm is listed in TABLE I.

III. Performance Results

This section presents simulation results for the adaptive iterative downlink LSTC-CDMA receiver over a quasi-static fading channel whereby the fading coefficient is constant within a frame, but changes independently from one frame to another. The constituent codes are nonsystematic convolutional codes with the code rate R of 1/2, memory order of 3, and the generating polynomial $g_1 = 15_8$ and $g_2 = 17_8$. The spreading sequence is a gold sequence with processing gain of 7. The proposed system is simulated with 2 transmit and 2 receive antennas with 130 information bits in each frame per layer for each user. Each layer consists of 266 encoded symbols per frame.

A comparison of the convergence speeds of LMS and PFGLMS algorithm is shown in Fig. 4, whereby the convergence speeds of PFGLMS adaptive iterative receiver is about seven times faster than that of LMS. The average Mean Square Error (MSE) of adaptive PFGLMS detector is lower than that of LMS detector. The performance of the 2 transmit and 2 receive antennas for 5 users under time domain approach is depicted in Fig. 5. The result shows that the performance of the adaptive iterative receiver based on PFGLMS algorithm has a significant improvement in the first iteration and gradually improves for the higher iterations, compared to that of the receiver based on LMS algorithm. The BER curves also show that the PFGLMS iterative receiver approaches the interference free bound and has an excellent tracking ability in the scattering environment.

IV. Conclusion

In this paper, we present an adaptive iterative receiver for Layered Space-Time Coded CDMA based on the Partially Filtered Gradient LMS algorithm, compared to LMS algorithm. The simulation results show that the proposed adaptive iterative receiver based on PFGLMS algorithm yields a faster convergence speed and better tracking ability with a slightly increase in the complexity in term of multiplication and addition. Due to the higher reliability of the Co-Channel Interference (CCI) and Multiple Access Interference (MAI) estimation, this performance results prove that the proposed adaptive iterative receiver can effectively mitigate the CCI and MAI using the interference suppression and cancellation techniques.

References

[1] R. L.-U. Choi, K. B. Letaief, and R. D. Murch, "MIMO CDMA antenna systems," *Proc. of IEEE ICC*, vol. 2, pp. 990-994, 2000.

[2] L. Mailaender, "Linear MIMO Chip Equalization for CDMA Downlink," *Proc. of IEEE SPAWC*, June 2003.

[3] S. Marinkovic, "Interference mitigation in CDMA and space-time coded MIMO systems," Thesis (Ph. D.) Telecommunications Laboratory, Dept. of Electrical and Information Engineering, University of Sydney, 2002.

[4] J. Li, K. B. Letaief, and Z. Cao, "Adaptive cochannel interference cancellation in space-time coded communication systems," *IEEE Trans. on Communication*, vol. 50, pp. 1580-1583, October 2002.

[5] C. Teekapakvisit, V. D. Pham, and B. Vucetic, "An Adaptive Iterative Receiver for Space-time coding MIMO Systems," *3rd Workshop on the Internet, Telecommunications and Signal Processing*, 2004.

[6] Y. Sun, M. L. Honig, and V. Tripathi, "Adaptive, iterative, reduced-rank equalization for MIMO channels," *Proc. of MILCOM*, October 2002.

[7] S. S. Haykin, *Adaptive filter theory*, 4th ed., Prentice Hall, 2002.

[8] J. S. Lim, "Fast adaptive filtering algorithm based on exponentially weighted least-square errors," *Electronics Letters*, October 1999.

TABLE I
COMPLEXITY COMPARISON BETWEEN LMS AND PFGLMS ALGORITHM

Algorithm	Number of multiplications	Computational Complexity (K=5, I=20, M=2, N=2, L=7)
Conventional-LMS	$KI[M(2L+1)+2KN-1]$	4900
PFGLMS	$KI[M(4L+1)+4KN-3]$	9500

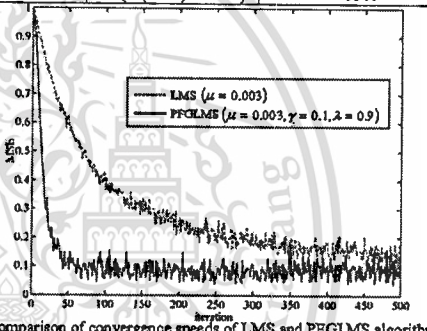

Fig. 4 Comparison of convergence speeds of LMS and PFGLMS algorithm.

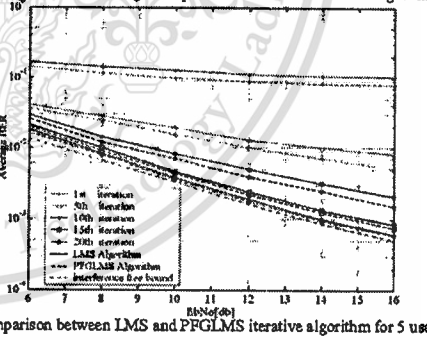

Fig.5 Comparison between LMS and PFGLMS iterative algorithm for 5 users.